Reliability of Complex System under Operation Process Influence – Analytical Approach

Krzysztof Kołowrocki[1], Ewa Kuligowska[2] and Joanna Soszyńska-Budny[3]

[1] Gdynia Maritime University, Gdynia, Poland
(E-mail: k.kolowrocki@wn.am.gdynia.pl)
[2] Gdynia Maritime University, Gdynia, Poland
(E-mail: e.kuligowska@wn.am.gdynia.pl)
[3] Gdynia Maritime University, Gdynia, Poland
(E-mail: joannas@am.gdynia.pl)

Abstract. The paper presents an analytical method applied to the reliability evaluation of a multistate system subjected to a variable multistate operation process. A semi-Markov process is applied to construct the multistate model of the system operation process considering the system reliability states changing process with memory about this process past states changing. Analytical linking of the system operation process model with the system reliability model is proposed to get a general reliability model of the complex system operating at varying in time operation conditions and to find its reliability characteristics. The results are illustrated by practical application to reliability evaluation of a port grain transportation system.
Keywords: Multistate system, operation process, complex system, reliability, analytical modelling.

1 Introduction

The reliability analysis of a system subjected to a varying in time its operation process very often leads to complicated calculations, especially in the case when we assume the system multistate reliability model and the multistate model of its operation process [1-10,12]. On the other hand, the complexity of the systems' operation processes and their influence on changing in time the systems' reliability structures and their components reliability parameters are very often met in real practice [3,4,6,11,12]. Thus, the practical importance of an approach linking the system reliability models and the system operation processes models into an integrated general model in reliability assessment of real technical systems is evident. To get much more general solutions of the problem, we deal with the multistate reliability model of the system and multistate model of its operation process considering the system reliability states changing process with memory about this process past states changing. This general analytical model with memory is presented and applied to a port grain transportation system reliability characteristics determination.

16[rd] ASMDA Conference Proceedings, 30 June – 4 July 2015, Piraeus, Greece

2 System operation process

We assume that a system during its operation at the fixed moment t, $t \in \langle 0,+\infty)$, may be at one of ν, $\nu \geq 2$, operations states z_b, $b, l = 1,2,\ldots,\nu$. Consequently, we mark by $Z(t)$, $t \in \langle 0,+\infty)$, the system operation process, that is a function of a continuous variable t, taking discrete values at the set $\{z_1, z_2, \ldots, z_\nu\}$ of the system operation states. We assume a semi-Markov model [2,4] of the system operation process $Z(t)$ and we mark by θ_{bl} its random conditional sojourn times at the operation states z_b, when its next operation state is z_l, $b, l = 1,2,\ldots,\nu$, $b \neq l$.

Consequently, the operation process may be described by the following parameters [6]:

- the vector $[p_b(0)]_{1\times\nu}$, of the initial probabilities of the system operation process $Z(t)$ staying at the particular operation states z_b, $b = 1,2,\ldots,\nu$, at the moment $t = 0$;
- the matrix $[p_{bl}]_{\nu\times\nu}$ of the probabilities of the system operation process $Z(t)$ transitions between the operation states z_b and z_l, $b, l = 1,2,\ldots,\nu$, $b \neq l$;
- the matrix $[H_{bl}(t)]_{\nu\times\nu}$ of the conditional distribution functions of the system operation process $Z(t)$ conditional sojourn times θ_{bl} at the operation states, $b, l = 1,2,\ldots,\nu$, $b \neq l$.

From the formula for total probability, it follows that the unconditional distribution functions of the sojourn times θ_b, $b = 1,2,\ldots,\nu$, of the system operation process $Z(t)$ at the operation states z_b, $b = 1,2,\ldots,\nu$, are given by [2]-[3], [6]

$$H_b(t) = \sum_{l=1}^{\nu} p_{bl} H_{bl}(t), \quad t \in \langle 0,+\infty), \quad b = 1,2,\ldots,\nu. \tag{1}$$

Hence, the mean values $E[\theta_b]$ of the system operation process $Z(t)$ unconditional sojourn times θ_b, $b = 1,2,\ldots,\nu$, at the operation states are given by

$$M_b = E[\theta_b] = \sum_{l=1}^{\nu} p_{bl} M_{bl}, \quad b = 1,2,\ldots,\nu, \tag{2}$$

where M_{bl} are the mean values of the lifetimes θ_{bl}.

The limit values of the system operation process $Z(t)$ transient probabilities at the particular operation states $p_b(t) = P(Z(t) = z_b)$ are given by [1], [3], [6]

$$p_b = \lim_{t\to\infty} p_b(t) = \frac{\pi_b M_b}{\sum_{l=1}^{v} \pi_l M_l}, \quad b = 1,2,\dots,v, \tag{3}$$

where M_b, $b = 1,2,\dots,v$, are given by (2)(2), while π_b are the steady probabilities of the vector $[\pi_b]_{1xv}$ given in [6].
Lemma 1. If the distribution of sojourn times θ_{bl}, are exponential of the form

$$H_{bl}(t) = 1 - \exp[-\alpha_{bl} t], \; t \in \langle 0, +\infty), \; b, l = 1,2,\dots,v, \; b \neq l, \tag{4}$$

then the sojourn times θ_b, $b = 1,2,\dots,v$, of the system operation process $Z(t)$ at the operation states z_b, $b = 1,2,\dots,v$, have distribution (1) of the form

$$H_b(t) = 1 - \sum_{l=1}^{v} p_{bl} \exp[-\alpha_{bl} t]), \; t \in \langle 0, +\infty), \; b = 1,2,\dots,v, \tag{5}$$

and the mean value $E[\theta_b]$ and the varriance $D[\theta_b]$ of the system operation process $Z(t)$ unconditional sojourn times θ_b, $b = 1,2,\dots,v$, at the operation states are given by

$$M_b = E[\theta_b] = \sum_{l=1}^{v} \frac{p_{bl}}{\alpha_{bl}}, \tag{6}$$

$$D_b = D[\theta_b] = 2\sum_{l=1}^{v} \frac{p_{bl}}{(\alpha_{bl})^2} - \left(\sum_{l=1}^{v} \frac{p_{bl}}{(\alpha_{bl})^2} \right)^2. \tag{7}$$

If we denote by $N_b(t)$, $b = 1,2,\dots,v$, the conditional number of changes of the system operation process' states before the moment t, $t \in \langle 0, +\infty)$, at the operation state z_b, $b = 1,2,\dots,v$, then considering *Lemma 1* and *Proposition 3.5c* from [6], we get the following result.
Lemma 2. If the distribution of sojourn times θ_{bl}, are exponential of the form (4)(4), then the distribution of the conditional number $N_b(t)$, $b = 1,2,\dots,v$, of changes of the system operation process' states before the moment t, $t \in \langle 0, +\infty)$, at the operation state z_b, $b = 1,2,\dots,v$, is approximately given by

$$P(N_b(t) = k) \cong F_{N(0,1)}\left(\frac{(k+1)M_b - t}{\sqrt{D_b t / M_b}} \right) - F_{N(0,1)}\left(\frac{k M_b - t}{\sqrt{D_b t / M_b}} \right), \tag{8}$$

where $F_{N(0,1)}(t)$ is a standard normal distribution function and M_b and D_b are determined respectively by (6)(6) and (7).

3 Analytical approach to reliability evaluation of multistate complex system

3.1 General theoretical backgrounds

In the multistate reliability analysis to define the system with degrading components, we assume that:

– n is the number of the system components,
– E_i, $i = 1,2,...,n$, are components of a system,
– all components and a system under consideration have the reliability state set $\{0,1,...,z\}$, $z \geq 1$,
– the reliability states are ordered, the reliability state 0 is the worst and the reliability state z is the best,
– $T_i(u)$, $i = 1,2,...,n$, are independent random variables representing the lifetimes of components E_i in the reliability state subset $\{u,u+1,...,z\}$, while they were in the reliability state z at the moment $t = 0$,
– $T(u)$ is a random variable representing the lifetime of a system in the reliability state subset $\{u,u+1,...,z\}$ while it was in the reliability state z at the moment $t = 0$,
– the system states degrades with time t,
– $E_i(t)$ is a component E_i reliability state at the moment t, $t \in \langle 0,+\infty)$, given that it was in the reliability state z at the moment $t = 0$,
– $s(t)$ is a system S reliability state at the moment t, $t \in \langle 0,+\infty)$, given that it was in the reliability state z at the moment $t = 0$.

Further, we assume that the changes of the operation states of the system operation process $Z(t)$ have an influence on the system multistate components E_i, $i = 1,2,\ldots,n$, reliability and the system reliability structure as well. Consequently, we denote the system multistate component E_i, $i = 1,2,\ldots,n$, conditional lifetime in the reliability state subset $\{u,u+1,\ldots,z\}$ while the system is at the operation state z_b, $b = 1,2,\ldots,v$, by $T_i^{(b)}(u)$ and its conditional reliability function by the vector

$$[R_i(t,\cdot)]^{(b)} = [1,\ [R_i(t,1)]^{(b)},\ ...,\ [R_i(t,z)]^{(b)}],$$

with the coordinates defined by

$$[R_i(t,u)]^{(b)} = P(T_i^{(b)}(u) > t | Z(t) = z_b) \ \text{ for } t \in \langle 0,+\infty),$$
$$u = 1,2,\ldots,z,\ b = 1,2,\ldots,v.$$

Similarly, we denote the system conditional lifetime in the reliability state subset $\{u, u+1,\dots,z\}$ while the system is at the operation state z_b, $b = 1,2,\dots,v$, by $T^{(b)}(u)$ and the conditional reliability function of the system by the vector

$$[\boldsymbol{R}(t,\cdot)]^{(b)} = [1,\ [\boldsymbol{R}(t,1)]^{(b)},\ \dots,\ [\boldsymbol{R}(t,z)]^{(b)}],$$

with the coordinates defined by

$$[\boldsymbol{R}(t,u)]^{(b)} = P(T^{(b)}(u) > t | Z(t) = z_b) \tag{9}$$

for $t \in \langle 0,+\infty)$, $u = 1,2,\dots,z$, $b = 1,2,\dots,v$.

In the case when the system operation time θ is large enough, the coordinates of the unconditional reliability function of the system defined by are given by [6]

$$\boldsymbol{R}(t,u) \cong \sum_{b=1}^{v} p_b [\boldsymbol{R}(t,u)]^{(b)} \text{ for } t \in \langle 0,+\infty),\ ,\ u = 1,2,\dots,z, \tag{10}$$

where $[\boldsymbol{R}(t,u)]^{(b)}$, $u = 1,2,\dots,z$, $b = 1,2,\dots,v$, are the coordinates of the system conditional reliability functions defined by (9) and p_b, $b = 1,2,\dots,v$, are the system operation process limit transient probabilities defined by (3).

The application of the above formula and other particular results for selected systems given in [3,6] allow to find the reliability evaluations of various real complex technical systems having "no memory" like for instance considered in [7] the port grain transportation system.

3.2 System reliability states changing process with memory

We assume that the changes of the operation states of the system operation process $Z(t)$ have an influence on the system multistate components E_i, $i = 1,2,\dots,n$, reliability and the system reliability structure as well. Moreover, in particular, we assume that the system components' reliability depend on the number of operation states changes of the system operation process. Consequently, we denote the system multistate component E_i, $i = 1,2,\dots,n$, conditional lifetime in the reliability state subset $\{u, u+1,\dots,z\}$ while the system is at the operation state z_b, $b = 1,2,\dots,v$, after k, $k = 0,1,\dots$, changes of the system operation states by $[T_i(u)]_k^{(b)}$ and its conditional reliability function by the vector

$$[R_i(t,\cdot)]_k^{(b)} = [1,\ [R_i(t,1)]_k^{(b)},\ \dots,\ [R_i(t,z)]_k^{(b)}], \tag{11}$$

with the coordinates defined by

$$[R_i(t,u)]_k^{(b)} = P([T_i\ (u)]_k^{(b)} > t | Z(t) = z_b) \tag{12}$$

for $t \in \langle 0,+\infty)$, $u = 1,2,\ldots,z$, $b = 1,2,\ldots,v$, $k = 0,1,\ldots$.

Similarly, we denote the system conditional lifetime in the reliability state subset $\{u, u+1,\ldots,z\}$ while the system is at the operation state z_b, $b = 1,2,\ldots,v$, after k, $k = 0,1,\ldots$, changes of the system operation states by $[T(u)]_k^{(b)}$ and the conditional reliability function of the system by the vector

$$[\boldsymbol{R}(t,\cdot)]_k^{(b)} = [1,\ [\boldsymbol{R}(t,1)]_k^{(b)},\ ...,\ [\boldsymbol{R}(t,z)]_k^{(b)}],$$

with the coordinates defined by

$$[\boldsymbol{R}(t,u)]_k^{(b)} = P([T(u)]_k^{(b)} > t | Z(t) = z_b) \tag{13}$$

for $t \in \langle 0,+\infty)$, $u = 1,2,\ldots,z$, $b = 1,2,\ldots,v$, $k = 0,1,\ldots$.

Under those assumptions, considering (8) and (10),we can get the following result.

Theorem 1. The unconditional reliability function of the multistate system subjected to multistate operation process and composed of components with their conditional reliability functions at the operation state z_b, $b = 1,2,\ldots,v$, after k, $k = 0,1,\ldots$, changes of the system operation states defined by (11)-(12) is given by

$$\boldsymbol{R}(t,\cdot) = [1,\ \boldsymbol{R}(t,1),\ ...,\ \boldsymbol{R}(t,z)\ ], \tag{14}$$

where

$$\boldsymbol{R}(t,u) \cong \sum_{b=1}^{v} p_b \left(\sum_{k=0}^{\infty} P(N_b(t) = k)[\boldsymbol{R}(t,u)]_k^{(b)} \right), \tag{15}$$

for $t \in \langle 0,+\infty)$, $u = 1,2,\ldots,z$, where the distribution $P(N_b(t) = k)$, $t \in \langle 0,+\infty)$, $k = 0,1,\ldots$, is determined by (8) and $[\boldsymbol{R}(t,u)]_k^{(b)}$ are the conditional reliability functions of the system defined by (13).

4 Port grain transportation system reliability evaluation

4.1 Port grain transportation system operation process

We consider the port grain transportation system, presented in Figure 1, assigned to handle the clearing of exported and imported grain.

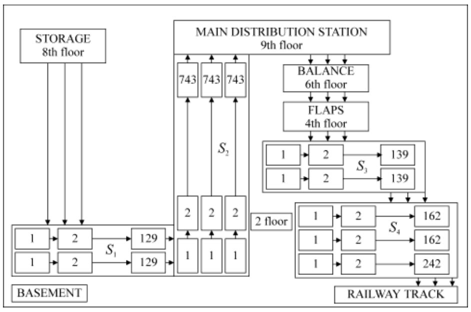

Figure 1. The scheme of the port grain transportation system structure at the operation state z_1

The port grain transportation system function is loading railway trucks with grain. The railway truck loading is performed in the following successive grain transportation system steps:

- gravitational passing of grain from the storage placed on the 8th elevator floor through 45 hall to horizontal conveyors placed in the elevator basement,
- transport of grain through horizontal conveyors to vertical bucket elevators transporting grain to the main distribution station placed on the 9th floor,
- gravitational dumping of grain through the main distribution station to the balance placed on the 6th floor,
- dumping weighed grain through the complex of flaps placed on the 4th floor to horizontal conveyors placed on the 2nd floor,
- dumping of grain from horizontal conveyors to worm conveyors,
- dumping of grain from worm conveyors to railway trucks.

In loading the railway trucks with grain the following presented in Figure 1 transportation subsystems take part: S_1 – horizontal conveyors of the first type, S_2 – vertical bucket elevators, S_3 – horizontal conveyors of the second type, S_4 – worm conveyors.

Taking into account the operation process of the considered transportation system, described by its operators, we distinguish its following $\nu = 3$ operation states:

z_1 – the system operation with the largest efficiency when all components of subsystems S_1, S_2, S_3 and S_4 are used,

z_2 – the system operation with less efficiency system when the first conveyor of subsystem S_1, the first and second elevators of subsystem S_2,the first conveyor of subsystem S_3, and the first and second conveyors of subsystem S_4, are used,

z_3 – the system operation with least efficiency when only the first conveyor of subsystem S_1, the first elevator of subsystem S_2, the first conveyor of subsystem S_3, and the first conveyor of subsystem S_4, are used.

Considering the system operators opinion, we assume the vector of approximate values of the initial probabilities

$$[p_b(0)]_{1x3} \cong [0.333, 0.333, 0.333]$$

of the system operation process staying at the particular states z_b at the time t = 0 and the matrix of probabilities of transitions between the operation states

$$[p_{bl}]_{3x3} \cong \begin{bmatrix} 0 & 0.333 & 0.667 \\ 0.444 & 0 & 0.556 \\ 0.333 & 0.667 & 0 \end{bmatrix} \tag{16}$$

Moreover, we assume the following matrix of the conditional distribution functions of the system sojourn times θ_{bl}, $b, l = 1, 2, 3,$

$$[H_{bl}(t)]_{3x3} = \begin{bmatrix} 0 & 1-e^{-5t} & 1-e^{-10t} \\ 1-e^{-40t} & 0 & 1-e^{-50t} \\ 1-e^{-10t} & 1-e^{-20t} & 0 \end{bmatrix} \tag{17}$$

Further, applying (5) and considering (16)-(17) we get the following unconditional distribution functions of the system sojourn times θ_b, $b = 1, 2, 3,$

$$H_1(t) = 1 - 0.333e^{-5t} - 0.667e^{-10t}, \;\; H_2(t) = 1 - 0.444e^{-40t} - 0.556e^{-50t},$$
$$H_3(t) = 1 - 0.333e^{-10t} - 0.667e^{-20t},$$

the mean values and their variances

$$M_1 \cong 0.1333, \; M_2 \cong 0.0222, \; M_3 \cong 0.0667,$$
$$D_1 \cong 0.0396, \; D_2 \cong 0.0010, \; D_3 \cong 0.0010. \tag{18}$$

After considering the above data and applying (18), the following limit values of the system operation process transient probabilities (3) at the operation states are determined and given by

$$p_1 \cong 0.5313, \quad p_2 \cong 0.1094, \quad p_3 \cong 0.3594,$$

From the above results, after applying *Lemma 2*, we imediatelly get the following conclusion.

Corollary 1. The distributions of the conditional numbers $N_b(t)$, of changes of the port grain transportation system operation process' states before $b=1,2,3$, of the moment t, $t \in \langle 0,+\infty)$, at the operation state z_b, $b=1,2,3$, are approximatelly given by (8), where M_b and D_b, b = 1,2,3, are given by (18).

4.2 Port grain transportation system reliability

Taking into account the efficiency of the considered in Section 4.1 port grain transportation system we distinguish the following three reliability states of the systems and its components:

- state 2 – the state ensuring the largest efficiency of the system and its conveyors,
- state 1 – the state ensuring less efficiency of the system caused by throwing grain off the system conveyors,
- state 0 – the state involving failure of the system.

The considered transportation system reliability analysis in the case of the system reliability states changing without memory is performed in [7]. In this section it is assumed that that the system reliability structure and its subsystems and components reliability parameters depend on its changing in time operation states and the exponential multistate reliability functions of the system components different in various operation states and dependent on the numbers of the system operation process changes in the past system operation are assumed. Considering those assumptions, we assume that the port grain transportation system subsystems S_υ, $\upsilon = 1,2,3.4$, are composed of three-state, i.e. z = 3, components $E_{ij}^{(\upsilon)}$, $\upsilon = 1,2,3,4$, having the conditional reliability functions while the system is at the operation state z_b, $b=1,2,3$, after k, $k = 0,1,\ldots$, changes of the system operation process states given by the vectors

$$[R_{ij}^{(\upsilon)}(t,\cdot)]_k^{(b)} = [1,[R_{ij}^{(\upsilon)}(t,1)]_k^{(b)}, [R_{ij}^{(\upsilon)}(t,2)]_k^{(b)}],$$

with the exponential coordinates

$$[R_{ij}^{(\upsilon)}(t,u)]_k^{(b)} = \exp[-[\lambda_{ij}^{(\upsilon)}(u)]_k^{(b)} t] = \exp[-[\lambda_{ij}^{(\upsilon)}(u)]^{(b)} \cdot c(k) \cdot t],$$

where $[\lambda_{ij}^{(\upsilon)}(u)]^{(b)}$ for $i = 1,2,\ldots,k^{(b)}$, $j = 1,2,\ldots,l_i^{(b)}$, $\upsilon = 1,2,3,4$, $b = 1,2,3$, $u = 1,2$, are given in Table 1 and $c(k) = (2k+1)/(k+1)$, $k = 0,1,\ldots$.

Considering that the system is a series system composed of subsystems S_1, S_2, S_3 and S_4, its conditional reliability functions at the particular operation states z_b, $b = 1,2,3$, after $k, k = 0,1,\ldots$, changes of system operation states are given by

$$[\boldsymbol{R}(t,\cdot)]_k^{(b)} = [1,\ [\boldsymbol{R}(t,1)]_k^{(b)},\ [\boldsymbol{R}(t,\cdot 2)]_k^{(b)}],\ \ t \in \langle 0,+\infty),\ \ k = 0,1,\ldots, \tag{19}$$

where after applying (9.59)-(9.60) given in [3] and the data given in Table 1, the coordinates at the particular operation states are as follows

Table 1. List of system components and parameters at different operation states

Subsystem	**Components** $E_{ij}^{(\upsilon)}$	**Parameters** $[\lambda_{ij}^{(\upsilon)}(u)]^{(b)}$					
		z_1		z_2		z_3	
		$u = 1$	$u = 2$	$u = 1$	$u = 2$	$u = 1$	$u = 2$
S_1	Belt conveyors of the 1st type	$k^{(1)} = 2$, $l_1^{(1)} = l_2^{(1)} = 129$		$k^{(2)} = 1$, $l_1^{(2)} = 129$		$k^{(3)} = 1$, $l_1^{(3)} = 129$	
	1 belt	0.0125	0.0150	0.0110	0.0120	0.0100	0.0105
	2 drums	0.0015	0.0020	0.0010	0.0012	0.0009	0.0011
	117 channelled rollers	0.0050	0.0100	0.0030	0.0060	0.0020	0.0040
	9 supporting rollers	0.0040	0.0080	0.0020	0.0030	0.0010	0.0020
S_2	Vertical bucket elevators	$k^{(1)} = 3$, $l_1^{(1)} = l_2^{(1)} = l_3^{(1)} = 743$		$k^{(2)} = 2$, $l_1^{(2)} = l_2^{(2)} = 743$		$k^{(3)} = 1$, $l_1^{(3)} = 743$	
	1 belt	0.0250	0.030	0.020	0.0240	0.0180	0.0220
	2 drums	0.0015	0.002	0.0012	0.0014	0.0011	0.0013
	740 buckets	0.0300	0.035	0.0220	0.0250	0.0200	0.0240
S_3	Belt conveyors of the 2nd type	$k^{(1)} = 2$, $l_1^{(1)} = l_2^{(1)} = 139$		$k^{(2)} = 1$, $l_1^{(2)} = 139$		$k^{(3)} = 1$, $l_1^{(3)} = 139$	
	1 belt	0.0125	0.015	0.011	0.0120	0.0100	0.0105
	2 drums	0.0015	0.002	0.001	0.0012	0.0009	0.0011
	117 channelled rollers	0.0050	0.010	0.003	0.0060	0.0020	0.0040
	19 supporting rollers	0.0040	0.008	0.002	0.0030	0.0010	0.0020
S_4	Chain worm conveyors	$k^{(1)} = 3$		$k^{(2)} = 2$		$k^{(3)} = 1$	
	Conveyors of the 1st type	$l_1^{(1)} = l_2^{(1)} = 162$		$l_1^{(2)} = l_2^{(2)} = 162$		$l_1^{(3)} = 162$	
	2 driving wheels	0.005	0.006	0.002	0.004	0.001	0.003
	160 links	0.012	0.014	0.008	0.010	0.007	0.009
	Conveyor of the 2nd type	$l_3^{(1)} = 242$		-		-	
	2 driving wheels	0.022	0.024	-	-	-	-
	240 links	0.034	0.040	-	-	-	-

$$
\begin{aligned}
[\boldsymbol{R}(t,1)]_k^{(1)} = {} & 24\exp[-55.903c(k)t] - 24\exp[-47.699c(k)t] \\
& - 24\exp[-33.675c(k)t] + 24\exp[-25.471c(k)t] - 24\exp[-47.699c(k)t] \\
& - 12\exp[-57.833c(k)t] - 12\exp[-56.5795c(k)t] - 12\exp[-56.5395c(k)t] \\
& - 12\exp[-53.973c(k)t] + 12\exp[-49.629c(k)t] + 12\exp[-48.3355c(k)t] \\
& + 12\exp[-35.605c(k)t] + 12\exp[-34.3515c(k)t] + 12\exp[-34.3115c(k)t] \\
& + 12\exp[-31.745c(k)t] - 12\exp[-27.401c(k)t] - 12\exp[-26.1075c(k)t] \\
& - 12\exp[-26.1475c(k)t] + 12\exp[-48.3755c(k)t] - 8\exp[-78.131c(k)t] \\
& + 8\exp[-69.927c(k)t] + 6\exp[-58.5095c(k)t] + 6\exp[-58.4695c(k)t] \\
& + 6\exp[-57.216c(k)t] + 6\exp[-54.6495c(k)t] + 6\exp[-54.6095c(k)t] \\
& - 6\exp[-50.2655c(k)t] - - 6\exp[-49.012c(k)t]\ 6\exp[-50.3055c(k)t] \\
& - 6\exp[-36.2815c(k)t] - 6\exp[-36.2415c(k)t] - 6\exp[-34.988c(k)t] \\
& - 6\exp[-32.4215c(k)t] - 6\exp[-32.3815c(k)t] + 6\exp[-28.0775c(k)t] \\
& + 6\exp[-28.0375c(k)t] + 6\exp[-26.784c(k)t] + 4\exp[-80.061c(k)t] \\
& + 4\exp[-78.8075c(k)t] + 4\exp[-78.7675c(k)t] + 4\exp[-76.201c(k)t] \\
& - 4\exp[-70.6035c(k)t] - 4\exp[-70.5635c(k)t] - 4\exp[-71.857c(k)t] \\
& - 3\exp[-59.146c(k)t] - 3\exp[-55.286c(k)t] + 3\exp[-50.942c(k)t] \\
& + 3\exp[-36.918c(k)t] + 3\exp[-33.058c(k)t] - 3\exp[-28.714c(k)t] \\
& - 2\exp[-80.7375c(k)t] - 2\exp[-80.6975c(k)t] - 2\exp[-79.444c(k)t] \\
& - 2\exp[-76.8775c(k)t] - 2\exp[-76.8375c(k)t] + 2\exp[-72.4935c(k)t] \\
& + 2\exp[-71.24c(k)t] + 2\exp[-72.5335c(k)t] + \exp[-81.374c(k)t] \\
& + \exp[-77.514c(k)t] - \exp[-73.17c(k)t]
\end{aligned} \tag{20}
$$

$$
\begin{aligned}
[\boldsymbol{R}(t,2)]_k^{(1)} = {} & 24\exp[-66.37c(k)t] - 24\exp[-56.722c(k)t] \\
& + 24\exp[-30.788c(k)t] - 24\exp[-40.436c(k)t] - 12\exp[-68.622c(k)t] \\
& - 12\exp[-67.711c(k)t] - 12\exp[-67.631c(k)t] - 12\exp[-64.118c(k)t] \\
& + 12\exp[-58.974c(k)t] + 12\exp[-58.063c(k)t] + 12\exp[-57.983c(k)t] \\
& + 12\exp[-42.688c(k)t] + 12\exp[-41.777c(k)t] + 12\exp[-41.697c(k)t] \\
& + 12\exp[-38.184c(k)t] - 12\exp[-33.04c(k)t] - 12\exp[-32.129c(k)t] \\
& - 12\exp[-32.049c(k)t] - 8\exp[-92.304c(k)t] + 8\exp[-82.656c(k)t] \\
& + 6\exp[-69.963c(k)t] + 6\exp[-69.883c(k)t] + 6\exp[-68.972c(k)t] \\
& + 6\exp[-65.459c(k)t] + 6\exp[-65.379c(k)t] - 6\exp[-60.315c(k)t] \\
& - 6\exp[-60.235c(k)t] - 6\exp[-59.324c(k)t] - 6\exp[-44.029c(k)t] \\
& - 6\exp[-43.949c(k)t] - 6\exp[-43.038c(k)t] - 6\exp[-39.525c(k)t] \\
& - 6\exp[-39.445c(k)t] + 6\exp[-34.381c(k)t] + 6\exp[-34.301c(k)t] \\
& + 6\exp[-33.39c(k)t] + 4\exp[-94.556c(k)t] + 4\exp[-93.645c(k)t]
\end{aligned}
$$

$$+\ 4\exp[-93.565c(k)t] + 4\exp[-90.052c(k)t] - 4\exp[-84.908c(k)t]$$
$$-\ 4\exp[-83.997c(k)t]\ - 4\exp[-83.917c(k)t]\ -\ 3\exp[-71.224c(k)t]$$
$$-\ 3\exp[-66.72c(k)t] + 3\exp[-61.576c(k)t] + 3\exp[-45.29c(k)t]$$
$$+\ 3\exp[-40.786c(k)t] - 3\exp[-35.642c(k)t]\ - 2\exp[-95.897c(k)t]$$
$$-\ 2\exp[-95.817c(k)t] -\ 2\exp[-94.906c(k)t] -\ 2\exp[-91.393c(k)t]$$
$$-\ 2\exp[-91.313c(k)t] +\ 2\exp[-86.249c(k)t] +\ 2\exp[-86.169c(k)t]$$
$$+\ 2\exp[-85.258c(k)t] +\ \exp[-97.158c(k)t] +\ \exp[-92.654c(k)t]$$
$$-\ \exp[-87.51c(k)t] \tag{21}$$

$$[\boldsymbol{R}(t,1)]_k^{(2)} = 4\exp[-18.3704c(k)t]\ -\ 2\exp[-34.6728c(k)t]$$
$$-\ 2\exp[-19.6544c(k)t] +\ \exp[-35.9568c(k)t] \tag{22}$$

$$[\boldsymbol{R}(t,2)]_k^{(2)} = 4\exp[-21.6516c(k)t]\ -\ 2\exp[-40.1784c(k)t]$$
$$-\ 2\exp[-23.2596c(k)t] +\ \exp[-41.7864c(k)t] \tag{23}$$

$$[\boldsymbol{R}(t,1)]_k^{(3)} = \exp[-16.462c(k)t] \tag{24}$$

$$[\boldsymbol{R}(t,2)]_k^{(3)} = \exp[-20.248c(k)t] \tag{25}$$

From the above results and from *Theorem 1* and *Corollary 1*, we get the unconditional reliability function (14) of the port grain transportation system given by

$$\boldsymbol{R}(t,\cdot) = [1,\ \boldsymbol{R}(t,1),\ \boldsymbol{R}(t,2)\ ],$$

where

$$\boldsymbol{R}(t,1) \cong \sum_{b=1}^{3} p_b (\sum_{k=0}^{\infty} P(N_b(t)=k)[\boldsymbol{R}(t,u)]_k^{(b)})$$
$$\cong 0.5313(\sum_{k=0}^{100} P(N_1(t)=k)[\boldsymbol{R}(t,1)]_k^{(1)}) + 0.1094(\sum_{k=0}^{100} P(N_2(t)=k)[\boldsymbol{R}(t,1)]_k^{(2)})$$
$$+ 0.3594(\sum_{k=0}^{100} P(N_3(t)=k)[\boldsymbol{R}(t,1)]_k^{(3)}) \tag{26}$$
$$\boldsymbol{R}(t,2) \cong \sum_{b=1}^{3} p_b (\sum_{k=0}^{\infty} P(N_b(t)=k)[\boldsymbol{R}(t,2)]_k^{(b)})$$
$$\cong 0.5313(\sum_{k=0}^{100} P(N_1(t)=k)[\boldsymbol{R}(t,2)]_k^{(1)}) + 0.1094(\sum_{k=0}^{100} P(N_2(t)=k)[\boldsymbol{R}(t,2)]_k^{(2)})$$
$$+ 0.3594(\sum_{k=0}^{100} P(N_3(t)=k)[\boldsymbol{R}(t,2)]_k^{(3)}) \tag{27}$$

are the conditional reliability functions of the system defined by (15), where $P(N_b(t)=k)$, $k = 0,1,\ldots$, are calculated according to (8) and (18) and $\boldsymbol{R}(t,u)]_k^{(b)}$ are the conditional reliability functions of the system defined by (19)-(25).
The approximate expected values of the system unconditional lifetimes in the reliability state subsets $\{1,2\}$, $\{2\}$, calculated from the results given by (26)-(27), are

$$\mu(1) \cong 0.0404, \ \mu(2) \cong 0.0345.$$

Further, the mean values of the unconditional lifetimes in the particular reliability states 1, 2, respectively are:

$$\overline{\mu}(1) = \mu(1) - \mu(2) = 0.0059 \text{ year}, \ \overline{\mu}(2) = \mu(2) = 0.0345 \text{ year}.$$

The expected values of the system unconditional lifetime in the reliability state subsets {1,2}, {2}, calculated for port grain transportation system in the case of the system reliability states changing without memory is performed in [7] and given by

$$\mu(1) \cong 0.0744 \text{ month}, \ \mu(2) \cong 0.0624 \text{ month}.$$

Further, the mean values of the system unconditional lifetimes in the particular reliability states 1, 2, respectively are [7]:

$$\overline{\mu}(1) \cong 0.0120 \text{ month}, \ \overline{\mu}(2) \cong 0.0624 \text{ month}.$$

Conclusions

The integrated general model of complex systems' reliability, linking their reliability models and their operation processes models and considering variable at different operation states their reliability structures and their components reliability parameters is constructed and applied to the reliability evaluation of the port grain transportation system composed of three series-parallel subsystems linked in series. The considered transportation system reliability analysis in the case of the system reliability states changing with memory that have influence on the system components reliability parameters is performed. The predicted reliability characteristics of the system are different from those determined for this system in the case its reliability states changing without memory considered in [7]. This fact justifies the sensibility of considering real systems at the variable operation conditions with components that have reliability functions dependent of the past system operation process state changes that is appearing out in a natural way from practice. This approach, upon the good accuracy of the systems' operation processes and the systems' components reliability parameters identification, makes their reliability prediction more precise and convergent to reality.

References

1. Grabski, F. and Jaźwiński, J. Functions of Random Variables in Problems of Reliability, Safety and Logistics, WKŁ, Warsaw, 2009 (in Polish).
2. F. Grabski. Semi-Markov Processes: Applications in System Reliability and Maintenance, 1st Edition, Elsevier Science & Technology, 2014.
3. K. Kołowrocki. Reliability of Large and Complex Systems, 2nd Edition, Elsevier Science & Technology, Oxford, 2014.
4. K. Kołowrocki and E. Kuligowska. Monte Carlo simulation application to reliability evaluation of port grain transportation system operating at variable conditions, Journal of Polish Safety and Reliability Association, Summer Safety and Reliability Seminars 4{1, 2013, 73-81.
5. K. Kołowrocki, E. Kuligowska and J. Soszyńska-Budny. Monte Carlo Simulation for optimization of object operation process and reliability, Journal of KONBiN 4{24, 2012, 79-92.
6. K. Kołowrocki and J. Soszyńska-Budny. Reliability and Safety of Complex Technical Systems and Processes: Modeling – Identification – Prediction – Optimization, Springer, London-Dordrecht-Heidelberg-New York, 2011.
7. K. Kołowrocki and J. Soszyńska-Budny. Modeling reliability of complex transportation system, Proc. Europen Safety and Reliability Conference-ESREL, Wrocław, 2014, 312.
8. E. Kuligowska. Monte Carlo simulation for reliability assessment and optimization of an system to varying operation conditions, Journal of Polish Safety and Reliability Association, Summer Safety and Reliability Seminars 4{2, 2013, 205-218.
9. E. Kuligowska. Preliminary Monte Carlo approach to complex system reliability analysis, Journal of Polish Safety and Reliability Association, Summer Safety and Reliability Seminars 3{1, 2012, 59-71.
10. E. Kuligowska. Reliability analysis of a system subjected to two-state operation process, Scientific Journals Maritime University of Szczecin 1 (36) (2013) 100-104.
11. J. Soszyńska. Reliability and risk evaluation of a port oil pipeline transportation system in variable operation conditions, International Journal of Pressure Vessels and Piping 87{2-3, 2010, 81-87.
12. J. Soszyńska. Systems reliability analysis in variable operation conditions, International Journal of Reliability, Quality and Safety Engineering. Special Issue: System Reliability and Safety 14{6, 2007, 617-634.
14. E. Zio and M. Marseguerra. Basics of the Monte Carlo Method with Application to System Reliability, LiLoLe, Hagen, 2002.

Identification of complex technical system components reliability models

Krzysztof Kolowrocki[1], and Joanna Soszynska-Budny[2]

[1] Gdynia Maritime University, Gdynia, Poland
(E-mail: katmatkk@am.gdynia.pl)
[2] Gdynia Maritime University, Gdynia, Poland
(E-mail: joannas@am.gdynia.pl)

Abstract. The paper is concerned with the methods for identification of unknown parameters of reliability models of multistate components of a complex technical system operating at variable conditions and their practical application. The multistate reliability model of a complex technical system component is constructed and the procedure of identifying its unknown reliability parameters is presented. In this reliability model, it is assumed that the conditional reliability functions of the multistate components at the system particular operation states are exponential. There are presented the methods of estimating unknown parameters of the exponential distribution of the system multistate component lifetimes in the reliability state subsets. The maximum likelihood method is applied to estimating unknown intensities of the component departure from the reliability state subsets at different system operation states in the case when there are in disposal empirical data coming from the process of system component reliability states changing for different kinds of the empirical investigations including the cases of small number of realizations and non-completed investigations. In the case when there are no empirical data, the procedure is based on the approximate opinions coming from experts. There is also suggested the goodness-of-fit method applied to testing the hypotheses concerned with the exponential form of the reliability function of the system multistate component at variable operations conditions. The methods are applied to the components of an exemplary system and a maritime ferry technical system unknown reliability parameters statistical identification.

1 Introduction

Many real technical systems belong to the class of complex systems. First of all, it is concerned with the large numbers of components and subsystems they are built and with their operating complexity. The changes of the operation states of the system operation process cause the changes of the system reliability structure and also the changes of its multistate components reliability parameters. The general joint model linking the system reliability model with the model of its operation process allowing for the reliability analysis of the complex technical systems operating at variable conditions is constructed in [6], [9]. To apply this general model practically in the evaluation and prediction of real complex technical systems reliability it is necessary to elaborate the

16th ASMDA Conference Proceedings, 30 June – 4 July 2015, Piraeus, Greece

statistical methods concerned with determining the unknown parameters of the proposed model [1]-[5], [10]-[12]. Particularly, in the part of the system model concerned with its reliability, the unknown parameters of the conditional reliability functions of the system multistate components at various operation states should be identified [7]-[9]. It is also necessary elaborating the methods of testing the hypotheses concerned with the conditional reliability functions [13]-[16] of the multistate components at the system various operation states [9].

2 Theoretical backgrounds

In the multistate reliability analysis of a system to define its ageing components we assume that [9], [13]-[16]:

- E is a component of a system,
- a components E has the reliability state set $\{0,1,...,z\}$, $z \geq 1$,
- the reliability states are ordered, the state 0 is the worst and the state z is the best,
- $T(u)$ is a random variable representing the lifetime of component E in the state subset $\{u,u+1,...,z\}$, while it was in the state z at the moment $t = 0$,
- the component reliability states degrade with time t,
- $e(t)$ is a component E state at the moment t, $t \in <0,\infty)$, given that it was in the state z at the moment $t = 0$.

The above assumptions mean that the states of the system degrading components may be changed in time only from better to worse.
Under those assumption, a vector

$$R(t,\cdot) = [R(t,0),R(t,1),...,R(t,z)], \ t \in <0,\infty), \tag{1}$$

where

$$R(t,u) = P(e(t) \geq u \mid e(0) = z) = P(T(u) > t), \ t \in <0,\infty), \ u = 0,1,...,z, \tag{2}$$

is the probability that the component E is in the state subset $\{u,u+1,\ldots,z\}$ at the moment t, $t \in <0,\infty)$, while it was in the state z at the moment $t = 0$, is called the multi-state reliability function of a component E.
Particularly, for $u = 0$, in (1) and (2) we have

$$R(t,0) = P(e(t) \geq 0 \mid e(0) = z) = P(T(0) > t) = 1, \ t \in <0,\infty). \tag{3}$$

Further, we assume that the system during its operation process is taking $\nu, \nu \in N$, different operation states $z_1, z_2, \ldots, z_\nu$, and we define the system operation process $Z(t)$, $t \in <0,+\infty)$, with discrete operation states from the set $\{z_1, z_2, \ldots, z_\nu\}$. since the changes of operation states of the multistate system operation process $Z(t)$ have an influence on the reliability functions of the system components then we mark by $T^{(b)}(u)$ the conditional lifetime $T^{(b)}(u)$ of the system component in the reliability states subset $\{u, u+1, \ldots, z\}$, $u = 1,2,\ldots,z$. Consequently, we mark the conditional multistate reliability function of the system component when the system is in the operation state z_b, $b = 1,2,\ldots,\nu$, by

$$[R(t,\cdot)]^{(b)} = [1, [R(t,1)]^{(b)}, \ldots, [R(t,z)]^{(b)}], \tag{4}$$

where

$$[R(t,u)]^{(b)} = P(T^{(b)}(u) > t | Z(t) = z_b) \text{ for } t \in <0,\infty), \ u = 1,2,\ldots,z, \ b = 1,2,\ldots,\nu, \tag{5}$$

is the conditional reliability function standing the probability that the conditional lifetime $T^{(b)}(u)$ of the system component in the reliability states subset $\{u, u+1, \ldots, z\}$ is greater than t, while the system operation process $Z(t)$ is in the operation state z_b, $b = 1,2,\ldots,\nu$. Further, we assume that the coordinates of the vector of the conditional multistate reliability function (4) are exponential reliability functions of the form

$$[R(t,u)]^{(b)} = \exp[-[\lambda(u)]^{(b)} t] \text{ for } t \in <0,\infty), \ u = 1,2,\ldots,z, \ b = 1,2,\ldots,\nu. \tag{6}$$

Te above assumptions mean that the density function of the system component conditional life time $T^{(b)}(u)$ in the reliability states subset $\{u, u+1, \ldots, z\}$, $u = 1,2,\ldots,z$, at the operation state z_b, $b = 1,2,\ldots,\nu$, is exponential of the form

$$[f(t,u)]^{(b)} = [\lambda(u)]^{(b)} \exp[-[\lambda(u)]^{(b)} t] \text{ for } t \in <0,\infty), \tag{7}$$

where $[\lambda(u)]^{(b)}$, $[\lambda(u)]^{(b)} \geq 0$, is an unknown intensity of departure from this subset of the reliability states.

3 Procedures of identification of complex technical system components reliability models

3.1 Procedure of the system components reliability data collection

3.1.1 Data coming from components reliability states changing processes

To estimate the unknown parameters of the system components multistate reliability models, during the experiment, we should collect necessary statistical data dependently of the fixed kinds of the experiments and the collected statistical data considered in distinguished in [9] *Cases 1-6*. To illustrate the methods we will consider only *Case 2* described below.

Case 2. The estimation of the component intensity of departure from the reliability states subset on the basis of the realizations of the component lifetimes up to the first departure from the reliability states subset on several experimental posts – Non-completed investigations, the same observation time on all experimental posts.

We assume that during the time $\tau^{(b)}$, $\tau^{(b)} > 0$, we have been observing the realizations of the component lifetimes $T^{(b)}(u)$ in the reliability states subset $\{u, u+1, \ldots, z\}$, $u = 1,2,\ldots,z$, at the operation state z_b, $b = 1,2,\ldots,\nu$, on $n^{(b)}$ identical experimental posts. We assume that at the beginning of the experiment all components are new identical components staying at the best reliability state z and that during the fixed observation time $\tau^{(b)}$ not all components have left the reliability states subset $\{1,2,\ldots,z\}$, i.e. $m^{(b)}$, $m^{(b)} < n^{(b)}$, observed components reached the worst reliability state 0. It means that the number $m^{(b)}(u)$ of components that have left the reliability states subset $\{u, u+1, \ldots, z\}$, $u = 1,2,\ldots,z$, is less or equal to $n^{(b)}$, i.e. $m^{(b)}(u) \le n^{(b)}$, $u = 1,2,\ldots,z$. Further, we mark by $A^{(b)}(u) = \{t_i^{(b)}(u) : i = 1,2,\ldots,m^{(b)}(u)\}$, $u = 1,2,\ldots,z$, the set of the moments $t_i^{(b)}(u)$, $i = 1,2,\ldots,m^{(b)}(u)$, $u = 1,2,\ldots,z$, of departures from the reliability states subset $\{u, u+1, \ldots, z\}$, $u = 1,2,\ldots,z$, of the component on the $i-$th observational post, i.e. the realizations of the identical component lifetimes $T_i^{(b)}(u)$, $i = 1,2,\ldots,n^{(b)}$, to the first departure from the reliability states subsets, that are the independent random variables with the exponential distribution defined by the density function (7).

3.1.2 Data coming from experts

On the basis of the expert opinions the approximate values

$$[\hat{\mu}(u)]^{(b)}, \; u = 1,2,\ldots,z, \; b = 1,2,\ldots,\nu,$$

of the mean values

$$[\mu(u)]^{(b)} = E[T(u)]^{(b)}, \; u = 1,2,\ldots,z, \; b = 1,2,\ldots,\nu,$$

of the system components lifetimes $[T(u)]^{(b)}$, $u = 1,2,\ldots,z$, $b = 1,2,\ldots,\nu$, in the reliability states subsets $\{u, u+1, \ldots, z\}$, $u = 1,2,\ldots,z$, while the system is operating in the operation state z_b, $b = 1,2,\ldots,\nu$, should be fixed.

3.2 Procedures of evaluating the system components unknown intensities of departure from the reliability state subsets

3.2.1 Data coming from components reliability states changing processes

On the basis of statistical data described in Section 3.1.1, we want to estimate the value of this unknown intensity of departure $[\hat{\lambda}(u)]^{(b)}$ from the reliability states subset $\{u, u+1, \ldots, z\}$, $u = 1,2,\ldots,z.$
The formulae for the kind of experiment considered in *Case 2* is presented below [9].
Case 2. In this case, the maximum likelihood evaluation of the unknown component intensity of departure $\lambda^{(b)}(u)$ from the reliability states subset $\{u, u+1, \ldots, z\}$, $u = 1,2,\ldots,z,$ is

$$\hat{\lambda}^{(b)}(u) = \frac{m^{(b)}(u)}{\sum_{i=1}^{m^{(b)}(u)} t_i^{(b)}(u) + \tau^{(b)}[n^{(b)} - m^{(b)}(u)]}, \quad u = 1,2,\ldots,z. \tag{8}$$

Assuming the observation time $\tau^{(b)}$ as the moment of departure from the reliability states subset $\{u, u+1, \ldots, z\}$, $u = 1,2,\ldots,z,$ of the components that have not left this reliability states subset we get so called pessimistic evaluation of the intensity of departure $\lambda^{(b)}(u)$ from the reliability states subset $\{u, u+1, \ldots, z\}$, $u = 1,2,\ldots,z,$ of the form

$$\hat{\lambda}^{(b)}(u) = \frac{n^{(b)}}{\sum_{i=1}^{m^{(b)}(u)} t_i^{(b)}(u) + \tau^{(b)}[n^{(b)} - m^{(b)}(u)]}, \quad u = 1,2,\ldots,z. \tag{9}$$

3.2.2 Data coming from experts

On the basis of the approximate values $[\hat{\mu}(u)]^{(b)}$, $u = 1,2,\ldots,z,$ $b = 1,2,\ldots,\nu,$ of the mean values $[\mu(u)]^{(b)} = E[T(u)]^{(b)}$, $u = 1,2,\ldots,z,$ $b = 1,2,\ldots,\nu,$ of the system components lifetimes $[T(u)]^{(b)}$, $u = 1,2,\ldots,z,$ $b = 1,2,\ldots,\nu,$ in the reliability states subsets $\{u, u+1, \ldots, z\}$, $u = 1,2,\ldots,z,$ while the system is operating in the operation state z_b, $b = 1,2,\ldots,\nu,$ coming from experts and described in Section 3.1.2, we want to estimate the values $[\hat{\lambda}(u)]^{(b)}$ of the components unknown intensities $[\lambda(u)]^{(b)}$ of departure from the reliability states subset $\{u, u+1, \ldots, z\}$, $u = 1,2,\ldots,z,$ while the system is operating in the operation state z_b, $b = 1,2,\ldots,\nu.$

The formula for all system components is given by the following approximate equation [9]

$$[\lambda(u)]^{(b)} \cong [\hat{\lambda}(u)]^{(b)} = \frac{1}{[\hat{\mu}(u)]^{(b)}}, \; u = 1,2,\ldots,z, \;\; b = 1,2,\ldots,\nu. \tag{10}$$

4 Applications

4.1 Statistical identification of exemplary system components reliability

4.1.1 Defining parameters of exemplary system components reliability models and data collection

The considered exemplary system reliability structure changing at the various operation states and its components and their unknown reliability parameters are described in [9]. At all the system operation process states z_b, $b = 1,2,3,4,$ defined in [9], we distinguish the following four reliability states 0, 1, 2 3, of the system and its components. Moreover, we fix that there are possible the transitions between the components reliability states only from better to worse ones. From the above, the subsystems S_υ, $\upsilon = 1,2,$ are composed of four-state, i.e. z = 3, components $E_{ij}^{(\upsilon)}$, $\upsilon = 1,2,$ with the conditional four-state reliability functions given by the vector

$$[R_{ij}^{(\upsilon)}(t,\cdot)]^{(b)} = [1, \; [R_{ij}^{(\nu)}(t,1)]^{(b)}, [R_{ij}^{(\upsilon)}(t,2)]^{(b)}, [R_{ij}^{(\upsilon)}(t,3)]^{(b)}], \;\; b = 1,2,3,4, \tag{11}$$

with the exponential co-ordinates

$$[R_{ij}^{(\upsilon)}(t,1)]^{(b)} = \exp[-[\lambda_{ij}^{(\upsilon)}(1)]^{(b)}], \;\; [R_{ij}^{(\upsilon)}(t,2)]^{(b)} = \exp[-[\lambda_{ij}^{(\upsilon)}(2)]^{(b)}],$$
$$[R_{ij}^{(\upsilon)}(t,3)]^{(b)} = \exp[-[\lambda_{ij}^{(\upsilon)}(3)]^{(b)}], \tag{12}$$

different at various operation states z_b, $b = 1,2,3,4,$ and with the intensities of departure from the reliability state subsets $\{1,2,3\}$, $\{2,3\}$, $\{3\}$, respectively

$[\lambda_{ij}^{(\upsilon)}(1)]^{(b)}$, $[\lambda_{ij}^{(\upsilon)}(2)]^{(b)}$, $[\lambda_{ij}^{(\upsilon)}(3)]^{(b)}$, $b = 1,2,3,4.$

4.1.2 Collecting data coming from exemplary system components reliability states changing processes

We arbitrarily suppose that we have in disposal data collected from the exemplary system components reliability states changing processes due to *Case*

2. Namely, we have in disposal the following data for particular components $E_{ij}^{(\upsilon)}$, $\upsilon = 1,2,$ of the exemplary system:

- the numbers of identical experiment posts $n^{(b)} = n_{ij}^{(b)}$,
- the observation times $\tau^{(b)} = \tau_{ij}^{(b)}$,
- the numbers $m^{(b)}(u) = m_{ij}^{(b)}(u)$ of components that have left the reliability state subsets $\{u, u+1, \ldots, 3\}$, $u = 1,2,3,$
- the sets $A^{(b)}(u) = A_{ij}^{(b)}(u) = \{t_i^{(b)}(u) : i = 1,2,\ldots,m^{(b)}(u)\}$ of realizations $t_i^{(b)}(u)$ $= t_{ij}^{(b)}(u)$ of the component lifetimes $T_{ij}^{(b)}(u)$ in the reliability state subsets $\{u, u+1, \ldots, 3\}$, $u = 1,2,3,$ at the operation state z_b, $b = 1,2,3,4$.

For instance, we suppose that the collected data for the component $E_{11}^{(1)}$ of the subsystem S_1 at the operation state z_1 are as follows:

$n^{(1)} = 40,\ \tau^{(1)} = 2600,\ m^{(1)}(1) = 32,$

$A^{(1)}(1) = \{$30, 44, 209, 240, 263, 265, 280, 285, 288, 289, 289, 302, 307, 350, 381,400, 430, 441, 452, 490, 490, 790, 837, 852, 856, 869, 1176,1191, 1253, 1697, 1700, 2454}, (13)

$n^{(1)} = 40,\ \tau^{(1)} = 2600,\ m^{(1)}(2) = 32,$

$A^{(1)}(2) = \{$30, 37, 37, 60, 63, 65, 69, 69, 80, 85, 88, 302, 307, 350, 352, 381, 400,430, 441, 462, 470, 490, 637, 652, 656, 669, 776, 891, 1053, 1597,1600, 2254} (14)

$n^{(1)} = 40,\ \tau^{(1)} = 2600,\ m^{(1)}(3) = 32,$

$A^{(1)}(3) = \{$20, 27, 37, 60, 63, 65, 69, 69, 80, 85, 88, 302, 307, 350, 352, 381, 400, 430, 441, 462, 470, 490, 637, 652, 656, 669, 776, 891, 1053, 1597,1600, 2054}. (15)

The first realizations $t_1^{(1)}(1) = 30,$ $t_1^{(1)}(2) = 30,$ $t_1^{(1)}(3) = 20$ and the second realizations $t_2^{(1)}(1) = 44,$ $t_2^{(1)}(2) = 37,$ $t_2^{(1)}(3) = 27$ of the component $E_{11}^{(1)}$ lifetimes $T_{11}^{(1)}(1),$ $T_{11}^{(1)}(2),$ $T_{11}^{(1)}(3)$ in the reliability state subsets $\{1,2,3\}$, $\{2,3\}$, $\{3\}$ taken from the sets $A_1^{(1)}(1),$ $A_1^{(1)}(2)$ and $A_1^{(1)}(3)$ are presented in Figure 1.

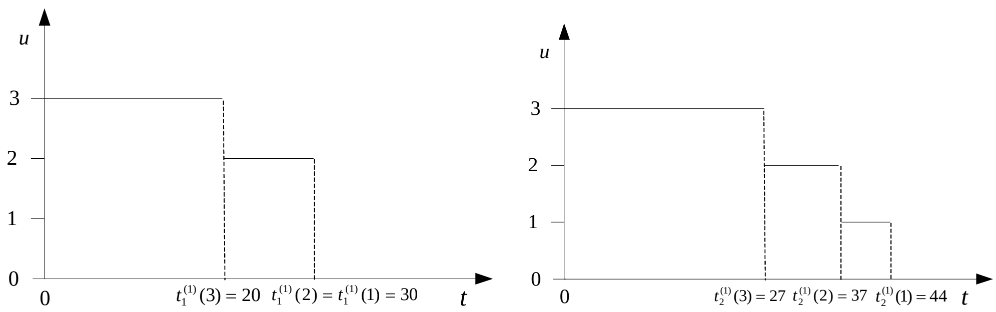

Fig. 1. The realizations of the components $E_{11}^{(1)}$ lifetimes $T_{11}^{(1)}(1)$, $T_{11}^{(1)}(2)$ and $T_{11}^{(1)}(3)$ in the reliability state subsets $\{1,2,3\}$, $\{2,3\}$ and $\{3\}$

4.1.3 Evaluating exemplary system components intensities of departures from reliability state subsets on basis of data coming from components reliability states changing processes

As by the arbitrary assumption, there are data collected from the exemplary system components reliability states changing processes, then their reliability models identification using the methods of Section 3.2.1 is possible. To identify the intensities of departures from the reliability state subsets, we can use statistical data included in Section 4.1.2 and the formula (8) in order to find the approximate values $[\hat{\lambda}_{ij}^{(\upsilon)}(1)]^{(b)}$, $[\hat{\lambda}_{ij}^{(\upsilon)}(2)]^{(b)}$ and $[\hat{\lambda}_{ij}^{(\upsilon)}(3)]^{(b)}$ of the subsystems S_υ, $\upsilon = 1,2,$ components unknown intensities $[\lambda_{ij}^{(\upsilon)}(1)]^{(b)}$, $[\lambda_{ij}^{(\upsilon)}(2)]^{(b)}$ and $[\lambda_{ij}^{(\upsilon)}(3)]^{(b)}$ of departure respectively from the reliability states subsets $\{1,2,3\}$, $\{2,3\}$, $\{3\}$, while the system is operating at the operation state z_b, $b = 1,2,3,4,$ and we can use the formula (9) to get their pessimistic evaluations. To illustrate this procedure, we find the evaluations $[\hat{\lambda}_{11}^{(1)}(1)]^{(1)}$, $[\hat{\lambda}_{11}^{(1)}(2)]^{(1)}$ and $[\hat{\lambda}_{11}^{(1)}(3)]^{(1)}$ of the intensities $[\lambda_{11}^{(1)}(1)]^{(1)}$, $[\lambda_{11}^{(1)}(2)]^{(1)}$ and $[\lambda_{11}^{(1)}(3)]^{(1)}$ of departures respectively from the reliability state subsets $\{1,2,3\}$, $\{2,3\}$ and $\{3\}$ of the component $E_{11}^{(1)}$ of the subsystem S_1, while the system is operating in the operation state z_1.
We proceed as follows:
- from data given by (13), we have

$$n^{(1)} = 40,\ \tau^{(1)} = 2600,\ m^{(1)}(1) = 32,$$
$$\sum_{i=1}^{m^{(1)}(1)} t_1^{(1)}(1) = 30 + 44 + \ldots + 1700 + 2454 = 20200,$$

then, according to (8), the evaluations $[\hat{\lambda}_{11}^{(1)}(1)]^{(1)}$ of the intensity $[\lambda_{11}^{(1)}(1)]^{(1)}$ of departure from the reliability state subset $\{1,2,3\}$ is

$$[\hat{\lambda}_{11}(1)]^{(1)} = \frac{m^{(1)}(1)}{\sum_{i=1}^{m^{(1)}(1)} t_i^{(1)}(1) + \tau^{(1)}[n^{(1)} - m^{(1)}(1)]}$$
$$= \frac{32}{20200 + 2600[40 - 32]} \cong 0.0008 \quad (16)$$

and according to (9), its pessimistic evaluation is

$$[\hat{\lambda}_{11}(1)]^{(1)} = \frac{n^{(1)}}{\sum_{i=1}^{m^{(1)}(1)} t_i^{(1)}(1) + \tau^{(1)}[n^{(1)} - m^{(1)}(1)]} = \frac{40}{20200 + 2600[40-32]} \cong 0.0010.$$

- from data given by (14), we have

$$n^{(1)} = 40, \ \tau^{(1)} = 2600, \ m^{(1)}(2) = 32,$$
$$\sum_{i=1}^{m^{(1)}(2)} t_1^{(1)}(2) = 30 + 37 + \ldots + 1600 + 2254 = 15853,$$

then, according to (8), the evaluations $[\hat{\lambda}_{11}^{(1)}(2)]^{(1)}$ of the intensity $[\lambda_{11}^{(1)}(2)]^{(1)}$ of departure from the reliability state subset $\{2,3\}$ is

$$[\hat{\lambda}_{11}(2)]^{(1)} = \frac{m^{(1)}(2)}{\sum_{i=1}^{m^{(1)}(2)} t_i^{(1)}(2) + \tau^{(1)}[n^{(1)} - m^{(1)}(2)]}$$
$$= \frac{32}{15853 + 2600[40-32]} \cong 0.0009 \quad (17)$$

and according to (9), its pessimistic evaluation is

$$[\hat{\lambda}_{11}(2)]^{(1)} = \frac{n^{(1)}}{\sum_{i=1}^{m^{(1)}(2)} t_i^{(1)}(2) + \tau^{(1)}[n^{(1)} - m^{(1)}(2)]} = \frac{40}{15853 + 2600[40-32]} \cong 0.0011.$$

- from data given by (15), we have

$$n^{(1)} = 40, \ \tau^{(1)} = 2600, \ m^{(1)}(3) = 32,$$
$$\sum_{i=1}^{m^{(1)}(3)} t_1^{(1)}(3) = 20 + 27 + \ldots + 1600 + 2054 = 15633,$$

then, according to (8), the evaluations $[\hat{\lambda}_{11}^{(1)}(3)]^{(1)}$ of the intensity $[\lambda_{11}^{(1)}(3)]^{(1)}$ of departure from the reliability state subset $\{3\}$ is

$$[\hat{\lambda}_{11}(3)]^{(1)} = \frac{m^{(1)}(3)}{\sum_{i=1}^{m^{(1)}(3)} t_i^{(1)}(3) + \tau^{(1)}[n^{(1)} - m^{(1)}(3)]}$$
$$= \frac{32}{15633 + 2600[40-32]} \cong 0.0009 \quad (18)$$

and according to (9), its pessimistic evaluation is

$$[\hat{\lambda}_{11}(3)]^{(1)} = \frac{m^{(1)}(3)}{\sum_{i=1}^{m^{(1)}(3)} t_i^{(1)}(3) + \tau^{(1)}[n^{(1)} - m^{(1)}(3)]} = \frac{40}{15633 + 2600[40-32]} \cong 0.0011.$$

This way, we may obtain the evaluations of the unknown intensities of departure for all remaining system components. Substituting the evaluations of the intensities of departures respectively into the formulae (12), we get the exponential coordinates of the exemplary system components reliability functions (11) that after successful testing can be used for the evaluation and prediction of this system reliability.

4.1.4 Identifying exemplary system multistate components conditional exponential reliability functions on basis of data coming from system components reliability states changing processes

As by the arbitrary assumption, there are data collected from the system components reliability states changing processes, then it is possible to verify the hypotheses on the exponential forms of the system components conditional reliability functions. To this end, we use the procedure given in [9]. Applying this procedure and using the statistical data from Section 4.1.2 and the results from Section 4.1.3, we may verify the hypotheses on the conditional exponential four-state exemplary system components reliability functions $[R_{ij}^{(\upsilon)}(t,\cdot)]^{(b)}$, $\upsilon = 1,2,$ $b = 1,2,3,4,$ at the particular operation states z_b, $b = 1,2,3,4.$ To do this, we need a sufficient number of realizations of the system components lifetime in the reliability state subsets. This condition is satisfied for the statistical data that are partly presented in Section 4.1.2. Considering the evaluated values of the unknown intensities of the component $E_{11}^{(1)}$ departure from the reliability state subsets given by (16)-(18), we formulate the null hypothesis H_0 concerned with the form of its multistate reliability $[R(t,\cdot)]^{(1)}$ in the following form:

H_0 : The conditional multistate reliability function of the system component $E_{11}^{(1)}$ at the operation state z_1

$$[R_{11}^{(1)}(t,\cdot)]^{(1)} = [1,\ [R_{11}^{(1)}(t,1)]^{(1)},\ [R_{11}^{(1)}(t,2)]^{(1)},\ [R_{11}^{(1)}(t,3)]^{(1)}\ ],$$

has the exponential reliability function coordinates of the forms

$[R_{11}^{(1)}(t,1)]^{(1)}$ = exp[-0.0008t], $[R_{11}^{(1)}(t,2)]^{(1)}$ = exp[-0.0009t],
$[R_{11}^{(1)}(t,3)]^{(1)}$ = exp[-0.0009t] for $t \in < 0, \infty)$.

Application of the goodness-of-fit method [9] allow to accept the above hypothesis.

4.2 Statistical identification of maritime ferry technical system components reliability

4.2.1 Defining parameters of ferry technical system components reliability models and data collection

The considered ferry technical system reliability structure changing at the various operation states and its components and their unknown safety parameters are described in [9].

At all the system operation states z_b, $b = 1,2,\ldots,18$, defined in [9], we distinguish the following five safety states 0, 1, 2, 3, 4 of the system and its components, defined in [9]. Moreover, we fix that there are possible the transitions between the components reliability states only from better to worse ones.

From the above, the ferry technical subsystems S_υ, $\upsilon = 1,2,\ldots,5$ are composed of five-state, i.e. $z = 4$, components $E_{ij}^{(\upsilon)}$, $\upsilon = 1,2,\ldots,5$ having the conditional five-state reliability functions

$$[R_{ij}^{(\upsilon)}(t,\cdot)]^{(b)} = [1,\ [R_{ij}^{(v)}(t,1)]^{(b)},[R_{ij}^{(\upsilon)}(t,2)]^{(b)},\ [R_{ij}^{(\upsilon)}(t,3)]^{(b)},\ [R_{ij}^{(\upsilon)}(t,4)]^{(b)}], \qquad (19)$$

$b = 1,2,\ldots,18,$

with the exponential coordinates

$$[R_{ij}^{(\upsilon)}(t,1)]^{(b)} = \exp[-[\lambda_{ij}^{(\upsilon)}(1)]^{(b)}],\quad [R_{ij}^{(\upsilon)}(t,2)]^{(b)} = \exp[-[\lambda_{ij}^{(\upsilon)}(2)]^{(b)}],$$
$$[R_{ij}^{(\upsilon)}(t,3)]^{(b)} = \exp[-[\lambda_{ij}^{(\upsilon)}(3)]^{(b)}],\quad [R_{ij}^{(\upsilon)}(t,4)]^{(b)} = \exp[-[\lambda_{ij}^{(\upsilon)}(4)]^{(b)}], \qquad (20)$$

and with the intensities of departure from the reliability state subsets $\{1,2,3,4\}$, $\{2,3,4\}$, $\{3,4\}$, $\{4\}$, respectively

$$[\lambda_{ij}^{(\upsilon)}(1)]^{(b)},\ [\lambda_{ij}^{(\upsilon)}(2)]^{(b)},\ [\lambda_{ij}^{(\upsilon)}(3)]^{(b)},\ [\lambda_{ij}^{(\upsilon)}(4)]^{(b)},\ b = 1,2,\ldots,18,$$

different at the particular operation states z_b, $b = 1,2,\ldots,18$, where $i = 1$ and $j = 1$ for $\upsilon = 1$, $i = 1$ and $j = 1,2,3,4$, $i = 2$ and $j = 1,2$, $i = 3,4,5,6,7$ and $j = 1$ for $\upsilon = 2$, $i = 1,2,3,4,5$ and $j = 1$ for $\upsilon = 3$, $i = 1,2$ and $j = 1$ for $\upsilon = 4$, $i = 1,2,3$ and $j = 1$ for $\upsilon = 5$.

4.2.2 Collecting data on ferry technical system components reliability models coming from experts

We have the approximate realizations

$[\hat{\mu}_{ij}^{(\upsilon)}(u)]^{(b)}$, $\upsilon = 1,2,3,4,5$ $u = 1,2,3,4,$ $b = 1,2,\ldots,18,$

of the mean values $[\mu_{ij}^{(\upsilon)}(u)]^{(b)} = E[[T_{ij}^{(\upsilon)}(u)]^{(b)}],$ $\upsilon = 1,2,3,4,5$ $u = 1,2,3,4,$ $b = 1,2,\ldots,18,$ of the conditional lifetimes $[T_{ij}^{(\upsilon)}(u)]^{(b)},$ $\upsilon = 1,2,3,4,5$ $u = 1,2,3,4,$ $b = 1,2,\ldots,18,$ in the reliability state subsets $\{u, u+1,\ldots,4\}$, $u = 1,2,3,4,$ of the components $E_{ij}^{(\upsilon)}$ of the ferry technical subsystems S_{υ}, $\upsilon = 1,2,3,4,5,$ at the particular operation states z_b, $b = 1,2,\ldots,18,$ estimated on the basis of the expert opinions. For instance, the approximate mean values $[\hat{\mu}_{11}^{(1)}(u)]^{(2)}$ of the ferry subsystem S_1 components conditional lifetimes $[T_{11}^{(1)}(u)]^{(2)}$ at the operation states z_2 are:

$$[\hat{\mu}_{11}^{(1)}(1)]^{(2)} = 30,\ [\hat{\mu}_{11}^{(1)}(2)]^{(2)} = 25,\ [\hat{\mu}_{11}^{(1)}(3)]^{(2)} = 22,\ [\hat{\mu}_{11}^{(1)}(4)]^{(2)} = 20. \quad (21)$$

4.2.3 Evaluating ferry technical system components intensities of departures from reliability state subsets on basis of data coming from experts

To evaluate approximately the parameters of multistate reliability functions of the ferry technical system components the statistical data coming from experts partly presented in Section 5.2.2 can be used. The statistical data collected in [9] and the formula (10) application yield the approximate values $[\hat{\lambda}_{ij}^{(\upsilon)}(u)]^{(b)}$ of the subsystems S_{υ}, $\upsilon = 1,2,3,4,5,$ components unknown intensities $[\lambda_{ij}^{(\upsilon)}(u)]^{(b)}$ of departure from the safety state subsets $\{1,2,3,4\}$, $\{2,3,4\}$, $\{3,4\}$, $\{4\}$, while the system is operating at the operation state z_b, $b = 1,2,\ldots,18.$ For instance, substituting into (10) the values the mean lifetimes given by (21), we obtain the approximate evaluations of the unknown intensities of departure of component $E_{11}^{(1)}$ of the subsystem S_1 from the safety state subsets $\{1,2,3,4\}$, $\{2,3,4\}$, $\{3,4\}$, $\{4\}$, while the ferry technical system is operating at the operation state z_2, that respectively amount

$$[\hat{\lambda}_{ij}^{(1)}(1)]^{(2)} = \frac{1}{[\hat{\mu}_{ij}^{(1)}(1)]^{(2)}} = \frac{1}{30} \cong 0.033,\ [\hat{\lambda}_{ij}^{(1)}(2)]^{(2)} = \frac{1}{[\hat{\mu}_{ij}^{(1)}(2)]^{(2)}} = \frac{1}{25} \cong 0.040,$$

$$[\hat{\lambda}_{ij}^{(1)}(2)]^{(2)} = \frac{1}{[\hat{\mu}_{ij}^{(1)}(2)]^{(2)}} = \frac{1}{22} \cong 0.045,\ [\hat{\lambda}_{ij}^{(1)}(2)]^{(2)} = \frac{1}{[\hat{\mu}_{ij}^{(1)}(2)]^{(2)}} = \frac{1}{20} \cong 0.050. \quad (22)$$

The evaluations of all unknown intensities of departure from the reliability state subsets $\{1,2,3,4\}$, $\{2,3,4\}$, $\{3,4\}$, $\{4\}$ of components of the ferry technical system operating at various operation states, can be obtained in the same way. Substituting the obtained evaluations of the intensities of departures respectively into the formulae (19)-(20), we get the exponential coordinates of the ferry technical system five-state components reliability functions that after arbitrary acceptance can be used for the evaluation and prediction of this system reliability characteristics.

4.2.4 Identifying ferry technical system multistate components conditional exponential relability functions on basis of data coming from experts

As there are no data collected from the ferry technical system components safety states changing processes, then it is not possible to verify the hypotheses on the exponential forms of this system components conditional reliability functions. We arbitrarily assume that these reliability functions are exponential and using the results of the previous section and the relationships (19)-(20) we fix their forms. For instance, using the evaluations (22) of the previous section and (19)-(20), we conclude that at the system operation state z_2, the subsystem S_1 component $E_{11}^{(1)}$ has the reliability function

$$[R_{11}^{(1)}(t,\cdot)]^{(2)} = [1,\ [R_{11}^{(1)}(t,1)]^{(2)},\ [R_{11}^{(1)}(t,2)]^{(2)},\ [R_{11}^{(1)}(t,3)]^{(2)},\ [R_{11}^{(1)}(t,4)]^{(2)}\ ],$$

with the exponential reliability function coordinates of the forms

$$[R_{11}^{(1)}(t,1)]^{(2)} = \exp[-0.033t],\ [R_{11}^{(1)}(t,2)]^{(2)} = \exp[-0.040t],$$
$$[R_{11}^{(1)}(t,3)]^{(2)} = \exp[-0.045t],\ [R_{11}^{(1)}(t,4)]^{(2)} = \exp[-0.05t].$$

This way arbitrarily fixed the exponential coordinates of the ferry technical system components reliability functions can be used for the evaluation and prediction of this system safety characteristics.

Conclusions

The proposed statistical methods of identification of the unknown parameters of the multistate components reliability models allow us for their practical applications in reliability evaluation and prediction of real complex multistate technical systems. These methods can be applied to estimating the reliability characteristics of various maritime, port and shipyard transportation systems oand other technical systems operating at variable conditions. The results are expected to be the basis to the reliability of complex technical systems optimization and their operation processes effectiveness and cost optimization as well. Thus, proposed methods for evaluating unknown parameter of the piece-wise exponential reliability function with a special stress on small samples and unfinished investigations are very important in everyday industrial practice.

References

1. T. Aven. Reliability evaluation of multistate systems with multistate components. IEEE Transactions on Reliability, 34, 473{479, 1985.
2. J. Collet. Some remarks on rare-event approximation. IEEE Transactions on Reliability, 45, 106{108, 1996.
3. P. Giudici and S. Figini. Applied data mining for business and industry. John Wiley & Sons Ltd, 2009.
4. S. Helvacioglu and M. Insel. Expert system applications in marine technologies. Ocean Engineering, 35, 11,12, 1067{1074, 2008.
5. O. Hryniewicz. Lifetime tests for imprecise data and fuzzy reliability requirements. Reliability and Safety Analyses under Fuzziness. Onisawa T. and Kacprzyk J., Eds., Physica Verlag, Heidelberg, 169-182, 1995.
6. K. Kołowrocki. Reliability of Large and Complex Systems. Elsevier, 2014.
7. K. Kołowrocki and J. Soszyńska. Methods and algorithms for evaluating unknown parameters of components reliability of complex technical systems. Journal of Polish Safety and Reliability Association, Summer Safety & Reliability Seminars, 4, 2, 223{230, 2009.
8. K. Kołowrocki and J. Soszyńska. Safety and risk evaluation of a ferry technical system. Journal of Polish Safety and Reliability Association, Summer Safety & Reliability Seminars, 4, 1, 159{172, 2010.
9. K. Kołowrocki and J. Soszyńska-Budny. Reliability and Safety of Complex Technical Systems and Processes: Modeling-Identification-Prediction-Optimization. Elsevier, 2014.
10. J.A. Rice. Mathematical statistics and data analysis. Duxbury. Thomson Brooks/Cole. University of California. Berkeley, 2007.
11. S. Vercellis. Data mining and optimization for decision making. John Wiley & Sons Ltd, 2009.
12. A.G. Wilson, T.L. Graves, M.S. Hamada MS et al. Advances in data combination, analysis and collection for system reliability assessment. Statistical Science, 21, 4, 4, 514{531, 2006.
13. J. Xue. On multi-state system analysis. IEEE Transactions on Reliability, 34, 329{337, 1985.
14. J. Xue and K. Yang. Dynamic reliability analysis of coherent multi-state systems. IEEE Transactions on Reliability, 4, 44, 683{688, 1995.
15. J. Xue and K. Yang. Symmetric relations in multi-state systems. IEEE Transactions on Reliability, 4, 44, 689{693, 1995.
16. K. Yu, I. Koren and Y. Guo. Generalized multistate monotone coherent systems. IEEE Transactions on Reliability, 43, 242{250, 1994.

Modelling and Statistical Identification of Complex Technical System Operation Process

Krzysztof Kolowrocki[1], and Joanna Soszynska-Budny[2]

[1] Gdynia Maritime University, Gdynia, Poland
(E-mail: katmatkk@am.gdynia.pl)
[2] Gdynia Maritime University, Gdynia, Poland
(E-mail: joannas@am.gdynia.pl)

Abstract. The paper is concerned with the methods and procedures for identification of unknown parameters of a general probability model of a complex technical system operation process and their practical application. The general multistate model of a complex technical system operation process is proposed and the procedure of identifying its basic unknown parameters is presented. There are also suggested typical distribution functions describing the system operation process conditional sojourn times at particular operation states and the procedure of identifying their unknown parameters is proposed. An illustration of the proposed methods and procedures practical application to identifying the port oil piping transportation system operation process and its characteristics prediction is presented.

1 Introduction

Modeling the complex system operation process is complicated because of the large number of the operation states, impossibility of their precise defining and exact describing the transitions between them. The changes of the operation states of the system operation process cause the changes of the system reliability structure and also the changes of its components reliability parameters. The general joint model linking the system reliability model with the model of its operation process is constructed in [1] and [2]. To apply this general model practically to the evaluation and prediction of real complex technical systems reliability it is necessary to elaborate the statistical methods concerned with determining the unknown parameters of the proposed model. Particularly, concerning the system operation process, the methods of estimating the probabilities of the initials system operation states, the probabilities of transitions between the system operation states and the distributions of the sojourn times of the system operation process at the operation states should be proposed [3]. The methods of testing the hypotheses concerned with the conditional sojourn times of the system operation process at the operation states should be also elaborated.

16th ASMDA Conference Proceedings, 30 June – 4 July 2015, Piraeus, Greece

2 Mathematical model of complex technical system operation process

We assume that the system during its operation process is taking $v, v \in N$, different operation states $z_1, z_2, \ldots, z_v$. Further, we define the system operation process $Z(t)$, $t \in <0,+\infty)$, with discrete operation states from the set $\{z_1, z_2, \ldots, z_v\}$. Moreover, we assume that the system operation process $Z(t)$ is a semi-Markov process [1]-[9], with the conditional sojourn times θ_{bl} at the operation states z_b when its next operation state is z_l, $b, l = 1,2,\ldots,v$, $b \neq l$.
Under these assumptions, the system operation process may be described by:

– the vector $[p_b(0)]_{1\times v}$ of the initial probabilities $p_b(0) = P(Z(0) = z_b)$, $b = 1,2,\ldots,v$, of the system operation process $Z(t)$ staying at the operation states at the moment $t = 0$;
– the matrix $[p_{bl}]_{v\times v}$ of probabilities p_{bl}, $b, l = 1,2,\ldots,v$, $b \neq l$, of the system operation process $Z(t)$ transitions between the operation states z_b and z_l;
– the matrix $[H_{bl}(t)]_{v\times v}$ of conditional distribution functions $H_{bl}(t) = P(\theta_{bl} < t)$, $b, l = 1,2,\ldots,v$, $b \neq l$, of the system operation process $Z(t)$ conditional sojourn times θ_{bl} at the operation states.

The mean values of the conditional sojourn times θ_{bl} of the system operation process $Z(t)$ are given by

$$M_{bl} = E[\theta_{bl}] = \int_0^\infty t dH_{bl}(t), \quad b, l = 1,2,\ldots,v, \quad b \neq l. \tag{1}$$

From the formula for total probability, it follows that the unconditional distribution functions of the sojourn times θ_b, $b = 1,2,\ldots,v$, of the system operation process $Z(t)$ at the operation states z_b, $b = 1,2,\ldots,v$, are given by [1], [2]

$$H_b(t) = \sum_{l=1}^{v} p_{bl} H_{bl}(t), \quad b = 1,2,\ldots,v. \tag{2}$$

Hence, the mean values $E[\theta_b]$ of the system operation process $Z(t)$ unconditional sojourn times θ_b, $b = 1,2,\ldots,v$, at the operation states are given by

$$M_b = E[\theta_b] = \sum_{l=1}^{v} p_{bl} M_{bl}, \quad b = 1,2,\ldots,v, \tag{3}$$

where M_{bl} are defined by the formula (1).

The limit values of the system operation process $Z(t)$ transient probabilities at the particular operation states

$$p_b(t) = P(Z(t) = z_b)\ ,\ t \in < 0,+\infty),\ \ b = 1,2,\dots,v, \tag{4}$$

are given by [1]-[9]

$$p_b \ = \lim_{t\to\infty} p_b(t) = \frac{\pi_b M_b}{\sum_{l=1}^{v} \pi_l M_l},\ \ b = 1,2,\dots,v, \tag{5}$$

where M_b, $b = 1,2,\dots,v,$ are given by (3), while the steady probabilities π_b of the vector $[\pi_b]_{1xv}$ satisfy the system of equations

$$\begin{cases} [\pi_b] = [\pi_b][p_{bl}] \\ \sum_{l=1}^{v} \pi_l = 1. \end{cases} \tag{6}$$

Other interesting characteristics of the system operation process $Z(t)$ possible to obtain are its total sojourn times $\hat{\theta}_b$ at the particular operation states z_b, $b = 1,2,\dots,v,$ during the fixed system operation time. It is well known [2], [6] that the system operation process total sojourn times $\hat{\theta}_b$ at the particular operation states z_b, for sufficiently large operation time θ, have approximately normal distributions with the expected value given by

$$\hat{M}_b = E[\hat{\theta}_b] = p_b\theta,\ \ b = 1,2,\dots,v, \tag{7}$$

where p_b are given by (5).

3 Procedure of identifying unknown parameters of complex technical system operation process

3.1 Methodology of description of the complex technical system

The description of the complex technical systems should include at least the following items:
- the system designation,
- the system operation conditions,
- the system subsystem and components.

3.2 Methodology of defining the parameters of the system operation process

To make the estimation of the unknown parameters of the system operations process the experiment delivering the necessary statistical data should be precisely planned.

Firstly, before the experiment, we should perform the following preliminary steps [3]:

i) to analyze the system operation process;

ii) to fix or to define its following general parameters:

- the number of the operation states of the system operation process v,
- the operation states of the system operation process z_1, z_2, …, z_v;

iii) to fix the possible transitions between the system operation states;

iv) to fix the set of the unknown parameters of the system operation process semi-Markov model.

3.3 Procedure of the system operation process data collection

To estimate the unknown parameters of the system operations process, during the experiment, we should collect necessary statistical data performing the following steps [3]:

i) to fix and to collect the following statistical data necessary to evaluating the probabilities of the initial states of the system operations process:

- the duration time of the experiment Θ,
- the number of the observed realizations of the system operation process $n(0)$,
- the numbers of staying of the operation process respectively in the operations states z_1, z_2, …, z_v, at the initial moment $t = 0$ of all $n(0)$ observed realizations of the system operation process $n_1(0)$, $n_2(0)$, …, $n_v(0)$, where $n_1(0)$ + $n_2(0)$ + $n_v(0)$ = $n(0)$, in the form of the vector $[n(0)]_{1xv}$;

ii) to fix and to collect the following statistical data necessary to evaluating the transient probabilities between the system operation states:

- the numbers n_{bl}, b, l = 1,2,...,v, $b \neq l$, of the transitions of the system operation process from the operation state z_b to the operation state z_l during all observed realizations of the system operation process in the form of the matrix $[n_{bl}]_{vxv}$;
- the numbers $n_b = n_{b1} + n_{b2} + \ldots + n_{bv}$, b = 1,2,...,v, of departures of the system operation process from the operation states z_b in the form of the column $[n_b]_{vx1}$;

iii) to fix and to collect the following statistical data necessary to evaluating the unknown parameters of the distributions of the conditional sojourn times of the system operation process in the particular operation states:

- the realizations θ_{bl}^k, k = 1,2, …, n_{bl}, b, l = 1,2,...,v, $b \neq l$, of the conditional sojourn times θ_{bl} of the system operations process at the operation state z_b when the next transition is to the operation state z_l during the observation time Θ.

3.4 Procedure of evaluating the unknown parameters of the system operation proces

After collecting the statistical data, it is possible to estimate the unknown parameters of the system operation process performing the following steps [3]:
i) to determine the vector $[p(0)]_{1x\nu}$ of the realizations of the probabilities $p_b(0)$, $b = 1,2,\ldots,\nu,$ of the initial states of the system operation process, according to the formula

$$p_b(0) = \frac{n_b(0)}{n(0)} \text{ for } b = 1,2,\ldots,\nu; \tag{8}$$

ii) to determine the matrix $[p_{bl}]_{\nu x\nu}$ of the realizations of the probabilities p_{bl}, $b,l = 1,2,\ldots,\nu,$ of the system operation process transitions from the operation state z_b to the operation state z_l, according to the formula

$$p_{bl} = \frac{n_{bl}}{n_b} \text{ for } b,l = 1,2,\ldots,\nu,\ b \neq l,\ p_{bb} = 0,\ b = 1,2,\ldots,\nu; \tag{9}$$

iii) to determine the following empirical characteristics of the realizations of the conditional sojourn time of the system operation process at the operation states:
- the realizations of the mean values $\bar{\theta}_{bl}$ of the conditional sojourn times θ_{bl} of the system operation process at the operation state z_b when the next transition is to the operation state z_l , according to the formula

$$\bar{\theta}_{bl} = \frac{1}{n_{bl}} \sum_{k=1}^{n_{bl}} \theta_{bl}^k,\ b,l = 1,2,\ldots,\nu,\ b \neq l \tag{10}$$

- the number $\bar{r}_{bl}$, of the disjoint intervals $I_j = < a_{bl}^j, b_{bl}^j)$, $j = 1,2,..\bar{r}_{bl}$, that include the realizations θ_{bl}^k, $k = 1,2,..n_{bl}$, of the conditional sojourn times θ_{bl}, the lengths d_{bl} and the ends a_{bl}^j, b_{bl}^j of these intervals and the numbers n_{bl}^j of the realizations θ_{bl}^k in these intervals [2].

3.5 Procedure of identifying the distributions of the system conditional sojourn times at operation states

To formulate and next to verify the hypothesis concerning the form of the distribution function $H_{bl}(t)$ of the system conditional sojourn time θ_{bl} on the basis of its realizations θ_{bl}^k, $k = 1,2,\ldots,n_{bl}$, it is necessary to proceed according to the following scheme:

- to construct and to plot the realization of the histogram of the system conditional sojourn time θ_{bl} at the operation state, defined by the following formula

$$\bar{h}_{n_{bl}}(t) = \frac{n_{bl}^{j}}{n_{bl}} \text{ for } t \in I_{j}, \tag{11}$$

- to analyze the realization of the histogram, comparing it with the graphs of the density functions $h_{bl}(t)$ of the previously distinguished distributions, to select one of them and to formulate the null hypothesis H_0, concerning the unknown form of the distribution function $H_{bl}(t)$ of the conditional sojourn time θ_{bl},
- to estimate the parameters of the selected distribution of the conditional sojourn times of the system operation process at the operation state in the way given in [2],
- to verify the hypothesis H_0 using the chi-square test [2].

3.6 Procedure of identifying the mean values of the system conditional sojourn times at operation states

After identifying the matrix $[h_{bl}(t)]_{\nu\times\nu}$ of the conditional density functions of the system conditional sojourn times θ_{bl}, $b,l = 1,2,\ldots,\nu$, $b \neq l$, in operation states corresponding to the matrix $[H_{bl}(t)]_{\nu\times\nu}$ of distribution functions, it is possible to determine the mean values of the system conditional sojourn times at the operation states either using (1) or the direct formulae for the distinguished distributions fixed in [2]. In the case when the identification of the conditional density functions of the system conditional sojourn times θ_{bl}, $b,l = 1,2,\ldots,\nu$, $b \neq l$, in operation states is not possible we may determine the approximate empirical values of the system conditional sojourn times in the operation states according to the formula (10) or use their approximate values coming from experts.

4 Statistical identification of exemplary system components reliability

4.1 Description of port oil piping transportation system operation process

The considered port oil piping transportation system is the main part of the Oil Terminal in Dębogórze that is designated for the reception from ships, the storage and sending by carriages or by cars the oil products such like petrol and oil. It is also designated for receiving from carriages or cars, the storage and loading the tankers with oil products. The considered terminal is composed of three parts *A*, *B* and *C*, linked by the piping transportation systems with the pier.

The scheme of this terminal is presented in Figure 1. The unloading of tankers is performed at the pier placed in the Port of Gdynia. The pier is connected with terminal part *A* through the transportation subsystem S_1 built of two piping lines composed of steel pipe segments with diameter of 600 mm. In the part *A* there is a supporting station fortifying tankers pumps and making possible further transport of oil by the subsystem S_2 to the terminal part *B*. The subsystem S_2 is built of two piping lines composed of steel pipe segments of the diameter 600 mm. The terminal part *B* is connected with the terminal part *C* by the subsystem S_3. The subsystem S_3 is built of one piping line composed of steel pipe segments of the diameter 500 mm and two piping lines composed of steel pipe segments of diameter 350 mm. The terminal part *C* is designated for the loading the rail cisterns with oil products and for the wagon sending to the railway station of the Port of Gdynia and further to the interior of the country.

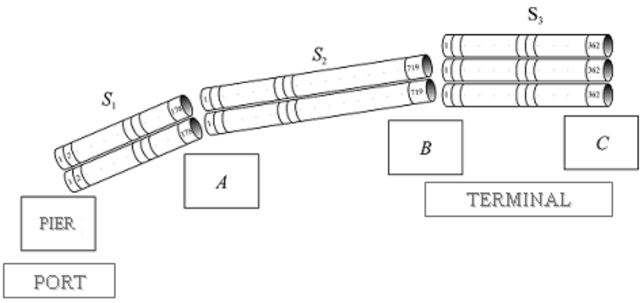

Fig. 1. The scheme of the port oil piping transportation system.

The oil pipeline system consists three subsystems:
- the subsystem S_1 composed of two identical pipelines, each composed of 178 pipe segments of length 12m and two valves,
- the subsystem S_2 composed of two identical pipelines, each composed of 717 pipe segments of length 12m and two valves,
- the subsystem S_3 composed of three different pipelines, each composed of 360 pipe segments of either 10 m or 7,5 m length and two valves.

4.2 Defining the parameters of the port oil piping transportation system operation process

Taking into account the expert opinion on the operation process of the considered port oil pipeline transportation system we fix [10]:
- the number of the pipeline system operation process states $\nu = 7$ and we distinguish the following as its seven operation states:

- an operation state z_1 – transport of one kind of medium from the terminal part B to part C using two out of three pipelines of the subsystem S_3,

- an operation state z_2 – transport of one kind of medium from the terminal part C (from carriages) to part B using one out of three pipelines of S_3,
- an operation state z_3 – transport of one kind of medium from the terminal part B through part A to pier using one out of two pipelines of the subsystem S_2 and one out of two pipelines of the subsystem S_1,
- an operation state z_4 – transport of two kinds of medium from the pier through parts A and B to part C using one out of two pipelines of the subsystem S_1, one out of two pipelines of the subsystem S_2 and two out of three pipelines of the subsystem S_3,
- an operation state z_5 – transport of one kind of medium from the pier through part A to B using one out of two pipelines of the subsystem S_1 and one out of two pipelines of the subsystem S_2,
- an operation state z_6 – transport of one kind of medium from the terminal part B to C using two out of three pipelines of the subsystem S_3, and simultaneously transport one kind of medium from the pier through part A to B using one out of two pipelines of the subsystem S_1 and one out of two pipelines of the subsystem S_2,
- an operation state z_7 – transport of one kind of medium from the terminal part B to C using one out of three pipelines of the subsystem S_3, and simultaneously transport second kind of medium from the terminal part C to B using one out of three pipelines of the subsystem S_3.

Moreover, we fix that there are possible the transitions between all system operation states. Thus, the unknown parameters of the system operation process semi-Markov model are:

- the initial probabilities $p_b(0)$, $b = 1,2,\ldots,7$, $b \neq l$, of the pipeline system operation process transients in the particular states z_b at the moment $t = 0$,
- the transition probabilities p_{bl}, $b,l = 1,2,\ldots,7$, of the pipeline system operation process from the operation state z_b into the operation state z_l,
- the distributions of the conditional sojourn times θ_{bl}, $b,l = 1,2,\ldots,7$, $b \neq l$, in the particular operation states and their mean values.

To identify all these parameters of the pipeline system operation process the collected statistical data about this process presented in [2] are needed.

4.3 The port oil piping transportation system operation process data collection

The collected statistical data necessary to evaluating the initial transient probabilities of the piping system operation process in the particular states are:

- the pipeline system operation process observation/experiment time $\Theta = 329$ days = 47 weeks,
- the number of the pipeline system operation process realizations $n(0) = 41$,

- the vector of realization $n_b(0)$ of the number of the pipeline system operation process transients in the particular operation states z_b at the initial moment t = 0

$[n_b(0)] = [14,2,0,0,9,8,8]$.

The collected statistical data necessary to evaluating the transition probabilities of the pipeline system operation process between the operation states are:
- the matrix realization n_{bl} of the numbers of pipeline system operation process transitions from the state z_b into the state z_l during the experiment time $\Theta = 329$ days

$$[n_{bl}]_{7x7} = \begin{bmatrix} 0 & 1 & 1 & 0 & 24 & 5 & 14 \\ 1 & 0 & 0 & 0 & 0 & 0 & 4 \\ 1 & 0 & 0 & 0 & 0 & 0 & 0 \\ 0 & 0 & 0 & 0 & 0 & 0 & 1 \\ 21 & 1 & 0 & 1 & 0 & 10 & 10 \\ 2 & 0 & 0 & 0 & 14 & 0 & 5 \\ 17 & 2 & 0 & 0 & 7 & 7 & 0 \end{bmatrix},$$

- the column of realization n_b of the total numbers of the pipeline system operation process transitions from the operation state z_b during the experiment time $\Theta = 329$ days

$[n_b]_{7x1} = [45,5,1,1,43,21,33]^T$.

The exemplary collected statistical data necessary to evaluating the unknown parameters of the distributions of the conditional sojourn times of the port oil pipeline transportation system operation process at the operation states the variable θ_{15} are as follows:
- the number of realizations $n_{15} = 24$,
- the realizations:

$\theta_{15}^1 = 930$, $\theta_{15}^2 = 3840$, $\theta_{15}^3 = 1290$, $\theta_{15}^4 = 480$, $\theta_{15}^5 = 5575$,
$\theta_{15}^6 = 4680$, $\theta_{15}^7 = 4350$, $\theta_{15}^8 = 2100$, $\theta_{15}^9 = 840$, $\theta_{15}^{10} = 2460$,
$\theta_{15}^{11} = 1560$, $\theta_{15}^{12} = 1020$, $\theta_{15}^{13} = 1860$, $\theta_{15}^{14} = 960$, $\theta_{15}^{15} = 930$,
$\theta_{15}^{16} = 910$, $\theta_{15}^{17} = 480$, $\theta_{15}^{18} = 410$, $\theta_{15}^{19} = 960$, $\theta_{15}^{20} = 480$,
$\theta_{15}^{21} = 1440$, $\theta_{15}^{22} = 4710$, $\theta_{15}^{23} = 540$, $\theta_{15}^{24} = 5180$.

4.4 Evaluating unknown basic parameters of port oil piping transportation system operation process

On the basis of the statistical data, using the formulae given in Section III, it is possible to evaluate
- the vector of realizations

$[p(0)]_{1x7} = [0.34, 0.05, 0, 0, 0.23, 0.19, 0.19]$

of the initial probabilities $p_b(0)$, $b = 1,2,...7,$ (8) of the pipeline system operation process transients at the operation states z_b at the moment *t* = 0,
- the matrix of realizations

$$[p_{bl}]_{7x7} = \begin{bmatrix} 0 & 0.022 & 0.022 & 0 & 0.534 & 0.111 & 0.311 \\ 0.2 & 0 & 0 & 0 & 0 & 0 & 0.8 \\ 1 & 0 & 0 & 0 & 0 & 0 & 0 \\ 0 & 0 & 0 & 0 & 0 & 0 & 1 \\ 0.488 & 0.023 & 0 & 0.023 & 0 & 0.233 & 0.233 \\ 0.095 & 0 & 0 & 0 & 0.667 & 0 & 0238 \\ 0.516 & 0.064 & 0 & 0 & 0.226 & 0.194 & 0 \end{bmatrix}, \qquad (12)$$

of the transition probabilities p_{bl}, $b,l = 1,2,...,7,$ (9) of the pipeline system operation process between the states.

4.5 Identifying distributions of conditional sojourn times at operation states of port oil piping transportation system

On the basis of statistical data, it is possible to determine the empirical characteristics of the conditional sojourn times of the pipeline system operation process at the operation states. Particularly, for θ_{15}, we have:
- the realizations of the mean value of the conditional sojourn times θ_{15}, calculated according to (10)

$$\bar{\theta}_{15} = \frac{1}{24}\sum_{k=1}^{24}\theta_{15}^{k} = 1999.4 \quad b,l = 12,...,7 \quad b \neq l,$$

- the number $\bar{r}_{15} = 5$ of the disjoint intervals that include the realizations θ_{15}^{k} of the conditional sojourn times θ_{15}, the length $d_{15} = 1291$ and the ends a_{bl}^{j}, b_{bl}^{j} of these intervals:

$$a_{15}^{1} = 0,\ b_{15}^{1} = a_{15}^{2} = 1291,\ b_{15}^{2} = a_{15}^{3} = 2582,\ b_{15}^{3} = a_{15}^{4} = 3873,$$
$$b_{15}^{4} = a_{15}^{5} = 5164,\ b_{15}^{5} = 6455, \qquad (13)$$

- the numbers n_{15}^{j} of the realizations θ_{15}^{k} in these intervals

$$n_{15}^{1} = 13,\ \ n_{15}^{2} = 5,\ n_{15}^{3} = 1,\ \ n_{15}^{4} = 4,\ \ n_{15}^{5} = 1. \tag{14}$$

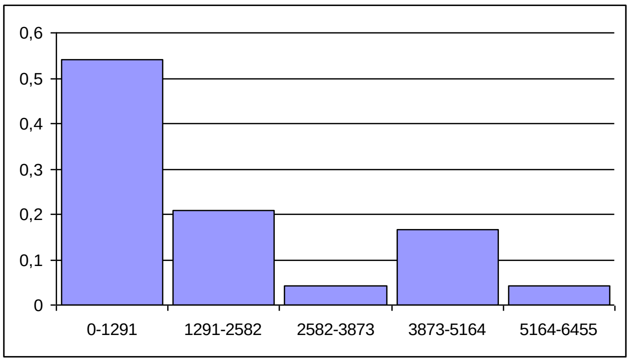

Fig. 2. Histogram of the conditional sojourn time θ_{15}

The realization of the histogram defined by (11) of the system conditional sojourn time θ_{15} constructed on the basis of the empirical results (13)-(14) is presented in Figure 2.
Using the procedure given in [2] we may verify the hypotheses on the distributions of the conditional sojourn times θ_{bl}, $b,l = 1,2,\ldots,7$, $b \neq l$, at the operation states. For instance, the conditional sojourn time θ_{15} has a chimney distribution with the density function

$$h_{15}(t) = \begin{cases} 0, & t < 0, \\ 0.0003, & 0 \le t < 1721.67, \\ 0.00007, & 1721.67 \le t < 6886.67, \\ 0, & t \ge 6886.67. \end{cases} \tag{15}$$

4.6 Identifying mean values of system conditional sojourn times at operation states of port oil piping transportation system

For the distributions identified in Section IV E, using the formula (1), we can find the mean values of the conditional sojourn times in the particular operation states. For instance, after applying (1) and (15), we get $M_{15} = 1999.4.$ In the remaining cases, because of lack of sufficiently large sets of empirical data for testing the hypotheses, it is possible to find only the approximate values of the mean values $M_{bl} = E[\theta_{bl}]$ of the conditional sojourn times at the operation states, using (10), that are as follow:

$$M_{12} = 1920,\ M_{13} = 480,\ \ M_{16} = 1250,\ M_{17} = 1129.6,$$
$$M_{21} = 9960,\ M_{27} = 810,\ M_{31} = 575,\ M_{47} = 380,$$
$$M_{51} = 874.7,\ M_{52} = 480,\ \ M_{54} = 300,\ M_{56} = 436.3,$$
$$M_{57} = 1042.5,\ M_{71} = 874.1.$$

This way, the port oil piping transportation system operation process is approximately identified and we may predict its main characteristics.

5 Port piping transportation system operation process prediction

Applying (3), the unconditional mean sojourn times of the piping system operation process at the operation states are:

$$M_1 \cong 1610.52,\ \ M_2 \cong 2640,\ \ M_3 = 575,\ \ M_4 = 380,$$
$$M_5 \cong 789.35,\ \ M_6 \cong 475.76,\ \ M_7 \cong 1497.16. \tag{16}$$

Considering (12) in the system of equations (6), we get its following solution

$$\pi_1 \cong 0.291,\ \ \pi_2 \cong 0.027,\ \ \pi_3 \cong 0.006,\ \ \pi_4 \cong 0.007,$$
$$\pi_5 \cong 0.301,\ \ \pi_6 \cong 0.144,\ \ \pi_7 \cong 0.224.$$

Hence and from (16), after applying (5), it follows that the limit values of the piping system operation process transient probabilities $p_b(t)$ at the operation states z_b are given by

$$p_1 = 0.395,\ \ p_2 = 0.060,\ \ p_3 = 0.003,\ \ p_4 = 0.002,$$
$$p_5 = 0.200,\ \ p_6 = 0.058,\ \ p_7 = 0.282.$$

Substituting the above transient probabilities at operation states into (7), we get the mean values of the port oil piping transportation system operation process total sojourn times at the particular operation states during $\theta = 1$ year:

$$\hat{M}_1 \cong 144,\ \hat{M}_2 \cong 22,\ \hat{M}_3 \cong 1,\ \ \hat{M}_4 \cong 1,\ \ \hat{M}_5 \cong 73,\ \ \hat{M}_6 \cong 21,\ \hat{M}_7 \cong 103 \text{ days.}$$

Conclusions

The way of the identification of the operation process of complex system including the formulae and procedures for estimating unknown parameters of the operation process semi-Markov and its characteristics prognosis is proposed. Its application to the port oil piping transportation system operation process unknown parameters estimation and operation characteristic prediction proves of the proposed formulae and procedures high practical importance.

The proposed statistical methods of identification of the unknown parameters of the multistate components reliability models allow us for their practical applications in reliability evaluation and prediction of real complex multistate technical systems. These methods can be applied to estimating the reliability characteristics of various maritime, port and shipyard transportation systems oand other technical systems operating at variable conditions. The results are expected to be the basis to the reliability of complex technical systems optimization and their operation processes effectiveness and cost optimization as well. Thus, proposed methods for evaluating unknown parameter of the piece-wise exponential reliability function with a special stress on small samples and unfinished investigations are very important in everyday industrial practice.

References

1. K. Kołowrocki. Reliability of Large and Complex Systems. Elsevier, 2014.
2. K. Kołowrocki and J. Soszyńska-Budny. Reliability and Safety of Complex Technical Systems and Processes: Modeling-Identification-Prediction-Optimization. Elsevier, 2011.
3. K. Kołowrocki and J. Soszyńska. Methods and algorithms for evaluating unknown parameters of components reliability of complex technical systems. Journal of Polish Safety and Reliability Association, Summer Safety & Reliability Seminars, 4, 2, 223{230, 2009.
4. F. Ferreira and A. Pacheco. Comparison of level-crossing times for Markov and semi-Markov processes. Stat & Probab Lett 77(2), 151{157, 2007.
5. P.W. Glynn and P.J. Haas. Laws of large numbers and functional central limit theorems for generalized semi-Markov processes. Stoch Model 22(2), 201{231, 2006.
6. F. Grabski, Semi-Markov Models of Systems Reliability and Operations Analysis. System Research Institute, Polish Academy of Science, (in Polish), 2002.
7. K. Kołowrocki and J. Soszyńska. A general model of industrial systems operation processes related to their environment and infrastructure. J Pol Saf Relib Assoc, Summer Safety & Reliability Seminars, vol. 2(2), 223{226, 2008.
8. N. Limnios and G. Oprisan. Semi-Markov Processes and Reliability. Birkhauser, Boston, 2005.
9. S. Mercier. Numerical bounds for semi-Markovian quantities and application to reliability. Methodol and Comput in Appl Probab. 10(2), 179{198, 2008.
10. J. Soszyńska. Reliability and risk evaluation of a port oil pipeline transportation system in variable operation conditions. Int J Pres Vessel and Pip, vol. 87, no 2-3, 81{87, 2010.

Complex System Operation Process Realizations Uniformity Testing

Krzysztof Kolowrocki[1], and Joanna Soszynska-Budny[2]

[1] Gdynia Maritime University, Gdynia, Poland
(E-mail: katmatkk@am.gdynia.pl)
[2] Gdynia Maritime University, Gdynia, Poland
(E-mail: joannas@am.gdynia.pl)

Abstract. The paper is concerned with the methods for statistical data uniformity testing and identifying unknown parameters of a general probability model of a complex technical system operation process and their practical application. The general model of a complex technical system operation process is introduced. The procedure of statistical data sets uniformity testing is proposed and applied to the empirical realizations of sojourn times at system operation states coming from realizations of a maritime ferry operation process collected during spring and winter into separate two sets of data. After that, the identification of the maritime ferry technical system operation process is performed and the identified process is applied to its operation characteristics prediction.

1 Introduction

The general joint model linking the system reliability model with the model of its operation process is constructed in [1] and [2]. To apply this general model practically to the evaluation and prediction of real complex technical systems reliability it is necessary to elaborate the statistical methods concerned with determining the unknown parameters of the proposed model. Particularly, concerning the system operation process, the methods of estimating the probabilities of the initials system operation states, the probabilities of transitions between the system operation states and the distributions of the sojourn times of the system operation process at the particular operation states should be proposed. The methods of testing the hypotheses concerned with the conditional sojourn times of the system operation process at particular operation states should be also elaborated. In the case when the statistical data are coming from different experiments, before the system operation identification, the investigation of these data uniformity is necessary.

2 Mathematical model of complex technical system operation process

16th ASMDA Conference Proceedings, 30 June – 4 July 2015, Piraeus, Greece

We assume that the system during its operation process is taking $v, v \in N$, different operation states $z_1, z_2, \dots, z_v$. Further, we define the system operation process $Z(t)$, $t \in <0,+\infty)$, with discrete operation states from the set $\{z_1, z_2, \dots, z_v\}$. Moreover, we assume that the system operation process $Z(t)$ is a semi-Markov process [1]-[9] with the conditional sojourn times θ_{bl} at the operation states z_b when its next operation state is z_l, $b, l = 1,2,\dots,v$, $b \neq l$.
Under these assumptions, the system operation process may be described by [10]:

– the vector $[p_b(0)]_{1 \times v}$ of the initial probabilities $p_b(0) = P(Z(0) = z_b)$, $b = 1,2,\dots,v$, of the system operation process $Z(t)$ staying at the operation states at the moment $t = 0$;
– the matrix $[p_{bl}]_{v \times v}$ of probabilities p_{bl}, $b, l = 1,2,\dots,v$, $b \neq l$, of the system operation process $Z(t)$ transitions between the operation states z_b and z_l;
– the matrix $[H_{bl}(t)]_{v \times v}$ of conditional distribution functions $H_{bl}(t) = P(\theta_{bl} < t)$, $b, l = 1,2,\dots,v$, $b \neq l$, of the system operation process $Z(t)$ conditional sojourn times θ_{bl} at the operation states.

The mean values of the conditional sojourn times θ_{bl} of the system operation process $Z(t)$ are given by

$$M_{bl} = E[\theta_{bl}] = \int_0^\infty t dH_{bl}(t), \ \ b, l = 1,2,\dots,v, \ \ b \neq l. \tag{1}$$

From the formula for total probability, it follows that the unconditional distribution functions of the sojourn times θ_b, $b = 1,2,\dots,v$, of the system operation process $Z(t)$ at the operation states z_b, $b = 1,2,\dots,v$, are given by [1]-[2]

$$H_b(t) \ = \ \sum_{l=1}^{v} p_{bl} H_{bl}(t), \ \ b = 1,2,\dots,v. \tag{2}$$

Hence, the mean values $E[\theta_b]$ of the system operation process $Z(t)$ unconditional sojourn times θ_b, $b = 1,2,\dots,v$, at the operation states are given by

$$M_b = E[\theta_b] \ = \ \sum_{l=1}^{v} p_{bl} M_{bl} \ , \ b = 1,2,\dots,v, \tag{3}$$

where M_{bl} are defined by the formula (1).
The limit values of the system operation process $Z(t)$ transient probabilities at the particular operation states

$$p_b(t) = P(Z(t) = z_b), \; t \in < 0, +\infty), \;\; b = 1,2,\ldots,v, \tag{4}$$

are given by [1]-[9]

$$p_b = \lim_{t \to \infty} p_b(t) = \frac{\pi_b M_b}{\sum_{l=1}^{v} \pi_l M_l}, \;\; b = 1,2,\ldots,v, \tag{5}$$

where M_b, $b = 1,2,\ldots,v$, are given by (3), while the steady probabilities π_b of the vector $[\pi_b]_{1xv}$ satisfy the system of equations

$$\begin{cases} [\pi_b] = [\pi_b][p_{bl}] \\ \sum_{l=1}^{v} \pi_l = 1. \end{cases} \tag{6}$$

Other interesting characteristics of the system operation process $Z(t)$ possible to obtain are its total sojourn times $\hat{\theta}_b$ at the particular operation states z_b, $b = 1,2,\ldots,v$, during the fixed system operation time. It is well known [2], [5] that the system operation process total sojourn times $\hat{\theta}_b$ at the particular operation states z_b, for sufficiently large operation time θ, have approximately normal distributions with the expected value given by

$$\hat{M}_b = E[\hat{\theta}_b] = p_b \theta, \;\; b = 1,2,\ldots,v, \tag{7}$$

where p_b are given by (5).

3 Procedure of experimental statistical data uniformity analysis

We consider test λ [2] that can be used for testing whether two independent samples of realizations of the conditional sojourn times at the operation states of the system operation process are drawn from the population with the same distribution. We assume that we have two independent samples of non-decreasing ordered realizations

$$\theta_{bl}^{1k}, \;\; k = 1,2,\ldots,n_{bl}^{1}, \text{ and } \theta_{bl}^{2k}, \;\; k = 1,2,\ldots,n_{bl}^{2}, \tag{8}$$

of the sojourn times θ_{bl}^{1} and θ_{bl}^{2} $b, l \in \{1,2,\ldots,v\}$, $b \neq l$, respectively composed of n_{bl}^{1} and n_{bl}^{2} realizations and we mark their empirical distribution functions by

$$H_{bl}^{1}(t) = \frac{1}{n_{bl}^{1}} \#\{k : \theta_{bl}^{1k} < t, k \in \{1,2,\ldots,n_{bl}^{1}\}\}, \quad t \geq 0, \tag{9}$$

and

$$H_{bl}^{2}(t) = \frac{1}{n_{bl}^{2}} \#\{k : \theta_{bl}^{2k} < t, k \in \{1,2,\ldots,n_{bl}^{2}\}\}. \quad t \geq 0, \tag{10}$$

Then, according to Kolmogorov-Smirnov theorem [7], the sequence of distribution functions given by the equation

$$Q_{n_1 n_2}(\lambda) = P(D_{n_1 n_2} < \frac{\lambda}{\sqrt{n}}) \tag{11}$$

defined for $\lambda > 0,$ where

$$n_1 = n_{bl}^{1}, \quad n_2 = n_{bl}^{2}, \quad n = \frac{n_1 n_2}{n_1 + n_2}, \tag{12}$$

and

$$D_{n_1 n_2} = \max_{-\infty < t < +\infty} \left| H_{bl}^{1}(t) - H_{bl}^{2}(t) \right|, \tag{13}$$

is convergent, as $n \to \infty,$ to the limit distribution function

$$Q(\lambda) = \sum_{k=-\infty}^{+\infty} (-1)^k e^{-2k^2 \lambda^2}, \quad \lambda > 0. \tag{14}$$

The distribution function $Q(\lambda)$ given by (14) is called λ distribution and its Tables of values are available.

The convergence of the sequence $Q_{n_1 n_2}(\lambda)$ to the λ distribution $Q(\lambda)$ means that for sufficiently large n_1 and n_2 we may use the following approximate formula

$$Q_{n_1 n_2}(\lambda) \cong Q(\lambda). \tag{15}$$

Hence, it follows that if we define the statistic

$$U_n = D_{n_1 n_2} \sqrt{n}, \tag{16}$$

where $D_{n_1 n_2}$ is defined by (13), then by (14) and (15), we have

$$P(U_n < u) = P(D_{n_1 n_2}\sqrt{n} < u) = P(D_{n_1 n_2} < \frac{u}{\sqrt{n}})$$

$$= Q_{n_1 n_2}(u) \cong Q(u) \text{ for } u > 0. \tag{17}$$

This result means that in order to formulate and next to verify the hypothesis that the two independent samples of the realizations of the system operation process conditional sojourn times θ_{bl}^1 and θ_{bl}^2, $b, l \in \{1,2,\ldots,\nu\}$, $b \neq l$, at the operation state z_b when the next transition is to the operation state z_l are coming from the population with the same distribution, it is necessary to proceed according to the following scheme:

- to fix the numbers of realizations n_{bl}^1 and n_{bl}^2 in the samples;
- to collect the realizations (8) of the conditional sojourn times θ_{bl}^1 and θ_{bl}^2 of the system operation process in the samples;
- to find the realization of the empirical distribution functions $H_{bl}^1(t)$ and $H_{bl}^2(t)$ defined by (9) and (10) respectively, in the following forms:

$$H_{bl}^1(t) = \begin{cases} \dfrac{n_{bl}^{11}}{n_{bl}^1} = 0, & t \leq \theta_{bl}^{11} \\ \dfrac{n_{bl}^{1k}}{n_{bl}^1}, & \theta_{bl}^{1k-1} < t \leq \theta_{bl}^{1k}, \quad k = 2,3,\ldots,n_{bl}^1, \\ \dfrac{n_{bl}^{1n_{bl}^1+1}}{n_{bl}^1} = 1, & t \geq \theta_{bl}^{1n_{bl}^1} \end{cases} \tag{18}$$

where

$$n_{bl}^{11} = 0, \; n_{bl}^{1n_{bl}^1+1} = n_{bl}^1, \tag{19}$$

and

$$n_{bl}^{1k} = \#\{j : \theta_{bl}^{1j} < \theta_{bl}^{1k}, \; j \in \{1,2,\ldots,n_{bl}^1\}\}, \; k = 2,3,\ldots,n_{bl}^1, \tag{20}$$

is the number of the sojourn time θ_{bl}^1 realizations less than its realization θ_{bl}^{1k}, $k = 2,3,\ldots,n_{bl}^1$,

$$H_{bl}^{2}(t)=\begin{cases}\frac{n_{bl}^{21}}{n_{bl}^{2}}=0, & t\le\theta_{bl}^{21}\\ \frac{n_{bl}^{2k}}{n_{bl}^{2}}, & \theta_{bl}^{2k-1}<t\le\theta_{bl}^{2k}, \quad k=2,3,\ldots,n_{bl}^{2},\\ \frac{n_{bl}^{2n_{bl}^{2}+1}}{n_{bl}^{2}}=1, & t\ge\theta_{bl}^{2n_{bl}^{2}}\end{cases} \tag{21}$$

where

$$n_{bl}^{21}=0\,,\ n_{bl}^{2n_{bl}^{2}+1}=n_{bl}^{2}, \tag{22}$$

and

$$n_{bl}^{2k}=\#\{j:\theta_{bl}^{2j}<\theta_{bl}^{2k},\ j\in\{1,2,\ldots,n_{bl}^{2}\}\},\ k=2,3,\ldots,n_{bl}^{2}, \tag{23}$$

is the number of the sojourn time θ_{bl}^{2} realizations less than its realization θ_{bl}^{2k}, $k=2,3,\ldots,n_{bl}^{2}$;

- to calculate the realization of the statistic u_n defined by (16) according to the formula

$$u_n=d_{n_{bl}^{1}n_{bl}^{2}}\sqrt{n}, \tag{24}$$

where

$$d_{n_{bl}^{1}n_{bl}^{2}}=\max\{d_{n_{bl}^{1}n_{bl}^{2}}^{1},\ d_{n_{bl}^{1}n_{bl}^{2}}^{2}\}, \tag{25}$$

$$d_{n_{bl}^{1}n_{bl}^{2}}^{1}=\max\{\left|H_{bl}^{1}(\theta_{bl}^{1k})-H_{bl}^{2}(\theta_{bl}^{1k})\right|,k\in\{1,2,\ldots,n_{bl}^{1}\}\}, \tag{26}$$

$$d_{n_{bl}^{1}n_{bl}^{2}}^{2}=\max\{\left|H_{bl}^{1}(\theta_{bl}^{2k})-H_{bl}^{2}(\theta_{bl}^{2k})\right|,k\in\{1,2,\ldots,n_{bl}^{2}\}\}, \tag{27}$$

$$n=\frac{n_{bl}^{1}n_{bl}^{2}}{n_{bl}^{1}+n_{bl}^{2}}; \tag{28}$$

- to formulate the null hypothesis H_0 in the following form:

H_0 : The samples of realizations (8) are coming from the populations with the same distributions;

- to fix the significance level α of the λ test;
- to read from the Tables of λ distribution the value $u = \lambda_0$ such that the following equality holds

$$P(U_n < u) = Q(u) = Q(\lambda_0) = 1 - \alpha; \tag{29}$$

- to determine the critical domain in the firm $(u, +\infty)$;
- to compare the obtained value u_n of the realization of the statistics U_n with the read from Tables value $u = \lambda_0$;
- to decide on the formulated hypothesis H_0 in the following way: if the value u_n does not belong to the critical domain, i.e. $u_n \le u$, then we do not reject the hypothesis H_0, otherwise if the value u_n belongs to the critical domain, i.e. $u_n > u$, then we reject the hypothesis H_0.

In the case when the null hypothesis H_0 is not rejected we may join the statistical data from the considered two separate sets into one new set of data and if there are no other sets of statistical data we proceed with the data of this new set in the way described in [8]. Otherwise, if there are other sets of statistical data we select the next one of them and perform the procedure of this section for data from this set and data from the previously formed new set. We continue this procedure up to the moment when the store of the statistical data sets is exhausted.

4 Maritime ferry operation process uniformity testing

We use the two-sample λ test described in Section III to verify the hypotheses that spring and winter realizations of the maritime ferry [7] conditional sojourn times at the operation states are from the populations with the same distribution. For instance, the procedure of testing the uniformity of data collected at the operation state z_1 when the next operation state was z_2 is as follows: For spring and winter data, the conditional sojourn times θ_{12}^1 and θ_{12}^2 have the empirical distribution functions

$$H^1{}_{12}(t)=\begin{cases}0, & t\le 15,\\ 1/42, & 15<t\le 20,\\ 2/42, & 20<t\le 25,\\ 3/42, & 25<t\le 33,\\ 4/42, & 33<t\le 35,\\ 5/42, & 35<t\le 37,\\ 6/42, & 37<t\le 40,\\ 8/42, & 40<t\le 43,\\ 9/42, & 43<t\le 44,\\ 13/42, & 44<t\le 45,\\ 14/42, & 45<t\le 46,\\ 15/42, & 46<t\le 47,\\ 17/42, & 47<t\le 50,\\ 18/42, & 50<t\le 52,\\ 19/42, & 52<t\le 53,\\ 21/42, & 53<t\le 55,\\ 22/42, & 55<t\le 57,\\ 23/42, & 57<t\le 58,\\ 24/42, & 58<t\le 59,\\ 26/42, & 59<t\le 60,\\ 27/42, & 60<t\le 61,\\ 29/42, & 61<t\le 62,\\ 30/42, & 62<t\le 63,\\ 32/42, & 63<t\le 65,\\ 33/42, & 65<t\le 67,\\ 34/42, & 67<t\le 68,\\ 35/42, & 68<t\le 71,\\ 36/42, & 71<t\le 72,\\ 38/42, & 72<t\le 75,\\ 39/42, & 75<t\le 78,\\ 40/42, & 78<t\le 84,\\ 41/42, & 84<t\le 97,\\ 1, & t>97;\end{cases}\qquad H^2{}_{12}(t)=\begin{cases}0, & t\le 12,\\ 1/40, & 12<t\le 15,\\ 3/40, & 15<t\le 18,\\ 4/40, & 18<t\le 19,\\ 5/40, & 19<t\le 20,\\ 6/40, & 20<t\le 25,\\ 7/40, & 25<t\le 33,\\ 9/40, & 33<t\le 34,\\ 10/40, & 34<t\le 36,\\ 11/40, & 36<t\le 37,\\ 14/40, & 37<t\le 40,\\ 15/40, & 40<t\le 41,\\ 16/40, & 41<t\le 44,\\ 17/40, & 44<t\le 46,\\ 18/40, & 46<t\le 48,\\ 20/40, & 48<t\le 50,\\ 21/40, & 50<t\le 53,\\ 22/40, & 53<t\le 55,\\ 23/40, & 55<t\le 57,\\ 24/40, & 57<t\le 59,\\ 25/40, & 59<t\le 60,\\ 27/40, & 60<t\le 61,\\ 28/40, & 61<t\le 62,\\ 29/40, & 62<t\le 63,\\ 30/40, & 63<t\le 65,\\ 34/40, & 65<t\le 67,\\ 35/40, & 67<t\le 69,\\ 36/40, & 69<t\le 75,\\ 38/40, & 75<t\le 80,\\ 39/40, & 80<t\le 90,\\ 1, & t>90.\end{cases}$$

The null hypothesis is H_0: The winter and spring data at the operation state z_1 when the next operation state was z_2 are from the population with the same distribution.

To verify this hypothesis we will apply the two-sample λ test at the significance level $\alpha = 0.05$. Using the above empirical distributions we form a common *Table 1* composed of all their values. In *Table 1*, the values t_k are joint together all realizations θ_{12}^{1k}, $k = 1,2,\ldots,n_{12}^1$, and θ_{12}^{2k}, $k = 1,2,\ldots,n_{12}^2$, of the conditional sojourn times θ_{12}^1 and θ_{12}^2, i.e. they are all discontinuity points of the empirical distribution function $H^1{}_{12}(t)$ and $H^2{}_{12}(t)$ were they have jumps in their values $H^1{}_{12}(t_k)$ and $H^2{}_{12}(t_k)$.

Table 1. Joint empirical distribution function

$t_k = \theta_{12}^{1k} \vee \theta_{12}^{2k}$	$H^1{}_{12}(t_k)$	$H^2{}_{12}(t_k)$	$\lvert H^1{}_{12}(t_k) - H^2{}_{12}(t_k)\rvert$
12	0	0	0
15	0	1/40	0.025
18	1/42	3/40	0.051
19	1/42	4/40	0.076
20	1/42	5/40	0.101
25	2/42	6/40	0.102
33	3/42	7/40	0.104
34	4/42	9/40	0.129
35	4/42	10/40	0.156
36	5/42	10/40	0.131
37	5/42	11/40	0.156
40	6/42	14/40	0.207
41	8/42	15/40	0.185
43	8/42	16/40	0.209
44	9/42	16/40	0.186
45	13/42	17/40	0.115
46	14/42	17/40	0.092
47	15/42	18/40	0.093
48	17/42	18/40	0.045
50	17/42	20/40	0.095
52	18/42	21/40	0.096
53	19/42	21/40	0.073
55	21/42	22/40	0.05
57	22/42	23/40	0.051
58	23/42	24/40	0.052
59	24/42	24/40	0.029
60	26/42	25/40	0.006
61	27/42	24/40	0.032
62	29/42	28/40	0.009
63	30/42	29/40	0.011
65	32/42	30/40	0.012
67	33/42	34/40	0.064
68	34/42	35/40	0.065
69	35/42	35/40	0.042
71	35/42	36/40	0.067
72	36/42	36/40	0.043
75	38/42	36/40	0.005
78	39/42	38/40	0.021

80	40/42	38/40	0.002
84	40/42	39/40	0.023
90	41/42	39/40	0.001
97	41/42	1	0.024
>97	1	1	0

Next, according to (25)-(27), from Table 1, we get

$$d_{4240} = \max_{t_k} \left| H^1{}_{12}(t_k) - H^2{}_{12}(t_k) \right| \cong 0.209,$$

and according to (28)

$$n_{12} = \frac{42 \cdot 40}{42 + 40} = 20.48.$$

Thus, the realization u_n of the statistics (24) is

$$u_n = d_{4240}\sqrt{n_{12}} = 0.209\sqrt{20.48} \cong 0.946.$$

From the table of the λ distribution for the significance level $\alpha = 0.05$, according to (29), we get the critical value $\lambda_0 = u \cong 1.36$. Since

$$u_n \cong 0.946 < u = 1.36,$$

then we do not reject the null hypothesis H_0.

After proceeding in an analogous way with data in the remaining operation states we can obtain the same conclusions that the sprig data sets and the winter data sets are from the populations with the identical distributions.

5 Statistical identification of maritime ferry operation process

To identify all parameters of the considered maritime ferry operation process [7] the statistical data coming from this process is needed. The joint statistical data that has been collected during spring and winter are:

- the number of the ship operation process states $\nu = 18$;
- the ferry operation process observation time $\Theta = 82$ days;
- the number of the ferry operation process realizations $n(0) = 82$;
- the vector of realizations of the numbers of the ferry operation process staying at the operation states z_b at the initial moment $t = 0$

$$[n_b(0)]_{1x18} = [82, 0, \ldots, 0];$$

- the matrix of realizations n_{bl} of the numbers of the ferry operation process $Z(t)$ transitions from the state z_b into the state z_l during the observation time $\Theta = 82$ days

$$[n_{bl}]_{18x18} = \begin{bmatrix} 0\,82\ \ 0\ldots 0\ \ 0 \\ 0\ \ 0\ 82\ldots 0\ \ 0 \\ \ldots \\ 0\ \ 0\ \ 0\ldots 0\,82 \\ 82\ 0\ \ 0\ldots\ 0\ \ 0 \end{bmatrix};$$

- the vector of realizations of the total numbers of the ferry operation process transitions from the operation state z_b during the observation time $\Theta = 82$ days

$[n_b]_{18x1} = [82,82,\ldots,82]^T$.
On the basis of the above statistical data it is possible to evaluate
- the vector of realizations

$[p(0)] = [1, 0, 0\ldots, 0, 0]$,

of the initial probabilities $p_b(0)$, $b = 1,2,\ldots,18,$ of the ferry operation process transients at the operation states z_b at the moment $t = 0$
- the matrix of realizations

$$[p_{bl}] = \begin{bmatrix} 0\,1\,0\ldots 0\,0 \\ 0\,0\,1\ldots 0\,0 \\ \ldots \\ 0\,0\,0\ldots 0\,1 \\ 1\,0\,0\ldots 0\,0 \end{bmatrix}, \tag{30}$$

of the transition probabilities p_{bl}, $b,l = 1,2,\ldots,18,$ of the system operation process $Z(t)$ from the operation state z_b into the operation state z_l.
The statistical data allow that applying the same methods as in [8], we may verify the hypotheses about the conditional distribution functions $H_{bl}(t)$ of the maritime ferry operation process sojourn times θ_{bl}, $b = 1,2,\ldots,17,$ $l = b+1$ and $b = 18,$ $l = 1$ at the state z_b while the next transition is to the state z_l on the base of their joint realizations θ_{bl}^j, $j = 1,2,\ldots,82.$ For instance, the conditional sojourn time θ_{12} has a normal distribution with the density function

$$h_{12}(t) = \frac{1}{18.256\sqrt{2\pi}} \exp[-\frac{(t-51.415)^2}{666.563}], \quad t \in (-\infty, \infty).$$

Next for the verified distributions, the mean values $M_{bl} = E[\theta_{bl}],\ b, l = 1,2,\ldots,18,$ $b \neq l,$ (1) of the system operation process $Z(t)$ conditional sojourn times at the operation states can be determined:

$$M_{12} = 51.415,\ M_{34} = 36.176,\ M_{67} = 37.268,\ M_{78} = 6.807,\ M_{89} = 19,$$
$$M_{910} = 46.614,\ M_{1011} = 2.829,\ M_{1112} = 4.459,\ M_{1213} = 25.091,\ M_{1314} = 513.689,$$
$$M_{1415} = 51.182,\ M_{1516} = 33.807,\ M_{181} = 18.039. \quad (31)$$

In the remaining cases, because of lack of sufficiently extensive empirical data, the mean values $M_{bl} = E[\theta_{bl}]$ can be estimated by application the formula for the empirical mean [8] giving the following their approximate values:

$$M_{23} = 2.533,\ M_{45} = 52.393,\ M_{56} = 530.188,\ M_{1617} = 4.448,\ M_{1718} = 5.473. \quad (32)$$

6 Maritime ferry operation process prediction

After applying (3) and the results (31)-(32), the unconditional mean sojourn times of the maritime ferry operation process at the particular operation states are:

$$M_1 = 51.415,\ M_2 = 2.533,\ M_3 = 36.176,\ M_4 = 52.393,\ M_5 = 530.188,$$
$$M_6 = 37.268,\ M_7 = 6.807,\ M_8 = 19,\ M_9 = 46.614,\ M_{10} = 2.829,\ M_{11} = 4.459,$$
$$M_{12} = 25.091,\ M_{13} = 513.689,\ M_{14} = 51.182,\ M_{15} = 31.807,\ M_{16} = 4.448,$$
$$M_{17} = 5.473,\ M_{18} = 18.039. \quad (33)$$

Considering (30) in the system of equations (6), we get its following solution

$$\pi_1 = \pi_2 = \pi_3 = \pi_4 = \pi_5 = \pi_6 = \pi_7 = \pi_8 = \pi_9 = \pi_{10} = \pi_{11} = \pi_{12} = \pi_{13} =$$
$$\pi_{14} = \pi_{15} = \pi_{16} = \pi_{17} = \pi_{18} \cong 0.056$$

Hence and from (33), after applying (5), it follows that the limit values of the maritime ferry operation process transient probabilities at the operation states $z_b,\ b = 1,2,\ldots,18,$ are:

$p_1 = 0.036,\ p_2 = 0.002,\ p_3 = 0.025,\ p_4 = 0.036,\ p_5 = 0.368,\ p_6 = 0.026,$
$p_7 = 0.005,\ p_8 = 0.013,\ p_9 = 0.032,\ p_{10} = 0.002,\ p_{11} = 0.003,\ p_{12} = 0.017,$
$p_{13} = 0.356,\ p_{14} = 0.036,\ p_{15} = 0.023,\ p_{16} = 0.003,\ p_{17} = 0.004,\ p_{18} = 0.013,$

Substituting the above transient probabilities at operation states into (7), we can get the mean values of the maritime ferry operation process total sojourn times at the particular operation states during $\theta = 1$ year:

$\hat{M}_1 = 13.14,\ \hat{M}_2 = 0.73,\ \hat{M}_3 = 9.13,\ \hat{M}_4 = 13.14,\ \hat{M}_5 = 134.32,\ \hat{M}_6 = 9.49,$
$\hat{M}_7 = 1.83,\ \hat{M}_8 = 4.75,\ \hat{M}_9 = 11.68,\ \hat{M}_{10} = 0.73,\ \hat{M}_{11} = 0.10,\ \hat{M}_{12} = 6.21,$
$\hat{M}_{13} = 129.94,\ \hat{M}_{14} = 13.14,\ \hat{M}_{15} = 8.40,\ \hat{M}_{16} = 1.10,\ \hat{M}_{17} = 1.46,$
$\hat{M}_{18} = 4.75$ days.

Conclusions

The way of the uniformity testing of statistical data coming from different sets of realizations of the same complex technical system operation process before joining them into one common set of data and identifying its unknown operation parameters and prognosis its operation characteristics was presented and practically applied. The results of its application to the empirical data uniformity testing and the parameters identifying of the maritime ferry operation process and the operation characteristic prognosis justifies the proposed methods and procedures practical importance in everyday practice concerned with the complex transportation systems operation processes identification and prediction.

References

1. K. Kołowrocki. Reliability of Large and Complex Systems. Elsevier, 2014.
2. K. Kolowrocki and J. Soszynska. Safety and risk evaluation of Stena Baltica ferry in variable operation conditions. Electron J Reliab Risk Anal: Theory Appl, vol. 2, No 4, 168{180, 2009.
3. F. Ferreira and A. Pacheco. Comparison of level-crossing times for Markov and semi-Markov processes. Stat & Probab Lett vol. 77(2), 151{157, 2007.
4. P.W. Glynn and P.J. Haas. Laws of large numbers and functional central limit theorems for generalized semi-Markov processes. Stoch Model vol. 22(2), 201{231, 2006.
5. F. Grabski. Semi-Markov Models of Systems Reliability and Operations Analysis. System Research Institute, Polish Academy of Science, (in Polish), 2002.
6. K. Kołowrocki and J. Soszyńska. A general model of industrial systems operation processes related to their environment and infrastructure, J Pol Saf Reliab Assoc, Summer Safety & Reliability Seminars, vol. 2(2), 223{226, 2008.

7. K. Kołowrocki and J. Soszyńska-Budny. Reliability and Safety of Complex Technical Systems and Processes: Modeling-Identification-Prediction-Optimization. Springer, 2011.
8. K. Kołowrocki and J. Soszyńska. Statistical identification of complex technical system operation process. Proc. 16th Conference of ASMDA International Conference – ASMDA 2015, Piraeus, Greece, Vol. …, …-…, 2015.
9. N. Limnios and G. Oprisan. Semi-Markov Processes and Reliability. Birkhauser, Boston, 2005.
10. K. Kołowrocki and J. Soszyńska. Methods and algorithms for evaluating unknown parameters of operation processes of complex technical systems. Proc. 3rd Summer Safety and Reliability Seminars – SSARS 2009, Gdańsk-Sopot, vol. 2, 211{222, 2009.
11. S. Mercier. Numerical bounds for semi-Markovian quantities and application to reliability. Methodol and Comput in Appl Probab. 10(2), 179{198, 2008.

Reliability of large one-dimensional nanosystems

Krzysztof Kołowrocki[1] and Mateusz Torbicki[2]

[1] Gdynia Maritime University, Morska, 81-87, Gdynia, Poland
(E-mail: k.kolowrocki@wn.am.gdynia.pl)
[2] Gdynia Maritime University, Morska, 81-87, Gdynia, Poland
(E-mail: m.torbicki@wn.am.gdynia.pl)

Abstract. Basic notions and agreements on reliability of one-dimensional nanosystems are introduced. The asymptotic approach to the one-dimensional nanosystem reliability investigation is presented and the nanosystem limit reliability function is defined. Auxiliary theorems on limit reliability functions of one-dimensional nanosystems composed of large number of independent components are formulated and the classes of limit reliability functions for a homogeneous series nanosystems are fixed. A model of a one-dimensional series nanosystem with dependent nanocomponents is created and the class of limit reliability functions identical with the class in the previous case is fixed as well. Moreover, the asymptotic approach application to reliability evaluation of an exemplary one-dimensional nanosystems with dependent nanocomponents is presented and its accuracy is discussed and illustrated.
Keywords: nanosystem, reliability, series nanosystem, asymptotic approach

1 Introduction

A nanosystem is a device which is built of individual nanocomponents and is a system engineered in a nanoscale, i.e. at least one of its dimensions is in size range of 1 to 100 nanometers, while 1 nanometer is equal to 10^{-9} meter. Thus, nanosystems are very small in the above sense but they may be composed of a huge number of nanocomponents and in this sense they can be considered as large systems. Sometimes, the exact reliability function of the nanosystem could be given by very complicated formula when a number of nanocomponents that make up a nanosystem is very large, mostly when lifetimes of nanocomponents are dependent on each other. Therefore, using the exact results of the nanosystems reliability evaluation in practical purpose is often very hard. The asymptotic approach to reliability evaluation of nanosystems can solve this problem. Namely, if we assume that the number of nanocomponents tends to infinity and find the limit reliability function of this nanosystem we can receive a simplified reliability function which approximate the exact reliability function.

16th ASMDA Conference Proceedings, 30 June – 4 July 2015, Piraeus, Greece

The results of this paper concern the asymptotic approach to the reliability evaluation of large one-dimensional nanosystems composed of independent nanocomponents and also nanosystems in which the nanocomponents are dependent of each other and the dependence between them is decreasing when the distance between them tends to infinity.

2 Reliability of one-dimensional nanosystems

We consider a one-dimensional nanosystem composed of $n \in N_{+}$, neighbouring nanocomponents $E_1, E_2, \ldots, E_n$, arranged in order shown in Figure 1.

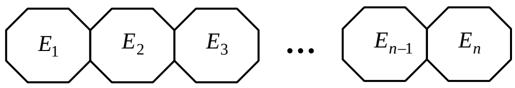

Fig. 1. A scheme of a one-dimensional nanosystem.

We denote by $s_i(t)$, $t \in < 0,+\infty)$, $i=1,\ldots,n$, a nanocomponent E_i displacement stochastic process which is equal to 0 when a nanocomponent E_i is displaced from its initial position at the moment t and otherwise it is equal to 1.
We assume that a nanocomponent E_i, $i=1,\ldots,n$, cannot be displaced from its initial position at the moment $t = 0$ and we denote by T_i a non-negative continuous random variable that reflects the time at which a nanocomponent E_i becomes displaced from its initial position. Moreover, the random variable T_i, $i=1,\ldots,n$, will also be called the time up to displacement of a nanocomponent E_i from its initial position.
According to above assumptions we can conclude that

$T_i=t_i$ if and only if $s_i(t_i^-)=1$ and $s_i(t_i)=0$ for $t_i \in (0,+\infty)$, $i=1,\ldots,n$.

Definition 2.1. A nanocomponent E_i, $i=1,\ldots,n$, is failed if it is displaced from its initial position.
We mark by

$$F_i(t)= P(T_i \le t),\ t \in (-\infty,+\infty),\ i=1,\ldots,n, \tag{2.1}$$

the distribution function of the time up to displacement T_i of the nanocomponent E_i and by

$$R_i(t)=P(T_i > t),\ t \in (-\infty,+\infty),\ i=1,\ldots,n, \tag{2.2}$$

a reliability function of a nanocomponent E_i.

Corollary 2.1. The following relationship

$$F_i(t) + R_i(t)=1,\ t \in (-\infty,+\infty),\ i=1,\ldots,n, \tag{2.3}$$

between the distribution function $F_i(t)$, $i=1,\ldots,n$, of a nanocomponent E_i and its reliability function $R_i(t)$ is satisfied.

Definition 2.2. We call a one-dimensional nanosystem homogeneous if all its nanocomponents have the same reliability function $R(t)$, $t \in (-\infty,+\infty)$, i.e.

$$R_i(t) = R(t),\ t \in (-\infty,+\infty),\ i=1,\ldots,n. \tag{2.4}$$

Moreover, we denote by $s(t)$, $t \in [0,+\infty)$, a nanosystem failure stochastic process which is equal to 0 when a nanosystem is failed at the moment t, $t \in< 0,+\infty)$, and otherwise it is equal to 1.
We assume that a nanosystem is not failed at the moment $t = 0$ and we mark by T a non-negative continuous random variable that represents the time at which a nanosystem becomes failed. Further, the random variable T will also be called the time up to nanosystem failure or the nanosystem lifetime.
According to above assumptions we can conclude that

$T = t$ if and only if $s(t^-)=1$ and $s(t)=0$ for $t \in (0,+\infty)$.

We mark by

$$\boldsymbol{F}(t)=P(T \le t),\ t \in (-\infty,+\infty), \tag{2.5}$$

the distribution function of the nanosystem lifetime and by

$$\boldsymbol{R}(t)=P(T > t),\ t \in (-\infty,+\infty), \tag{2.6}$$

the reliability function of the nanosystem.

Definition 2.3. A function given by

$$\boldsymbol{R}_n(t) = P(T > t),\ t \in (-\infty,+\infty), \tag{2.7}$$

where $T=\varphi(T_1,\ T_2,\ldots,\ T_n)$, is called the reliability function of the one-dimensional nanosystem composed of n nanocomponents E_i, $i=1,\ldots,n$. The function φ that depends on the nanosystem model and expresses the relationship between the nanosystem lifetime and its nanocomponents times up to their displacements from the initial positions is called the one-dimensional nanosystem reliability structure function.

Definition 2.4. A one-dimensional nanosystem composed of n nanocomponents E_i, $i=1,\ldots,n$, is called series if its lifetime T is given by

$$T = \min_{1\le i\le n}\{T_i\}, \tag{2.8}$$

where T_i are the nanocomponents E_i displacement times.

Definition 2.5. The nanocomponents E_i, $i=1,\ldots,n$, displacement times T_i are independent random variables if and only if

$$\boldsymbol{R}\,(t_1, t_2,\ldots, t_n) = P(T_1 > t_1,\ T_2 > t_2,\ ...,\ T_n > t_n) = \prod_{i=1,\ldots,n} R_i(t_i),$$

where $\boldsymbol{R}$ is a joint reliability function of a nanocomponents E_i and

$$R_i(t_i) = \boldsymbol{R}(-\infty,\ldots,-\infty,t_i,-\infty,\ldots,-\infty),\ i=1,\ldots,n,$$

are the reliability functions of the nanocomponents E_i defined by (2.2).

Corollary 2.2. If nanocomponents E_i, $i=1,\ldots,n$, displacement times T_i of the one-dimensional series nanosystem are independent random variables, then the reliability function of this nanosystem is given by

$$\boldsymbol{R}_n(t) = \prod_{i=1,\ldots,n} R_i(t)$$

and in the case when the nanosystem is homogeneous

$$\boldsymbol{R}_n(t) = [R(t)]^n, \tag{2.9}$$

where $R_i(t)$ and $R(t)$, $t \in (-\infty,+\infty)$, are the reliability functions of its nanocomponents defined respectively by (2.2) and (2.4).

We may also consider more complex case when the nanocomponents E_i, $i=1,\ldots,n$, displacement times T_i of the one-dimensional nanosystem are dependent random variables. A particular case of nanocomponents' dependence considered in this paper is formulated in the following assumption.

Assumption 2.1. The dependence between T_i and T_j, $i,j=1,\ldots,n$, decreases with the increasing distance $d(i,\ j)$ between them in that way they became independent when this distance tends to infinity.

3 Asymptotic approach to reliability of one-dimensional nanosystems

For convenience in the theoretical considerations we assume that the distributions of the one-dimensional nanosystem's nanocomponents' displacement times and the nanosystem lifetime T do not have to be concentrated in the interval $< 0,+\infty)$. It means that a reliability function of the nanosystem lifetime $\boldsymbol{R}(t)$, $t \in (-\infty,+\infty)$, does not have to fulfill the condition

$$\boldsymbol{R}(t) = 1 \text{ for } t \in (-\infty,0).$$

Despite that, the properties of that reliability function do not change. Hence, between a reliability function $\boldsymbol{R}(t)$, $t \in (-\infty,+\infty)$, and a distribution function $\boldsymbol{F}(t)$, $t \in (-\infty,+\infty)$, the following relationship

$$\boldsymbol{R}(t) + \boldsymbol{F}(t) = 1 \text{ for } t \in (-\infty,+\infty) \tag{3.1}$$

holds. Thus, the next corollary is clear.

Corollary 3.1. A reliability function $\boldsymbol{R}(t)$ is non-increasing, right-continuous and

$$\boldsymbol{R}(-\infty) = 1, \boldsymbol{R}(+\infty) = 0.$$

Definition 3.1. A reliability function $\boldsymbol{R}(t)$ is called degenerate if there exists $t_0 \in (-\infty,+\infty)$, such that

$$\boldsymbol{R}(t) = 1 \text{ for } t < t_0 \text{ and } \boldsymbol{R}(t) = 0 \text{ for } t \geq t_0.$$

Corollary 3.2. A function

$$\overline{\boldsymbol{R}}(t) = \exp[-\overline{V}(t)], \ t \in (-\infty,+\infty),$$

is a reliability function if and only if a function $\overline{V}(t)$ is non-negative, non-decreasing, right continuous, $\overline{V}(-\infty) = 0, \overline{V}(+\infty) = +\infty$. At the same time, $\overline{V}(t)$ can be identically equal to $+\infty$ in an interval.

Agreement 3.1. If we use symbol $\overline{V}(t)$ in next considerations we always mean a function of properties given in *Corollary 3.2* and if $\overline{V}(t)$ is identically equal to $+\infty$ we assume that $\exp[-\overline{V}(t)]=0$.

Moreover, if we say that $\overline{V}(t)$ is a non-negative, non-decreasing or non-increasing and right-continuous we consider the intervals where $\overline{V}(t) \neq +\infty$.
At the same time, we mark the set of continuity points of a reliability function $\overline{\boldsymbol{R}}(t)$ by $C_{\overline{\boldsymbol{R}}}$ and the set of continuity points of a function $\overline{V}(t)$ and points such that $\overline{V}(t) = +\infty$ by $C_{\overline{V}}$.
According to *Definition 3.1*, *Corollaries 3.1-3.2* and *Agreement 3.1*, we introduce the following definitions.

Definition 3.2. A function $\overline{V}(t)$ is called degenerate if there exists $t_0 \in (-\infty,+\infty)$ such that

$$\overline{V}(t) = 0 \text{ for } t < t_0 \text{ and } \overline{V}(t) = +\infty \text{ for } t \geq t_0.$$

Hence, the next corollary is obvious.

Corollary 3.3. A reliability function

$$\overline{\boldsymbol{R}}(t) = \exp[-\overline{V}(t)\,],\ t \in (-\infty,+\infty),$$

is degenerate if and only if a function $\overline{V}(t)$ is degenerate.
The asymptotic approach to the reliability of nanosystems depends on the investigation of limit distributions of a standardized random variable $(T - b_n)/a_n$, where T is the lifetime of a one-dimensional nanosystem and $a_n > 0, b_n \in (-\infty,+\infty)$ are suitably chosen numbers called normalizing constants. Since

$$P((T - b_n)/a_n > t) = P(T > a_n t + b_n) = \boldsymbol{R}_n(a_n t + b_n),$$

where $\boldsymbol{R}_n(t)$ is a reliability function of a one-dimensional nanosystem composed of n nanocomponents, then the next definition is natural.

Definition 3.4. A reliability function $\mathfrak{R}(t)$ is called a limit reliability function or an asymptotic reliability function of a one-dimensional nanosystem having a reliability function $\boldsymbol{R}_n(t)$ if there exist normalizing constants $a_n > 0, b_n \in (-\infty,+\infty)$ such that

$$\lim_{n\to+\infty} \boldsymbol{R}_n(a_n t + b_n) = \mathfrak{R}(t) \text{ for } t \in C_{\mathfrak{R}}.$$

Consequently, if the asymptotic reliability function $\mathfrak{R}(t)$ of a nanosystem is known, then for sufficiently large $n \in N_+$, the approximate formula

$$\boldsymbol{R}_n(t) \cong \mathfrak{R}((t-b_n)/a_n),\ t \in (-\infty,+\infty), \tag{3.2}$$

may be used instead of the nanosystem exact reliability function $\boldsymbol{R}_n(t)$.
Moreover, from the condition

$$\lim_{n\to+\infty} \boldsymbol{R}_n(a_n t + b_n) = \mathfrak{R}(t) \ \text{ for } t \in C_{\mathfrak{R}},$$

it follows that setting

$\alpha_n = a a_n,\ \beta_n = b a_n + b_n,$

where $a > 0$ and $b \in (-\infty,+\infty)$, we obtain that

$$\lim_{n\to+\infty} \boldsymbol{R}_n(\alpha_n t + \beta_n) = \lim_{n\to+\infty} \boldsymbol{R}_n(\alpha_n(at+b)+b_n) = \mathfrak{R}(at+b) \text{ for } t \in C_{\mathfrak{R}}.$$

Thus, if $\mathfrak{R}(t)$ is the limit reliability function of a nanosystem, then $\mathfrak{R}(at+b)$ with arbitrary $a > 0$ and $b \in (-\infty,+\infty)$ is its limit reliability function as well. That fact justifies the next definition.

Definition 3.5. The limit reliability functions $\mathfrak{R}_0(t)$ and $\mathfrak{R}(t)$ are said to be of the same type if there exist numbers $a > 0$ and $b \in (-\infty,+\infty)$ such that

$$\mathfrak{R}_0(t) = \mathfrak{R}(at+b) \text{ for } t \in (-\infty,+\infty).$$

Agreement 3.2. We write $x(n) = o(y(n))$, where $x(n)$ and $y(n)$ are positive functions, when $x(n)$ is of order much less than $y(n)$ in a sense

$$\lim_{n\to+\infty} \frac{x(n)}{y(n)} = 0.$$

4 Limit reliability of the one-dimensional nanosystem with independent nanocomponents

The investigations of limit reliability functions of homogeneous one-dimensional nanosystems with independent nanocomponents are based on next lemma.

Lemma 4.1. If

(i) $\overline{\mathfrak{R}}(t) = \exp[-\overline{V}(t)]$, is a non-degenerate reliability function,

(ii) $\overline{\boldsymbol{R}}_n(t)$ is the reliability function of a homogeneous series nanosystem with independent nanocomponents defined by (2.9),

(iii) $a_n > 0, b_n \in (-\infty, +\infty)$,

then

$$\lim_{n \to +\infty} \overline{\boldsymbol{R}}_n(a_n t + b_n) = \overline{\mathfrak{R}}(t) \text{ for } t \in C_{\overline{\mathfrak{R}}} \tag{4.1}$$

if and only if

$$\lim_{n \to +\infty} nF(a_n t + b_n) = \overline{V}(t) \text{ for } t \in C_{\overline{V}}. \tag{4.2}$$

Lemma 4.1 is an essential tool in finding limit reliability functions of series nanosystems. Its various proofs may be found in Barlow and Proschan[1], Gniedenko[4] and Kołowrocki[5]. It is the basis for determining classes of all possible limit reliability functions of these nanosystems as well. These class is fixed by the next theorem proved in Barlow and Proschan[1], Gniedenko[4] and Kołowrocki[5].

Theorem 4.1. The only non-degenerate limit reliability functions of the homogeneous one-dimensional series nanosystem with independent nanocomponents are:

$\overline{\mathfrak{R}}_1(t) = \exp[-(-t)^{-\alpha}]$ for $t < 0$ and $\overline{\mathfrak{R}}_1(t) = 0$ for $t \geq 0$, $\alpha > 0$,

$\overline{\mathfrak{R}}_2(t) = 1$ for $t < 0$ and $\overline{\mathfrak{R}}_2(t) = \exp[-t^{\alpha}]$ for $t \geq 0$, $\alpha > 0$,

$\overline{\mathfrak{R}}_3(t) = \exp[-\exp[t]]$ for $t \in (-\infty, \infty)$.

5 Limit reliability of the one-dimensional nanosystem with dependent nanocomponents

To investigate the limit reliability functions of one-dimensional homogeneous series nanosystems with dependent nanocomponents which satisfy *Assumption 2.1* we can use the following modification of *Lemma 4.1*.

Theorem 5.1. If the joint reliability function of the homogeneous series one-dimensional nanosystem is given by

$$\boldsymbol{R}(t_1, t_2, \ldots, t_n) = (\prod_{i=1,\ldots,n} R(t_i)) \cdot \prod_{i<j=1,\ldots,n} h(|i-j|, R(t_i), R(t_j)), \tag{5.1}$$

for $t_1, \ldots, t_n \in (-\infty, +\infty)$, where $R(t)$ is a reliability function of the nanocomponents,

$$h : N_+ \times [0,1]^2 \to [0,1], \tag{5.2}$$

$$\lim_{k \to +\infty} h(k, x, y) = 1, x, y \in [0,1], \tag{5.3}$$

$$h(k, x, y) = h(k, y, x), \ \ x, \ \ y \in [0,1], \ k \in N_+, \tag{5.4}$$

$$h(k, 1, y) = 1, \ \ y \in [0,1], \ k \in N_+, \tag{5.5}$$

$$h(\cdot, x, y) \text{ is increasing for fixed } x, y \in [0,1], \tag{5.6}$$

$$h(k, \cdot, x) \text{ is increasing for fixed } k \in N_+, x \in [0,1], \tag{5.7}$$

$\overline{\boldsymbol{\mathfrak{R}}}(t) = \exp[-\overline{V}(t)]$, $t \in (-\infty, +\infty)$, is a non-degenerate reliability function, $a_n > 0, b_n \in (-\infty, +\infty)$, and

$$h(1, R(a_n t + b_n), R(a_n t + b_n)) = 1 - o(1/n^2), \tag{5.8}$$

then

$$\lim_{n \to +\infty} \overline{\boldsymbol{R}}_n(a_n t + b_n) = \overline{\boldsymbol{\mathfrak{R}}}(t) \text{ for } t \in C_{\overline{\boldsymbol{\mathfrak{R}}}} \tag{5.9}$$

if and only if

$$\lim_{n \to +\infty} nF(a_n t + b_n) = \overline{V}(t) \ \text{ for } t \in C_{\overline{V}}. \tag{5.10}$$

Proof: Since $\boldsymbol{R}(t_1, \ldots, t_n)$, $t_i \in (-\infty, +\infty)$, $i = 1, \ldots, n$, given by (5.1), is a joint reliability function and at the same time, for all $i < j$, $i, j = 1,2,\ldots,n$, then we get

$$\lim_{|i-j| \to +\infty} P(T_i > t_i, T_j > t_j) = \lim_{|i-j| \to +\infty} \boldsymbol{R}_n(-\infty, \ldots, -\infty, t_i, -\infty, \ldots, -\infty, t_j, -\infty, \ldots, -\infty)$$

$$= \lim_{|i-j| \to +\infty} R(t_i)\, R(t_j) \cdot h(|i-j|, R(t_i), R(t_j)) = R(t_i)\, R(t_j) \text{ for } t_i, t_j \in (-\infty, +\infty).$$

Thus, the considered reliability model of the nanosystem defined by (5.1)-(5.8) fulfills *Assumption 2.1.* Obviously, from (5.1), we have

$$\overline{\boldsymbol{R}}_n(t) = R^n(t) \cdot \prod_{i=1,\dots,n} \left[h(i, R(t), R(t))\right]^{n-i}, t \in (-\infty,+\infty).$$

Then, according to conditions (5.2) and (5.6) we receive

$$\prod_{i=1,\dots,n} \left[h(1, R(t), R(t))\right]^{n-i} \le \prod_{i=1,\dots,n} \left[h(i, R(t), R(t))\right]^{n-i} \le 1, t \in (-\infty,+\infty). \tag{5.11}$$

Further, let $a_n > 0, b_n \in (-\infty,+\infty),$ be constants such that the condition (5.8) is fulfilled. Hence, from (5.8) we get

$$\lim_{n\to+\infty} \prod_{i=1,\dots,n} [h(1, R(a_n t + b_n), R(a_n t + b_n))]^{n-i} = \lim_{n\to+\infty} \prod_{i=1,\dots,n} [1 - o(1/n^2)]^{n-i} =$$

$$\lim_{n\to+\infty} [1 - o(1/n^2)]^{(n-1)n/2} = \lim_{n\to+\infty} \exp[-o(1/n^2)(n-1)n/2] = \exp[0] = 1$$

for all $t \in (-\infty,+\infty).$ Thus, according to the squeeze theorem

$$\lim_{n\to+\infty} \prod_{i=1,\dots,n} [h(i, R(a_n t + b_n), R(a_n t + b_n))]^{n-i} = 1, t \in (-\infty,+\infty). \tag{5.12}$$

Assume that

$$\lim_{n\to+\infty} nF(a_n t + b_n) = \overline{V}(t) \text{ for } a_n > 0, b_n \in (-\infty,+\infty), \ t \in C_{\overline{V}}. \tag{5.13}$$

Obviously, using (5.12) and (5.13) for $t \in C_{\overline{V}}$ we have

$$\lim_{n\to+\infty} \overline{\boldsymbol{R}}_n(a_n t + b_n) = \lim_{n\to+\infty} R^n(a_n t + b_n) = \lim_{n\to+\infty} \exp[-nF(a_n t + b_n)] =$$
$$= \exp[-\overline{V}(t)] = \overline{\boldsymbol{\mathfrak{R}}}(t).$$

Next, we assume that

$$\lim_{n\to+\infty} \overline{\boldsymbol{R}}_n(a_n t + b_n) = \overline{\boldsymbol{\mathfrak{R}}}(t) = \exp[-\overline{V}(t)] \text{ for } a_n > 0, b_n \in (-\infty,+\infty) \text{ and } t \in C_{\overline{\mathfrak{R}}}.$$

Hence, according to (5.12) for $t \in C_{\overline{V}}$ we get

$$\lim_{n\to+\infty} \overline{\boldsymbol{R}}_n(a_n t + b_n) = \lim_{n\to+\infty} R^n(a_n t + b_n) = \exp[-\overline{V}(t)],$$

and

$$\lim_{n\to+\infty} R^n(a_n t + b_n) = \lim_{n\to+\infty} \exp[-nF(a_n t + b_n)] = \exp[-\overline{V}(t)],$$

so consequently

$$\lim_{n\to+\infty} nF(a_n t + b_n) = \overline{V}(t) \text{ for } t \in C_{\overline{V}},$$

what completes the proof. □

Theorem 5.2. The only non-degenerate limit reliability functions of the homogeneous one-dimensional series system with dependent nanocomponents, which fulfill assumptions from *Theorem 5.1*, are the same as functions from *Theorem 4.1*.

Example 5.1. Consider the joint reliability function of the homogeneous one-dimensional series system with dependent nanocomponents given by (5.1) in which

$h(k, x, y) = 1 - c\cdot[(1-x)(1-y)]^{q\cdot k}$ for $c \in (0,1]$, $q > 1$, $x, y \in [0,1]$, $k \in N_+$.

It is easy to prove that function h satisfies conditions (5.2) - (5.7). Moreover, if we assume that

$$\lim_{n\to+\infty} nF(a_n t + b_n) = \overline{V}(t) \text{ for } t \in C_{\overline{V}},$$

for $a_n > 0, b_n \in (-\infty,+\infty)$, we obtain

$$\lim_{n\to+\infty} \frac{h(1, R(a_n t + b_n), R(a_n t + b_n)) - 1}{1/n^2} =$$
$$= \lim_{n\to+\infty} (1 - c[(1-R(a_n t + b_n))(1-R(a_n t + b_n))]^q - 1)\cdot n^2 =$$
$$= \lim_{n\to+\infty} -c\cdot F^{2q}(a_n t + b_n)\cdot n^2 = \lim_{n\to+\infty} -c\cdot[nF(a_n t + b_n)]^{2q}\cdot n^{2-2q} =$$

$$= -c[\bar{V}(t)]^{2q} \cdot 0 = 0, \quad c \in (0,1],\ q > 1,\ t \in C_{\bar{V}}.$$

Hence,

$h(1, R(a_n t+b_n), R(a_n t+b_n))$= 1- $o(1/n^2)$ for $n \in N_+, t \in C_{\bar{V}}$,

so the considering joint reliability function fulfills assumption from *Theorem 5.1*. Moreover, if we assume that c=1, q=1.1 and

$$R(t) = \begin{cases} 1, & t < 0 \\ \exp[-\lambda t], & t \ge 0, \end{cases}$$

where λ >0, then reliability function of that one-dimensional series nanosystem is given by

$$\boldsymbol{R}_n(t) = \begin{cases} 1, & t < 0 \\ e^{-\lambda n t} \cdot \prod_{i=1,\ldots,n} (1-[1-e^{-\lambda t}]^{2.2i})^{n-i}, & t \ge 0. \end{cases}$$

Since for a_n=1/(λn) and b_n=0, we have

$$\lim_{n \to +\infty} nF(a_n t + b_n) = 0 \ \text{ for } \ t < 0$$

and

$$\lim_{n \to +\infty} nF(a_n t + b_n) = \lim_{n \to +\infty} n(1 - e^{\frac{-\lambda t}{\lambda n}}) = \lim_{n \to +\infty} (t - no(1/n)) = t \ \text{ for } \ t \ge 0,$$

then by *Theorem 5.1* the asymptotic reliability function of this nanosystem is

$$\bar{\mathfrak{R}}_2(t) = \begin{cases} 1, & t < 0 \\ \exp[-t], & t \ge 0. \end{cases}$$

Thus, using the formula (3.2) for n=20 and λ=1/(4sec), we can approximate the nanosystem's exact reliability function $\bar{\boldsymbol{R}}_{20}(t)$ by

$$\bar{\boldsymbol{R}}_{20}(t) \cong \bar{\mathfrak{R}}_2(5t) = \begin{cases} 1, & t < 0 \\ \exp[-5t], & t \ge 0. \end{cases}$$

The expected value of this nanosystem lifetime T and its standard deviation, in seconds, calculated on the basis of the above approximate result, respectively are:

$E[T] \cong 1/5$ sec, $\sigma \cong 1/5$ sec.

The differences between the values of nanosystem exact reliability function and the values of its approximate reliability function are shown in *Table 2* and illustrated in *Figure 2*. It can be learned that they are small, what justifies using the asymptotic approximation.

t [sec]	$\overline{\boldsymbol{R}}_{20}(t)$	$\overline{\mathfrak{R}}_2((t-b_n)/a_n)$	$\overline{\boldsymbol{R}}_{20}(t)-\overline{\mathfrak{R}}_2(5t)$
0	1	1	0
0.1	0.603188	0.606531	-0.003343
0.2	0.358887	0.367879	-0.008992
0.3	0.210364	0.223130	-0.012766
0.4	0.121435	0.135335	**-0.013900**
0.5	0.069032	0.082085	-0.013053
0.6	0.038647	0.049787	-0.011140
0.7	0.021310	0.030197	-0.008888
0.8	0.011574	0.018316	-0.006741

Table 1. The differences between the values of the nanosystem exact and approximate reliability functions.

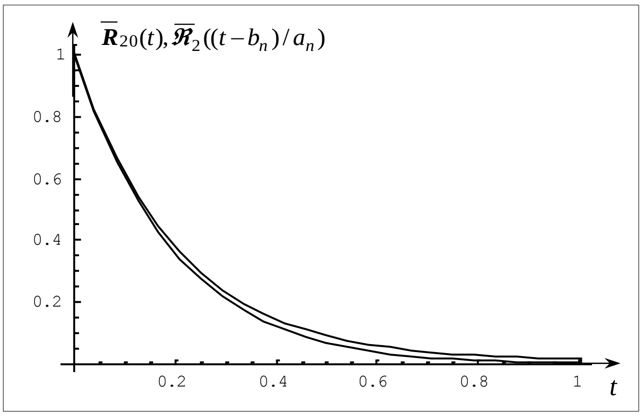

Fig. 2. The graphs of the exact and approximate reliability functions of the exemplary homogeneous series one-dimensional nanosystem.

7 Conclusion

In Ebrahimi[3], we can find investigation of the asymptotic reliability function of homogeneous series nanosystem in which times up to displacement of nanocomponents from their initial positions are dependent and this dependence decreasing with increasing the distance between nanocomponents. To create the joint reliability function of that nanosystem the copula functions are used there.
In this paper, a classes of the reliability function is fixed for the one-dimensional homogeneous series nanosystem with assumed dependencies between lifetimes of nanocomponents decreasing when the distance between nanocomponents tends to infinity. The fixed class of its possible asymptotic reliability functions is the same as the class of asymptotic reliability functions of this nanosystem when its nanocomponents are independent. Thus, we can use a theorems similar to the lemmas which allow us to investigate limit reliability function of the one-dimensional homogeneous series nanosystem with independent times up to displacement of nanocomponents to investigate the limit reliability functions of nanosystems with dependent nanocomponents. And finally, that result allows us to determinate the class of limit reliability functions of these nanosystems and to approximate their exact reliability functions when the times up to displacement of nanocomponents are dependent.

References

1. R. E. Barlow and F. Proschan. *Statistical Theory of Reliability and Life Testing. Probability Models*. Holt Rinehart and Winston, Inc., New York, 1975.
2. N. Ebrahimi. *Assessing a linear nanosystem's limiting reliability from its components*. Journal of Applied Probability 45, 879-887, 2008.
3. N. Ebrahimi. *Assessing the reliability function of nanocomponents*, Journal of Applied Probability 48, 31-42, 2011.
4. B. W. Gniedenko. Sur la distribution limite du terme maximum d'une serie aleatoire, *Annals of Mathematics* 44, 432–453, 1943.
5. K. Kołowrocki. *On a class of limit reliability functions for series-parallel and parallel-series systems*, Gdynia Maritime University Press, 1993.
6. K. Kołowrocki. *Reliability of large systems*, Encyclopedia of Quantitative Risk Analysis and Assessment, ISBN 978-0-470-03549-8, John Wiley & Sons, Vol. 4, 1466-1471, 2008.
7. K. Kołowrocki. *Reliability of Large and Complex Systems*, Elsevier, 2014.

Monte-Carlo Reliability Evaluation of Multiple Choice Forms Recognition Algorithms

Samuel Kosolapov[1]

[1] ORT Braude Academic College of Engineering, Karmiel, Israel
(E-mail: ksamuel@braude.ac.il)

Abstract. Multiple Choice Forms are widely used during exams in which respondents are asked to select the best possible answer out of the choices from the list. Scanning and analysis of Multiple Choice Forms by using standard or specialized flatbed scanner is reliable, but slow. In the frames of developed Camera Based FFS (Fast Feedback System), Multiple Choice Forms are photographed by a Smartphone's camera and obtained images are immediately processed by a Smartphone's software. Considering that in the real life form's illumination, smartphone's position and orientation are not optimal, reliable recognition of the forms require sophisticated algorithms. Additionally, barrel and pincushion image distortions of smartphone's cameras must be taken into account. In order to fasten development and reliability evaluation of the algorithms in test, Monte-Carlo simulator was developed. After setting the simulation parameters (distance from camera to the form, orientation angles of the camera relative to the form, etc.), synthetic test-image of the form is created. The algorithm in test processes this image, and statistics of recognition reliability is collected. Results of the simulation shows that reliability of Camera Based FFS is high enough to be used in the real class.
.

Keywords: Monte-Carlo simulation, Image Processing, Multiple Choice Quiz.

1 Introduction

Multiple-Choice Quiz (MCQ) is a well-known form of an exam in which students are asked to answer to the specially formulated question by selecting the best possible answer out of the choices from the list. This type of exam is known more than 100 years and is widely used in many universities (Kehoe [1]). Traditionally, during MCQ, students blacken selection boxes (or circles) on the printed on the paper MCQ Form. In the simplest form, educator checks the forms manually. Better option is to scan the forms by using flatbed scanner and process scanned images by using dedicated for that software. It is clear, that in this case students get grades after significant delay. In the frames of Camera Based FFS (Fast Feedback System), MCQ Forms are photographed by a smartphone's camera and obtained images are immediately processed by a smartphone's software (Kosolapov et al. [2], Gershikov and Kosolapov [3], Xian [4]). It is clear, that in this case student can get grades relatively fast (during minutes); hence this system can be referred as Fast Feedback System (FFS).

16th ASMDA Conference Proceedings, 30 June – 4 July 2015, Piraeus, Greece

Although the idea of using a camera instead of slow scanner looks trivial, it should be taken into account, that scanner operates in the stable environment, hence quality of the scanned images are always excellent, so that processing of the scanned images is simple and reliable. When smartphone's camera is used to photograph MCQ Form, quality of the obtained images is much worse because of lower resolution, uneven illumination and image distortions by the lens of the camera.

Operation of the camera-based FFS is similar to the operation of camera-based 2D barcode scanner. On Fig. 1 presented typical 2D barcode. The barcode has three positioning elements (markers). When smartphone' camera takes the image of the 2D barcode, size and orientation of the 2D barcode are not exact. By using positions of three marker's, parameters of the rotation and scaling can be evaluated, and image registration can be executed. Then barcode info can be easily extracted from the pattern between the markers (Hara and Watabe [5]).

Fig. 1. Exemplary 2D barcode having three positioning elements (markers)

Important difference between 2D barcodes and MCQ Forms is in their physical size: most of the MCQ Forms have standard A4 size, whereas typical 2D barcode is much smaller. Our preliminary evaluations revealed that for the camera-based FFS size A5 is preferable as logistically as technically. On Fig. 2 presented MCQ Form optimized for camera-based FFS. The form has 6 black circle markers that can be used to evaluate parameters of the transform of the MCQ Form image (photographed by smartphone' camera) to the image having predefined size, orientation and position. The form has three blocks of rectangle selection boxes having predefined sizes and positions. Lines of selection boxes labeled as T1, T2, and T3 used to encode number of the test (quiz) in the range from 000 to 999. Lines labeled ID6...ID9 encoded four last digits of the student' ID. Alternatively, number of student in the class list can be used. Lines of selection boxes labeled as Q01...Q10 are designed to collect numbers of selected answers. Up to 10 answers can be collected. This number is good enough for the concept of FFS, according to which lecturer asks questions during the lecture. Asking bigger number of questions during the lecture is impractical. MCQ Form has additional rectangular markers, which can be used to validate proper image registration.

A big number of MCQ Form variants, camera types and image recognition algorithms can be selected. It would be impractical to test all possible variants physically. Fortunately, adequate smartphone's camera models are known (Sukmock and Byongoh [6], Claus [7]).

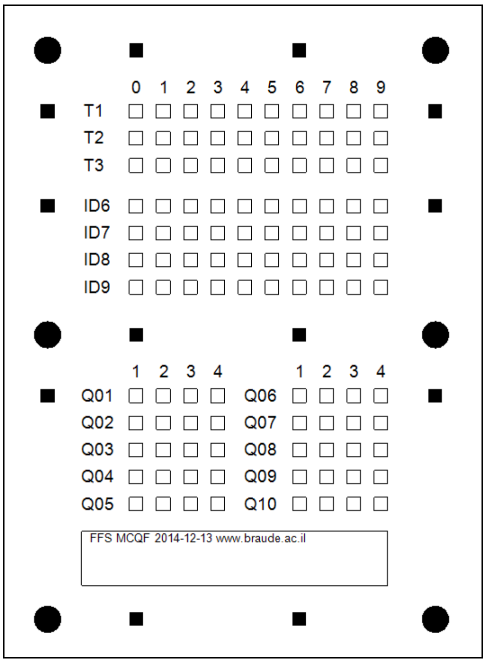

Fig. 2. MCQ Form optimized for camera-based FFS

By using proper camera model, one can create synthetic image of the MCQ Form and process it by using selected image processing algorithms. Considering big number of FFS parameters, it is clear that Monte-Carlo approach must be used to evaluate accuracy and reliability of the configuration in test.

This article describes Monte-Carlo simulator designed to evaluate accuracy and reliability of the selected image processing algorithms used to process the MCQ Form. During simulations, simplified model of the MCQ Form presented in the Fig.2 was used. Simulator was created by using MS Visual Studio 2013 C# .NET.

Section 2 describes classical pinhole camera model modified to take into account typical for smartphone's cameras image distortions.

Section 3 describes implementation of Affine Transform and Bilinear Transform used in the simulator.

Section 4 describes main blocks of the Monte-Carlo simulator and typical results obtained during simulator operation.

2 Modified Pinhole Camera Model

In order to take into account barrel and pincushion camera distortions and different MCQ Form position and orientation relative to the camera, classic pinhole camera model was modified. Fig. 3 presents Modified Pinhole Camera

Model (MPCM). Camera contains lens (1) and CCD or CMOS image sensor (2), box and camera electronics (not shown).

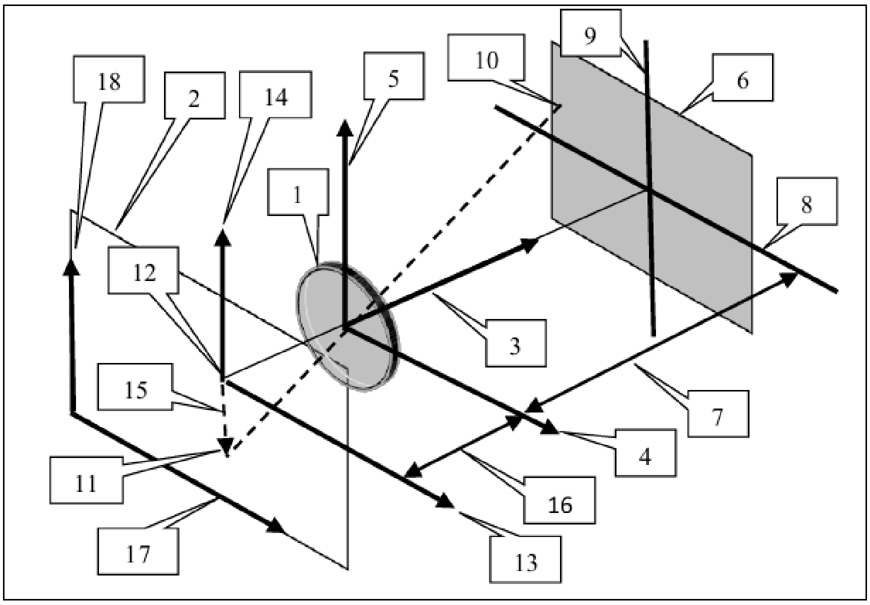

Fig. 3. Modified Pinhole Camera Model

MPCM has a number of coordinate systems. Origin of the main 3D coordinate system is at the center of the lens (1). Direction of axis "Z" (3) coincides with the direction of the main optical axis of the lens (1). Axis "X" (4) and axis "Y" (5) are normal to the axis "Z" (3). Flat MCQ Form (6) is positioned on the distance D (7) from the center of the lens (1) normally to the direction of the axis "Z" (3). Auxiliary axis " X' " (8) is parallel to the axis "X" (4), and auxiliary axis " Y' " (9) is parallel to the axis Y (5). In the frames of the classical pinhole model, 3D geometrical point P (10) (on the surface of the MCQ Form (6)) having coordinates {X,Y,Z} in the main coordinate system, is projected to the 2D point P' (11) on the CCD (2).
2D coordinates of the point P' can be presented in the auxiliary CCD 2D coordinate system {x, y}. Center (12) of this coordinate system is in the center of the CCD (2). Axis "x" (13) is parallel to the axis "X" (4) and axis "y" (14) is parallel to the axis "Y" (5). Distance of point P' (11) from the center of the CCD (12) will be referred later as "r" (15). This parameter will be used to describe barrel and pincushion distortions. Distance (16) between lens (1) and CCD (2) can be calculated by using well-known lens law in the frames of the geometrical optics. However, practically, distance D (7) between MCQ Form (6) and the lens (1) is significantly bigger than typical focal lens of the CCD camera. In this case, distance (16) is practically equals to focal length of the lens "F" and then, one can evaluate {x,y} as $x = F*X/Z$ and $y=F*Y/Z$.

Above evaluation does not takes into account typical for the simple smartphone's cameras barrel and pincushion distortions. Fig. 4 presents deformation of rectangular grid resulted from barrel and pincushion distortion.

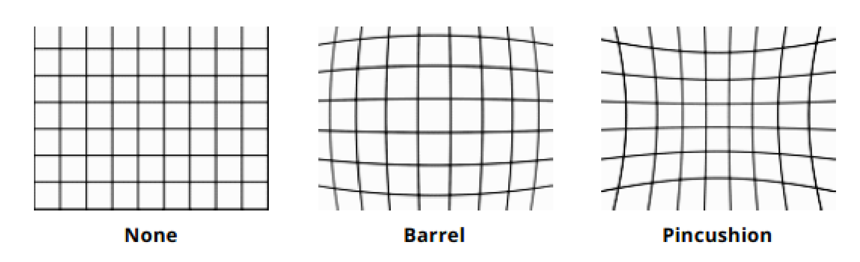

Fig. 4. Barrel and Pincushion distortions

It is clear, that during real life MCQ Form photographing, direction of the camera main optical axis (direction of "Z" axis (3)) is not normal to the surface of MCQ Form (6). In the MPCM, effect of camera rotation and translation is modelled as translation and rotation of the MCQ Form in the main XYZ coordinate system. Dashed line (19) (see Fig. 5) represents rotation of the form about "Y" axis and dashed line (20) represents rotation of the MCQ Form about "X" axis. Rotation about axis "Z" and form translation are obvious and thus not shown.

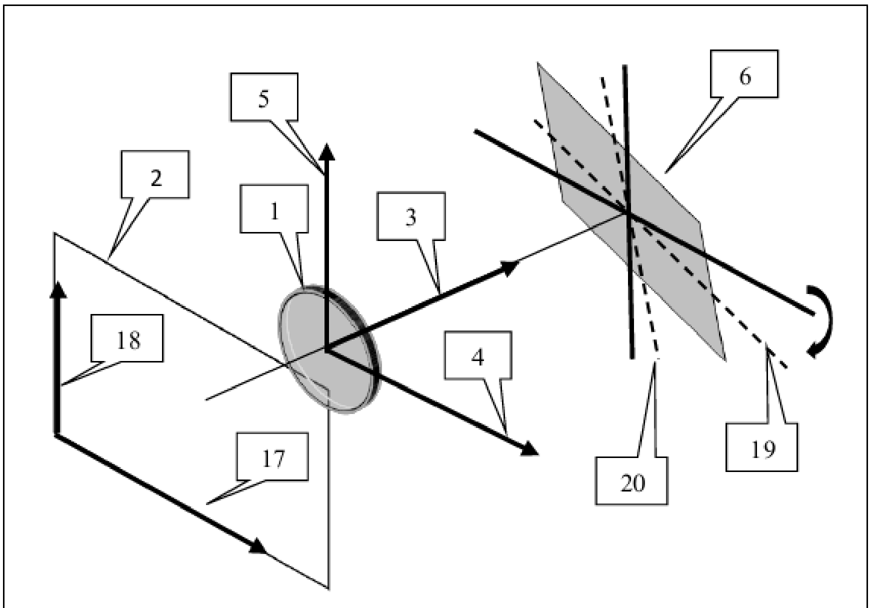

Fig. 5. Effect of camera rotation and translation.

Fig. 6 presents extract of the C# code calculating 3D coordinates {X, Y, Z} of some point P (10) positioned on the surface of the MCQ Form (6) after rotation by using 3D coordinates of this point {x,y,z} before rotation and relevant angles. Obviously, proper degrees-radians conversion must be applied.

```
// Rotate over Z
X = x * Math.Cos(angleZ) - y * Math.Sin(angleZ);
Y = x * Math.Sin(angleZ) + y * Math.Cos(angleZ);

//Rotate Over Y and X
Z =  z + z*Math.Sin( angleX ) + z*Math.Sin(angleY);

X = X * Math.Cos(angleY);
Y = Y * Math.Cos(angleX);
```

Fig. 6. C# Code used to model MCQ Form rotation

Additionally, it should be taken into account, that 2D {x,y} coordinates of the P' point (11) in the physical 2D coordinate system (12,13,14) are not convenient for the computer-based Image Processing algorithms. Computer treats image on the image sensor as a 2D array of pixels, and array indexes {row, col} must be positive. Conversion between {x,y} of the point P' (measured in mm) and correspondent pair {row, col} measured in pixels (see axis (17) representing "col" and axis (18) representing "row") is obvious, when proper image sensor parameters are known..
Fig. 7 presents the code calculating {row, col} of the point P' (11) by using {X,Y,Z} coordinates of the point P (10), after taking into account rotation and translation described above. Sizes of CCD image sensor in pixels and pixel sizes in mm are used during conversion. Barrel and pincushion distortions are modelled by using well-known radially symmetrical barrelFactor. Practical values and tolerances of the camera model parameters are described in the Section 4.

3 Affine and Bilinear Transform

Result of camera model "operation" is an image ("ccd Bitmap") which is expected to look as if it was created by real-life camera. In order to simplify operation of simulator, only four corner circle markers and one block of selection boxes were used. To further simplify simulator, only centers of markers and selection boxes were marked as black pixels on the white background of the "ccd Bitmap". This bitmap represents scaled, rotated, translated and distorted image of the simplified MCQ Form. Registration of this bitmap results in "std Bitmap". Currently, registration was executed by using two transform algorithms: Affine Transform and Bilinear Transform. In order to calculate six parameters {a11…a23} of the Affine Transform (Fig. 8), one must know positions of three markers on the source image {"ccd Bitmap") and required positions of the markers on the registered image ("std Bitmap"). Then, by solving six equations, {a11….a23} can be calculated. Formulae for the calculations of six parameters of the Affine Transform were obtained by using MAPLE 18 symbolic software.

```
public void PositionFromXYZ(
        double XinMM,
        double YinMM,
        double ZinMM,
        out double barrelFactor,
        out sPixelPosition position)
{
    double x, y, row, col, r ;

    x = +FinMM * XinMM / ZinMM;
    y = +FinMM * YinMM / ZinMM;

    row = y / (double) ccdPixelHeightInMM;
    col = x / (double) ccdPixelWidthInMM;
    r = Math.Sqrt(row * row + col * col);

    barrelFactor = 1 + K1 * r + K2 * r * r;

    row = row * barrelFactor;
    col = col * barrelFactor;

    row = row + (double) ccdSizeInPixels.Height / 2.0;
    col = col + (double) ccdSizeInPixels.Width / 2.0;

    position.Row = (int)( row + 0.5);
    position.Col = (int)( col + 0.5);
}
```

Fig. 7. C# Code of the modified pinhole camera model (MPCM)

```
stdPosition.Col = (int)
                   (  a11 * ccdPosition.Col
                    + a12 * ccdPosition.Row
                    + a13 +0.5);
stdPosition.Row = (int)
                   (  a21 * ccdPosition.Col
                    + a22 * ccdPosition.Row
                    + a23 + 0.5);
```

Fig. 8. Equations of the Affine Transform

Exemplary formula for "a12" is presented in the Fig. 9. In this example, "m1c" represents column of the center of Marker #1 in the "ccd bitmap". In the real application, this value must be extracted from the real image from camera. In this simulation, this value is obtained as result of calculations described in the Section 2. During Monte-Carlo simulation pseudo-random "error values" were added to "centers" in order to simulate error of the marker recognition algorithm. Parameter "stdM2c" means column of the center of marker #2 on the "std Bitmap". Practically, this value is set as scaled value of the marker position on the real MCQ Form. For example, if MCQ Form width was designed as 150 mm and marker #2 is positioned 15 mm from the right, then stdM2c was calculated as (150-15)*4 = 540 pixels. Determinant ("det") and other parameters of the Affine Transform were calculated in the same way.

```
a12 = (
          m1c * stdM2c
        - m1c * stdM3c
        - m2c * stdM1c
        + m2c * stdM3c
        + m3c * stdM1c
        - m3c * stdM2c) / det;
```

Fig. 9. Exemplary calculation of "a12" (Affine Transform)

Affine Transform is linear transform. Hence, it cannot compensate for the barrel and pincushion distortions. In attempt to compensate above distortions, Bilinear Transform was used in the simulations. Fig. 10 presents equations for this transform.

```
stdPosition.Col = (int)
                   (  a11
                    + a12 * ccdPosition.Col
                    + a13 * ccdPosition.Row
                    + a14 * ccdPosition.Col * ccdPosition.Row
                    + 0.5);
stdPosition.Row = (int)
                   (  a21
                    + a22 * ccdPosition.Col
                    + a23 * ccdPosition.Row
                    + a24 * ccdPosition.Col * ccdPosition.Row
                    + 0.5);
```

Fig. 10. Equations of Bilinear Transform

In order to find eight parameters of the Bilinear Transform, eight linear equations must be symbolically solved. Positions of the four markers must be known. Fig. 11 presents exemplary calculations of the parameter "a11" of the Bilinear Transform.

```
a11 = (
      m1c * m1r * m2c * m3r * stdM4c
    - m1c * m1r * m2c * m4r * stdM3c
    - m1c * m1r * m2r * m3c * stdM4c
    + m1c * m1r * m2r * m4c * stdM3c
    + m1c * m1r * m3c * m4r * stdM2c
    - m1c * m1r * m3r * m4c * stdM2c
    - m1c * m2c * m2r * m3r * stdM4c
    + m1c * m2c * m2r * m4r * stdM3c
    + m1c * m2r * m3c * m3r * stdM4c
    - m1c * m2r * m4c * m4r * stdM3c
    - m1c * m3c * m3r * m4r * stdM2c
    + m1c * m3r * m4c * m4r * stdM2c
    + m1r * m2c * m2r * m3c * stdM4c
    - m1r * m2c * m2r * m4c * stdM3c
    - m1r * m2c * m3c * m3r * stdM4c
    + m1r * m2c * m4c * m4r * stdM3c
    + m1r * m3c * m3r * m4c * stdM2c
    - m1r * m3c * m4c * m4r * stdM2c
    - m2c * m2r * m3c * m4r * stdM1c
    + m2c * m2r * m3r * m4c * stdM1c
    + m2c * m3c * m3r * m4r * stdM1c
    - m2c * m3r * m4c * m4r * stdM1c
    - m2r * m3c * m3r * m4c * stdM1c
    + m2r * m3c * m4c * m4r * stdM1c) / det;
```

Fig. 11. Exemplary calculation of "a11" (Bilinear Transform)

One can see that calculations of the Bilinear Transform parameters are time consuming, so that this transform must be used only in case when there are serious reasons to do this.

4 Monte-Carlo Simulator

Fig. 12 presents block-chart of the main blocks of Monte-Carlo simulator. Before entering Monte-Carlo loop, simulator sets parameters of the MPCM which will not be changed in the Monte-Carlo loop. Name of those parameters, units and typical values can be seen in Fig. 13. Then, simplified MCQ Form of A5 size is created. For simplicity, only positions of the centers of the four corner markers and centers of the 10x15 selection boxes are calculated. Then, Monte-Carlo loop is entered. First, pseudo-random set of variable MPCM parameters is calculated by using flat distribution. Name or those variable parameters, units, typical values and tolerances can be seen in Fig. 14.

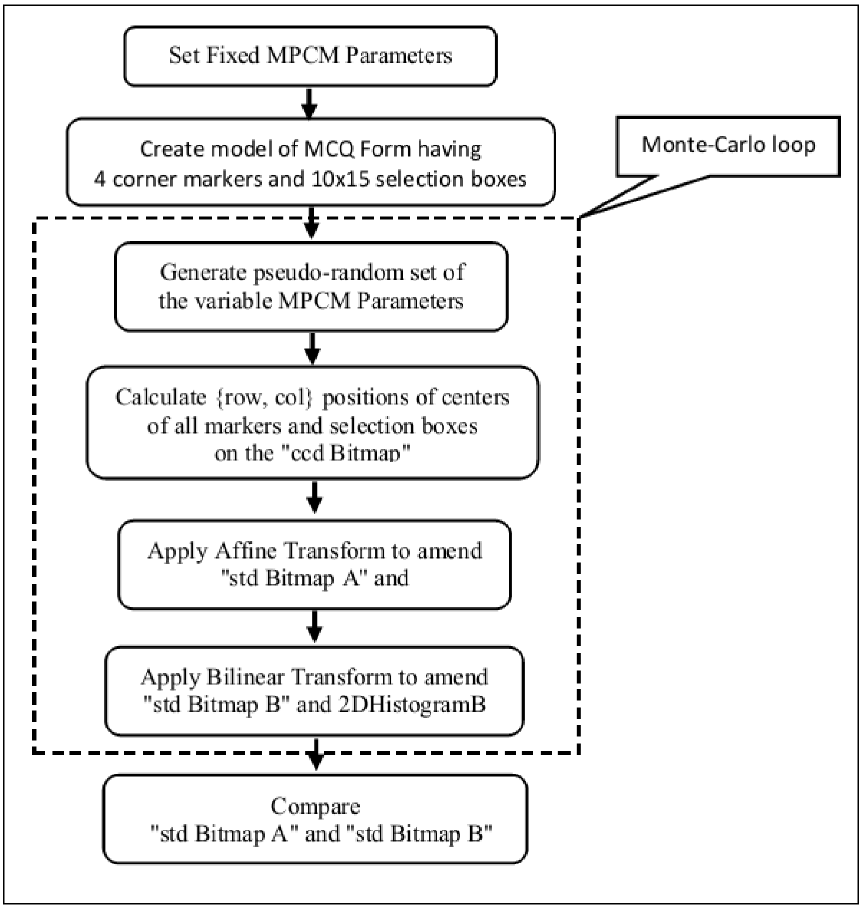

Fig. 12. Block-chart of the main steps of the Monte-Carlo simulator

Fixed Monte-Carlo Simulator Parameters			
#	**Parameter**	**Units**	**Value**
1	Camera Focal Length	mm	10
2	CCD Pixel Size	mm	0.01
3	CCD width	pixels	1224
4	CCD height	pixels	1632
5	MCQ Form width	mm	150
6	MCQ Form height	mm	200
7	Marker step	mm	15
8	STD Image width	pixels	600
9	STD Image height	pixels	800

Fig. 13. Fixed parameters of the Monte-Carlo Simulator

Variable MPCM Parameters				
#	Parameter	Units	Value	Tolerance
1	Distance to MCQ Form	mm	200	50
2	Camera X Shift	mm	0	30
3	Camera Y Shift	mm	0	30
4	Camera rotation over X axis	deg	0	10
5	Camera rotation over Y axis	deg	0	10
6	Camera rotation over Z axis	deg	0	10
7	K1	-	1E-7	5E-8
8	K2	-	1E-7	5E-8
9	Marker Recognition Algorithm Error	pixels	0	2

Fig. 14. Variable parameters of the Monte-Carlo Simulator

On the next step, simulator (by using as fixed as variable parameters of the MPCM) calculates {row, col} positions of the centers of the four corner markers and all selection boxes as described in the Section 2. Then parameters of Affine Transform and Bilinear Transform are calculated as described in the Section 3. Calculated Affine Transform parameters are used to calculate final {row, col} positions of the four markers and all the selection boxes on the "std Bitmap A". Calculated Bilinear Transform parameters are used to calculate final {row, col} positions of the four markers and all the selection boxes on the "std Bitmap B". Fig 15 presents typical "std Bitmap A" (left) and "std Bitmap B" (right).

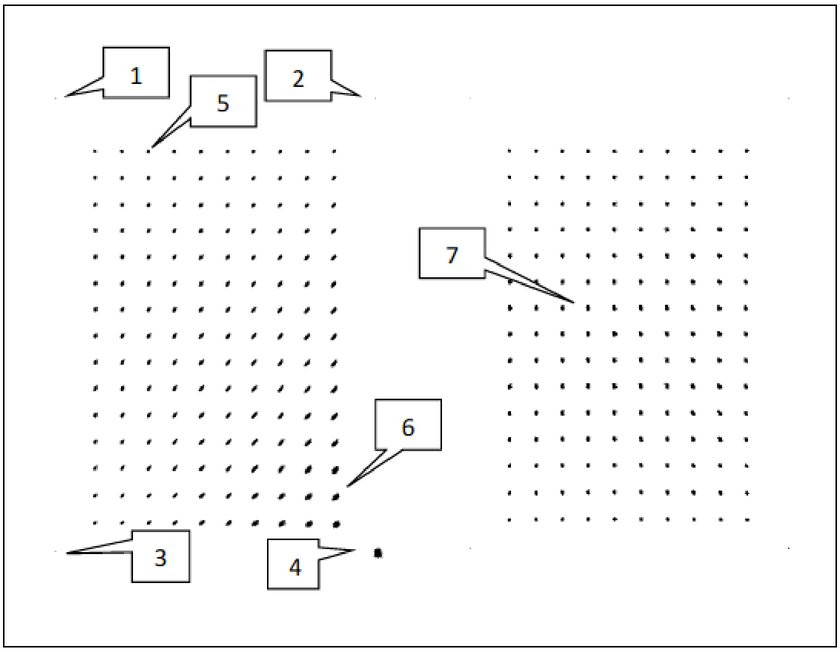

Fig. 15. Exemplary result of Monte-Carlo Simulator

In the original "std Bitmap A" one can see that centers of the three markers used in the Affine Transform resulted in a single pixel black points (those points cannot be seen in the scaled down Fig. 15 and thus, are marked as (1) (2) and (3)). This means that Affine Transform calculates final positions of those three markers correctly for any pseudo-random combination of the MPCM parameters. However, the fourth marker (which was not used by the Affine Transform) can be clearly seen as blob of black pixels (4), and not as a single black pixel. This means that Affine Transform is not adequate in this case. Size of this blob is about 15 pixels. It can be seen that centers of the selection boxes are also seen as blobs of black pixels. Typical size of the blob in the left top part of the "std Image A" (5) is about 4 pixels. Typical size of the blob in the right bottom part of the "std Image A" (6) is about 10 pixels. Size of selection box is 15 pixels. This means that Affine Transform is not exact enough to ensure reliable recognition of the "blacken" and "non-blacken" selection boxes. Bilinear Transform provides much better results. All four markers are single pixel points (not seen in the scaled down Fig, 15). It can be seen that selection boxes appears as blobs of black pixels, but of much smaller sizes. Blobs of maximal sizes are positioned at the center (7) and their size is less than five pixels. This means that Bilinear Transform has accuracy that is good enough for the reliable recognition of "blacken" and "non-blacken" selection boxes.

Additionally 2DHistogramA and 2DHistogramB were calculated. After Monte-Carlo loop is finished, 2DHistogramA and 2DHistogramB contains number of times the specific pair {row, col} was used. By using well-known statistical methods, more detailed analysis of the reliability of algorithms in test can be provided. As a result of this analysis, final number of black circle markers on the current design of MCQ Form (Fig. 2) was set to six. Then, upper and bottom parts of the MCQ Form can be processed independently: on the first stage, top and middle markers are used to calculate parameters of the "upper" Bilinear Transform. Then "T" and "ID" selection boxes are processed. On the second stage, middle and bottom markers are used to calculate parameters of the "bottom" Bilinear Transform. Then "Q" selection boxes are processed. In this case, sizes of the "blobs" are nearly twice smaller. This means that positions of the selection boxes on the "std Bitmap" does not depend on variations of the PMCM parameters in the selected ranges. In this case recognition of "blacken" and "non-blacken" selection boxes is trivial and reliable enough for the practical usage in the Camera-Based FFS.

Conclusions

Results of the operation of the developed Monte-Carlo simulator shows that design of MCQ Form having six markers used to calculate parameters of Bilinear Transform enables to create reliable implementation of the camera-based FFS.

References

1. J. Kehoe. Writing multiple-choice test items. Practical Assessments, Research & Education. 4(9), 2008.
2. S. Kosolapov, N.Sabag et al. Evaluation of Two Camera-Based Approaches for Collecting Student Feedback. Education Alternatives. Vol 12 (1173-1182), 2014.
3. E. Gershikov and S. Kosolapov. On Image Based Fast Feedback Systems for Academic Evaluation. International Journal of Signal Processing Systems. Vol 3, No 1, (19-24), 2014.
4. L. Xian. Optical Marks Recognition (OMR) Engine. Code Projects.
5. Masahiro Hara, Motoaki Watabe, et al. Optically readable two-dimensional code and method and apparatus using the same, patent US 5726435 A, 1998.
6. L. Sukmock, K. Byongoh et al. Accurate determination of distortion for smartphone cameras. Applied Optics, Vol 53, No 29, 2014.
7. D. Claus. A rational function lens distortion model for general cameras. Accurate determination of distortion for smartphone cameras. Computer Vision and Pattern Recognition 2005, CVPR. IEEE Computer Society Conference (Vol 1).

Interpretation of the evolution of the Homogeneous Markov System as the deformation of a viscoelastic medium. The 3D case.

Lubonja Kostika, George Tsaklidis

Department of Mathematics, Aristotle University of Thessaloniki, Greece

Abstract

Every attainable structure of a closed continuous time homogeneous Markov system (HMS) with *n* states is considered as a point-particle of $\boldsymbol{R}^n$. Then, the motion of an attainable structure corresponds to the motion of the respective point-particle in $\boldsymbol{R}^n$. Under the assumption that ‘‘the motion of every particle at every time point is due to its interaction with its surroundings’’, $\boldsymbol{R}^n$ (and in particular the set of the attainable structures of the HMS or alternatively of the underlying Markov chain) becomes a continuum. So the evolution of the set of the attainable structures corresponds to the motion of the continuum. For the case of a three-dimensional HMS (n=3), it is stated that the concept of the two-dimensional isotropic viscoelasticity can further be used to interpret the three-state HMS's evolution.

1. Introduction

In this paper we consider a continuous-time homogeneous Markov system (HMS) with state space S={1,2,…,n}. The members of the system could be particles, biological organisms, parts of human population, etc. Every member of the system may be in one and only one of the states 1,2,…,n at some time point t, and it can move from some state *i* to some other state j in the time interval [t,t+Δt] with transition probability $p_{ij}\cdot\Delta t$, for every $t \epsilon \boldsymbol{R}^+$. Then, every attainable structure of the continuous time HMS with *n* states and fixed size is considered as a point-particle of $\boldsymbol{R}^n$. Thus, the motion of an attainable structure corresponds to the motion of the respective point-particle in $\boldsymbol{R}^n$.

Under the assumption that the motion of every particle at every time point is due to its interaction with its surroundings, $\boldsymbol{R}^n$ is further seen as a continuum (Tsaklidis, (1998, 1999), Tsaklidis and Soldatos (2003), Maaita et al (2013)) and, hence, the evolution of the set of the HMS attainable structures corresponds to the deformation of the continuum. This turns to be a realistic assumption, since the motion of every point-particle depends entirely on its position in $\boldsymbol{R}^n$. Under these considerations, the concepts of the state of stress and the relevant stress tensor can be associated with an *n* dimensional HMS (i.e., a HMS with *n* states, abbreviated as *n*-D HMS) and, as far as the present paper is concerned these are initially detailed in an example application dealing with a 3D HMS in Tsaklidis (1999).

Then, given the rate of transition probabilities matrix of the HMS a question is raised on whether the set of the attainable structures of the continuous time HMS may be considered as a viscoelastic continuum and, in this context, it is further examined whether the deformation of such a model could explain the evolution of the HMS.

We stress here that the aforementioned HMS can generally represent any Markov system whose evolution is driven by a continuous time Markov chain (MC). So the interpretation of such a system as a continuum, can be equivalently be considered as the continuum viewpoint of the relevant Markov chain itself. In other words the material behavior can be assigned to the HMS or alternatively to the MC which “generates” the HMS. This

16th ASMDA Conference Proceedings, 30 June – 4 July 2015, Piraeus, Greece

consideration refers to any homogeneous Markov system and not only to the model of the special type examined in Tsaklidis (1998, 1999), Tsaklidis and Soldatos (2003), Maaita et al (2013), denoted as HMS. By taking the above consideration into account we will retain the same symbolism, HMS, by which we will generally refer to any homogeneous Markov system driven ("generated") by a continuous time MC and not only to the Markov model of the partcular type examined in Tsaklidis (1998, 1999), Tsaklidis and Soldatos (2003), Maaita et al (2013).

The study follows the steps of the methodology presented in Maaita et al (2013), in which the 3D HMS was successfully interpreted, through the deformation of a linearly elastic medium. It was further mentioned that the evolution of an n-D HMS may be interpreted through the deformation of an *n-1* dimensional, anisotropic, linearly elastic solid. Apart from the above concepts, the present project develops further the 3D HMS example application, and the evolution of the HMS is interpreted through the deformation of a 2D viscoelastic continuum, i.e., the Kelvin-Voigt model (Christensen (1982), Mase (1970)).

The Kelvin-Voigt model can interpret the motion of a continuum which exhibits a elastic and also viscous behavior, that are common and characteristic properties for real continua. This model consists of a combination of a spring and a dashpot, coupled in parallel, as shown in Figure 1. The elastic behavior of the spring is described by Hooke's law while the viscous behavior of the dashpot is described by the Newton's law for viscous fluids. If any of the two properties is not considered, the model is reduced either to the elastic or to the Newtonian (or non-Newtonian) fluid model. The increased number of dimensions, as compared with the number of dimensions considered in Tsaklidis and Soldatos (2003), results in an increase of the number of the Partial Differential Equations (PDEs) describing the motion of the present HMS and, consequently, it complicates the associated calculations. Using the field equations of viscoelasticity, an explicit form of the stress tensor involved can still be evaluated analytically.

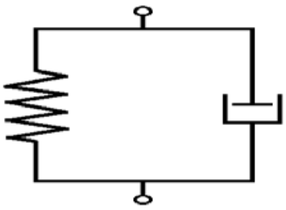

Figure 1. The Kelvin-Voight model

It is therefore concluded that, under certain assumptions, the evolution of a 3D HMS may successfully be interpreted through the deformation of a 2D viscoelastic Kelvin-Voigt model. The interpretation of the evolution of HMSs through the deformation laws of viscoelastic continua gives rise to further fruitful thoughts regarding the manner in which well-known concepts and features met in classical and finite viscoelasticity (e.g., anisotropy, strain energy) may be associated to HMSs and be exploited appropriately. For example, the adoption of anisotropy could imply the existence of special directions or regions on the field of the attainable structures, where the system evolves in the same or different ways. This would lead to conclusions regarding the interpretation and the special features of the HMS. Therefore, if the HMS represents a system of biological sea organisms, anisotropy could indicate different environmental behavior due to sea streams or neighborhood with bacteria colonies, etc.

2. The continuous time HMS as a viscoelastic medium.

For a continuous time HMS it is assumed that the transition probability of moving from some state *i* to *j* in the time interval $[t, t+\Delta t]$ is given by the relation

$$p_{ij}(t, t+\Delta t) = q_{ij}\Delta t + o(\Delta t), \tag{1}$$

where $q_{ij} \geq 0$ is the rate of transition from *i* to *j* and the $o(\Delta t)$ denotes a quantity that becomes negligible when compared to *Δt* as $\Delta t \to 0$, $\underset{\Delta t \to 0}{\lim}(o(\Delta t)/\Delta t) = 0$. In the general case the non-homogenous Markov systems' transitions intensities q_{ij} may be time depended.

In what follows, let $\mathbf{x(t)} = (x_i(t))_{i\in S}$ denote the n×1 state vector of the HMS, the *i-th* component of which is the probability of a systems' member to possess state *i* at time *t*. Then the probabilistic law for the transitions given in (1) leads to the equation

$$x_j(t+\Delta t) = x_i(t)\left(q_{ij}\Delta t + \delta_{ij}\right) + o(\Delta t), \tag{2}$$

where repeated indices denote summation over their range and δ_{ij} stands for the Kronecker delta, having the value 1 when *i=j* and 0 otherwise. From (2) the Kolmogorov equation can be derived, i.e.,

$$\dot{\mathbf{x}}^T(\mathrm{t}) = \mathbf{x}^T(t)\cdot\mathbf{Q}, \tag{3}$$

where $\dot{\mathbf{x}}\mathbf{(t)}$ denotes the derivative of the vector **x(t)** with respect to $t, \mathbf{Q} = \left(q_{ij}\right)_{i,j\in S}$ is the matrix of transitions intensities and the superscript ^{T} denotes transposition of the respective vector (or matrix).

Equation (3) represents the motion of a stochastic structure in $\boldsymbol{R}^n$. If we consider every structure of the HMS moving according to (3) as a "particle" of the n-dimensional space we can assign material behavior to $\boldsymbol{R}^n$. From (3) we conclude that the velocity $\dot{\mathbf{x}}\mathbf{(t)}$ of each particle depends only on its position, **x(t)**. So we can assume that the motion of every particle, at every time *t*, depends on the interaction of that particle with its surroundings (the infinitesimal continuum around the point **x(t)**). Thus, the HMS may be considered as a continuum moving according to Eq. (3).

Now, from (3) we get that the trajectory of every initial HMS's structure **x(t)** moving in $\boldsymbol{R}^n$ is given by

$$\mathbf{x}^T(t) = \mathbf{x}^T(0)\mathrm{e}^{\mathbf{Q}\mathrm{t}},\ t \geq 0. \tag{4}$$

As the initial state vectors **x(0)** run over all stochastic *n*-tuples, we get the respective set of the solutions **x(t)** given by (4), which is denoted by *A(t)* and called "the set of the attainable structures." Let $A_n(t)$ be the region of $\boldsymbol{R}^n$ defined by *A(t)*. We are interested in the motion-evolution of the continuum possessing the region $A_n(0) \subset \boldsymbol{R}^n$ at time $t = 0$, in the velocity field defined by (3).

Now, Eq. (3) represents a system of n linear differential equations (DEs). Because of the stochasticity condition

$$\mathrm{x}_1(t) + .. + \mathrm{x}_n(t) = 1$$

the variables $x_i(t)$, $i=1,2,..,n$, are depended and the motion takes place on the hyperplane

$$(\Pi): \mathrm{x}_1 + .. + \mathrm{x}_n = 1.$$

In order to express the motion taking place on the ($n-1$ -dimensional) hyperplane (Π) using only $n-1$ coordinates, we introduce a new coordinate system as follows. Firstly, we assume, without loss of generality, that **Q** is an irreducible matrix. In this case, a stochastic stability point, $\boldsymbol{\pi}$, exists for which $\boldsymbol{\pi}^{\mathrm{T}} \cdot \mathbf{Q} = \mathbf{0}^T$. Consider at $\boldsymbol{\pi}$ a new orthogonal coordinate system $\{\mathbf{f}_1, \mathbf{f}_2, .., \mathbf{f}_n\}$ where $\mathbf{f}_1$, $\mathbf{f}_2$,…, $\mathbf{f}_n$ belongs to the hyperplane (Π) and $\mathbf{f}_n \perp \Pi$, and let

$$\mathbf{F} = [\mathbf{f}_1, \mathbf{f}_2, .., \mathbf{f}_n] = [\mathbf{F}_1 \,|\, \mathbf{f}_n],$$

where $\mathbf{F}_1 = [\mathbf{f}_1 \,|\, \mathbf{f}_2 \,|\, .. \,|\, \mathbf{f}_{n-1}]$. Equation (3) expressed with respect to the coordinate system $\{\mathbf{f}_1 \,|\, \mathbf{f}_2 \,|\, .. \,|\, \mathbf{f}_{n-1}\}$, with origin to $\boldsymbol{\pi}$, become $\dot{\mathbf{z}}^{\mathbf{T}}\mathbf{(t)} = \mathbf{z}^{\mathbf{T}}\mathbf{(t)} \cdot \mathbf{W}$, or simply

$$\dot{\mathbf{z}}^{\mathbf{T}} = \mathbf{z}^{\mathbf{T}} \cdot \mathbf{W} \tag{5}$$

where $\mathbf{z} = (z_1, z_2, .., z_{n-1})^T$ and

$$\mathbf{W} = \mathbf{F_1}^{\mathbf{T}}\mathbf{Q}\mathbf{F_1} \, . \tag{6}$$

The system of the n DEs of (3) is now reduced to the equivalent system of the (n−1) DEs given in (5). So, Eq. (5) can be used instead of (3) in order to study the dynamical evolution-motion of the HMS-continuum taking place on (Π). Note that since tr **G** = tr **Q** < 0, the field defined by (5) is compressible.

Now, every part of the “material continuum” $A_n(t)$, t ≥ 0, is supposed to be subjected to surface forces. Then the $n\times 1$ stress vector $\mathbf{t}^{\mathrm{n}}(\mathrm{t})$ is defined at every point P enclosed by the infinitesimal surface S, where **n** is the $n\times 1$ outward unit normal of the surface element ΔS of S. The state of stress at P is given by the set $\mathbf{t}^{\mathrm{n}}$ generated from all the unit vectors **n**, according to the formula

$$\mathbf{t}^{(\hat{\mathbf{n}})} = \mathbf{T} \cdot \mathbf{n},$$

where **T** is the symmetric n × n stress tensor.

The stress tensor $\mathbf{T} = (t_{ij}(\mathbf{z}, t))$, $i,j=1,2,..,n-1$, should satisfy Cauchy’s equation of motion

$$divT(\mathbf{z}, t) + b(\mathbf{z}, t) = \rho(\mathbf{z}, t) \cdot \mathbf{a}(\mathbf{z}, t) \tag{7}$$

at every point P of the medium, where **z** is the position vector of the point P (with respect to the new coordinate system), $\rho(\mathbf{z}, t)$ is the material density at the point P at time t, $\mathbf{a}(\mathbf{z}, t)$ is the acceleration at the point P at time t and $b(\mathbf{z}, t)$ represents a vector of possible body forces given by the description of a particular HMS.

The acceleration $\mathbf{a}(\mathbf{z}, t)$ appearing in the (7) is given by

$$\mathbf{a}(\mathbf{z}, t) = \frac{\partial \mathbf{v}}{\partial t} + \nabla \mathbf{v} \cdot \mathbf{v}$$

where $\mathbf{v} = v_{ij}$ stands for the velocity (z), and the (i,j)-entry of the (n−1×n−1) matrix $\nabla\mathbf{v}$ equals $\frac{\partial v_i}{\partial z_j}$. Since by (5), the velocity is time independent, we get

$$\mathbf{a}(\mathbf{z},\mathrm{t}) = \nabla\mathbf{v}\cdot\mathbf{v} = \mathbf{W}^{\mathbf{T}}\dot{\mathbf{z}} = \left(\mathbf{W}^2\right)^{\mathbf{T}}\mathbf{z}.$$

Thus

$$\mathbf{a}(\mathbf{z},t) = \mathbf{a}(\mathbf{z}) = \left(\mathbf{W}^2\right)^{\mathbf{T}}\mathbf{z}. \tag{8}$$

Let $\mathbf{E} = \left(\varepsilon_{ij}\right)$ be the $(n-1)\times(n-1)$ Eulerian strain tensor with

$$\varepsilon_{ij} = \left(\frac{du_i}{dx_j} + \frac{du_j}{dx_i} - \frac{du_m}{dx_i}\frac{du_m}{dx_j}\right), \tag{9}$$

where $\mathbf{u} = \left(u_i\right)$ represents the displacement vector Since the features of the HMS give no rise to consider it as an inhomogeneous or anisotropic medium, we will focus attention to the case of a homogeneous isotropic viscoelastic continuum and specific the Kelvin-Voigt model. For this case the stress tensor $\mathbf{T} = \left(t_{ij}\right)$, *i, j* = 1 2, becomes (Meille and Garbozci (2001), Mase (1970), Roylance (2001))

$$t_{ij} = \left(\left(K-G\right)\cdot\varepsilon_{\kappa\kappa} - \eta\cdot\dot{\varepsilon}_{\kappa\kappa}\right)\cdot\delta_{ij} + 2\cdot G\cdot\varepsilon_{ij} + 2\cdot\eta\cdot\dot{\varepsilon}_{ij}, \tag{10}$$

where K is the bulk modulus, G is the shear modulus, η is the shear viscosity and $\dot{\varepsilon}_{\kappa\kappa}$ is the rate of strain. The parameters $\lambda=(K-G)$ and G are referred also as the *Lame parameters.*

3. The case of the 3D continuous time HMS

For the case of the 3D (irreducible) HMS, i.e., for S = {1, 2, 3}, the intensity matrix has the form

$$\mathbf{Q} = \begin{pmatrix} -q_{12}-q_{13} & q_{12} & q_{13} \\ q_{21} & -q_{21}-q_{23} & q_{23} \\ q_{31} & q_{32} & -q_{31}-q_{32} \end{pmatrix}, \tag{11}$$

where $q_{ij} \geq 0$ for i≠j, and the diagonal elements are nonnegative. The stability point $\boldsymbol{\pi}$ of the HMS is the stochastic, left eigenvector of the intensity matrix (11) associated with the eigenvalue 0, i.e., $\boldsymbol{\pi}^{\mathrm{T}}\cdot\mathbf{Q} = \mathbf{0}^{\mathbf{T}}$ and $\boldsymbol{\pi}^{\mathrm{T}}\mathbf{1} = \mathbf{1}^{\mathbf{T}}$, where $\mathbf{1}$ is the column vector of 1's. The base vectors of the orthogonal coordinate system {$\mathbf{f}_1$, $\mathbf{f}_2$, $\mathbf{f}_3$}, with origin at $\boldsymbol{\pi}$, can be chosen to be

$$\mathbf{f}_1 = \left(-\sqrt{\frac{2}{3}},\sqrt{\frac{1}{6}},\sqrt{\frac{1}{6}}\right)^T, \mathbf{f}_2 = \left(0,-\sqrt{\frac{1}{2}},\sqrt{\frac{1}{2}}\right)^T, \mathbf{f}_3 = \left(\sqrt{\frac{1}{3}},\sqrt{\frac{1}{3}},\sqrt{\frac{1}{3}}\right)^T. \tag{12}$$

Then,

$$\mathbf{F}_1 = \begin{pmatrix} -\sqrt{\frac{2}{3}} & \sqrt{\frac{1}{6}} & \sqrt{\frac{1}{6}} \\ 0 & -\sqrt{\frac{1}{2}} & \sqrt{\frac{1}{2}} \end{pmatrix}^T . \tag{13}$$

According to (5), the motion of a particle-structure is expressed on the 2D hyperplane (Π) by the equation

$$\mathbf{z}^T(t) = \left(z_1(t), z_2(t)\right) = \mathbf{z}^T(0)\,\mathrm{e}^{\mathbf{W}t} . \tag{14}$$

Then, since

$$\mathbf{u}(\mathbf{z};t,t+\Delta t) = \mathbf{z}(t+\Delta t) - \mathbf{z}(t), \tag{15}$$

the components ε_{ij} of the continuum's strain tensor can be evaluated using (9).

In order to examine if the 3D HMS can be interpreted as a density-homogeneous viscoelastic medium (that is $\rho(\mathbf{z},t)=\rho(t)$ for every $\mathbf{z}$ and t) we have to check if Cauchy's equation of motion, (7), is justified while substituting for the required acceleration and density, using (8). Moreover we have to check if the continuity equation

$$\frac{d\rho}{dt} + \rho \cdot div(\mathbf{v}) = 0 , \tag{16}$$

is satisfied, where $\mathbf{v} = \dot{\mathbf{z}}$ stands for the velocity.

The mass forces appearing in (7) to meet the general case, are here set equal to **0**. The final system of Cauchy's equation of motion is of the form:

$$\begin{aligned} \rho(\alpha_{11}z_1 + \alpha_{12}z_2) = {} & \frac{d\lambda}{dz_1}\left(\varepsilon_{11} + \varepsilon_{22}\right) - \frac{dn}{dz_1}\left(\dot{\varepsilon}_{11} + \dot{\varepsilon}_{22}\right) + 2\varepsilon_{11}\frac{dG}{dz_1} + 2\dot{\varepsilon}_{11}\frac{dn}{dz_1} \\ & + 2\frac{dG}{dz_2}\varepsilon_{12} + 2\frac{dn}{dz_2}\dot{\varepsilon}_{12} , \end{aligned} \tag{17}$$

$$\begin{aligned} \rho(\alpha_{21}z_1 + \alpha_{22}z_2) = {} & 2\frac{dG}{dz_1}\varepsilon_{21} + 2\frac{dn}{dz_1}\dot{\varepsilon}_{21} + \frac{d\lambda}{dz_2}\left(\varepsilon_{11} + \varepsilon_{22}\right) - \frac{dn}{dz_2}\left(\dot{\varepsilon}_{11} + \dot{\varepsilon}_{22}\right) \\ & + 2\frac{dG}{dz_2}\varepsilon_{22} + 2\frac{dn}{dz_2}\dot{\varepsilon}_{22} \end{aligned} \tag{18}$$

The above system cannot be solved in terms of the (unknown) parameters G, λ and η, because there are three unknown parameters but only two equations. So, <u>we assume here that the shear viscosity η depends only on time t</u>. We notice here that such an space-independence assumption for the parameters G and λ can be seen to violate the consideration of the HMS as a real continuum (in the sense that $G, \lambda \to -\infty$ for some t). Then the above system (17)-(18) becomes a system of two unknown parameters

$$\rho(\alpha_{11}z_1 + \alpha_{12}z_2) = \frac{d\lambda}{dz_1}\left(\varepsilon_{11} + \varepsilon_{22}\right) + 2\varepsilon_{11}\frac{dG}{dz_1} + 2\frac{dG}{dz_2}\varepsilon_{12}$$

$$\rho(\alpha_{21}z_1+\alpha_{22}z_2)=2\frac{dG}{dz_1}\varepsilon_{21}+\frac{d\lambda}{dz_2}\left(\varepsilon_{11}+\varepsilon_{22}\right)+2\frac{dG}{dz_2}\varepsilon_{22}.$$

In order to solve the above underdetermined system of PDEs, we can work either numerically or seek for solutions of some special forms, for example separable solutions in the form

$$\lambda(\mathbf{z},t)=\mathrm{Z}_1(z_1)\mathrm{T}_1(\mathrm{t})+\mathrm{Z}_2(z_2)\mathrm{T}_2(\mathrm{t})\ ,\ G(\mathbf{z},t)=K_1(z_1)\mathrm{T}_1(\mathrm{t})+K_2(z_2)\mathrm{T}_4(\mathrm{t}).$$

Then the system of the two PDEs (17)–(18), which determines the motion of the HMS-continuum, now considered as a 2D continuum, becomes a system of two ODEs which can be solved in terms of λ and G:

$$\rho\left(a_{11}z_1+a_{12}z_2\right)=\left(\varepsilon_{11}+\varepsilon_{22}\right)\mathrm{T}_1(\mathrm{t})\frac{\partial Z_1}{\partial z_1}+2\varepsilon_{11}\,\mathrm{T}_3(\mathrm{t})\frac{\partial K_1}{\partial z_1}+2\varepsilon_{12}\,\mathrm{T}_4(\mathrm{t})\frac{\partial K_2}{\partial z_2}$$

$$\rho\left(a_{21}z_1+a_{22}z_2\right)=2\varepsilon_{21}\,\mathrm{T}_3(\mathrm{t})\frac{\partial K_1}{\partial z_1}+2\varepsilon_{22}\,\mathrm{T}_4(\mathrm{t})\frac{\partial K_2}{\partial z_2}+\left(\varepsilon_{11}+\varepsilon_{22}\right)\mathrm{T}_2(\mathrm{t})\frac{\partial Z_2}{\partial z_2}.$$

Now we have to check if the above system of ODEs (corresponding to Cauchy's equation of motion given by (7)), is justified while substituting for the required acceleration and density, using (8) and the continuity equation (16). The mass forces appearing in (7) to meet the general case, are set equal to **0**. If the system of the ODEs is justified then the 2D continuum corresponding to the 3D HMS, as explained in Sec. 2, can be used in order to interpret the evolution of the HMS. The procedure of solving the system (17)–(18) will be presented clearly by means of the example provided in the next section.

3.1 The energy of the HMS

The rate of the energy, E, of the HMS is given by

$$\frac{dK}{dt}+\frac{dU}{dt}=\frac{dE}{dt}, \tag{19}$$

where U stands for the internal energy and K for the kinetic energy. The rate of the internal energy is given by

$$\frac{dU}{dt}=\frac{tr(\mathbf{W}\cdot\mathbf{T})}{\rho}\quad , \tag{20}$$

while the rate of the kinetic energy can be easily calculated by means of (5).

4. An illustrative example

Consider a closed continuous-time HMS with state space S = {1, 2, 3} and intensity matrix

$$\mathbf{Q}=\begin{pmatrix}-4.7 & 4 & 0.7\\ 4.02 & -4.22 & 0.2\\ 0.2 & 2 & -2.2\end{pmatrix}$$

(as given in Maaita et al, 2013), The stability point of the HMS is the stochastic, left eigenvector of the intensity matrix (11) associated with the eigenvalue 0, that is $\boldsymbol{\pi}^{\mathrm{T}} \cdot \mathbf{Q} = \mathbf{0}^{\mathbf{T}}$ and $\boldsymbol{\pi}^{\mathrm{T}} \times \mathbf{1} = \mathbf{1}^{\mathbf{T}}$. It is found that $\boldsymbol{\pi}^{\mathrm{T}}$ =(0.389,0.447,0.164).

The base vectors of the orthogonal coordinate system {$\mathbf{f}_1$, $\mathbf{f}_2$, $\mathbf{f}_3$}, with origin at $\boldsymbol{\pi}$, can be chosen to be those given by (12). Then, by (13) and (6), the matrix **W** appearing in the reduced matrix Eq. (5), which expresses the motion on the hyperplane (Π), is found to be

$$\mathbf{W} = \mathbf{F}_1^T \mathbf{Q} \mathbf{F}_1 = \begin{pmatrix} -6.81 & 1.96876 \\ 3.3082 & -4.31 \end{pmatrix},$$

with eigenvalues

$$\lambda_1 = -840716, \ \lambda_2 = -271824.$$

Since λ_1, $\lambda_2 < 0$, the velocity field $\dot{\mathbf{z}}^{\mathbf{T}} = \mathbf{z}^{\mathbf{T}} \cdot \mathbf{W}$ is compressible.

Now, using (14) with $\mathbf{z}(0) = \left(z_1(0), z_2(0)\right)^T$, we get the equations of motion

$$z_1(t) = \left(0.72e^{-8.402t} + 0.28e^{-2.718t}\right) z_{10} + \left(-0.582e^{-8.402t} + 0.582e^{-2.718t}\right) z_{20}$$

$$z_2(t) = \left(-0.346e^{-8.402t} + 0.346e^{-2.718t}\right) z_{10} + \left(0.28e^{-8.402t} + 0.72e^{-2.718t}\right) z_{20}.$$

Then from (15) we derive the components of the displacement vector:

$$u_1(z;t,t+\Delta t) = z_1(t+\Delta t) - z_1(t) = \left(-1+0.72e^{-8.402\Delta t} + 0.28e^{-2.718\Delta t}\right) z_1 \\ + \left(-0.582e^{-8.402\Delta t} + 0.582e^{-2.718\Delta t}\right) z_2 \ ,$$

$$u_2(z;t,t+\Delta t) = z_2(t+\Delta t) - z_2(t) = \left(-0.346e^{-8.402\Delta t} + 0.346e^{-2.718\Delta t}\right) z_1 \\ + \left(-1+0.28e^{-8.402\Delta t} + 0.72e^{-2.718\Delta t}\right) z_2.$$

From (9) the entries of the strain tensor $\mathbf{E} = (\varepsilon_{ij})$ can be evaluated to be

$$\varepsilon_{11} = -1.5 - 0.319e^{-16.804t} - 0.082e^{-11.12t} + 1.44e^{-8.402t} - 0.0992e^{-5.436t} + 0.56e^{-2.718t} \tag{21}$$

$$\varepsilon_{12} = \varepsilon_{21} = 0.258e^{-16.804t} - 0.052e^{-11.12t} - 0.928e^{-8.402t} - 0.206e^{-5.436t} + 0.928e^{-2.718t} \tag{22}$$

$$\varepsilon_{22} = -1.5 - 0.209e^{-16.804t} + 0.137e^{-11.12t} + 0.56e^{-8.402t} - 0.429e^{-5.436t} + 1.44e^{-2.718t}, \tag{23}$$

and then, by (10), the components $t_{ij} = \left(\left(K - G\right) \cdot \varepsilon_{\kappa\kappa} - \eta \cdot \dot{\varepsilon}_{\kappa\kappa}\right) \cdot \delta_{ij} + 2 \cdot G \cdot \varepsilon_{ij} + 2 \cdot \eta \cdot \dot{\varepsilon}_{ij}$, of the stress tensor $\mathbf{T} = (t_{ij})$ can be derived.

By substituting for **a(z,** t) and **T(z**, t) in Cauchy's equation of motion, (7), assuming the body forces to be equal to zero, we get the system of the PDEs

$$\rho\cdot(52.889z_1-36.787z_2)=$$
$$=\left(-3-0.528e^{-16.804t}+0.056e^{-11.12t}+2e^{-8.402t}-0.528e^{-5.436t}+2e^{-2.718t}\right)\frac{d\lambda}{dz_1}$$

$$+2\left(-1.5-0.319e^{-16.804t}-0.082e^{-11.12t}+1.44e^{-8.402t}-0.099e^{-5.43648t}+0.56e-^{2.718t}\right)\frac{dG}{dz_1}$$

$$+2\left(0.258e^{-16.804t}-0.052e^{-11.12t}-0.928e^{-8.402t}-0.206e^{-5.436t}+0.928e^{-2.718t}\right)\frac{dG}{dz_2}\quad(24)$$

and

$$\rho\cdot(-21.893z_1+25.089z_2)=$$
$$=\left(-3-0.528e^{-16.804t}+0.056e^{-11.12t}+2e^{-8.402t}-0.528e^{-5.436t}+2e^{-2.718t}\right)\frac{d\lambda}{dz_2}$$

$$+2\left(-1.5-0.319e^{-16.804t}-0.082e^{-11.12t}+1.44e^{-8.402t}-0.099e^{-5.43648t}+0.56e-^{2.718t}\right)\frac{dG}{dz_2}$$

$$+2\left(0.258e^{-16.804t}-0.052e^{-11.12t}-0.928e^{-8.402t}-0.206e^{-5.436t}+0.928e^{-2.718t}\right)\frac{dG}{dz_1}\quad(25)$$

In order to solve the system of the PDEs (24)–(25), we have to evaluate the density ρ(t). Now, by assuming that the material is homogeneous with respect to the density at every time t, (i.e., the density depends only on the time and not on the spatial coordinates), we get by using the continuity Eq. (16) and for the given velocity field, for which div(**v**)=11.12 that

$$\rho=\rho(0)\,\mathrm{e}^{11.12\,\mathrm{t}}.$$

Next, let us seek for a solution (λ,G) of the above underdetermined system (24)–(25) of PDEs, such that

$$\lambda(\mathbf{z},t)=\mathrm{Z}_1(z_1)\mathrm{T}_1(\mathrm{t})+\mathrm{Z}_2(z_2)\mathrm{T}_2(\mathrm{t})\ ,\quad G=K_1(z_1)\mathrm{T}_1(\mathrm{t})+K_2(z_2)\mathrm{T}_4(\mathrm{t}).\qquad(26)$$

Then the system (24)-(25) becomes

$$\rho\left(52.889z_1-36.787z_2\right)=\left(\varepsilon_{11}+\varepsilon_{22}\right)\mathrm{T}_1(\mathrm{t})\frac{\partial \mathrm{Z}_1}{\partial z_1}+2\varepsilon_{11}\,\mathrm{T}_3(\mathrm{t})\frac{\partial \mathrm{K}_1}{\partial z_1}+2\varepsilon_{12}\,\mathrm{T}_4(\mathrm{t})\frac{\partial \mathrm{K}_2}{\partial z_2}$$

$$\rho\left(-21.893z_1+25.089z_2\right)=\left(\varepsilon_{11}+\varepsilon_{22}\right)\mathrm{T}_2(\mathrm{t})\frac{\partial \mathrm{Z}_2}{\partial z_2}+2\varepsilon_{21}\,\mathrm{T}_3(\mathrm{t})\frac{\partial \mathrm{K}_1}{\partial z_1}+2\varepsilon_{22}\,\mathrm{T}_4(\mathrm{t})\frac{\partial \mathrm{K}_2}{\partial z_2},$$

from which we derive that

$$52.889\cdot\rho\cdot z_1=\left(\varepsilon_{11}+\varepsilon_{22}\right)\mathrm{T}_1(\mathrm{t})\frac{\partial \mathrm{Z}_1}{\partial z_1}+2\varepsilon_{11}\,\mathrm{T}_3(\mathrm{t})\frac{\partial \mathrm{K}_1}{\partial z_1}$$

$$-36.787 \cdot \rho \cdot z_2 = 2\varepsilon_{12}\, T_4(t) \frac{\partial K_2}{\partial z_2}$$

$$-21.893 \cdot \rho \cdot z_1 = 2\varepsilon_{21}\, T_3(t) \frac{\partial K_1}{\partial z_1}$$

and

$$25.089 \cdot \rho \cdot z_2 = 2\varepsilon_{22}\, T_4(t) \frac{\partial K_2}{\partial z_2} + \left(\varepsilon_{11} + \varepsilon_{22}\right) T_2(t) \frac{\partial Z_2}{\partial z_2},$$

where $\varepsilon_{ij}(t)$ are given by (21)–(23). The above system may be considered as a system of consistency equations for the motion of the HMS-continuum assuming the solution (λ, G) to be of the form (26). Using these equations we get by simple algebraic manipulations that

$$\lambda(\mathbf{z}, t) = \rho \cdot \left(\left(\frac{z_1^{\,2}}{2} + \alpha_1 \right) \cdot \frac{52.889\varepsilon_{21}(t) + 21.893\varepsilon_{11}(t)}{\varepsilon_{21}(t)\left(\varepsilon_{11}(t) + \varepsilon_{22}(t)\right)} + \left(\frac{z_2^{\,2}}{2} + \alpha_2 \right) \cdot \frac{25.089\varepsilon_{12}(t) + 36.787\varepsilon_{22}(t)}{\varepsilon_{12}(t)\left(\varepsilon_{11}(t) + \varepsilon_{22}(t)\right)} \right) \tag{27}$$

$$G(\mathbf{z}, t) = -\rho \cdot \left(\left(\frac{z_1^{\,2}}{2} + b_1 \right) \cdot \frac{21.787}{2\varepsilon_{21}(t)} + \left(\frac{z_2^{\,2}}{2} + b_2 \right) \cdot \frac{36.787}{2\varepsilon_{12}(t)} \right), \tag{28}$$

where α_1, α_2, b_1, and b_2 are real arbitrary constants.

Now from (27), (28) and the relation $K=\lambda+G$, we can derive the bulk modulus K. In figures 1 and 2 the solution (*K*(**z**.*t*), *G*(**z**,*t*)) is presented for t=0.01 and t=0.3, with $a_1 = a_2 = 0.2$ and $b_1 = b_2 = -0.5$. The shapes of the respective surfaces *K*(**z**.*t*) and *G*(**z**,*t*) remain the same also for larger values of t, while the values of *K*(**z**.*t*) and *G*(**z**,*t*) increase exponentially fast, because of their dependence on ρ(t) .

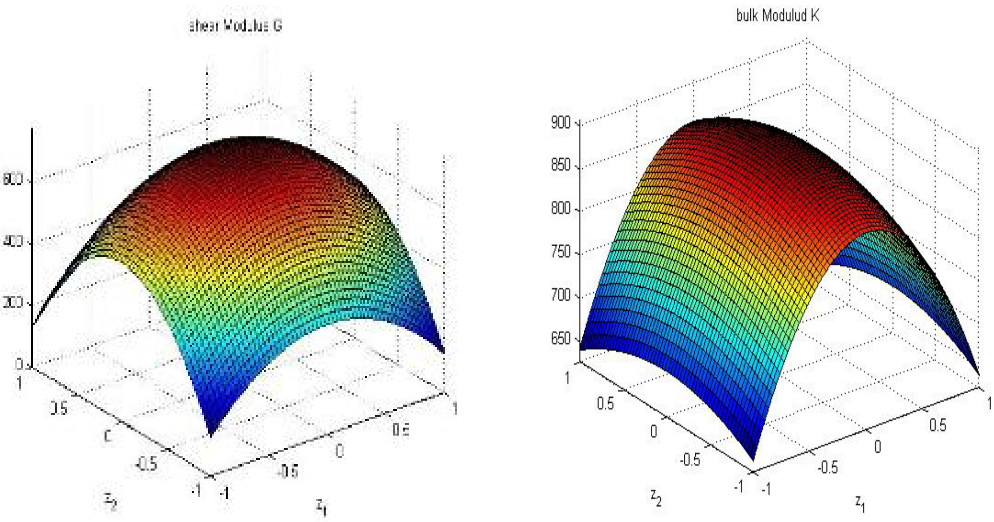

Figure 2. Shear *G*(**z**,*t*) and bulk modulus *K*(**z**.*t*) for t=0.01

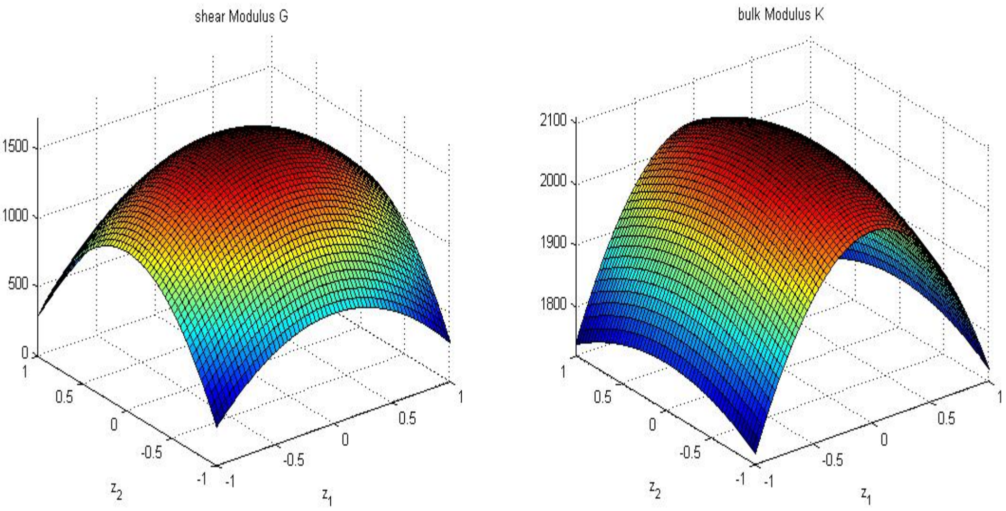

Figure 3. Shear $G(\mathbf{z},t)$ and bulk modulus $K(\mathbf{z}.t)$ for t=0.3

The shear viscosity, $\eta(t)$, which is not found by solving the PDEs, should be determined so as to allow for a natural interpretation. Now $\eta(t)$ should be proportional to pressure (alternatively to the density) and inversely proportional to the rate of shear strain (Dealy and Wang (2013), Lanzedorfer (2011)). Through those considerations the shear viscosity could be of the form

$$\eta(t) = \frac{\rho(t)(21.893 + 36.787)(0.23855 - t)}{2\dot{\varepsilon}_{12}(\mathrm{t})}, \tag{29}$$

where the quantity $(0.23855 - t)$ arises in order for η(t) to be positive, i.e., $\eta(\mathrm{t})>0$ for t >0 (see Figure 4), and the constant (21.893+36.787) is included in order for η(t) to have the same behavior as parameter G.

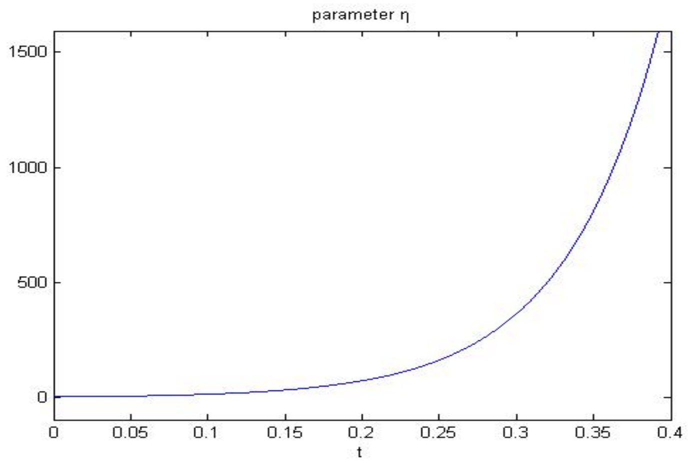

Figure 4. The shear viscosity, η(t).

4.1 The energy of the HMS

In order to evaluate the energy of the HMS-continuum, the internal energy may be firstly evaluated taking (20) into account. Then, by setting without loss of generality $\rho(0) = 1$,

$$\frac{dU}{dt} = \frac{\left(-6.81 \cdot t_{11} + 1.96876 \cdot t_{12} + 3.30822 \cdot t_{21} - 4.31 \cdot t_{22}\right)}{\rho}, \tag{30}$$

where the stresses t_{ij}, $i, j = 1, 2$, are derived by taking into account (27), (28) and (29).

The rate of change of the kinetic energy, *K(t),* can be evaluated using the velocity field (5) or equivalently (14). So,

$$\begin{aligned}\frac{dK}{dt} &= \left(-5.36e^{-16.8t} - 0.9e^{-11.12t} - 054e^{-5.43t}\right) z_{10}^2 \\ &+ \left(8.67e^{-16.8}t - 1.15e^{-11.12t} - 2.24e^{-5.43t}\right) z_{10} z_{20} \\ &+ \left(-3.5e^{-16.8t} + 1.52e^{-11.12t} - 2.32e^{-5.43t}\right) z_{20}^2 .\end{aligned} \tag{31}$$

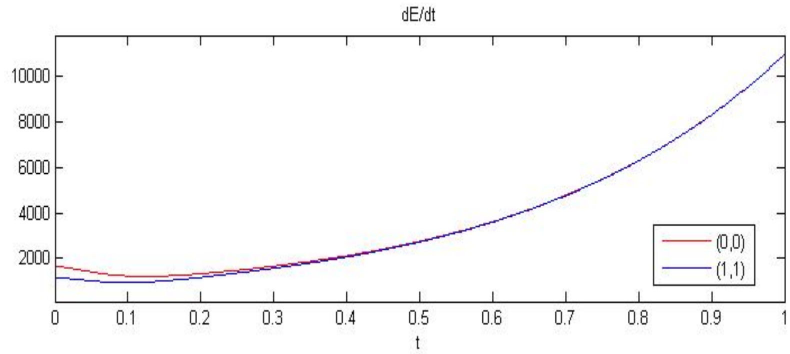

Figure 5. Rate of change of the Energy.

Next, by (30), (31), and (19), the rate of change of the whole energy, E (i.e., internal plus kinetic energy), can be easily derived. The rate of change of the energy, is presented for two different spatial initial conditions in Fig. 5. The (exponential) growth of the rate of change is due to the internal energy while the rate of change of the kinetic energy tends to 0. It should be emphasized here that the energy behavior of the system presented in Fig. 5, depends on the solution type selected for *G*(t), *K*(t), i.e., on (26), while other types of solutions for *G(*t), *K(*t) may lead to different energy behaviors.

4. Conclusion

Since the features of a HMS or equivalently of its underlying (generating) MC do not give rise to the determination of certain initial conditions concerning the evaluation of the parameters *K*, *G* and η, fixed numerical values cannot be given to them. Nevertheless, by assuming $\lambda(\mathbf{z},t)$ and $G(\mathbf{z},t)$ to be of the special form (26), and by choosing suitable constants α_1, α_2, b_1, b_2 (in (27)–(28)), we can assign positive values to *K* and *G* as expected by the theory of real continua. In the same way, we can assign via (29) positive values to the parameter η. The three parameters appear generally to be time-dependent and increase rapidly

(Hofmeister (1991)) because, by (27), (28) and (29), they are proportional to the density $\rho(t)$, which grows up exponentially fast.

Since under the assumption (26) the three parameters appearing in the study of real viscoelastic continua, retain their features (e.g. positiveness) while considered for the 3D HMS-continuum (using the Kelvin-Voight model), the evolution of the HMS can be interpreted as the deformation of a 2D homogeneous viscoelastic medium. Consequently suitable values could generally be assigned to the (arbitrary) constants appearing in the solutions $K(\mathbf{z},t)$, $G(\mathbf{z}, t)$, in order for the HMS to attain any special features.

Finally, the HMS-continuum (or alternatively the relative MC-continuum (via the set of the attainable structures)) interestingly reveals a functionally graded material (FGM) behavior since its parameters are continually changing in space and the values of K and G appear to be bigger near to the continuum "center", i.e., the stability point $\boldsymbol{\pi}$ (Bharti et al (2013), Makwana and Panchal (2014)). In other words the material is stress resistant especially near to $\boldsymbol{\pi}$.

Acknowledgment: We would like to thank Emeritus Prof. Nikolaos Charalampakis, (Department of Civil Engineering, Aristotle University Thessaloniki, Greece) for his useful remarks and indications in writing this paper.

References

[1] Bharti I., Gupta N. and Gupta K.M. *Novel Applications of Functionally Graded Nano, Optoelectronic and Thermoelectric Material.* International Journal of Materials. Mathematics and Manufacturing. Vol 1. No 3. 2013.

[2] Bridgman P. W. *The Viscosity of Liquids under Pressure.* Proceedings of the National Academy of Sciences of U.S.A. Vol 11. No 10. pp 603-606. 1925.

[3] Christensen R.M. *Theory of Viscoelasticity an Introduction.* Edition II. Academics Press. New York. 1982.

[4] Dealy J. M. and Wang J. *Viscosity and Normal Stresses Difference.* Melt reology and its Applications in the Plastic Industry. vol. XVI, 2013.

[5] Hofmeister A.M. *Pressure Derivatives of the Bulk Modulus.* Journal of Geophysical Research. Vol 96. pp 893-907. 1991.

[6] Lanzedorfer M. *Flow of Incompressible Fluids with Pressure-Depended viscosity.* Prague. 2011.

[7] Maaita J. O., Tsaklidis G. M and Meletidou E. The *Homogeneous Markov System as an Elastic Medium. The 3D case.* Communications in Statics-Theory and Methods. No 42. pp 2259 -2270. 2013.

[8] Makwana A. B and Panchal K. C. *A Review of Stress of Functionally Graded of Functionally Graded Material Plate with Cut-out.* International Journal of Engineering Research & Technology. Vol 3. Issue 3. 2014.

[9] Mase G. E. *Continuum Mechanics.* Schaums Outline McGraw-Hill Inc. 1970.

[10] Meille S. and Garbozci E.J. *Linear Elastic Properties of 2D and 3D Models of Porous Material Made From Elongated Objects.* Modelling Simul. Mat. Sci. Eng. Vol 9. pp 371-390. 2001.

[11] Roylance D. *Engineering Viscoelasticity*. Massachusetts Institute of Technology Cambridge. MA 02319. 2001.

[12] Tsaklidis G. M. *The stress tensor and the energy of a continuous time homogeneous Markov system with fixed size.* Applied Probability Trust. No 36. 1999.

[13] Tsaklidis G. M and Soldatos K. P. *Modelling of continuous time homogeneous Markov system with fixed size as an elastic solid: the 2D case.* Applied Mathematical Modeling. No 27. pp 877-887. 2003.

A Compound Scan Statistic Distribution with Applications in Risk Management*

Vasileios M. Koutras[1], Markos V. Koutras[2], and Femin Yalcin[3]

[1] Department of Statistics and Insurance Science, University of Piraeus, Greece (E-mail: vkoutras@icloud.com)
[2] Department of Statistics and Insurance Science, University of Piraeus, Greece (E-mail: mkoutras@unipi.gr)
[3] Department of Statistics and Insurance Science, University of Piraeus, Greece (E-mail: feminyalcin@yahoo.com.tr)

Abstract. In the present work we study the distribution of a random sum of random variables which is related to a binary scan statistic. The motivation of the model studied herein stems from several areas of applied science such as financial risk management, actuarial science, quality control and reliability, educational psychology, engineering etc.
Let T_k denote the waiting time for the first occurrence of "two successes which lie at most k places apart", (i.e. two successes separated by at most $k-2$ failures) in a sequence of binary success/fail trials ($k \geq 2$ is a positive integer). Assume further that $Y_1, Y_2, \ldots$ is a sequence of independent and identically distributed discrete random variables which are independent of T_k. In the present article we develop some results on the distribution of the compound random variable $S_k = \sum_{t=1}^{T_k} Y_t$ and illustrate how these results can be profitably used to study models pertaining to risk management problems, more specifically to supervisory bank capitalization monitoring.
Keywords: Waiting Times, Compound distributions, Binary scan statistics, Phase–type distributions, Bank supervision, Risk management.

1 Introduction

The motivation of the model studied in the present article stems from several areas of applied science such as financial risk management, actuarial science, quality control and reliability, educational psychology, engineering etc. Many problems encountered in these areas can be described through dichotomous (binary) variables $\xi_1, \xi_2, \ldots$ taking on the values 1 (success, S) or 0 (failure, F) and the interest focuses on random variables related to the time a predetermined criterion is satisfied (stopping rule).

As an example, let us consider the following model which is of special importance in financial risk management. Assume that a bank is subject to a

* This research has been co-financed by the European Union (European Social Fund – ESF) and Greek national funds through the Operational Program "Education and Lifelong Learning" of the National Strategic Reference Framework (NSRF) - Research Funding Program: Aristeia II. Investing in knowledge society through the European Social Fund.

16^{th} *ASMDA Conference Proceedings, 30 June – 4 July 2015, Piraeus, Greece*

sequence of stress tests over time. Using several indices related to the bank's economical health, the bank may be classified as appropriately functioning (low risk of defaulting) or not. For example, it is widely recognized that a bank's capitalization is of utmost importance and provides the main line of defense for absorbing unexpected losses; therefore it may be used as an important risk measure signaling an oncoming credit event, i.e. default. A measure of bank capitalization health is provided by the Capital Ratio, which is defined as (Tier1+Tier2)/Risk-Weighted Assets; for regulatory purposes, the Basel Accord has adopted a simple dichotomous classification that characterizes a bank either as undercapitalized or not, depending on whether its Capital Ratio falls below or above 8%; see e.g. Demstez *et al.*[5]; Flannery and Sorescu[8]; Estrella *et al.*[7], Goldberg and Hudgins[11]; Lindquist[17], Berger *et al.*[2], Koutras and Drakos[16].

Apparently, the outcomes of the series of stress tests may be modeled by the aid of a sequence of binary variables $\xi_1, \xi_2, \ldots$ taking on the values 1 (success, S) or 0 (failure, F) where 1 designates an undercapitalized bank (i.e. a bank that failed in the stress test) and 0 for a well-capitalized one. A plausible criterion to consider that a bank is susceptible to default would be to have at least two negative stress tests that are very close to each other, e.g. when an outcome of the form SS, SFS, $SFFS$ is observed.

The aforementioned model can be accommodated in the following general set-up. Let $\xi_1, \xi_2, \ldots$ be an infinite sequence of binary outcomes and denote by T_k the waiting time for the first occurrence of two successes which lie at most k places apart from each other, i.e. they are separated by at most $k-2$ failures ($k \geq 2$ is a positive integer). Clearly, T_k counts the number of trials required to observe for the first time one of the patterns

$$SS, SFS, \ldots, S\overbrace{F \ldots F}^{k-2}S.$$

For illustration, consider the sequence of outcomes

$$FFSFFFSFFFFSFFSFSS$$

then

$$T_2 = 18, \qquad T_3 = 17, \qquad T_4 = 15, \text{ and } \qquad T_5 = 7.$$

The random variable T_k is a special case of a *scan statistic*, see e.g. Glaz[9], Glaz and Naus[10], Greenberg[12], Saperstein[19], Chen and Glaz[4]. Note that, for $k = 2$ the random variable T_k is enumerating success runs of length $k = 2$ and therefore it follows a *geometric distribution of order 2*; the interested reader may consult the book by Balakrishnan and Koutras[1] for more details and results relating to waiting times for runs and scans.

Let us next assume that the times of the stress tests are random and denote by Y_1 the time when the first stress test takes place. Moreover, denote by Y_t the interarrival time between the $(t-1)$-th and t-th stress tests ($t \geq 2$). Then the total time till a default signal is created for the monitored bank (i.e. the time when the bank is considered susceptible to a future default) will be described by the random variable

$$S_k = \sum_{t=1}^{T_k} Y_t,$$

where $Y_1, Y_2, \ldots$ is a sequence of positive valued iid random variables, which are independent of T_k.

The simplest scenario for the sequence $\xi_t,\ t = 1, 2, \ldots$ which gives birth to the random variable T_k is when $\xi_t,\ t = 1, 2, \ldots$ is a sequence of iid trials with constant success probability $p = P[\xi_t = 1]$ and failure probability $q = 1 - p = P[\xi_t = 0]$ for $t = 1, 2, \ldots$. For the financial risk modeling application discussed earlier, this sequence might arise as follows. Let X_t denote the Capital Ratio of the bank subject to the stress test at time $t,\ t = 1, 2, \ldots$. Adopting the Basel Accord dichotomous classification we may consider that the bank failed the stress test if $X_t < 8\%$ and therefore $p = P[\xi_t = 1] = P[X_t > 0.08]$ and $q = P[\xi_t = 0] = P[X_t \leq 0.08]$. If $X_t,\ t = 1, 2, \ldots$ are considered as independent, then $\xi_t,\ t = 1, 2, \ldots$ will be independent as well and the sequence $\xi_t,\ t = 1, 2, \ldots$ will be a sequence of iid Bernoulli trials. A more realistic scenario could be created by assuming that X_t depends on the magnitude of the previous capitalization X_{t-1} or more generally on the capitalizations of more than one previous time instances. Under this assumption the resulting sequence $\xi_t,\ t = 1, 2, \ldots$ exhibits a first (or higher) order Markov dependence. In our presentation we shall deal with the iid model only and leave the more general set up for future research.

In the present study, we obtain the distribution and the moments of the compound scan statistic $S_k = \sum_{t=1}^{T_k} Y_t$ using some recursive and nonrecursive formulae. Since the distribution of the scan statistic $T_k,\ k \geq 2$ can be represented as a phase-type distribution, we shall also establish some results for the probability mass function (pmf) of S_k by making use of the theory of phase-type distributions.

A discrete phase-type distribution of order d is the distribution of the random variable T that describes the time to absorption in a finite discrete time Markov chain with d transient states and one absorbing state. Let Λ_0 be the $(d+1) \times (d+1)$ transition probability matrix of the Markov chain and $\boldsymbol{\pi}_0 = (\pi_1, \pi_2, \ldots, \pi_{d+1})'$ the respective initial probability vector. Assume that the absorbing state of the Markov chain is labeled as state $d+1$. Then, the pmf of the discrete phase-type random variable T may be expressed as

$$P[T = t] = \boldsymbol{\pi}' \Lambda^{t-1} \boldsymbol{u},\ t = 1, 2, \ldots, \tag{1}$$

where Λ is the $d \times d$ substochastic matrix of Λ_0 deduced by removing the row and column associated with the absorbing state $d+1$, $\boldsymbol{\pi} = (\pi_1, \pi_2, \ldots, \pi_d)'$ is the respective initial transition probability vector (note that $\sum_{i=1}^{d} \pi_i = 1 - \pi_{d+1} \leq 1$), and $\boldsymbol{u} = (I_d - \Lambda)\,\mathbf{1}$ is a column vector including all transition probabilities from the transient states to the absorbing state. The symbol $\mathbf{1}$ denotes a column vector of size d whose all entries are 1 and I_d the $d \times d$ identity matrix. If T is a discrete phase-type random variable with pmf given in (1), we shall say that T follows a phase-type distribution of order d with parameters $\boldsymbol{\pi}$ and

Λ, symbolically $T \sim PH_d(\boldsymbol{\pi}, \Lambda)$. For more details on phase-type distributions and their properties, we refer to the books by Neuts[18] and He[13].

The structure of the present paper is as follows. In Section 2 we give some results for the distribution, probability generating function, and the moments of the compound scan statistic $S_k = \sum_{t=1}^{T_k} Y_t$. Section 3 addresses the problem of evaluating the pmf of S_k in the case where Y_t's are discrete random variables. We indicate how one can establish effective recursive schemes for the pmf of S_k and develop a nonrecursive formula for it when the positive valued iid random variables $Y_1, Y_2, \ldots$ have a phase-type distribution. Finally, in Section 4 we provide some plots for the distribution of the compound scan statistic along with some remarks on its shape and the effort required for the computations.

2 Generating functions and moments of the compound scan statistic

In this section we present some results for the evaluation of the probability mass function and the moments of $S_k = \sum_{t=1}^{T_k} Y_t$. The random variable T_k appearing in the random sum stands for the waiting time for the first occurrence of two successes which lie at most k places apart ($k \geq 2$) in a sequence of binary iid (Bernoulli) trials having probability of success p and probability of failure $q = 1 - p$.

Let us denote by

$$P_{S_k}(z) = E\left(z^{S_k}\right) = \sum_{t=1}^{\infty} P[S_k = t]\, z^t = \sum_{t=1}^{\infty} f_k(t)\, z^t$$

and

$$P_{T_k}(z) = E\left(z^{T_k}\right) = \sum_{t=1}^{\infty} P[T_k = t]\, z^t$$

the probability generating functions (pgf's) of S_k and T_k, respectively, and by

$$P_Y(z) = E\left(z^{Y_t}\right) = \sum_{x=1}^{\infty} P[Y_t = x]\, z^x$$

the common pgf of all Y_t's, $t = 1, 2, \ldots$. Making use of the well known formula for the pgf of a sum of random variables (see e.g. Bowers *et al.*[3]) we may express the pgf of S_k as follows

$$P_{S_k}(z) = P_{T_k}(P_Y(z)). \tag{2}$$

The pgf of T_k, $P_{T_k}(z)$, is given by (see Koutras[14])

$$P_{T_k}(z) = E\left(z^{T_k}\right) = \frac{(pz)^2 A(z)}{1 - qz - pq^{k-1}z^k},$$

where

$$A(z) = \sum_{i=0}^{k-2} (qz)^i = \frac{1 - (qz)^{k-1}}{1 - qz}.$$

Replacing $P_{T_k}(z)$ into (2) we readily deduce the next expression for the pgf of the compound scan statistic distribution

$$P_{S_k}(z) = E\left(z^{S_k}\right) = \frac{\left(pP_Y(z)\right)^2}{1 - qP_Y(z) - pq^{k-1}\left(P_Y(z)\right)^k} \frac{1 - \left(qP_Y(z)\right)^{k-1}}{1 - qP_Y(z)}. \quad (3)$$

Note that for the special case $k = 2$ the result coincides with the one given by Koutras and Eryilmaz[15] since in this case the scan statistic reduces to the waiting time for a success run of length 2.

Let us now turn our attention from probability generating functions to moment generating functions (mgf's). Denote by

$$M_{S_k}(z) = E\left(e^{zS_k}\right) = \sum_{t=1}^{\infty} P\left[S_k = t\right] e^{zt} = \sum_{t=1}^{\infty} f_k(t)\, e^{zt}$$

and

$$M_{T_k}(z) = E\left(e^{zT_k}\right) = \sum_{t=1}^{\infty} P\left[T_k = t\right] e^{zt}$$

the mgf's of S_k and T_k, respectively, and by

$$M_Y(z) = E\left(e^{zY_t}\right) = \begin{cases} \sum\limits_{x=1}^{\infty} P\left[Y_t = x\right] e^{zx} & \text{if } Y_t\text{'s are discrete,} \\ \int e^{zx} f_Y(x)\, dx & \text{if } Y_t\text{'s are continuous} \end{cases}$$

the common mgf of all Y_t's, $t = 1, 2, \ldots$. When Y_t's are iid continuous random variables, $f_Y(x)$ denotes the common probability density function (pdf) of the Y_t's. The mgf of S_k can then be expressed in terms of the pgf of T_k and the mgf of Y_t's as follows

$$M_{S_k}(z) = P_{T_k}\left(M_Y(z)\right).$$

Replacing $P_{T_k}(z)$ we obtain the next expression for the mgf of the compound scan statistic distribution

$$M_{S_k}(z) = E\left(z^{S_k}\right) = \frac{\left(pM_Y(z)\right)^2}{1 - qM_Y(z) - pq^{k-1}\left(M_Y(z)\right)^k} \frac{1 - \left(qM_Y(z)\right)^{k-1}}{1 - qM_Y(z)}. \quad (4)$$

Using the well known formulae for the mean and variance of a random sum of random variables,

$$E\left(S_k\right) = E\left(\sum_{t=1}^{T_k} Y_t\right) = E\left(T_k\right) E\left(Y_t\right),$$

$$Var\left(S_k\right) = Var\left(\sum_{t=1}^{T_k} Y_t\right) = E\left(T_k\right) Var\left(Y_t\right) + \left(E\left(Y_t\right)\right)^2 Var\left(T_k\right),$$

and the following expressions for the mean and variance of the scan statistic T_k (see Koutras[14])

$$E\left(T_k\right) = \frac{2 - q^{k-1}}{p\left(1 - q^{k-1}\right)},$$

$$Var(T_k) = \frac{q}{p^2} + (2k-1)\frac{q^{k-1}}{p(1-q^{k-1})^2} + \frac{q}{p^2(1-q^{k-1})^2},$$

we may readily deduce explicit expressions for the mean and the variance of S_k, namely

$$E(S_k) = \frac{2-q^{k-1}}{p(1-q^{k-1})}E(Y_t), \tag{5}$$

$$\begin{aligned} Var(S_k) &= \frac{2-q^{k-1}}{p(1-q^{k-1})}Var(Y_t) \\ &+ (E(Y_t))^2\left[\frac{q}{p^2} + (2k-1)\frac{q^{k-1}}{p(1-q^{k-1})^2} + \frac{q}{p^2(1-q^{k-1})^2}\right]. \end{aligned} \tag{6}$$

Formulae (3)-(6) can be used, at least for some simple special cases, to gain neat expressions for the pmf, pgf, and the moments of S_k.

As an illustration we mention that, if $k = 3$ and $Y_1, Y_2, \ldots$ have an exponential distribution with pdf

$$f_Y(y) = \theta e^{-\theta y},\ y > 0$$

then $M_Y(z) = E\left(e^{zY_t}\right) = \frac{\theta}{\theta - z}$, $z < \theta$ and the mgf of S_k reduces to

$$M_{S_3}(z) = \frac{(p\theta)^2\left[(p-2)\theta + z\right]}{p^2(p-2)\theta^3 + (2p+1)\theta^2 z - (p+2)\theta z^2}.$$

Likewise, if $k = 3$ and $Y_1, Y_2, \ldots$ have a geometric distribution with pmf

$$P[Y_t = y] = \theta(1-\theta)^{y-1},\ y = 1, 2, \ldots \text{ for } t = 1, 2, \ldots$$

then $P_Y(z) = E\left(z^{Y_t}\right) = \frac{\theta z}{1-(1-\theta)z}$ and the pgf of S_k reads

$$P_{S_3}(z) = \frac{(p\theta z)^2\left[(B(z))^2 - (1-p)^2\theta^2 z^2\right]}{((p\theta - 1)z + 1)\left[(B(z))^3 - p(1-p)^2\theta^3 z^3 - (1-p)\theta z(B(z))^2\right]}, \tag{7}$$

where $B(z) = (\theta - 1)z + 1$.

3 Evaluation of the probability mass function of the compound scan statistic

In the present section we shall discuss several methods for deriving the pmf of the compound scan statistic in the case where the random variables Y_t are discrete.

First of all, let us mention that, having at hand an explicit expression for the pgf of S_k (see (3)), one may easily establish a recursive scheme for the evaluation of $f_k(t) = P[S_k = t]$ at least for some simple special cases. For example if $k = 3$ and $Y_1, Y_2, \ldots$ follow a geometric distribution we have already deduced the pgf as indicated in formula (7). That result yields the following simple recursive scheme for $f_3(t) = P[S_3 = t]$, $t = 1, 2, \dots$

$$f_3(t) = 2(1 - p\theta) f_3(t-1) - \left[(1 - p\theta)^2 + (1 - p)^2 \theta^2\right] f_3(t-2)$$
$$- (1 - p)^2 (p - 2) \theta^3 \sum_{i=3}^{t-1} ((p - 2)\theta + 1)^{i-3} f_3(t - i), \; t \geq 3.$$

Using this recursion along with the obvious initial conditions $f_3(2) = (p\theta)^2$, $f_3(1) = 0$, one can easily proceed to the evaluation of the whole probability distribution of S_3.

We shall now proceed to the development of some general formulae for the evaluation of the pmf of S_k that exploit the theory of phase-type family of distributions. Eisele[6] obtained recursive schemes for the pmf of the random variable $S = \sum_{t=1}^{T} Y_t$ when $Y_1, Y_2, \dots$ is a sequence of positive valued iid discrete (or continuous) random variables with common pmf (or pdf) $f_Y(t)$ and T is a discrete random variable having a phase-type distribution of order d, that is, $T \sim PH_d(\boldsymbol{\pi}, \Lambda)$.

To implement Eisele's[6] recursive scheme we need to compute two sets of coefficients that are associated to the substochastic $d \times d$ matrix Λ. The first set $b_1, b_2, \dots, b_d$ is simply the set of coefficients of the characteristic polynomial of Λ, i.e.

$$\det(xI_d - \Lambda) = x^d + \sum_{i=1}^{d} b_i x^{d-i}$$

while the second one consists of the numbers $a_1, a_2, \dots, a_d$ generated by the following formulae

$$a_1 = P[T = 1] \text{ and } a_t = P[T = t] + \sum_{i=1}^{t-1} b_i P[T = t - i] \text{ for } t = 2, 3, \dots, d.$$

We are presenting next a lemma providing the set of coefficients involved in Eisele's[6] recursive scheme for the case of the compound scan statistic distribution.

Lemma 1. *For the distribution of the random variable T_k we have*

$$b_1 = p - 1, \; b_k = -p(1 - p)^{k-1}, \; b_2 = \dots = b_{k-1} = b_{k+1} = 0$$

and

$$a_i = \begin{cases} 0 & \text{for } i = 1, \\ p^2 (1 - p)^{i-2} & \text{for } i = 2, \dots, k, \\ 0 & \text{for } i = k + 1. \end{cases}$$

Proof. Balakrishnan and Koutras[1] have indicated that the distribution of T_k can be analyzed by imbedding it to an appropriate Markov chain with respective transition probability matrix

$$\Lambda_0 = \left[\begin{array}{cccccccc|c} 1-p & p & 0 & 0 & \cdots & 0 & 0 & 0 & 0 \\ 0 & 0 & 1-p & 0 & \cdots & 0 & 0 & 0 & p \\ 0 & 0 & 0 & 1-p & \cdots & 0 & 0 & 0 & p \\ 0 & 0 & 0 & 0 & \cdots & 0 & 0 & 0 & p \\ \vdots & \vdots & \vdots & \vdots & & \vdots & \vdots & \vdots & \vdots \\ 0 & 0 & 0 & 0 & \cdots & 0 & 1-p & 0 & p \\ 0 & 0 & 0 & 0 & \cdots & 0 & 0 & 1-p & p \\ 1-p & p & 0 & 0 & \cdots & 0 & 0 & 0 & 0 \\ \hline 0 & 0 & 0 & 0 & \cdots & 0 & 0 & 0 & 1 \end{array}\right]_{(k+2)\times(k+2)}$$

This in fact indicates that T_k belongs to the family of phase-type distributions, namely, $T_k \sim PH_{k+1}(\boldsymbol{\pi}, \Lambda)$ with $\boldsymbol{\pi} = (1, 0, \ldots, 0)' = \boldsymbol{e}_1$ and Λ the upper left $(k+1) \times (k+1)$ submatrix of Λ_0, that is,

$$\Lambda = \begin{bmatrix} 1-p & p & 0 & 0 & \cdots & 0 & 0 & 0 \\ 0 & 0 & 1-p & 0 & \cdots & 0 & 0 & 0 \\ 0 & 0 & 0 & 1-p & \cdots & 0 & 0 & 0 \\ 0 & 0 & 0 & 0 & \cdots & 0 & 0 & 0 \\ \vdots & \vdots & \vdots & \vdots & & \vdots & \vdots & \vdots \\ 0 & 0 & 0 & 0 & \cdots & 0 & 1-p & 0 \\ 0 & 0 & 0 & 0 & \cdots & 0 & 0 & 1-p \\ 1-p & p & 0 & 0 & \cdots & 0 & 0 & 0 \end{bmatrix}_{(k+1)\times(k+1)}.$$

It is not difficult to verify that the characteristic polynomial of Λ is given by

$$\det(xI_{k+1} - \Lambda) = x^{k+1} + (p-1)\,x^k + (-1)^k\,(p-1)^{k-1}\,px;$$

hence $b_1 = p - 1$, $b_k = -p\,(1-p)^{k-1}$, and $b_2 = \cdots = b_{k-1} = b_{k+1} = 0$.

On the other hand, it is obvious that $P[T_k = 0] = P[T_k = 1] = 0$ and

$$P[T_k = i] = (i-1)\,p^2 q^{i-2} \text{ for } 1 < i \le k.$$

Since T_k satisfies the following recurrence relation

$$P[T_k = i] = qP[T_k = i-1] + pq^{k-1}P[T_k = i-k] \text{ for } i > k,$$

we get $P[T_k = k+1] = (k-1)\,p^2 q^{k-1}$. Therefore

$$\begin{aligned} a_1 &= P[T_k = 1] = 0, \\ a_i &= P[T_k = i] + \sum_{j=1}^{i-1} b_j P[T_k = i-j] \\ &= (i-1)\,p^2 q^{i-2} + b_1 P[T_k = i-1] = p^2\,(1-p)^{i-2} \text{ for } 1 < i \le k, \\ a_{k+1} &= P[T_k = k+1] + \sum_{j=1}^{k} b_j P[T_k = k+1-j] \\ &= (k-1)\,p^2 q^{k-1} + b_1 P[T_k = k] + b_k P[T_k = 1] = 0. \end{aligned}$$

■

Eisele[6] obtained the next recursion for the pmf of the random variable $S = \sum_{t=1}^{T} Y_t$ when T has a discrete phase-type distribution of order d and $Y_1, Y_2, \ldots$ is a sequence of positive valued iid random variables independent of T:

$$P[S=t] = \sum_{j=1}^{\min(d,t)} a_j f_Y^{*j}(t) - \sum_{j=1}^{\min(d,t-1)} b_j \left(\sum_{u=1}^{t-1} P[S=u] f_Y^{*j}(t-u) \right)$$

for $t \geq 1$, where $f_Y^{*j}(t)$ is the j-th convolution of $Y_1, Y_2, \ldots, Y_j$, i.e.

$$f_Y^{*j}(t) = P\left[\sum_{i=1}^{j} Y_i = t \right], \; j = 1, 2, \ldots.$$

Making use of this result, we may now readily establish an efficient set of recurrence relations for S_k.

Proposition 1. *Assume that the support of the random variables $Y_1, Y_2, \ldots$ is $\{y_0, y_0+1, \ldots\}$ and denote by $f_Y^{*j}(t)$ the j-th convolution of $Y_1, Y_2, \ldots, Y_j$. Then the pmf of S_k obeys the following recursive scheme*

$$f_k(t) = \begin{cases} \sum\limits_{j=2}^{k} p^2 (1-p)^{j-2} f_Y^{*j}(t) & \\ -(p-1) \sum\limits_{u=1}^{t-1} f_k(u) P[Y=t-u] & \\ -p(1-p)^{k-1} \sum\limits_{u=1}^{t-1} f_k(u) f_Y^{*k}(t-u) & \text{if } t > y_0 k, \\ \sum\limits_{j=2}^{k} p^2 (1-p)^{j-2} f_Y^{*j}(t) & \\ -(p-1) \sum\limits_{u=1}^{t-1} f_k(u) P[Y=t-u] & \text{if } 1 < t \leq y_0 k, \end{cases}$$

with initial conditions $f_k(0) = f_k(1) = 0$.

Proof. Since T_k has a discrete phase-type distribution of order $k+1$ and $Y_1, Y_2, \ldots$ is a sequence of positive valued iid random variables independent of T_k, one can apply Eisele's[6] result to obtain the next recurrence relation for the pmf of $S_k = \sum_{t=1}^{T_k} Y_t$:

$$\begin{aligned} f_k(t) &= P[S_k = t] \\ &= \sum_{j=1}^{\min(d,t)} a_j f_Y^{*j}(t) - \sum_{j=1}^{\min(d,t-1)} b_j \left(\sum_{u=1}^{t-1} P[S_k=u] f_Y^{*j}(t-u) \right) \\ &= \sum_{j=1}^{\min(d,t)} a_j f_Y^{*j}(t) - \sum_{j=1}^{\min(d,t-1)} b_j \left(\sum_{u=1}^{t-1} f_k(u) f_Y^{*j}(t-u) \right) \text{ for } t \geq 2. \end{aligned}$$

The result follows immediately by replacing the coefficients a_j and b_j, $j = 1, 2, \ldots, k+1$ obtained in Lemma 1. ■

It is of interest to note that, when the random variables $Y_1, Y_2, \ldots$ follow a phase-type distribution, one can evaluate the pmf of S_k by the aid of an exact formula similar to (1). This can be achieved by exploiting the following important result provided by Neuts[18]:

Proposition 2 (Neuts[18]). *If $\{f_N(v)\}$ and $\{f_X(t)\}$ are the pmf's of two discrete phase-type distributions $PH_d(\boldsymbol{\pi}, \Lambda)$ and $PH_c(\boldsymbol{\rho}, M)$ of orders d and c, respectively, then the mixture*

$$\sum_{v=0}^{\infty} f_N(v)\, f_X^{*v}(t)$$

follows a phase-type distribution $PH_{cd}(\boldsymbol{\sigma}, \Sigma)$ of order cd, with parameters

$$\boldsymbol{\sigma} = \boldsymbol{\rho} \otimes \boldsymbol{\pi}\left(I_d - \alpha\Lambda\right)^{-1},$$

$$\Sigma = M \otimes I_d + \boldsymbol{u}\boldsymbol{\rho}' \otimes \left(I_d - \alpha\Lambda\right)^{-1}\Lambda,$$

where $\alpha = 1 - \boldsymbol{\rho}'\mathbf{1}$ and $\boldsymbol{u} = (I_c - M)\,\mathbf{1}$.

The notation $A \otimes B$ appearing above has been used to indicate the Kronecker product of two matrices A and B, that is, if $A = (a_{ij})_{n_1 \times n_2}$, then

$$A \otimes B = \begin{bmatrix} a_{11}B & a_{12}B & \cdots & a_{1n_2}B \\ a_{21}B & a_{22}B & \cdots & a_{2n_2B} \\ \vdots & \vdots & & \vdots \\ a_{n_11}B & a_{n_12}B & \cdots & a_{n_1n_2}B \end{bmatrix}.$$

Proposition 3. *Assume that the random variables $Y_1, Y_2, \ldots$ follow a phase-type distribution $PH_c(\boldsymbol{\rho}, M)$ of order c. Then $S_k = \sum_{t=1}^{T_k} Y_t$ follows a phase-type distribution $PH_{c(k+1)}(\boldsymbol{\sigma}, \Sigma)$ of order $c\,(k+1)$ with parameters*

$$\boldsymbol{\sigma} = \boldsymbol{\rho} \otimes \boldsymbol{e}_1\left(I_{k+1} - \alpha\Lambda\right)^{-1}$$

and

$$\Sigma = M \otimes I_{k+1} + \boldsymbol{u}\boldsymbol{\rho}' \otimes \left(I_{k+1} - \alpha\Lambda\right)^{-1}\Lambda,$$

where $\alpha = 1 - \boldsymbol{\rho}'\mathbf{1}$ and $\boldsymbol{u} = (I_c - M)\,\mathbf{1}$. Therefore, the pmf of S_k can be expressed as

$$f_k(t) = P\left[S_k = t\right] = \boldsymbol{\sigma}'\Sigma^{t-1}\left(I_{c(k+1)} - \Sigma\right)\mathbf{1},\ t = 1, 2, \ldots.$$

Proof. By conditioning on the value of the scan statistic T_k and then using the independence between T_k and Y_i's, we obtain

$$\begin{aligned} f_k(t) &= P\left[\sum_{i=1}^{T_k} Y_i = t\right] = \sum_{j=2}^{\infty} P\left[\sum_{i=1}^{T_k} Y_i = t \,\middle|\, T_k = j\right] P\left[T_k = j\right] \\ &= \sum_{j=2}^{\infty} P\left[\sum_{i=1}^{j} Y_i = t \,\middle|\, T_k = j\right] P\left[T_k = j\right] \\ &= \sum_{j=2}^{\infty} P\left[\sum_{i=1}^{j} Y_i = t\right] P\left[T_k = j\right] = \sum_{j=2}^{\infty} f_{T_k}(j)\, f_Y^{*j}(t). \end{aligned}$$

Since $Y_i \sim PH_c(\boldsymbol{\rho}, M)$, $i = 1, 2, \ldots$ and $T_k \sim PH_{k+1}(\boldsymbol{\pi}, \Lambda)$ with $\boldsymbol{\pi} = (1, 0, \ldots, 0)' = \boldsymbol{e}_1$ and

$$\Lambda = \begin{bmatrix} 1-p & p & 0 & 0 & \cdots & 0 & 0 & 0 \\ 0 & 0 & 1-p & 0 & \cdots & 0 & 0 & 0 \\ 0 & 0 & 0 & 1-p & \cdots & 0 & 0 & 0 \\ 0 & 0 & 0 & 0 & \cdots & 0 & 0 & 0 \\ \vdots & \vdots & \vdots & \vdots & & \vdots & \vdots & \vdots \\ 0 & 0 & 0 & 0 & \cdots & 0 & 1-p & 0 \\ 0 & 0 & 0 & 0 & \cdots & 0 & 0 & 1-p \\ 1-p & p & 0 & 0 & \cdots & 0 & 0 & 0 \end{bmatrix}_{(k+1)\times(k+1)},$$

we can easily apply Proposition 2 and the proof is complete. ∎

As an illustration, let $k = 3$ and assume that $Y_1, Y_2, \ldots$ have a geometric distribution with pmf

$$P[Y_i = y] = \theta(1-\theta)^{y-1}, \ y = 1, 2, \ldots \text{ for } i = 1, 2, \ldots$$

Then the distribution of $Y_1, Y_2, \ldots$ can be considered as a phase-type distribution $PH_c(\boldsymbol{\rho}, M)$ of order $c = 1$ with $\boldsymbol{\rho} = (1)_{1\times 1}$ and $M = (1-\theta)_{1\times 1}$. Using these quantities in the formulae given in Proposition 3 we obtain

$$\alpha = 1 - \boldsymbol{\rho}'\mathbf{1} = 0,$$

$$\boldsymbol{u} = (I_c - M)\,\mathbf{1} = (\theta)_{1\times 1},$$

$$\boldsymbol{\sigma} = \boldsymbol{\rho} \otimes \boldsymbol{e}_1 (I_4 - \alpha\Lambda)^{-1} = (\boldsymbol{e}_1)_{4\times 1},$$

and

$$\begin{aligned} \Sigma &= M \otimes I_4 + \boldsymbol{u}\boldsymbol{\rho}' \otimes (I_4 - \alpha\Lambda)^{-1}\Lambda \\ &= \begin{bmatrix} 1-\theta & 0 & 0 & 0 \\ 0 & 1-\theta & 0 & 0 \\ 0 & 0 & 1-\theta & 0 \\ 0 & 0 & 0 & 1-\theta \end{bmatrix} + \begin{bmatrix} \theta(1-p) & \theta p & 0 & 0 \\ 0 & 0 & \theta(1-p) & 0 \\ 0 & 0 & 0 & \theta(1-p) \\ \theta(1-p) & \theta p & 0 & 0 \end{bmatrix} \\ &= \begin{bmatrix} 1-\theta p & \theta p & 0 & 0 \\ 0 & 1-\theta & \theta(1-p) & 0 \\ 0 & 0 & 1-\theta & \theta(1-p) \\ \theta(1-p) & \theta p & 0 & 1-\theta \end{bmatrix}. \end{aligned}$$

It is now obvious that $\Sigma\mathbf{1} = (1, 1-\theta p, 1-\theta p, 1)' = \mathbf{1} - \theta p(\boldsymbol{e_2} + \boldsymbol{e_3})$ and $(I_4 - \Sigma)\,\mathbf{1} = \mathbf{1} - \Sigma\mathbf{1} = \theta p(\boldsymbol{e_2} + \boldsymbol{e_3})$. Therefore, the pmf of S_k can be evaluated by the matrix formula

$$f_3(t) = P[S_3 = t] = \theta p \boldsymbol{e}_1' \Sigma^{t-1}(\boldsymbol{e}_2 + \boldsymbol{e}_3), \ t = 1, 2, \ldots.$$

4 Numerical results

In Figures 1, 2, and 3 we have plotted the pmf of the compound scan statistic S_k for $k = 3$, $k = 4$, and $k = 5$, respectively, in the special case when $Y_1, Y_2, \ldots$ have a geometric distribution with pmf $P[Y_i = y] = \theta(1-\theta)^{y-1}$, for $i = 1, 2, \ldots$. In our analysis, we used two different sets of values for the parameters p and θ. As made clear from those figures, the shape of the distribution of S_k is unimodal in all the graphs.

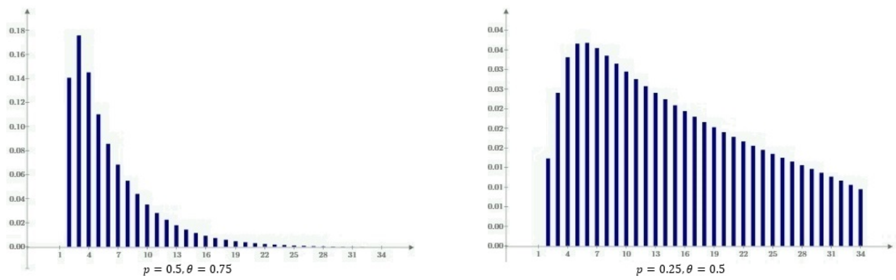

Fig. 1. Compound scan statistic distribution for $k = 3$

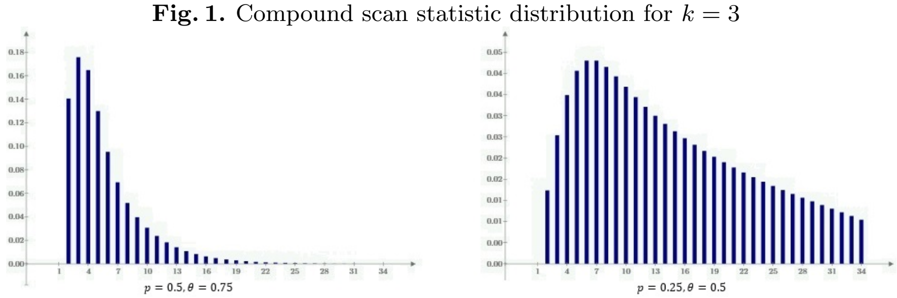

Fig. 2. Compound scan statistic distribution for $k = 4$

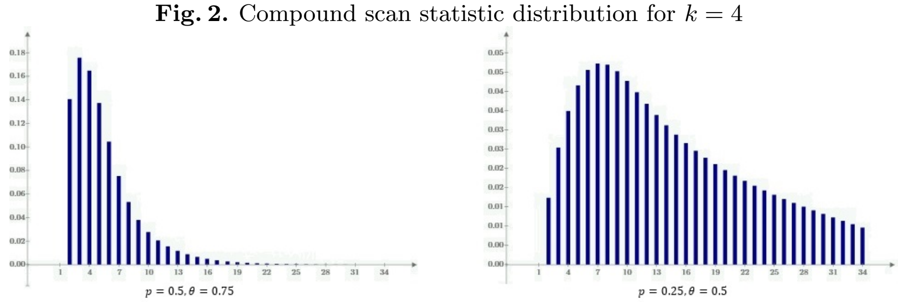

Fig. 3. Compound scan statistic distribution for $k = 5$

In Table 1, for a fixed k, namely $k = 3$, the CPU times for computing the pmf of S_k by the use of the recursive formula (given in Proposition 1) and the nonrecursive formula (given in Proposition 3) are presented. The recursive formula takes much more time than the nonrecursive one. Therefore, if the random variables $Y_1, Y_2, \ldots$ have a phase-type distribution, the matrix-based nonrecursive formula seems to be more efficient.

t	Method Used	CPU Time	t	Method Used	CPU Time
10	Recursive formula	$\leq$ 1 second	16	Recursive formula	$\approx$ 40 seconds
	Nonrecursive formula	$\leq$ 1 second		Nonrecursive formula	$\leq$ 1 second
12	Recursive formula	$\approx$ 2 seconds	18	Recursive formula	$\approx$ 5.5 minutes
	Nonrecursive formula	$\leq$ 1 second		Nonrecursive formula	$\leq$ 1 second
14	Recursive formula	$\approx$ 5 seconds	20	Recursive formula	$>$ 20 minutes
	Nonrecursive formula	$\leq$ 1 second		Nonrecursive formula	$\leq$ 1 second

Table 1. CPU times for $P\left[S_3 = t\right]$ for several values of t when Y_t's follow a geometric distribution

k	p	θ	μ	σ	$P\left[S_k > \mu\right]$	k	p	θ	μ	σ	$P\left[S_k > \mu\right]$
3	0.25	0.05	262.857	241.624	0.36947	10	0.25	0.05	166.494	127.446	0.38667
		0.25	52.571	47.888	0.36919			0.25	33.299	24.961	0.38872
		0.50	26.286	23.668	0.36492			0.50	16.649	12.143	0.38872
		0.75	17.524	15.592	0.36837			0.75	11.100	7.863	0.36067
		0.90	14.603	12.900	0.37048			0.90	9.250	6.434	0.36439
	0.50	0.05	55.111	40.209	0.39231		0.50	0.05	80.078	56.164	0.40258
		0.25	11.022	7.474	0.36904			0.25	16.016	10.647	0.38793
		0.50	5.511	3.348	0.38779			0.50	8.008	4.933	0.36708
		0.75	3.674	1.938	0.40674			0.75	5.339	3.006	0.38147
		0.90	3.062	1.449	0.24822			0.90	4.449	2.352	0.39098
	0.75	0.05	93.333	75.982	0.37654		0.75	0.05	53.333	36.999	0.40426
		0.25	18.667	14.697	0.37917			0.25	10.667	6.799	0.41472
		0.50	9.333	7.024	0.36164			0.50	5.333	2.981	0.38147
		0.75	6.222	4.456	0.34278			0.75	3.556	1.663	0.40674
		0.90	5.185	3.595	0.33208			0.90	2.963	1.194	0.54438
	0.90	0.05	44.669	31.163	0.40628		0.90	0.05	44.444	30.712	0.40528
		0.25	8.934	5.630	0.43316			0.25	8.889	5.533	0.43240
		0.50	4.467	2.386	0.39149			0.50	4.444	2.331	0.39098
		0.75	2.978	1.240	0.54438			0.75	2.963	1.194	0.54438
		0.90	2.482	0.808	0.34390			0.90	2.469	0.761	0.34390
	0.95	0.05	42.158	29.167	0.40103		0.95	0.05	42.105	29.057	0.40079
		0.25	8.432	5.223	0.39920			0.25	8.421	5.200	0.39900
		0.50	4.216	2.171	0.35105			0.50	4.211	2.157	0.35091
		0.75	2.811	1.076	0.49234			0.75	2.807	1.064	0.49234
		0.90	2.342	0.643	0.26898			0.90	2.339	0.630	0.26898
4	0.25	0.05	218.378	193.514	0.36943	20	0.25	0.05	160.340	123.813	0.40430
		0.25	43.676	38.249	0.37084			0.25	32.068	22.192	0.39727
		0.50	21.838	18.837	0.37510			0.50	16.034	10.729	0.38793
		0.75	14.559	12.363	0.36937			0.75	10.689	6.889	0.41472
		0.90	12.132	10.204	0.35409			0.90	8.908	5.618	0.43240
	0.50	0.05	85.714	66.240	0.38592		0.50	0.05	80.000	55.858	0.40258
		0.25	17.143	12.720	0.37075			0.25	16.000	10.583	0.38793
		0.50	8.571	6.014	0.38066			0.50	8.000	4.899	0.36708
		0.75	5.714	3.764	0.38889			0.75	5.333	2.981	0.38147
		0.90	4.762	3.008	0.39098			0.90	4.444	2.331	0.39098
	0.75	0.05	53.757	37.984	0.40519		0.75	0.05	53.333	36.998	0.40426
		0.25	10.751	7.008	0.41535			0.25	10.667	6.799	0.41472
		0.50	5.376	3.097	0.38174			0.50	5.333	2.981	0.38147
		0.75	3.584	1.751	0.40674			0.75	3.556	1.663	0.40674
		0.90	2.986	1.278	0.54438			0.90	2.963	1.194	0.54438
	0.90	0.05	44.467	30.771	0.40532		0.90	0.05	44.444	30.712	0.40528
		0.25	8.893	5.546	0.43242			0.25	8.889	5.533	0.43240
		0.50	4.447	2.338	0.39098			0.50	4.444	2.331	0.39098
		0.75	2.964	1.201	0.54438			0.75	2.963	1.194	0.54438
		0.90	2.470	0.768	0.34390			0.90	2.469	0.761	0.34390
	0.95	0.05	42.108	29.065	0.40080		0.95	0.05	42.105	29.057	0.40079
		0.25	8.422	5.201	0.39900			0.25	8.421	5.200	0.39900
		0.50	4.211	2.158	0.35091			0.50	4.211	2.157	0.35091
		0.75	2.807	1.065	0.49234			0.75	2.807	1.064	0.49234
		0.90	2.339	0.631	0.26898			0.90	2.339	0.630	0.26898
5	0.25	0.05	197.029	169.013	0.36928	30	0.25	0.05	160.019	112.539	0.40430
		0.25	39.406	33.333	0.36837			0.25	32.004	21.932	0.39727
		0.50	19.703	16.368	0.37288			0.50	16.002	10.595	0.38793
		0.75	13.135	10.710	0.35508			0.75	10.668	6.807	0.41472
		0.90	10.946	8.822	0.38585			0.90	8.890	5.540	0.43240
	0.50	0.05	82.667	61.586	0.39345		0.50	0.05	80.000	55.857	0.40258
		0.25	16.533	11.768	0.39148			0.25	16.000	10.583	0.38793
		0.50	8.267	5.522	0.36961			0.50	8.000	4.889	0.36708
		0.75	5.511	3.423	0.38147			0.75	5.333	2.981	0.38147
		0.90	4.593	2.715	0.39098			0.90	4.444	2.331	0.39098
	0.75	0.05	53.438	37.298	0.40435		0.75	0.05	53.333	36.998	0.40426
		0.25	10.688	6.863	0.41476			0.25	10.667	6.779	0.41472
		0.50	5.344	3.017	0.38147			0.50	5.333	2.981	0.38147
		0.75	3.563	1.691	0.40674			0.75	3.556	1.663	0.40674
		0.90	2.969	1.221	0.54438			0.90	2.963	1.194	0.54438
	0.90	0.05	44.447	30.719	0.40528		0.90	0.05	44.444	30.712	0.40528
		0.25	8.889	5.535	0.43240			0.25	8.889	5.533	0.43240
		0.50	4.445	2.332	0.39098			0.50	4.444	2.331	0.39098
		0.75	2.963	1.195	0.54438			0.75	2.963	1.194	0.54438
		0.90	2.469	0.762	0.34390			0.90	2.469	0.761	0.34390
	0.95	0.05	42.105	29.058	0.40079		0.95	0.05	42.105	29.057	0.40079
		0.25	8.421	5.200	0.39900			0.25	8.421	5.200	0.39900
		0.50	4.211	2.157	0.35091			0.50	4.211	2.157	0.35091
		0.75	2.807	1.064	0.49234			0.75	2.807	1.064	0.49234
		0.90	2.339	0.630	0.26898			0.90	2.339	0.630	0.26898

Table 2. Values of $\mu = E\left(S_k\right)$, σ, where $\sigma^2 = Var\left(S_k\right)$, and $P\left[S_k > \mu\right]$ for several values of k, p, and θ

Finally, in Table 2 we present the mean $\mu = E(S_k)$, the standard deviation σ, where $\sigma^2 = Var(S_k)$, and the probability $P[S_k > \mu]$ for several values of k, p, and θ. The mean times, standard deviations, and the respective probabilities provided in Table 2 may be of special interest for a regulator practicing the stress test model mentioned in the introduction, in order to set up a plan that will acquire specific achievements (e.g. initiate early signals for Capital Ratio deterioration of a monitored bank).

References

1. N. Balakrishnan and M.V. Koutras. *Runs and Scans with Applications*, Wiley, New York, 2002.
2. A. Berger, R. DeYoung, M. Flannery, D. Lee and O. Oztekin. How do large banking organizations manage their capital ratios? *Journal of Financial Services Research*, 34, 123–149, 2008.
3. N.L. Bowers, J.C. Hickman, H.U. Gerber, C.J. Nesbitt and D.A.Jones. *Actuarial Mathematics (2nd Edition)*, Society of Actuaries, Schaumburg, Illinois, 1997.
4. J. Chen and J. Glaz. Approximations and inequalities for the distribution of a scan statistic for 0-1 Bernoulli trials. *In Advances in Combinatorial Methods and Applications to Probability and Statistics (Ed. N. Balakrishnan)*, Birkhaeuser, Boston, 1997.
5. R. Demstez, M. Saidenberg and P. Strahan. Banks with something to lose: The disciplinary role of franchise value. *Federal Reserve Bank of New York Economic Policy Review*, 2, 1-14, 1996.
6. K.-T. Eisele. Recursions for compound phase distributions. *Insurance: Mathematics & Economics*, 38, 149–156, 2006.
7. A. Estrella, S. Park and S. Peristiani. Capital ratios as predictors of bank failure, *Federal Reserve Bank of New York Economic Policy Review*, 6, 33–52, 2000.
8. M. Flannery and S. Sorescu. Evidence of bank market discipline on subordinated debenture yields: 1983-1991. *Journal of Finance* 51, 1347–1377, 1996.
9. J. Glaz. Moving window detection for discrete-data. *IEEE Transactions on Information Theory*, 29, 457–462, 1983.
10. J. Glaz and J. Naus. Tight bounds and approximations for scan statistic probabilities for discrete data. *The Annals of Applied Probability*, 1, 306–318, 1991.
11. L. Goldberg and S. Hudgins. Depositor discipline and changing strategies for regulating thrift institutions, *Journal of Financial Economics*, 63, 263–274, 2002.
12. I. Greenberg. The first occurrence of n successes in N trials. *Technometrics*, 12, 627–634, 1970.
13. Q.-M. He. *Fundamentals of Matrix-Analytic Methods*, Springer, New York, 2014.
14. M.V. Koutras. On a waiting time distribution in a sequence of Bernoulli trials. *Annals of the Institute of Statistical Mathematics*, 48, 789–806, 1996.
15. M.V. Koutras and S. Eryilmaz. Compound geometric distribution of order k. Submitted for publication.
16. V.M. Koutras and K. Drakos. A migration approach for USA banks' capitalization: Are the 00s the same with the 90s? *International Review of Financial Analysis*, 30, 131–140, 2013.
17. K. Lindquist. Banks buffer capital: How important is risk? *Journal of International Money and Finance*, 23, 493–513, 2004.
18. M.F. Neuts. *Matrix-Geometric Solutions in Stochastic Models: An Algorithmic Approach*, The Johns Hopkins University Press, Baltimore, 1981.
19. B. Saperstein. On the occurrence of n successes within N Bernoulli Trials, *Technometrics*, 15, 809–818, 1973.

New bounds for the scan statistic distribution via a N-demimartingale approach

Markos V. Koutras[1] and Demetrios P. Lyberopoulos[2]

[1] Department of Statistics and Insurance Science, 80 Karaoli and Dimitriou street, University of Piraeus, Piraeus, Greece
(E-mail: `mkoutras@unipi.gr`)
[2] Department of Statistics and Insurance Science, 80 Karaoli and Dimitriou street, University of Piraeus, Piraeus, Greece
(E-mail: `dilyber@webmail.unipi.gr`)

Abstract. The concept of pattern arises in many applications comprising experimental trials with two or more possible outcomes in each trial. A binary scan of type r/k is a special pattern referring to success-failure strings of fixed length k that contain at least r-successes, where r, k are positive integers with $r \leq k$. The task of determining explicitly, in a sequence of independent and identically distributed binary trials (with probability of success p), the probability distribution of the waiting time $T_r^{(k)}$ for the first occurrence of a scan of type r/k becomes extremely difficult and computationally intractable, when r takes values either too large or not quite close to k. In the present work, some new maximal inequalities for nonnegative N-demi(super)martingales are proven and then new bounds for the cumulative distribution function of $T_r^{(k)}$ are obtained. A numerical study is also carried out for investigating the behavior of the new bounds for various values of the parameters r, k, p.
Keywords: scan statistic, bound, N-demimartingale, N-demisupermartingale, demimartingale, demisubmartingale, i.i.d. binary trials..

1 Introduction and Preliminaries

By $\mathbb{N}$ is denoted the set of all natural numbers, while $\mathbb{N}_0 := \mathbb{N} \cup \{0\}$. The symbol $\mathbb{R}$ stands for the set of all real numbers, while $\mathbb{R}_+ := \{x \in \mathbb{R} : x \geq 0\}$. If $d \in \mathbb{N}$, then $\mathbb{R}^d$ denotes the Euclidean space of dimension d. Moreover, $x \wedge y := \min\{x, y\}$, $x \vee y := \max\{x, y\}$ and $x^+ := x \vee 0$ for $x, y \in \mathbb{R}$. For $n \in \mathbb{N}$ and $i \in \{1, \dots, n\}$ the i-canonical projection from $\mathbb{R}^n$ onto $\mathbb{R}$ is denoted by π_i.

Throughout the paper we consider an arbitrary but fixed probability space (Ω, Σ, P). A set $N \in \Sigma$ with $P(N) = 0$ is called a P**-null set**. The family of all P-null sets is denoted by Σ_0. For any two Σ-measurable maps Z_1, Z_2 on Ω we write $Z_1 = Z_2$ $P-$ almost surely (P-a.s. for short), if $\{Z_1 \neq Z_2\} \in \Sigma_0$.

Let $\{X_n\}_{n\in\mathbb{N}}$ be a sequence of binary trials on (Ω, Σ, P), each resulting in either a *success* (that is the event $\{X_n = 1\}$) or a *failure* (that is $\{X_n = 0\}$) with probability $p \in (0, 1)$ or $q := 1-p$, respectively. Then, for any fixed $k \in \mathbb{N}$ and for each $m \in \mathbb{N}$ such that $m \leq k$, the sequence $X_n, X_{n+1}, \dots, X_{n+m-1}$ of random variables on Ω is said to be a **moving window (for $\{X_n\}_{n\in\mathbb{N}}$) of**

16^{th} *ASMDA Conference Proceedings, 30 June – 4 July 2015, Piraeus, Greece*

length m**.** In particular, the term **(**$P-$**)scan** or **(**$P-$**)generalized run of type** r/k refers to moving windows $X_n, X_{n+1}, \ldots, X_{n+m-1}$ of length $m \leq k$ such that the number of successes contained therein is (with non zero probability) at least r.

In what follows, we set $X_0 := 0$ *and assume that every sum over an empty index set is equal to zero.* For each $n \in \mathbb{N}$ and $k \in \mathbb{N}_0$ consider the random variable $Y_{n,k}$ on Ω defined by

$$Y_{n,k} := \sum_{j=\max\{n-k+1,1\}}^{n} X_j. \tag{1}$$

For any fixed $k \in \mathbb{N}$ the sequence $\{Y_{n,k}\}_{n\in\mathbb{N}}$ will be called **the enumerating process** of scanning width k for the sequence of binary trials $\{X_n\}_{n\in\mathbb{N}}$.

The random variable $T_r^{(k)}$ defined on Ω by means of

$$T_r^{(k)} := \min\{n \in \mathbb{N} : Y_{n,k} \geq r\}$$

is said to be **the waiting time for the first occurrence of a scan of type** r/k. The importance of the above waiting time arises from the widespread applicability of scan enumerating statistics in a substantial number of scientific areas such as reliability theory and molecular biology. For more details, we refer e.g. to Balakrishnan and Koutras [1].

In Bersimis et al. [2], a systematic approach for studying the waiting time $T_r^{(k)}$ for an *almost perfect run* (i.e. a r/k-scan with $r \in \{k-1, k-2\}$), in a sequence of Bernoulli trials, is made possible via a recursive scheme. In this paper, the problem of determining, in a sequence of independent and identically distributed (i.i.d. for short) binary trials, the probability distribution of the waiting time $T_r^{(k)}$ is investigated under a different perspective. More precisely, we focus on obtaining bounds for the cumulative distribution function (c.d.f. for short) of $T_r^{(k)}$ instead of computing it explicitly. Even though the latter may seem as a drawback to our approach, we should point out that on the other side of the balance the extracted results apply not only for almost perfect runs but also for any kind of scan. Furthermore, bounds are widely used in the study of scans and runs as an extensive literature related to this topic witnesses (cf e.g. [1] for more details).

Since it is clear that for any fixed $k \in \mathbb{N}$ the sequence $\{Y_{n,k}\}_{n\in\mathbb{N}}$ is not P-independent, and since it can be easily proven that for any fixed $k \in \mathbb{N}$ and for all $r, k, t \in \mathbb{N}$ with $r \leq k$ condition

$$\{T_r^{(k)} \leq t\} = \big\{\max_{1\leq n\leq t} Y_{n,k} \geq r\big\}$$

holds true, it seems reasonable enough to wonder whether maximal inequalities can be exploited for obtaining some upper and lower bounds for the c.d.f. $F_{r:k}(t;p) := P(T_r^{(k)} \leq t)$, see also e.g. [5], Chapters 2 and 3.

Motivated by the above question, in Section 2 and under the assumption of i.i.d. binary trials $\{X_n\}_{n\in\mathbb{N}}$, the membership of $\{Y_{n,k}\}_{n\in\mathbb{N}}$, for $k \in \mathbb{N}$ fixed, in the classes of demi(sub)martingales and N-demi(super)martingales is first examined and then a relative N-demimartingale result is given (see Proposition 1). Next, in Section 3, some new maximal inequalities for nonnegative N-demi(super)martingales are proven. As a consequence, some bounds for the c.d.f. of the waiting time $T_r^{(k)}$ in a sequence of i.i.d. binary trials are extracted in Section 4. This paper concludes with Section 5 (and its Appendix), where an investigation on the behavior of our new bounds for various values of the parameters r, k, p is carried out.

2 Some results related to the enumerating process

We first recall some notions more, needed in this section.

By $\sigma(Z) := \{Z^{-1}(B) : B \in \mathfrak{B}\}$ is denoted the σ-algebra generated by the Σ-measurable function Z, where $\mathfrak{B} := \mathfrak{B}(\mathbb{R})$ stands for the Borel σ-algebra of subsets of $\mathbb{R}$. Setting $T_Z := \{B \subseteq \mathbb{R} : \ Z^{-1}(B) \in \Sigma\}$, we clearly get that $\mathfrak{B} \subseteq T_Z$. Then we denote by $P_Z : T_Z \longrightarrow \mathbb{R}$ the **image measure of** P **under** Z. The restriction of P_Z to $\mathfrak{B}$ is denoted again by P_Z, while R_Z stands for the range of Z. The notation $\mathbf{B}(n,p)$, where $n \in \mathbb{N}$ and $p \in (0,1)$, stands for the law of binomial distribution. Moreover, its probability mass and cumulative distribution function at point $x \in \mathbb{R}$ will be denoted by $b(x; n, p)$ and $F_b(x; n, p)$, respectively.

The family of all real-valued P-integrable functions on Ω is denoted by $\mathcal{L}^1(P)$. Functions that are P-a.s. equal are not identified. The (unconditional) expectation of the random variable Z is denoted by $\mathbb{E}_P[Z]$. If $Z \in \mathcal{L}^1(P)$ and $\mathcal{F}$ is a σ-subalgebra of Σ, then each function $\widetilde{Z} \in \mathcal{L}^1(P \mid \mathcal{F})$ satisfying for each $F \in \mathcal{F}$ the equality $\int_F Z\,dP = \int_F \widetilde{Z}\,dP$ is said to be a **version of the conditional expectation of** Z **given** $\mathcal{F}$, and it will be denoted by $\mathbb{E}_P[Z \mid \mathcal{F}]$. Furthermore, for any $E \in \Sigma$ we set $P(E \mid F) := \mathbb{E}_P[\chi_E \mid \mathcal{F}]$, where χ_E stands for the indicator (or characteristic) function of the set E. Note that if W is a random variable on Ω then $\mathbb{E}_P[Z \mid W] = \mathbb{E}_P[Z \mid \sigma(W)] \ \ P \mid \sigma(W)$-a.s., while for any $A \in \Sigma$ with $P(A) > 0$ we have $\mathbb{E}_P[Z \mid A] = \frac{1}{P(A)} \int_A Z dP$.

Every family $\{\mathcal{F}_j\}_{j\in\mathbb{N}}$ of σ-subalgebras of Σ, such that $\mathcal{F}_j \subseteq \mathcal{F}_{j+1}$ for each $j \in \mathbb{N}$, is called a **filtration** for the measurable space (Ω, Σ). Moreover, a sequence $\{Z_j\}_{j\in\mathbb{N}}$ of random variables on Ω is said to be **adapted to a filtration** $\{\mathcal{F}_j\}_{j\in\mathbb{N}}$ if each Z_j is $\mathcal{F}_j$-measurable. If $\mathcal{F}_j = \sigma(\bigcup_{i=1}^{j} \sigma(Z_i))$ for each $j \in \mathbb{N}$, then $\{\mathcal{F}_j\}_{j\in\mathbb{N}}$ is said to be the **canonical filtration** for $\{Z_j\}_{j\in\mathbb{N}}$, and it will be denoted by $\{\mathcal{F}_j^{(Z)}\}_{j\in\mathbb{N}}$.

Definitions 1 Let $\{Z_j\}_{j\in\mathbb{N}}$ be a sequence in $\mathcal{L}^1(P)$. Then $\{Z_j\}_{j\in\mathbb{N}}$ is said to be:
(a) a P**-martingale** (with respect to $\{\mathcal{F}_j^{(Z)}\}_{j\in\mathbb{N}}$), if

$$\mathbb{E}_P[(Z_{j+1} - Z_j) f(Z_1, \ldots, Z_j)] = 0 \quad \text{for each } j \in \mathbb{N} \tag{2}$$

and for every measurable function f on $\mathbb{R}^j$ such that the above expectations exist.

(b) a P**-demimartingale**, if condition (2) but with "$\geq$" in the place of the equality is satisfied for every coordinatewise nondecreasing function f on $\mathbb{R}^j$ such that the above expectations exist.
(c) a P**-demisubmartingale**, if condition (2) but with "$\geq$" in the place of the equality is satisfied for every f as in (b) but with $f \geq 0$.
(d) a N**-demimartingale under** P, if condition (2) but with "$\leq$" in the place of the equality is satisfied for every f as in (b). In particular, if $f \geq 0$ then $\{Z_j\}_{j\in\mathbb{N}}$ is said to be a N**-demisupermartingale under** P**.**

Remark 1 Obviously, the class of all P-martingales is included in that of all P-demimartingales, which in its own turn is a subclass of all P - demisubmartingales. For more on Definitions 1 we refer to [5], Section 2.1. It is also clear that any N-demimartingale (under P) is also a N-demisupermartingale. For details on the last two classes of processes, see e.g. [5], Section 3.1.

In what follows, unless it is stated otherwise, we assume that $\{X_n\}_{n\in\mathbb{N}}$ *is a* P*-i.i.d. sequence of binary trials.*

The next result is an immediate consequence of the definition of conditional expectation and the monotonicity of the involved functions.

Lemma 1 *Let* $k \in \mathbb{N}$ *be arbitrary but fixed. For each* $n \in \mathbb{N}$ *with* $n \geq k$ *also let* f *be a coordinatewise nondecreasing real-valued function on* $\mathbb{R}^n$ *as well as* $\{h_{i,k}\}_{i\in\{1,\ldots,n\}}$ *be a sequence of such functions on* $\mathbb{R}^{i\wedge k}$*. Then for each* $n \in \mathbb{N}$ *with* $n \geq k$ *the following holds true:*

$$\eta_{n,k,0}(h_{i,k}; f) \leq \eta_{n,k,1}(h_{i,k}; f),$$

where

$$\eta_{n,k,x}(h_{i,k}; f) := \mathbb{E}_P[f(h_1(X_1), \ldots, h_n(X_{n-k+1}, \ldots, X_n)) \mid \{X_{n-k+1} = x\}]$$

for any $x \in \{0, 1\}$*. In particular,*

$$\mathbb{E}_P[f(Y_{1,k}, \ldots, Y_{n,k}) \mid \{X_{n-k+1} = 0\}] \leq \mathbb{E}_P[f(Y_{1,k}, \ldots, Y_{n,k}) \mid \{X_{n-k+1} = 1\}].$$

Lemma 2 *Let* $k \in \mathbb{N}$ *be arbitrary but fixed. Then the sequence* $\{Y_{n,k}\}_{n\in\mathbb{N}}$ *is neither a* P*-demisubmartingale nor a* N*-demisupermartingale under* P*.*

Proof. First fix on an arbitrary $k \in \mathbb{N}$. Then note that by (1) we get

$$Y_{n,k} - Y_{n-1,k} = X_n - X_{(n-k)^+} \quad \text{for each } n \in \mathbb{N}; \tag{3}$$

hence for each $n \in \mathbb{N}$ and for every measurable function f on $\mathbb{R}^n$ such that each expectation

$$H_{n,k}(f) := H_{n,k}(Y_{1,k}, \ldots, Y_{n,k}; f) := \mathbb{E}_P[(Y_{n+1,k} - Y_{n,k})f(Y_{1,k}, \ldots, Y_{n,k})]$$

exists, we obtain that the equalities

$$\mathbb{E}_P[(Y_{n+1,k} - Y_{n,k}) \mid \mathcal{F}_n^{(X)}] = \mathbb{E}_P[X_{n+1} \mid \mathcal{F}_n^{(X)}] - X_{(n-k+1)^+} = p - X_{(n-k+1)^+},$$

hold true $P \mid \mathcal{F}_n^{(X)}$-a.s., implying that

$$H_{n,k}(f) = \mathbb{E}_P[(p - X_{(n-k+1)^+})f(Y_{1,k}, \ldots, Y_{n,k})].$$

If in addition, f is coordinatewise nondecreasing, it follows by Lemma 1 that

$$H_{n,k}(f) = pq[\eta_{n,k,0}(h_{i,k}; f) - \eta_{n,k,1}(h_{i,k}; f)] \leq 0 \quad \text{for each } n \in \mathbb{N} \text{ with } n \geq k, \tag{4}$$

where $h_{i,k}(x_{(i-k+1)\vee 1}, \ldots, x_i) := \sum_{j=(i-k+1)\vee 1}^{i} x_j$ for each $k \in \mathbb{N}$ and for each $(x_{(i-k+1)\vee 1}, \ldots, x_i) \in \mathbb{R}^{i\wedge k}$, while it is immediate that

$$H_{n,k}(f) = p\mathbb{E}_P[f(Y_{1,k}, \ldots, Y_{n,k})] \geq 0 \quad \text{for each } n \in \mathbb{N} \text{ with } n < k. \tag{5}$$

Suppose now that $\{Y_{n,k}\}_{n\in\mathbb{N}}$ is a P-demisubmartingale. It then follows that for each $n \in \mathbb{N}$ and for every nonnegative coordinatewise nondecreasing function f on $\mathbb{R}^n$ such that $H_{n,k}(f)$ exists we have $H_{n,k}(f) \geq 0$. The latter together with an application of condition (4) for $f = \pi_n$ yields that $H_{n,k}(\pi_n) = 0$ for each $n \in \mathbb{N}$ with $n \geq k$. But since by assumption $\{X_n\}_{n\in\mathbb{N}}$ is P-independent, it follows that

$$P_{Y_{n,k}} = \mathbf{B}(n \wedge k, p) \quad \text{for each } n \in \mathbb{N}, \tag{6}$$

implying

$$\begin{aligned} H_{n,k}(\pi_n) &= \mathbb{E}_P[(Y_{n+1,k} - Y_{n,k})Y_{n,k}] \overset{(3)}{=} \mathbb{E}_P[X_{n+1}Y_{n,k}] - \mathbb{E}_P[X_{n-k+1}Y_{n,k}] \\ &\overset{(6)}{=} kp^2 - \mathbb{E}_P[X_{n-k+1}^2] - \sum_{j=n-k+2}^{n} \mathbb{E}_P[X_{n-k+1}X_j] = -pq; \end{aligned}$$

hence $0 = H_{n,k}(\pi_n) = -pq$ for each $n \in \mathbb{N}$ with $n \geq k$, a contradiction. Thus, $\{Y_{n,k}\}_{n\in\mathbb{N}}$ cannot be a P-demisubmartingale.

Moreover, suppose that $\{Y_{n,k}\}_{n\in\mathbb{N}}$ is a N-demisupermartingale under P. Then applying similar arguments with above but with considering $f = 1$ instead of $f = \pi_n$, we infer by condition (5) that $0 = H_{n,k}(1) = p$ for each $n < k$, which is not valid; hence $\{Y_{n,k}\}_{n\in\mathbb{N}}$ cannot be a N-demisupermartingale under P either. $\square$

Because of Lemma 2 none of the maximal inequalities applying either for demi(sub)martingales or for N-demi(super)martingales can be exploited in the case of the enumerating process $\{Y_{n,k}\}_{n\in\mathbb{N}}$, where $k \in \mathbb{N}$ is arbitrary but fixed. To overcome this difficulty, consider for any fixed $k \in \mathbb{N}$ the sequence $\{\widetilde{Y}_{n,k}\}_{n\in\mathbb{N}_0}$ of random variables on Ω defined by means of

$$\widetilde{Y}_{n,k} := \begin{cases} Y_{n,k}, & \text{if } n \in \{k, k+1, \ldots\} \\ Y_{k,k}, & \text{if } n \in \{1, \ldots, k-1\} \\ 0, & \text{if } n = 0, \end{cases} \tag{7}$$

and note that $R_{\widetilde{Y}_{n,k}} = \{0, \ldots, k\}$ for each $n \in \mathbb{N}$.

Proposition 1 *For any fixed $k \in \mathbb{N}$ the following hold true:*

(i) *The sequence* $\{Y_{n,k}\}_{n\in\mathbb{N}}$ *is adapted to* $\{\mathcal{F}_n^{(X)}\}_{n\in\mathbb{N}}$.

(ii) *The sequence* $\{\widetilde{Y}_{n,k}\}_{n\in\mathbb{N}}$ *is a* N*-demimartingale under* P. *Moreover, it is not a* P*-demisubmartingale.*

Proof. Assertion (i) is immediate by (1). As for (ii), first fix on an arbitrary $k \in \mathbb{N}$. By virtue of (i) we get that $\{\widetilde{Y}_{n,k}\}_{n\in\mathbb{N}}$ is adapted to $\{\mathcal{F}_n^{(X)}\}_{n\in\mathbb{N}}$. Furthermore, note that for each $n \in \mathbb{N}$ and for every coordinatewise nondecreasing function f on $\mathbb{R}^n$ such that each expectation

$$\widetilde{H}_{n,k}(f) := \widetilde{H}_{n,k}(\widetilde{Y}_{1,k},\ldots,\widetilde{Y}_{n,k};f) := \mathbb{E}_P[(\widetilde{Y}_{n+1,k} - \widetilde{Y}_{n,k})f(\widetilde{Y}_{1,k},\ldots,\widetilde{Y}_{n,k})]$$

exists, it follows by (7) that

$$\widetilde{H}_{n,k}(f) = \begin{cases} H_{n,k}(f), & \text{if } n \in \{k, k+1, \ldots\} \\ 0, & \text{if } n \in \{1, \ldots, k-1\}, \end{cases}$$

implying together with condition (4) that $\widetilde{H}_{n,k}(f) \leq 0$ for each $n \in \mathbb{N}$. The latter together with the clear fact that $\mathbb{E}_P[\widetilde{Y}_{n,k}] = kp < \infty$ for each $n \in \mathbb{N}$ yields that the sequence $\{\widetilde{Y}_{n,k}\}_{n\in\mathbb{N}}$ is a N-demimartingale under P.

Moreover, suppose that $\{\widetilde{Y}_{n,k}\}_{n\in\mathbb{N}}$ is also a P-demisubmartingale. It then follows that $\widetilde{H}_{n,k}(f) = 0$ for each $n \in \mathbb{N}$ and for every nonnegative coordinatewise nondecreasing function f on $\mathbb{R}^n$ such that each expectation $\widetilde{H}_{n,k}(f)$ exists. But then by the proof of Lemma 2, we infer for each $n \in \mathbb{N}$ with $n \geq k$ that $0 = \widetilde{H}_{n,k}(\pi_n) = H_{n,k}(\pi_n) = -pq$, a contradiction. □

The fact that the modified enumerating process $\{\widetilde{Y}_{n,k}\}_{n\in\mathbb{N}}$ is proved to be a N-demimartingale does not suffice by itself for extracting proper bounds for the c.d.f of the waiting time $T_r^{(k)}$. To this aim, some new maximal inequalities for nonnegative N-demi(super)martingales are proved in the next section.

3 Maximal inequalities for nonnegative N-demimartingales

Dai et al. [4] recently provided a counterexample for the validity of some Chow type maximal inequalities for N-demimartingales. This counterexample also applies to another well-known maximal inequality for N-demimartingales (see [3], Theorem 2.1 or better see e.g. [5], Theorem 3.2.1), which could have been of special interest for the purposes of this work, if it was true. The aim of this section is to provide some useful alternatives to Theorem 2.1 from [3] for sequences of P-a.s. nonnegative random variables.

Proposition 2 *If* $\{Z_j\}_{j\in\mathbb{N}}$ *is a* N*-demimartingale under* P *such that* $Z_j \geq 0$ P*-a.s. for each* $j \in \mathbb{N}$*, then for any fixed* $t \in \mathbb{N}$ *and for each* $\varepsilon > 0$ *the following inequality holds true:*

$$P\Big(\max_{1\leq j\leq t} Z_j > \varepsilon\Big) \leq 1 - \frac{1}{\varepsilon}\mathbb{E}_P[Z_1] + \frac{1}{\varepsilon}\sum_{l=1}^{t}\mathbb{E}_P[Z_l\chi_{\{Z_l>\varepsilon\}}]. \tag{8}$$

Proof. First fix on arbitrary $t \in \mathbb{N}$ and $\varepsilon > 0$. Define next the random variable $\tau_{t,\varepsilon} : \Omega \longrightarrow \mathbb{R}$ by means of

$$\tau_{t,\varepsilon}(\omega) := \begin{cases} \inf\{j \in \{1,\ldots,t\} : Z_j(\omega) > \varepsilon\}, & \text{if } \omega \in \bigcup_{j=1}^{t}\{Z_j > \varepsilon\} \\ t, & \text{if } \omega \in \bigcap_{j=1}^{t}\{Z_j \leq \varepsilon\} \end{cases}$$

for each $\omega \in \Omega$. Clearly, $\tau_{t,\varepsilon}$ is a $\mathcal{F}_t^{(Z)}$-measurable function and $R_{\tau_{t,\varepsilon}} = \{1,\ldots,t\}$; moreover, it is a coordinatewise nonincreasing function of $Z_1,\ldots,Z_t$.

The latter together with our assumption that $\{Z_j\}_{j\in\mathbb{N}}$ is a N-demimartingale under P yields that $\mathbb{E}_P[Z_1] \leq \mathbb{E}_P[Z_{\tau_{t,\varepsilon}\wedge t}]$ (cf. e.g. [5], Theorem 3.1.7), and so we get

$$\mathbb{E}_P[Z_1] \leq \mathbb{E}_P[Z_{\tau_{t,\varepsilon}}\chi_{\{\max_{1\leq j\leq t} Z_j > \varepsilon\}}] + \mathbb{E}_P[Z_t\chi_{\{\max_{1\leq j\leq t} Z_j \leq \varepsilon\}}],$$

which implies that

$$\varepsilon P\Big(\max_{1\leq j\leq t} Z_j \leq \varepsilon\Big) \geq \mathbb{E}_P[Z_1] - \mathbb{E}_P[Z_{\tau_{t,\varepsilon}}\chi_{\{\max_{1\leq j\leq t} Z_j > \varepsilon\}}]. \tag{9}$$

But since the last expectation equals

$$\sum_{l=1}^{t}\mathbb{E}_P[Z_{\tau_{t,\varepsilon}}\chi_{\{\max_{1\leq j\leq t} Z_j > \varepsilon, \tau_{t,\varepsilon}=l\}}] = \sum_{l=1}^{t}\mathbb{E}_P[Z_l\chi_{\{\max_{1\leq j\leq t} Z_j > \varepsilon, \tau_{t,\varepsilon}=l\}}]$$

and all random variables Z_n are P-a.s. nonnegative, it follows that

$$\mathbb{E}_P[Z_{\tau_{t,\varepsilon}}\chi_{\{\max_{1\leq j\leq t} Z_j > \varepsilon\}}] \leq \sum_{l=1}^{t}\mathbb{E}_P[Z_l\chi_{\{\max_{1\leq j\leq t} Z_j > \varepsilon, Z_l > \varepsilon\}}] = \sum_{l=1}^{t}\mathbb{E}_P[Z_l\chi_{\{Z_l > \varepsilon\}}].$$

The latter together with (9) entails that

$$\varepsilon - \varepsilon P\Big(\max_{1\leq j\leq t} Z_j > \varepsilon\Big) \geq \mathbb{E}_P[Z_1] - \sum_{l=1}^{t}\mathbb{E}_P[Z_l\chi_{\{Z_l > \varepsilon\}}];$$

hence we equivalently get condition (8). □

Another alternative to Theorem 2.1 from [3] is next presented.

Proposition 3 *If $\{Z_j\}_{j\in\mathbb{N}}$ is a N-demisupermartingale under P such that $Z_j \geq 0$ P-a.s. for each $j \in \mathbb{N}$, then for any fixed $t \in \mathbb{N}$ and for each $\varepsilon > 0$ the following inequality holds true:*

$$\varepsilon P\Big(\max_{1\leq j\leq t} Z_j \geq \varepsilon\Big) \leq \sum_{l=1}^{t}\mathbb{E}_P[Z_l\chi_{\{\max_{1\leq j\leq l} Z_j \geq \varepsilon\}}].$$

Proof. First fix on arbitrary $t \in \mathbb{N}$ and $\varepsilon > 0$. Define next the random variable $\widetilde{\tau}_{t,\varepsilon} : \Omega \longrightarrow \mathbb{R}$ by means of

$$\begin{aligned}\widetilde{\tau}_{t,\varepsilon}(\omega) &:= \widetilde{\tau}_{t,\varepsilon}(Z_1,\ldots,Z_t)(\omega) \\ &:= \begin{cases} \sup\{j \in \{1,\ldots,t\} : Z_j(\omega) \geq \varepsilon\}, & \text{if } \omega \in \bigcup_{j=1}^{t}\{Z_j \geq \varepsilon\} \\ 1, & \text{if } \omega \in \bigcap_{j=1}^{t}\{Z_j < \varepsilon\} \end{cases}\end{aligned}$$

for each $\omega \in \Omega$. Clearly, $\widetilde{\tau}_{t,\varepsilon}$ is a $\mathcal{F}_t^{(Z)}$-measurable function and $R_{\widetilde{\tau}_{t,\varepsilon}} = \{1,\ldots,t\}$; moreover, it is a coordinatewise nondecreasing function of $Z_1,\ldots,Z_t$.

The latter together with our assumption that $\{Z_j\}_{j\in\mathbb{N}}$ is a N - demisupermartingale under P yields that $\mathbb{E}_P[Z_1] \geq \mathbb{E}_P[Z_{\widetilde{\tau}_{t,\varepsilon}\wedge t}]$ (cf. e.g. [5], Theorem 3.1.7), and so we get

$$\mathbb{E}_P[Z_1] \geq \mathbb{E}_P[Z_{\widetilde{\tau}_{t,\varepsilon}}\chi_{\{\max_{1\leq j\leq t} Z_j\geq\varepsilon\}}] + \mathbb{E}_P[Z_1\chi_{\{\max_{1\leq j\leq t} Z_j<\varepsilon\}}]$$

or equivalently

$$\mathbb{E}_P[Z_1\chi_{\{\max_{1\leq j\leq t} Z_j\geq\varepsilon\}}] \geq \mathbb{E}_P[Z_{\widetilde{\tau}_{t,\varepsilon}}\chi_{\{\max_{1\leq j\leq t} Z_j\geq\varepsilon\}}].$$

But since all random variables Z_n are P-a.s. nonnegative, it follows that

$$\begin{aligned}\mathbb{E}_P[Z_{\widetilde{\tau}_{t,\varepsilon}}\chi_{\{\max_{1\leq j\leq t} Z_j\geq\varepsilon\}}] &\geq \mathbb{E}_P[Z_t\chi_{\{\max_{1\leq j\leq t} Z_j\geq\varepsilon\}\cap\{\max_{1\leq j\leq t-1} Z_j<\varepsilon, Z_t\geq\varepsilon\}}]\\ &\geq \varepsilon P\Big(\max_{1\leq j\leq t-1} Z_j<\varepsilon, Z_t\geq\varepsilon\Big);\end{aligned}$$

hence putting $\psi(t) := \psi(t;\varepsilon) := P(\max_{1\leq j\leq t} Z_j \geq \varepsilon)$, we obtain that

$$\varepsilon[\psi(t) - \psi(t-1)] \leq \mathbb{E}_P[Z_1\chi_{\{\max_{1\leq j\leq t} Z_j\geq\varepsilon\}}] \quad \text{for each } t\in\mathbb{N},$$

since t was chosen arbitrarily. Then by induction our proposition follows. □

4 Bounds for $F_{r:k}$ in a sequence of i.i.d. binary trials

Propositions 2 and 3 are exploited here for obtaining the bounds of interest for the c.d.f. of the waiting time $T_r^{(k)}$, see Corollaries 1 and 2, respectively.

Corollary 1 *For any fixed $k \in \mathbb{N}$ and for all $r,t \in \mathbb{N}$ with $r \leq k < t$ the following holds true:*

$$F_{r:k}(t;p) \leq u_1(r,k,t,p) := 1 - \frac{kp}{r-1} + \frac{t}{r-1}\sum_{y=r}^{k} yb(y;k,p).$$

Proof. First fix on arbitrary $r,k,t \in \mathbb{N}$ with $r \leq k < t$. Then note that by virtue of Proposition 1 we may apply Proposition 2 for $\{Z_j\}_{j\in\mathbb{N}} = \{\widetilde{Y}_{n,k}\}_{n\in\mathbb{N}}$ and $\varepsilon = r-1$. So, inequality (8) becomes

$$\begin{aligned}(r-1)P\Big(\max_{1\leq n\leq t}\widetilde{Y}_{n,k}\geq r\Big) \;&\leq\; (r-1) - \mathbb{E}_P[\widetilde{Y}_{1,k}] + \sum_{n=1}^{k}\mathbb{E}_P[\widetilde{Y}_{n,k}\chi_{\{\widetilde{Y}_{n,k}\geq r\}}]\\ &\quad + \sum_{n=k+1}^{t}\mathbb{E}_P[\widetilde{Y}_{n,k}\chi_{\{\widetilde{Y}_{n,k}\geq r\}}],\end{aligned}$$

implying together with conditions (7) and (6) as well as condition

$$\{T_r^{(k)} \leq t\} = \big\{\max_{k\leq n\leq t} Y_{n,k} \geq r\big\} \tag{10}$$

that

$$F_{r:k}(t;p) \le 1 - \frac{kp}{r-1} + \frac{t}{r-1}\sum_{y=r}^{k} yb(y;k,p),$$

which completes the proof. $\square$

Corollary 2 *For any fixed $k \in \mathbb{N}$ and for all $r, t \in \mathbb{N}$ with $r \le k < t$ the c.d.f. $F_{r:k}(t;p)$ is upper bounded by*

$$u_2(r,k,t,p) := \frac{t}{r}\sum_{y=r}^{k} yb(y;k,p) + \frac{1}{r}\sum_{l=k+1}^{t}\sum_{y=r+k-l}^{r-1} yb(y;k,p)[1 - F_b(r-1-y;l-k,p)].$$

Proof. First fix on arbitrary $r, k, t \in \mathbb{N}$ with $r \le k < t$.

Next note that Proposition 1 togetether with Remark 1 implies that we may apply Proposition 3 to get the inequality

$$rP\Big(\max_{1\le n\le t} \widetilde{Y}_{n,k} \ge r\Big) \le \sum_{l=1}^{t} \mathbb{E}_P[\widetilde{Y}_{l,k}\chi_{\{\max_{1\le n\le l}\widetilde{Y}_{n,k}\ge r\}}],$$

which taking into account conditions (7), (10) and (6), entails that

$$rF_{r:k}(t;p) \le \sum_{l=1}^{k} \mathbb{E}_P[Y_{k,k}\chi_{\{Y_{k,k}\ge r\}}] + \sum_{l=k+1}^{t} \mathbb{E}_P[Y_{l,k}\chi_{\{\max_{k\le n\le l} Y_{n,k}\ge r\}}]$$

or equivalently that

$$rF_{r:k}(t;p) \le k\sum_{y=r}^{k} yb(y;k,p) + \sum_{l=k+1}^{t} \mathbb{E}_P[Y_{k,k}\chi_{\{\max_{k\le n\le l} Y_{n,k}\ge r\}}]. \tag{11}$$

But since $Y_{n,k} = \sum_{j=1}^{n}(Y_j - Y_{j-1,k})$ for each $n \in \mathbb{N}$, we get by (3) that

$$Y_{l,k} - Y_{n,k} = \sum_{j=n+1}^{l}(X_j - X_{(j-k)^+}) = \sum_{j=n+1}^{l} X_j - \sum_{j=n-k+1}^{l-k} X_{j^+}.$$

for each $n, l \in \mathbb{N}$ such that $l > n$. Setting now

$$\widetilde{\varpi}_{r,k,t}(y) := P(Y_{k,k} = y, \max_{k\le n\le l} Y_{n,k} \ge r)$$

as well as

$$U(r,k,l,p) := \mathbb{E}_P[Y_{k,k}\chi_{\{\max_{k\le n\le l} Y_{n,k}\ge r\}}]$$

for any fixed $l \in \mathbb{N}$ with $l > k$ and for each $y \in \mathbb{N}_0$, it follows by (1) and the P-independence of the binary trials $\{X_n\}_{n\in\mathbb{N}}$, that for each $y \in \{0, \ldots, k\}$

$$\begin{aligned}
\widetilde{\varpi}_{r,k,t}(y) &= P\Big(Y_{k,k} = y, \max_{k\le n\le l}\Big(\sum_{j=k+1}^{n} X_j - \sum_{j=1}^{n-k} X_j\Big) \ge r - y\Big) \\
&\le P\Big(Y_{k,k} = y, \max_{k\le n\le l} \sum_{j=k+1}^{n} X_j \ge r - y\Big) \\
&= P\Big(Y_{k,k} = y, \sum_{j=k+1}^{l} X_j \ge r - y\Big) \\
&= b(y; k, p)[1 - F_b(r - 1 - y; l - k, p)],
\end{aligned}$$

which implies that

$$\begin{aligned}
U(r, k, l, p) &\le \sum_{y=1}^{r-1} yb(y; k, p)[1 - F_b(r - 1 - y; l - k, p)] + \sum_{y=r}^{k} yb(y; k, p) \\
&= \sum_{y=r+k-l}^{r-1} yb(y; k, p)[1 - F_b(r - 1 - y; l - k, p)] + \sum_{y=r}^{k} yb(y; k, p);
\end{aligned}$$

hence

$$\begin{aligned}
\sum_{l=k+1}^{t} U(r, k, l, p) \;\le\; &\sum_{l=k+1}^{t} \sum_{y=r+k-l}^{r-1} yb(y; k, p)[1 - F_b(r - 1 - y; l - k, p)] \\
&+ (t - k) \sum_{y=r}^{k} yb(y; k, p).
\end{aligned}$$

The latter together with (11) results in proving the corollary. □

The following result is an immediate consequence of Corollaries 1 and 2.

Proposition 4 *For any fixed $k \in \mathbb{N}$ and for all $r, t \in \mathbb{N}$ such that $r \le k < t$, the following holds true:*

$$F_{r:k}(t; p) \le (u_1 \wedge u_2)(r, k, t, p),$$

where u_1 and u_2 are as in Corollaries 1 and 2, respectively.

Remark 2 A first look in the upper bounds of Proposition 4 suggests that although we may not decide in general which of the two bounds is more efficient, $u_2(r, k, t, p)$ as a more sophisticated one is expected to outperform $u_1(r, k, t, p)$. Also note that Proposition 4 yields $\lim_{p\to 0^+} F_{r:k}(t; p) \le \lim_{p\to 0^+} u_2(r, k, t, p) = 0$, implying the intuitively natural fact that as the success probability p of each binary trial tends to zero, the probability $P(T_r^{(k)} \le t)$ does so.

5 Numerical Results

In the Appendix, a series of tables providing the computed values for the upper bounds of $F_{r:k}(t;p)$ given in Proposition 4, together with its minimum as well as with the exact or simulated (depending on the examined type of scan) c.d.f. of $T_r^{(k)}$, is presented. Note that for almost perfect runs the exact c.d.f. is computed by exploiting Proposition 1 of Bersimis et al. [2]; otherwise the computation of the empirical c.d.f. of $T_r^{(k)}$ is performed via simulation. More precisely, a sequence of i.i.d. binary trials with success probability p is generated each time and the number of trials needed until a scan of type r/k appears is recorded; the number of such sequences simulated equals 1000.

In Tables 1 to 4 the values in **bold** stand for the most appropriate bound between $u_1(r,k,t,p)$ and $u_2(r,k,t,p)$ at each time time t. Also note that in the last column each of these tables we compute the *relative error*

$$\frac{(u_1 \wedge u_2)(r,k,t,p) - \kappa(r,k,t,p)}{\kappa(r,k,t,p)}$$

for the upper bound ($r.e.$ for short), where $\kappa(r,k,t,p)$, for $p \in (0,1)$, $r,k \in \mathbb{N}$ with $r \le k$ and $t \ge k+1$, is the exact or simulated (depending on the examined type of scan) c.d.f..

Remarks. In brief, the performed numerical study suggested that:

(a) *For the case of almost perfect runs*, the relative error in general behaves as a nonincreasing function of p, for fixed r,k,t. The most common exception to this rule occurs for $t = k+1$ (compare Tables 1 and 2). Furthermore, the relative error usually increases whenever t does so and r,k,p remain the same. However, for some time intervals it may behave as follows: up to a trial, say t_1, increases with t, then it becomes a nonincreasing function of t until another trial, say t_2, and so forth (see Table 3); in other words, its graph versus time may resemble a multimodal function. It is also worth noticing that fixing on r,k,t the upper bound $u_2(r,k,t,p)$ proves to be the tightest one (as expected by Remark 2) for small values of p ($p \le 0.1$). On the contrary, the larger values the success probability takes the more $u_1(r,k,t,p)$ outperforms $u_2(r,k,t,p)$. For moderate or large p ($p > 0.2$), though, all upper bounds seem to be inadmissible. Here it should be noted that for any fixed triplet (r,k,p) the first upper bound tends to be more efficient as t increases, while the opposite happens for $u_2(r,k,t,p)$. The above facts are confirmed not only in Tables 1 to 3 but also by a similar numerical study conducted for the 3/5- and 5/6-almost perfect runs.

(b) The only pattern from those described in (a) that remains valid for scans other than almost perfect runs is that referring to which of the two upper bounds is tighter for the various values of t. All other comments made in there do not apply in general. In fact, for most r/k-scans with $r \notin \{k-2, k-1\}$ even the tightest of the upper bounds computes inadmissible values beyond some of the first t. However, exceptions as the one presented in Table 3 may occur.

Aknowledgements

This research has been co-financed by the European Union (European Social Fund - ESF) and Greek national funds through the Operational Program "Education and Lifelong Learning" of the National Strategic Reference Framework (NSRF) - Research Funding Program: Aristeia II. Investing in knowledge society through the European Social Fund.

References

1. N. Balakrishnan and M.V. Koutras. *Runs and scans with applications*, Wiley, New York, 2002.
2. S. Bersimis, M.V. Koutras, and G.K. Papadopoulos. Waiting Time for an Almost Perfect Run and Applications in Statistical Process Control. *Methodology and Computing in Applied Probability* 16, 207–222, 2014.
3. T.C. Christofides. Maximal inequalities for N-demimartingales. *Archives of Inequalities and Applications* 1, 387–397, 2003.
4. P. Dai, Y. Shen, S. Hu and W. Yang. Some results for demimartingales and N-demimartingales. *Journal of Inequalities and Applications* 2014:489, 2014.
5. B.L.S. Prakasa Rao. *Associated Sequences, Demimartingales and Nonparametric Inference*, Probability and its Applications, Springer Basel AG, 2012.

Appendix: Tables of Section 5

t	exact	u_1	u_2	$u_1 \wedge u_2$	r.e.
8	0.000011	0.860062	**0.000066**	0.000066	4.818
13	0.000038	0.860100	**0.001240**	0.001240	34.616
18	0.000058	0.860139	**0.009118**	0.009118	155.740
23	0.000082	0.860177	**0.034884**	0.034884	426.343
28	0.000105	0.860216	**0.092585**	0.092585	880.048
33	0.000129	0.860254	**0.195339**	0.195339	1518.700
38	0.000152	0.860293	**0.352587**	0.352587	2318.790
43	0.000175	0.860331	**0.568994**	0.568994	3242.170
48	0.000199	0.860370	**0.844688**	0.844688	4245.890
53	0.000222	**0.860408**	1.176250	0.860408	3868.670

Table 1. Computed bounds Vs exact c.d.f.: $(r, k) = (6, 7)$ and $p = 0.1$

t	exact	u_1	u_2	$u_1 \wedge u_2$	r.e.
8	0.000119	0.790670	**0.000702**	0.000702	4.907
13	0.000353	0.791088	**0.010881**	0.010881	29.846
18	0.000587	0.791507	**0.066946**	0.066946	113.129
23	0.000820	0.791926	**0.217233**	0.217233	263.807
28	0.001054	0.792344	**0.495718**	0.495718	469.297
33	0.001287	**0.792763**	0.911289	0.792763	614.641
38	0.001521	**0.793181**	1.452190	0.793181	520.384
43	0.001755	**0.793600**	2.095760	0.793600	451.235
48	0.001988	**0.794019**	2.816890	0.794019	398.340
53	0.002222	**0.794437**	3.593080	0.794437	356.571

Table 2. Computed bounds Vs simulated c.d.f.: $(r, k) = (6, 7)$ and $p = 0.15$

t	exact	u_1	u_2	$u_1 \wedge u_2$	r.e.
7	0.001999	0.811984	**0.010082**	0.010082	4.043
12	0.005456	0.820544	**0.051558**	0.051558	8.450
17	0.008892	0.829104	**0.171246**	0.171246	18.258
22	0.012317	0.837664	**0.392290**	0.392290	30.850
27	0.015729	0.846224	**0.718710**	0.718710	44.692
32	0.019130	**0.854784**	1.141880	0.854784	43.683
37	0.022519	**0.863344**	1.647090	0.863344	37.338
42	0.025897	**0.871904**	2.218100	0.871904	32.669
47	0.029262	**0.880464**	2.839810	0.880464	29.089
52	0.032616	**0.889024**	3.499370	0.889024	26.257

Table 3. Computed bounds Vs simulated c.d.f.: $(r,k) = (4,6)$ and $p = 0.15$

t	exact	u_1	u_2	$u_1 \wedge u_2$	r.e.
30	0.046	0.587144	**0.122368**	0.122368	1.660
32	0.047	0.595518	**0.147594**	0.147594	2.140
33	0.049	0.599705	**0.166470**	0.166470	2.397
37	0.052	0.616453	**0.305068**	0.305068	4.867
39	0.053	0.624826	**0.426376**	0.426376	7.045
41	0.054	0.633200	**0.593177**	0.593177	9.985
45	0.055	**0.649947**	1.091080	0.649947	10.817
47	0.056	**0.658321**	1.432420	0.658321	10.756
50	0.057	**0.670882**	2.067290	0.670882	10.770
52	0.061	**0.679255**	2.572470	0.679255	10.135
54	0.062	**0.687629**	3.141010	0.687629	10.091

Table 4. Computed bounds Vs simulated c.d.f.: $(r,k) = (14,28)$ and $p = 0.25$

A Bivariate Semiparametric Control Chart Based on Order Statistics

Markos V. Koutras and Elisavet M. Sofikitou

Department of Statistics and Insurance Science, School of Finance and Statistics, University of Piraeus, Piraeus, Greece
(E-mail: mkoutras@unipi.gr, esofikit@unipi.gr)

Abstract. In the present article, we introduce a new bivariate semiparametric Shewhart-type control chart which is based on the bivariate statistic $(X_{(r)},Y_{(s)})$, where $X_{(r)}$ and $Y_{(s)}$ are the order statistics of the respective X and Y test samples. The suggested bivariate control chart is very simple and consists a straightforward generalization of the well known univariate median (non-parametric) control chart.

An expression for the operating characteristic function of the new control chart is obtained. A key advantage of the chart is that, although the performance of it is typically affected by the dependence structure of the bivariate observations under study, the values of the false alarm rate and the in-control run length do not seem to change dramatically when different copulas are used. Tables are provided for the implementation of the chart for some typical ARL values and false alarm rates. The performance of the proposed chart is compared to that of the traditional χ^2 chart as well as to the nonparametric SN^2 and SR^2 charts introduced by Boone and Chakraborti [5].

Keywords: Order statistics, nonparametric control charts, semiparametric control charts, false alarm rate, average run length, statistical quality control, copulas.

1 Introduction

It is commonly believed that the quality improvement of a single product or of an entire production is the main purpose of Statistical Quality Control. This can be achieved through the identification and reduction of the natural variability (as much as possible), which is an inherent part of any process. In recent years, the non-parametric control charts have drawn the interest of many researchers, as they can be useful alternatives to their parametric counterparts in cases where there is no information on the distribution of the underlying process or where the distribution is not normal.

The construction of a non-parametric control chart is as follows. Firstly, a random reference sample is drawn from an unknown continuous distribution, which is assumed to be in-control. Based on this sample, reliable control limits are set using specific order statistics. Then successive test samples are collected in order to decide whether the process remains in control or has shifted to an out-of-control distribution.

16th ASMDA Conference Proceedings, 30 June – 4 July 2015, Piraeus, Greece

Janacek and Meikle [8] proposed a univariate non-parametric two-sided (Shewhart-type) control chart for the median. Due to the use of the median, the main advantage of this chart is that it is insensitive to measurement errors and can be used in situations that the quality characteristic involves ordinal data. Generalizing the above idea, Chakraborti *et al*. [6] suggested a chart for a test sample quantile. Recently, Balakrishnan *et al*. [4] improved the median chart and its extensions by incorporating an additional condition (based on the number of observations from the test sample falling between the control limits).

Extending the idea of Chakraborti *et al*. [6], we introduce a bivariate semiparametric control chart based on order statistics, which is actually a straightforward generalization of the classical univariate non-parametric control chart for the median. In Section 2, we perform a detailed study of the characteristics of the new control chart. Our numerical experimentation indicated that, although the new chart is typically affected by the dependence structure of the bivariate observations under study, the values of the false alarm rate do not change dramatically when different copulas or distributions are used. In Section 3, we compare the new chart to the traditional parametric χ^2 chart and also the nonparametric SN^2 and SR^2 charts of Boone and Chakraborti [5]. For this purpose, a simulation study was carried out. Finally, in Section 4, some concluding remarks, suggestions and recommendations are provided for the proposed chart.

2 A New Bivariate Semiparametric Control Chart

In order to interpret the new chart, we will describe a similar technique to the one commonly used for the construction of the univariate median control chart and its extensions. Firstly, let us assume that a random bivariate reference sample $(X_1^{(R)},Y_1^{(R)})$, $(X_2^{(R)},Y_2^{(R)})$, ..., $(X_m^{(R)},Y_m^{(R)})$ is collected from an in-control distribution which is described by a joint cumulative continuous distribution function (cdf) $F^{(R)}(x,y)=F(x,y)$ with marginal distributions $F_X(x)$ and $F_Y(y)$. Subsequently, successive test samples are independently drawn of each other (and also the reference sample) from the underlying process, in order to decide whether the process has shifted to an out-of-control cdf $F^{(T)}(x,y)=G(x,y)$ with marginal distributions $G_X(x)$ and $G_Y(y)$. For this reason, we choose four particular order statistics from the reference sample, which are used as control limits of the proposed chart, i.e.,

$$LCL_X = X_{a:m}^{(R)},\ UCL_X = X_{b:m}^{(R)},\ LCL_Y = Y_{c:m}^{(R)},\ UCL_Y = Y_{d:m}^{(R)},$$

with $1 \le a < b \le m$ and $1 \le c < d \le m$. After the test sample is collected, the *r*th and *s*th order statistics $X_{r:n}^{(T)}$ and $Y_{s:n}^{(T)}$, respectively. In particular, the underlying process is declared to be "in-control", if the following two conditions hold true:

$$X_{a:m}^{(R)} \le X_{r:n}^{(T)} \le X_{b:m}^{(R)} \text{ and } Y_{c:m}^{(R)} \le Y_{s:n}^{(T)} \le Y_{d:m}^{(R)} \qquad (1)$$

It is worth mentioning that if the medians of the test sample are used, both r, s are set equal to $(n+1)/2$, when n is odd and equal to $n/2$, when n is even.

For these cases, it is quite reasonable to resort to control limits symmetrically placed around the median, and therefore the design parameters *b* and *d* are selected as $b = m - a + 1$ and $d = m - c + 1$.

In the sequel, we shall be denoting by $C(u,v)$ and $D(u,v)$ the bivariate copulas associated with $F(x,y)$ and $G(x,y)$, respectively. Then, according to Sklar's theorem, Sklar [9], the joint distributions $F(x,y)$ and $G(x,y)$ are given by

$$F(x,y) = C(F_X(x), F_Y(y)) \text{ and } G(x,y) = D(G_X(x), G_Y(y)) \tag{2}$$

In general, a bivariate copula combines the joint cdf with its univariate margins and is used to describe the dependence structure between two random variables. If the marginal distributions are continuous, then the copula is unique.

If the test sample comes from a continuous cdf $G(x,y)$, the probability that the proposed chart does not signal is given by

$$p = p_{F,G}(m,n;a,b,c,d;r,s) = p(X_{a:m}^{(R)} \le X_{r:n}^{(T)} \le X_{b:m}^{(R)} \text{ and } Y_{c:m}^{(R)} \le Y_{s:n}^{(T)} \le Y_{d:m}^{(R)}) \tag{3}$$

which is, in fact, the operating characteristic function of the new chart, while $1 - p$ provides the signaling probability of an event. We will now introduce the following Lemma which will be used to calculate the above probability *p*.

Lemma 1. *Let* $(X_i, Y_i) \sim F(x,y),\ i = 1,2,...,n$ *with marginals* $F_X(x),\ F_Y(y)$ *and associated copula* $C(x,y)$. *Then the joint cdf of the random variables*

$$U_{r:n} = F_X(X_{r:n}) \text{ and } V_{s:n} = F_Y(Y_{s:n})$$

is given by the formula

$$F_{r,s:n}^{(C)}(u,v) = P\left(U_{r:n} \le u, V_{s:n} \le v\right) = \sum_{i=r}^{n} \sum_{j=s}^{n} \sum_{k} a_n\left(i,j,k\right) q_n^{(C)}\left(i,j,k;u,v\right)$$

for $1 \le r \le n$ *and* $1 \le s \le n$, *where*

$$\begin{aligned} q_n^{(C)}\left(i,j,k;u,v\right) = \left(C(u,v)\right)^k \times \left(u - C(u,v)\right)^{i-k} \times \left(v - C(u,v)\right)^{j-k} \\ \times \left(1 - u - v + C(u,v)\right)^{n-i-j+k}, \end{aligned} \tag{4}$$

$$a_n\left(i,j,k\right) = \frac{n!}{k!(i-k)!(j-k)!(n-i-j+k)!} = \binom{n}{k,\ i-k,\ j-k,\ n-i-j+k}$$

and the inner summation is performed for $max(0, i+i-n) \le k \le min(i,j)$.

Proof. It is obvious that

$$F_{r,s:n}^{(C)}(u,v) = P(F_X(X_{r:n}) \le u, F_Y(Y_{s:n}) \le v) = P(X_{r:n} \le F_X^{-1}(u), Y_{s:n} \le F_Y^{-1}(v))$$

and the result follows immediately on making use of the well known formula (see Arnold *et. al* [2] and David and Nagaraja [7])

$$\begin{aligned} P(X_{r:n} \le x, Y_{s:n} \le y) = \sum_{i=r}^{n} \sum_{j=s}^{n} \sum_{k=\max(0,i+j-n)}^{\min(i,j)} a_n(k,i,j)(F(x,y))^k (F_X(x) - F(x,y))^{i-k} \\ \times (F_Y(y) - F(x,y))^{j-k} (1 - F_X(x) - F_Y(y) + F(x,y))^{n-i-j+k}. \end{aligned}$$

The proof of the lemma is completed by taking into account the expression (2) and by noticing that $F(F_X^{-1}(u), F_Y^{-1}(v)) = C(F_X(F_X^{-1}(u), F_Y(F_Y^{-1}(v))) = C(u,v)$, $F_X(F_X^{-1}(u) = u$ and $F_Y(F_Y^{-1}(v)) = v$. ■

At this point, it should be mentioned that the copula of the random variables $U_{r:n} = F_X(X_{r:n})$ and $V_{s:n} = F_Y(Y_{s:n})$ is equal to the copula of the random variables $X_{r:n}$ and $Y_{s:n}$, i.e. $C_{X_{r:n},V_{s:n}}(u,v) = C_{U_{r:n},V_{s:n}}(u,v)$. For more information on this result, please refer to the paper of Anjos *et al.* [1] and Avérous *et al.* [3].

We can now establish the exact formula for the operating characteristic function (3) of the proposed chart.

Proposition 1. *The operating characteristic function of the control chart defined by* (1) *is given by*

$$p = p_{F,G}(m,n;a,b,c,d;r,s)$$

$$= \int_0^1\int_0^1 F_{r,s:n}^{(D)}(G_X(F_X^{-1}(u)), G_Y(F_Y^{-1}(v))) \frac{\partial^2}{\partial u \partial v} H^{(C)}(m;a,b,c,d;u,v)\, dudv \tag{5}$$

where $H^{(C)}(m;a,b,c,d;u,v) = \sum_{i_1=a}^{b-1}\sum_{j_1=c}^{d-1}\sum_{k_1=\max(0,i_1+j_1-m)}^{\min(i_1,j_1)} a_m(i_1, j_1, k_1)\, q_m^{(C)}(i_1, j_1, k_1; u, v)$

and $F_{r,s:n}^{(D)}(w,t)$ *is the joint cdf described in Lemma 1 for* $w = G_X(F_X^{-1}(u))$ *and* $t = G_Y(F_Y^{-1}(v))$.

Proof. Firstly, treating p of (3) as a mean with respect to the joint distribution of $X_{a:m}^{(R)}$, $X_{b:m}^{(R)}$, $Y_{c:m}^{(R)}$, $Y_{d:m}^{(R)}$, we write the desired probability in the equivalent form

$$P(F_X(X_{a:m}^{(R)}) \le F_X(X_{r:n}^{(T)}) \le F_X(X_{b:m}^{(R)}) \text{ and } F_Y(Y_{c:m}^{(R)}) \le F_Y(Y_{s:n}^{(T)}) \le F_Y(Y_{d:m}^{(R)}))$$

and then apply the conditioning-unconditioning principle on the random variables

$$U_{a:m} = F_X(X_{a:m}^{(R)}),\ U_{b:m} = F_X(X_{b:m}^{(R)}),\ V_{c:m} = F_Y(Y_{c:m}^{(R)}),\ V_{d:m} = F_Y(Y_{d:m}^{(R)})$$

to gain the integral expression

$$p = \int_0^1\int_0^{v_2}\int_0^1\int_0^{u_2} P(u_1 \le F_X(X_{r:n}^{(T)}) \le u_2 \text{ and } v_1 \le F_Y(Y_{s:n}^{(T)}) \le v_2)$$
$$\times f_{U_{a:m},U_{b:m};V_{c:m},V_{d:m}}(u_1,u_2,v_1,v_2) du_1 du_2 dv_1 dv_2, \tag{6}$$

where $f_{U_{a:m},U_{b:m};V_{c:m},V_{d:m}}(u_1,u_2,v_1,v_2)$ is the joint pdf of $U_{a:m}, U_{b:m}, V_{c:m}, V_{d:m}$.

Let us now write the probability appearing inside the quadruple integral in the following form

$$P[F_X^{-1}(u_1) \le X_{r:n}^{(T)} \le F_X^{-1}(u_2) \text{ and } F_Y^{-1}(v_1) \le Y_{s:n}^{(T)} \le F_Y^{-1}(v_2)] =$$

$$P[G_X(F_X^{-1}(u_1)) \le G_X(X_{r:n}^{(T)}) \le G_X(F_X^{-1}(u_2)), G_Y(F_Y^{-1}(v_1)) \le G_Y(Y_{s:n}^{(T)}) \le G_Y(F_Y^{-1}(v_2))]$$

and exploit the Lemma 1 to get

$$F_{r,s:n}^{(D)}(G_X(F_X^{-1}(u_2)),G_Y(F_Y^{-1}(v_2)))+F_{r,s:n}^{(D)}(G_X(F_X^{-1}(u_1)),G_Y(F_Y^{-1}(v_1)))$$
$$-F_{r,s:n}^{(D)}(G_X(F_X^{-1}(u_1)),G_Y(F_Y^{-1}(v_2)))-F_{r,s:n}^{(D)}(G_X(F_X^{-1}(u_2)),G_Y(F_Y^{-1}(v_1))). \quad (7)$$

Now by substituting the expression (7) in the integral (5) and changing the order of integration the following four integrals pop up

$$I_1=\int_0^1\int_0^1 F_{r,s:n}^{(D)}(G_X(F_X^{-1}(u_2)),G_Y(F_Y^{-1}(v_2)))\, f_{U_{b:m};V_{d:m}}(u_2,v_2)du_2dv_2$$
$$I_2=\int_0^1\int_0^1 F_{r,s:n}^{(D)}(G_X(F_X^{-1}(u_1)),G_Y(F_Y^{-1}(v_1)))\, f_{U_{a:m};V_{c:m}}(u_1,v_1)du_1dv_1$$
$$I_3=\int_0^1\int_0^1 F_{r,s:n}^{(D)}(G_X(F_X^{-1}(u_1)),G_Y(F_Y^{-1}(v_2)))\, f_{U_{a:m};V_{d:m}}(u_1,v_2)du_1dv_2$$
$$I_4=\int_0^1\int_0^1 F_{r,s:n}^{(D)}(G_X(F_X^{-1}(u_2)),G_Y(F_Y^{-1}(v_1)))\, f_{U_{b:m};V_{c:m}}(u_2,v_1)du_2dv_1,$$

where $f_{r,s:n}^{(C)}(u,v)$ is the joint density function of the cdf described in Lemma 1. In view of the above results the integral (6) reduces to

$$p=\int_0^1\int_0^1 F_{r,s:n}^{(D)}(G_X(F_X^{-1}(u)),G_Y(F_Y^{-1}(v)))$$
$$\times\left[f_{b,d:m}^{(C)}(u,v)+f_{a,c:m}^{(C)}(u,v)-f_{a,d:m}^{(C)}(u,v)-f_{b,c:m}^{(C)}(u,v)\right]dudv$$
$$=\int_0^1\int_0^1 F_{r,s:n}^{(D)}(G_X(F_X^{-1}(u)),G_Y(F_Y^{-1}(v)))\frac{\partial^2}{\partial u\partial v}H^{(C)}(m;\alpha,b,c,d;u,v)dudv,$$

where

$$H^{(C)}(m;a,b,c,d;u,v)=F_{b,d:m}^{(C)}(u,v)+F_{a,c:m}^{(C)}(u,v)-F_{a,d:m}^{(C)}(u,v)-F_{b,c:m}^{(C)}(u,v)$$
$$=\sum_{i_1=a}^{b-1}\sum_{j_1=c}^{d-1}\sum_{k_1=\max(0,i_1+j_1-m)}^{\min(i_1,j_1)} a_m(i_1,j_1,k_1)\; q_m^{(C)}(i_1,j_1,k_1;u,v).$$

Finally, a direct application of the previous lemma yields

$$F_{r,s:n}^{(D)}(G_X(F_X^{-1}(u)),G_Y(F_Y^{-1}(v)))=$$
$$\sum_{i=r}^{n}\sum_{j=s}^{n}\sum_{k=\max(0,i+j-n)}^{\min(i,j)} a_n(i,j,k)\; q_n^{(D)}(i,j,k;G_X(F_X^{-1}(u)),G_Y(F_Y^{-1}(v)))$$

where $q_n^{(D)}(i,j,k;u,v)$ is calculated by formula (4), with *C* replaced by *D*, and the proof is over. ■

An exact formula for the alarm rate of the new chart is given below.

Proposition 2. *If* $F_X=G_X$ *and* $F_Y=G_Y$, *then the Alarm Rate (AR) of the control chart can be expressed as follows*

$$AR=AR^{(C,D)}(m,n;a,b,c,d;r,s)=1-\int_0^1\int_0^1 F_{r,s:n}^{(D)}(u,v)\frac{\partial^2}{\partial u\partial v}H^{(C)}(m;a,b,c,d;u,v)\;dudv$$

or equivalently by

$$AR=1+\sum_{i=r}^{n}\sum_{j=s}^{n}\sum_{k=\max(0,i+j-n)}^{\min(i,j)} a_n(i,j,k)\sum_{i_1=a}^{b-1}\sum_{j_1=c}^{d-1}\sum_{k_1=\max(0,i_1+j_1-m)}^{\min(i_1,j_1)} a_m(i_1,j_1,k_1)$$
$$\times Q^{(C,D)}(i,j,k;i_1,j_1,k_1) \quad (8)$$

where

$$Q^{(C,D)}(i,j,k;i_1,j_1,k_1)=\int_0^1\int_0^1\frac{\partial}{\partial u}q_n^{(D)}(i,j,k;u,v)\times\frac{\partial}{\partial v}q_m^{(C)}(i_1,j_1,k_1;u,v)\,dudv,$$

$$q_n^{(D)}(i,j,k;u,v)=\sum_{r_1=0}^{i-k}\sum_{r_2=0}^{j-k}\sum_{r_3=0}^{n-i-j+k}\binom{i-k}{r_1}\binom{j-k}{r_2}\binom{n-i-j+k}{r_3}$$
$$\times(-1)^{i+j-r_1-r_2}u^{r_1}v^{r_2}(1-u-v)^{r_3}(D(u,v))^{n-k-r_1-r_2-r_3},$$

$$q_m^{(C)}(i_1,j_1,k_1;u,v)=\sum_{s_1=0}^{i_1-k_1}\sum_{s_2=0}^{j_1-k_1}\sum_{s_3=0}^{m-i_1-j_1+k_1}\binom{i_1-k_1}{s_1}\binom{j_1-k_1}{s_2}\binom{m-i_1-j_1+k_1}{s_3}$$
$$\times(-1)^{i_1+j_1-s_1-s_2}u^{s_1}v^{s_2}(1-u-v)^{s_3}(C(u,v))^{m-k_1-s_1-s_2-s_3}.$$

Proof. Since $F_X=G_X$ and $F_Y=G_Y$, we have $G_X(F_X^{-1}(u))=u$, $G_Y(F_Y^{-1}(v))=v$ and the formula (5) of Proposition 1 takes on the form

$$AR=AR^{(C,D)}(m,n;a,b,c,d;r,s)=1-\int_0^1\int_0^1F_{r,s:n}^{(D)}(u,v)\frac{\partial^2}{\partial u\partial v}H^{(C)}(m;a,b,c,d;u,v)\,dudv$$

Let us now apply integration by parts in double integral of the above expression. The first summand which appears is

$$I=\int_0^1\left(F_{r,s:n}^{(D)}(u,v)\frac{\partial}{\partial v}H^{(C)}(m;a,b,c,d;u,v)\right)\Bigg|_{u=0}^{1}dv\,,$$

where

$$\begin{aligned}H^{(C)}(m;a,b,c,d;u,v)&=F_{b,d:m}^{(C)}(u,v)+F_{a,c:m}^{(C)}(u,v)-F_{a,d:m}^{(C)}(u,v)-F_{b,c:m}^{(C)}(u,v)\\&=C_{U_b,V_d}(I_u(b,m-b+1),I_v(d,m-d+1))\\&\quad+C_{U_a,V_c}(I_u(a,m-a+1),I_v(c,m-c+1))\\&\quad-C_{U_a,V_d}(I_u(a,m-a+1),I_v(d,m-d+1))\\&\quad-C_{U_b,V_c}(I_u(b,m-b+1),I_v(c,m-c+1))\end{aligned}$$

and

$$I_x(a,b)=\frac{B_x(a,b)}{B(a,b)}=\frac{1}{B(a,b)}\int_0^x t^{a-1}(1-t)^{b-1}dt$$

denotes the incomplete beta function ratio. The integral I is equal to zero. This result is direct by taking into account the properties: $C(u,1)=u$, $C(1,v)=v$, $C(u,0)=C(0,v)=0$ and noticing that

$$H^{(C)}(m;a,b,c,d;1,v)=H^{(C)}(m;a,b,c,d;0,v)=0\,.$$

So, the AR can equivalently be written as

$$AR=1+\int_0^1\int_0^1\frac{\partial}{\partial u}F_{r,s:n}^{(D)}(u,v)\frac{\partial}{\partial v}H^{(C)}(m;a,b,c,d;u,v)\,dudv.$$

Taking into account Lemma 1, we get

$$AR = 1 + \sum_{i=r}^{n}\sum_{j=s}^{n}\sum_{k=\max(0,i+j-n)}^{\min(i,j)} a_n(i,j,k)\sum_{i_1=a}^{b-1}\sum_{j_1=c}^{d-1}\sum_{k_1=\max(0,i_1+j_1-m)}^{\min(i_1,j_1)} a_m(i_1,j_1,k_1)Q^{(C,D)}(i,j,k;i_1,j_1,k_1)$$

where

$$Q^{(C,D)}(i,j,k;i_1,j_1,k_1) = \int_0^1\int_0^1 \frac{\partial}{\partial u} q_n^{(D)}(i,j,k;u,v) \times \frac{\partial}{\partial v} q_m^{(C)}(i_1,j_1,k_1;u,v)\ dudv\ .$$

Observe next that the multiplicands appearing inside the double integral of the quantity

$$q_n^{(D)}(i,j,k;u,v) = (D(u,v))^k (u - D(u,v))^{i-k} (v - D(u,v))^{j-k} (1 - u - v + D(u,v))^{n-i-j+k}$$

can be expressed by the aid of the binomial expansion as

$$\begin{aligned}
\{u - D(u,v)\}^{i-k} &= \sum_{r_1=0}^{i-k}\binom{i-k}{r_1} u^{r_1}(-1)^{i-k-r_1}(D(u,v))^{i-k-r_1}\\
\{v - D(u,v)\}^{j-k} &= \sum_{r_2=0}^{j-k}\binom{j-k}{r_2} v^{r_2}(-1)^{j-k-r_2}(D(u,v))^{j-k-r_2}\\
\{1 - u - v + D(u,v)\}^{n-i-j+k} &= \sum_{r_3=0}^{n-i-j+k}\binom{n-i-j+k}{r_3}(1-u-v)^{r_3}(D(u,v))^{n-i-j+k-r_3}.
\end{aligned}$$

Algebraic operations can now be easily carried out to obtain the next alternative expression for

$$\begin{aligned}
q_n^{(D)}(i,j,k;u,v) = &\sum_{r_1=0}^{i-k}\sum_{r_2=0}^{j-k}\sum_{r_3=0}^{n-i-j+k}\binom{i-k}{r_1}\binom{j-k}{r_2}\binom{n-i-j+k}{r_3}\\
&\times(-1)^{i+j-r_1-r_2} u^{r_1} v^{r_2}(1-u-v)^{r_3}(D(u,v))^{n-k-r_1-r_2-r_3}
\end{aligned}$$

and similar results apply to the quantity $q_m^{(C)}(i_1,j_1,k_1;u,v)$. Combining all the above expressions we derive the *AR* and the proof is over. ■

It is worth mentioning that if $F_X = G_X$, $F_Y = G_Y$ and in addition $C = D$, the False Alarm Rate (*FAR*) of the suggested chart is obtained, i.e.

$$FAR = AR^{(C,C)}(m,n;a,b,c,d;r,s) = 1 - \int_0^1\int_0^1 F_{r,s:n}^{(C)}(u,v)\frac{\partial^2}{\partial u\partial v}H^{(C)}(m;a,b,c,d;u,v)\ dudv.$$

3 Performance Study - Numerical Comparisons

As already mentioned, in this Section we will present tables for the implementation of the new chart for some typical in-control *ARL* values and false alarm rates. The *ARL* and the *FAR* can be evaluated numerically for any choice of the design parameters. In order to reduce the parameters tabulated, from all the several available choices, r and s (with $r = s$) were set equal to $(n+1)/2$, because the medians of test and the reference sample were used, while a, b and c, d were chosen symmetrically ($b = m - a + 1$, $d = m - c + 1$). As a result, the control limits utilized are symmetric order statistics, i.e.

$$LCL_X = X_{a:m}^{(R)},\ UCL_X = X_{b:m}^{(R)} = X_{m-a+1:m}^{(R)},\ LCL_Y = Y_{c:m}^{(R)},\ UCL_Y = Y_{d:m}^{(R)} = Y_{m-c+1:m}^{(R)}\ .$$

The design parameters were suitably determined, to attain the pre-specified value of *ARL* and *FAR* as close to their target values as possible.

(m = 40)		Mean Shift ($\mu_{out} = \mu_X^{(T)} = \mu_Y^{(T)}$)								
n	(a,b) (c,d)	-2	-1.5	-1	0.5	0	0.5	1	1.5	2
				F-G-M Copula ($\theta_1 = \theta_2 = -0.3$)						
5	(4, 37)	0.98	0.85	0.50	0.16	**0.05**	0.16	0.50	0.85	0.98
	(5, 36)	1	0.91	0.62	0.23	**0.08**	0.23	0.60	0.91	0.99
	(6, 35)	1	0.95	0.70	0.31	**0.12**	0.30	0.71	0.95	1
11	(7, 34)	1	0.99	0.79	0.26	**0.05**	0.26	0.79	1	1
	(8, 33)	1	1	0.86	0.35	**0.08**	0.35	0.86	1	1
	(9, 32)	1	1	0.91	0.44	**0.13**	0.45	0.91	1	1
25	(9, 32)	1	1	0.93	0.35	**0.04**	0.35	0.94	1	1
	(10, 31)	1	1	0.97	0.46	**0.06**	0.46	0.97	1	1
	(11, 30)	1	1	0.99	0.54	**0.10**	0.58	0.99	1	1
				A-M-H Copula ($\theta_1 = \theta_2 = -0.3$)						
5	(4, 37)	0.98	0.85	0.49	0.15	**0.05**	0.16	0.49	0.85	0.98
	(5, 36)	0.99	0.92	0.60	0.23	**0.08**	0.23	0.61	0.92	0.99
	(6, 35)	1	0.95	0.71	0.30	**0.13**	0.30	0.70	0.95	1
11	(7, 34)	1	0.99	0.78	0.26	**0.05**	0.25	0.79	0.99	1
	(8, 33)	1	1	0.85	0.36	**0.09**	0.35	0.86	1	1
	(9, 32)	1	1	0.91	0.44	**0.13**	0.44	0.91	1	1
25	(9, 32)	1	1	0.94	0.34	**0.03**	0.35	0.94	1	1
	(10, 31)	1	1	0.97	0.47	**0.06**	0.46	0.97	1	1
	(11, 30)	1	1	0.98	0.58	**0.10**	0.58	0.99	1	1
				Clayton-Pareto Copula ($\theta_1 = \theta_2 = 2$)						
5	(4, 37)	0.97	0.81	0.46	0.14	**0.05**	0.15	0.47	0.81	0.97
	(5, 36)	0.99	0.88	0.56	0.21	**0.08**	0.22	0.57	0.88	0.98
	(6, 35)	0.99	0.93	0.66	0.28	**0.12**	0.28	0.66	0.92	0.99
11	(7, 34)	1	0.98	0.74	0.24	**0.05**	0.25	0.75	0.98	1
	(8, 33)	1	0.99	0.81	0.32	**0.08**	0.33	0.82	0.99	1
	(9, 32)	1	0.99	0.88	0.41	**0.13**	0.42	0.87	0.99	1
25	(9, 32)	1	1	0.90	0.32	**0.03**	0.33	0.91	1	1
	(10, 31)	1	1	0.90	0.43	**0.06**	0.44	0.95	1	1
	(11, 30)	1	1	0.97	0.53	**0.10**	0.53	0.98	1	1

Table I. *AR* for a given design

n	Mean Shift	Bivariate Normal Data				Bivariate t Data with 5 d.f.			
		SN^2	SR^2	χ^2	*New Chart*	SN^2	SR^2	χ^2	*New Chart*
		UCL=8.69	UCL=8.78	UCL=10.60	$a=c=166$	UCL=8.70	UCL=8.73	UCL=12.2	$a=c=166$
15	(0.0, 0.0)	199.96	199.63	202.05	199.785	206.289	200.296	196.207	201.14
	(0.2, 0.2)	75.35	66.42	**51.40**	66.18	53.46	**46.73**	74.60	57.85
	(0.4, 0.4)	18.94	15.19	**9.52**	15.04	11.79	**9.55**	15.32	11.26
	(0.6, 0.6)	6.52	4.94	**2.91**	4.71	4.80	**3.30**	4.07	**3.30**
	(0.8, 0.8)	2.92	2.29	**1.47**	2.20	2.05	1.78	1.70	**1.57**
	(1.0, 1.0)	1.75	1.41	**1.10**	1.37	1.43	1.29	1.15	**1.12**
		UCL=9.80	UCL=9.72	UCL=10.60	$a=250,\ c=245$	UCL=9.76	UCL=9.64	UCL=11.4	$a=250,\ c=245$
30	(0.0, 0.0)	204.98	198.08	199.79	201.022	199.81	197.77	199.68	198.68
	(0.3, 0.6)	3.37	2.21	**1.75**	2.88	6.72	**4.93**	6.45	5.02
	(0.3, 0.9)	1.38	1.10	**1.03**	1.23	2.58	1.91	1.7078	**1.64**
	(0.6, 0.3)	3.31	2.18	**1.75**	2.72	6.60	**4.94**	6.47	5.54
	(0.6, 0.9)	1.26	1.08	**1.03**	1.18	2.19	1.81	1.73	**1.55**
	(0.9, 0.3)	1.39	1.09	**1.03**	1.20	2.61	1.92	1.75	**1.72**
	(0.9, 0.6)	1.27	1.09	**1.03**	1.15	2.22	1.83	1.71	**1.60**
		UCL=10.08	UCL=10.05	UCL=10.60	$a=c=166$	UCL=10.06	UCL=10.0	UCL=11.1	$a=c=166$
50	(0.0, 0.0)	202.77	194.58	200.97	204.82	200.14	197.70	199.02	206.56
	(0.2, 0.2)	20.31	14.64	**12.50**	21.74	11.80	**9.77**	14.86	12.97
	(0.6, 0.6)	1.14	1.06	**1.04**	1.12	1.06	**1.03**	1.05	**1.03**
		UCL=10.08	UCL=10.05	UCL=10.60	$a=294,\ c=299$	UCL=10.06	UCL=10.0	UCL=11.1	$a=294,\ c=299$
	(0.3, 0.6)	1.70	1.25	**1.15**	1.52	1.27	**1.13**	1.17	**1.13**
	(0.9, 0.3)	1.05	**1.00**	**1.00**	1.02	**1.00**	**1.00**	**1.00**	**1.00**

Table II. Comparison of the ARL_{out} of control charts with approximately the same ARL_{in}

The performance of a control chart is usually assessed by checking its potential to detect process shifts as fast as possible. The typical method used is to pre-specify a common value for the *FAR* and then look at the out-of-control values (*AR*) for several process mean shifts. In Table I, we have considered three different *FAR* levels (from approximately 5 to 10%) for three copulas with standard normal marginal distributions. For our calculations we used the Farlie-Gumbel-Morgenstern, the Ali-Mikhail-Haq (A-M-H) and the Clayton-Pareto copula which are respectively given by

$$C_\theta(u,v) = uv[1+\theta_2(1-u)(1-v)], \qquad -1 \le \theta \le 1$$

$$C_\theta(u,v) = uv/[1+\theta_2(1-u)(1-v)]\ , \quad -1 \le \theta \le 1$$

$$C_\theta(u,v) = (u^{-\theta}+v^{-\theta}-1\ )\ , \qquad \theta > 0.$$

It should be mentioned that the suggested chart remains unaffected by the choice of the marginal distributions. Then, we computed the *AR* as the means $\mu_X^{(T)} = \mu_Y^{(T)}$ of the test sample shift from the in-control value $\mu_X^{(R)} = \mu_Y^{(R)} = 0$.

It is obvious that our chart is quite sensitive and capable of identifying process mean shifts quickly. In addition, the tables presented clearly indicate that no matter what copula is used the *FAR* is almost the same for fixed values of the parameters *m*, *n*, *r*, *s*, *a*, *b*, *c*, *d*, which can be used for the design of the new chart. Consequently, the performance of the chart might be typically affected by the dependence structure of the underlying characteristics, but the *FAR* does not change crucially. The same holds true for the in-control *ARL*, as we will see below.

In order to study and compare the performance of the proposed chart to its parametric and nonparametric counterparts, data from multivariate normal and *t* distribution (with 5 degrees of freedom) were generated and used for the calculation of the *ARL* values. It is worth mentioning here that the *t* distribution is one of the most popular multivariate non-normal distributions used in simulation studies. The distribution parameters utilized are the same as those considered in the publication of Boone and Chakraborti [5], which are presented below as follows

$$\mu = \begin{pmatrix} 0 \\ 0 \end{pmatrix},\ \Sigma\begin{pmatrix} 1 & 0.5 \\ 0.5 & 1 \end{pmatrix} \text{ and } \Sigma_{t(5)} = \begin{pmatrix} 0.6 & 0.3 \\ 0.3 & 0.6 \end{pmatrix}.$$

It is important to note that $\Sigma_{t(v)}$ was suitably chosen in order to achieve the same covariance matrix for both distributions. Moreover, we assume that $a = c$, when equal shifts occur and $a \ne c$ otherwise. In what follows, the new chart is compared to the SN^2 and SR^2 charts of Boone and Chakraborti [5] as well as to the traditional χ^2 in terms of its out-of-control *ARL*. The control limit values of SN^2, SR^2 and χ^2 were the same proposed by Boone and Chakraborti [5]. For the study, the ARL_{in} was set to 200 (or nearly) with *FAR* being equal to 0.005. To estimate the in and out-of-control *ARL* values for the proposed chart, the same assumptions were made, as previously. The results are presented in Tables II and III.

The simulation study carried out reveals that the charts perform very similarly. In the case that the data are multivariate normal, the χ^2 chart performs slightly better. This was expected as the parametric distributional assumption holds true. When the data are not normal, the charts seem to perform almost the same, with the new and the SR^2 chart performing sometimes better than the χ^2 chart. The SR^2 chart detects a shift more quickly than the SN^2 chart, which can be explained by the fact that the Wilcoxon signed-rank test is more powerful than the sign test in cases of symmetric and light-tailed distributions. Although the attained ARL_{in} values are sometimes higher than desired, it should be noted that the proposed chart detects shifts very quickly. Finally, the new chart seems to outperform the others, when both means shift unequally from their in-control values.

4 Conclusions

As the simulation study revealed, the new control chart offers a simple tool which is equivalent or slightly better, in terms of performance power, to the SR^2, SN^2 and χ^2 charts. Although the new chart is typically affected by the dependence structure of the characteristics under study, the values of *FAR* and ARL_{in} are almost the same when different distributions or copulas are used; this is an appealing property, since it could be used as a fully non-parametric control chart (although formally it should be labelled as a semiparametric one). Besides its simplicity, the implementation of the new chart does not require any assumptions on the form of the bivariate distribution that the characteristics under study follow. This is a strong advantage when compared to other non-parametric control charts available in the literature. For example, the SR^2 chart can only be used under the assumption of diagonal symmetry on the underlying bivariate distribution (otherwise its test statistic cannot be computed), while both the SN^2 and SR^2 charts require the inversibility of the estimation of the process covariance matrix. Hence, the new chart seems to be a highly useful tool to a quality practitioner, not only because of its simplicity and high performance but for offering a valid tool for cases where alternative non-parametric control charts cannot be used.

References

1. U.U. Anjos, N. Kolev and N.L. Tanaka. Copula Associated to Order Statistics, *Brazilian Journal of Probability and Statistics*, **19**, 2, 111-123, 2005.
2. B.C. Arnold, N. Balakrishnan and H.N. Nagaraja. *A First Course in Order Statistics*, Wiley, New York, 1992.
3. J. Avérous, C. Genest and S.C. Kochar. On the Dependence Structure of Order Statistics, *Journal of Multivariate Analysis*, **94**, 1, 159-171, 2005.
4. N. Balakrishnan, I.S. Triantafyllou and M.V. Koutras. A Distribution-Free Control Chart Based on Order Statistics, *Communications in Statistics: Theory and Methods*, **39**, 20, 3652-3677, 2010.
5. J.M. Boone and S. Chakraborti. Two Simple Shewhart-type Multivariate Nonparametric Control Charts, Applied Stochastic Models in Business and Industry, **28**, 2, 130-140, 2012.
6. S. Chakraborti, P. Van Der Laan and M.A. van de Wiel. A Class of Distribution-Free Control Charts, *Journal of the Royal Statistical Society: Series C (Applied Statistics)*, **53**, 3, 443-462, 2004.
7. H.A. David and H.N. Nagaraja. *Order Statistics*, Wiley, Hoboken, New Jersey, 2003.

8. G.J. Janacek and S.E. Meikle. Control Charts Based on Medians, *Journal of the Royal Statistical Society: Series D (The Statistician)*, **46**, 1, 19–31, 1997.
9. A. Sklar. Fonctions de Répartition à *n* Dimensions et Leurs Marges, *Publications de l'Institut de Statistique de l'Université de Paris*, **8**, 229–231, 1959.

Reliability and Risk Function Improvement of Bulk Cargo Transportation System

Kwiatuszewska-Sarnecka Bozena[1]

[1] Department of Mathematics, Maritime University Gdynia, ul. Morska 83, 81-226 Gdynia, Poland,
(E-mail: b.sarnecka@wn.am.gdynia.pl)

Abstract. In the paper the basic notions of the ageing multistate systems reliability analysis are introduced. The system multistate components and the multistate system reliability functions are defined and the mean values of the multistate system lifetimes in the reliability state subsets and in the particular reliability states are determined. The notion of the multistate system risk function and the moment of the system exceeding the critical reliability state are introduced. The series and series - parallel reliability structures of the multistate systems with ageing components with hot single reserve are defined and their reliability functions and mean values are determined. Further, in the developed reliability models, it is assumed that the system's components have the multistate Weibull reliability functions with various parameters in their different reliability state subsets. Under this assumption, the proposed multistate system reliability models are applied in maritime transport to the reliability analysis of a bulk cargo transportation system and its reliability function, moreover other main characteristics are determined.

Keywords: multistate system, reliability function, risk function, redundancy

1 Introduction

Taking into account the complexity of the failure processes of real technical systems, it seems reasonable to expand the two-state approach to multi-state approach [1] in the system reliability analysis. The assumption that the system is composed of multistate components with reliability states degrading in time [2] gives possibility for more precise analysis of its reliability. This assumption allows us to distinguish a system reliability critical state, which exceeded is either dangerous for the environment or does not assure the necessary level of the effectiveness of its operations process. Then, an important system reliability characteristic is the time to the moment of exceeding the system reliability critical state and its distribution, which is called the system risk function. This distribution is strictly related to the system multistate reliability function, which is a basic characteristic of the multistate system. Next, the assumption that the system's components have single hot reserve gives the possibility to improve the

16th ASMDA Conference Proceedings, 30 June – 4 July 2015, Piraeus, Greece

system's reliability and extend the time to the moment of exceeding the system reliability critical state. This approach may be successfully applied to a wide class of real ageing technical systems, for instance to reliability analysis, identification and prediction of the bulk cargo terminal transportation system, which is demonstrated in the paper.

2 Multistate approach to system reliability analysis

In the multistate reliability analysis to define a system composed of n, $n \in N$ ageing components we assume that:

– E_i, $i = 1,2,...,n$, are components of a system,
– all components and a system under consideration have the set of reliability states $\{0,1,...,z\}$, $z \geq 1$,
– the reliability states are ordered, the state 0 is the worst and the state z is the best,
– the component and the system reliability states degrade with time t,
– $T_i(u)$, $i = 1,2,...,n$, $n \in N$, are independent random variables representing the lifetimes of components E_i in the reliability state subset $\{u,u + 1,...,z\}$, while they were in the reliability state z at the moment $t = 0$,
– $T(u)$ is a random variable representing the lifetime of a system in the reliability state subset $\{u,u + 1,...,z\}$, while it was in the reliability state z at the moment $t = 0$,
– $s_i(t)$ is a component E_i reliability state at the moment t, $t \in \langle 0,\infty)$, given that it was in the reliability state z at the moment $t = 0$,
– $s(t)$ is the system reliability state at the moment t, $t \in \langle 0,\infty)$, given that it was in the reliability state z at the moment $t = 0$.

The above assumptions mean that the reliability states of the ageing system and components may be changed over time only from better to worse.
Definition 1. A vector

$$R_i(t,\cdot) = [R_i(t,0), R_i(t,1), \ldots, R_i(t,z)], \text{ for } t \in \langle 0,\infty),\ i = 1,2,...,n, \tag{1}$$

where

$$R_i(t,u) = P(s_i(t) \geq u \mid s_i(0) = z) = P(T_i(u) > t) \tag{2}$$

for $t \in \langle 0,\infty), u = 0,1,\ldots,z,$ is the probability that the component E_i is in the reliability state subset $\{u, u+1,\ldots,z\}$ at the moment t, $t \in \langle 0,\infty)$, while it was in the reliability state z at the moment $t = 0$, is called the multistate reliability function of a component E_i.
Definition 2. A vector

$$\boldsymbol{R}(t,\cdot) = [\boldsymbol{R}(t,0), \boldsymbol{R}(t,1), \ldots, \boldsymbol{R}(t,z)],\ t \in \langle 0,\infty), \tag{3}$$

where

$$\boldsymbol{R}(t,u) = P(s(t) \geq u \mid s(0) = z) = P(T(u) > t) \tag{4}$$

for $t \in \langle 0,\infty)$, $u = 0,1,...,z$, is the probability that the system is in the reliability state subset $\{u,u + 1,...,z\}$ at the moment t, $t \in \langle 0,\infty)$, while it was in the reliability state z at the moment $t = 0$, is called the multistate reliability function of a system. The reliability functions $R_i(t,u)$ and $\boldsymbol{R}(t,u)$, $t\in\langle 0,\infty)$, u = 0,1,...,z, defined by (2) and (4) are called the coordinates of the components and the system multistate reliability functions $R_i(t,\cdot)$ and $\boldsymbol{R}(t,\cdot)$ are given by respectively (1) and (3). It is clear that from Definition 1 and Definition 2, for $u=0$, we have $R_i(t,0) = 1$ and $\boldsymbol{R}(t,0)=1$.

Under the above definitions, the mean value of the system lifetime $T(u)$ in the reliability state subset $\{u,u+1,...,z\}$ is given by

$$\mu(u)=\int_0^\infty \boldsymbol{R}(t,u)dt,\ u = 1,2,\ldots,z. \tag{5}$$

Moreover, the mean values of the system lifetimes in particular reliability states are given by

$$\bar{\mu}(u)=\mu(u)-\mu(u+1),\ u = 0,1,...,z-1,\ \bar{\mu}(z)=\mu(z), \tag{6}$$

where $\mu(u)$ u = 0,1,...,z are given by (5).

Further, if r is the system critical reliability state, then the system risk function is given by [2], [3]

$$\boldsymbol{r}(\boldsymbol{t})=1-\boldsymbol{R}(\boldsymbol{t},\boldsymbol{r}),\ t\in\langle 0,\infty), \tag{7}$$

and if $\boldsymbol{\tau}$ is the moment when the system risk function exceeds a permitted level δ, then if $\boldsymbol{r}^{-1}(\boldsymbol{t})$ exists we have

$$\boldsymbol{\tau}=\boldsymbol{r}^{-1}(\delta), \tag{8}$$

where $\boldsymbol{r}^{-1}(\boldsymbol{t})$ is the inverse function of the risk function $\boldsymbol{r}(\boldsymbol{t})$.

Now, after introducing the notion of the multistate reliability analysis, we may define basic multistate reliability structures.

Definition 3. A multistate system is called a series if its lifetime $T(u)$ in the reliability state subset $\{u,u+1,...,z\}$ is given by $T(u) = \min_{1\le i\le n}\{T_i(u)\}$, u = 1,2,...,z.

The reliability function of the multistate series system is given by the vector

$$\boldsymbol{R}(t,\cdot) = [1, \boldsymbol{R}(t,1), ..., \boldsymbol{R}(t,z)] \tag{9}$$

with the coordinates

$$\boldsymbol{R}(t,u) = \prod_{i=1}^{n} R_i(t,u),\ t\in<0,\infty),\ u = 1,2,...,z. \tag{10}$$

Definition 4. A multistate system is called series-parallel if its lifetime $T(u)$ in the reliability state subset $\{u,u+1,...,z\}$ is given by $T(u) = \max_{1\le i\le k_n}\{\min_{1\le j\le l_i}\{T_{ij}(u)\}\}$, u = 1,2,...,z.

The reliability function of the regular multistate series-parallel system is given by the vector

$$\boldsymbol{R}(t,\cdot) = [1, \boldsymbol{R}(t,1), ..., \boldsymbol{R}(t,z)], \tag{11}$$

with the coordinates

$$\boldsymbol{R}(t,u) = 1-\prod_{i=1}^{k_n}[1-\prod_{j=1}^{l_i} R_{ij}(t,u)],\ t\in(-\infty,\infty),\ u = 1,2,...,z, \tag{12}$$

where k_n is the number of series subsystems linked in parallel and l_i is the number of components in the series subsystem.

3 Multistate approach to system reliability improvement analysis

Definition 5. A multi-state series system is called a series system with a hot reserve of its components if its lifetime $T^{)}(u)$ in the state subset $\{u,u+1,...,z\}$ is given by [5] $T(u) = \min_{1 \le i \le n}\{\max_{1 \le j \le 2}\{T_{ij}(u)\}\}$, $u = 1,2,...,z$,

where $T_{i1}(u)$ are the lifetimes of the system's basic components and $T_{i2}(u)$ are the lifetimes of their reserve components.

The scheme of this kind of series system is shown in *Figure 1*.

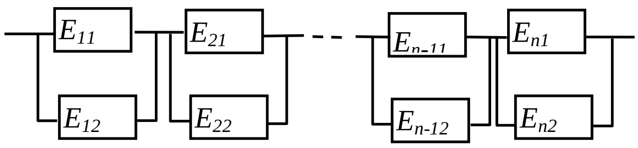

Figure 1. The scheme of a series system with a hot reserve of its components**.**

The reliability function of the non-homogeneous multi-state series system with a hot reserve of its components is given by a vector

$$\boldsymbol{IR}(t,\cdot) = [1, \boldsymbol{IR}(t,1),..., \boldsymbol{IR}(t,z)], \tag{13}$$

where

$$\boldsymbol{IR}(t,u) = \prod_{i=1}^{n}[1-[F_i(t,u)]^2], \; t \in <0,\infty), \; u = 1,2,...,z. \tag{14}$$

Definition 5. A multistate system is called series-parallel system with a hot reserve of its components if its lifetime $T(u)$ in the reliability state subset $\{u,u+1,...,z\}$ is given by $T(u) = \max_{1 \le i \le k_n}\{\min_{1 \le j \le l_i}\{\max_{1 \le k \le 2}\{T_{ijk}(u)\}\}\}$, $u = 1,2,...,z$,

where $T_{ij1}(u)$ are the lifetimes of the system's basic components and $T_{ij2}(u)$ are the lifetimes of the reserve components.
The reliability function of the regular multistate series-parallel system with a hot reserve of its components is given by the vector

$$\boldsymbol{IR}(t,\cdot) = [1, \boldsymbol{IR}(t,1),..., \boldsymbol{IR}(t,z)], \tag{15}$$

with the coordinates

$$\boldsymbol{IR}(t,u) = 1-\prod_{i=1}^{k_n}[1-\prod_{j=1}^{l_i}[1-[F_{ij}(t,u)]^2], \; t \in (-\infty,\infty), \; u = 1,2,...,z, \tag{16}$$

where k_n is the number of series subsystems linked in parallel and l_i is the number of components in the series subsystem.

4 Bulk cargo transportation system - technical description

The considered bulk cargo terminal placed at the Baltic seaside is designated for storage and reloading of bulk cargo such as different kinds of fertilizers e.g.:

ammonium sulphate, but its main area of activity is to load bulk cargo on board the ships for export. There are two independent transportation systems:
1. The system of reloading rail wagons. 2. The system of loading vessels.
Cargo is brought to the terminal by trains consisting of self discharging wagons, which are discharged to a hopper and then by means of conveyors are transported into the one of four storage tanks (silos). Loading of fertilizers from storage tanks on board the ship is done by means of a special reloading system, which consists of several belt conveyors and one bucket conveyor, which allows for the transfer of bulk cargo in a vertical direction. Researched system is a system of belt conveyors, reffered to as the transport system. In the conveyor reloading system, we distinguish three bulk cargo transportation subsystems, the belt conveyors S_1, S_2 and S_3. The conveyor loading system is composed of six bulk cargo transportation subsystems, the dosage conveyor S_4, the horizontal conveyor S_5, the horizontal conveyor S_6, the sloping conveyor S_7, the dosage conveyor with buffer S_8, and the loading system S_9.
The bulk cargo transportation subsystems are built, respectively:
- the subsystem S_1 composed of 1 rubber belt, 2 drums, a set of 121 bow rollers, and a set of 23 belt supporting rollers,
- the subsystem S_2 composed of 1 rubber belt, 2 drums, a set of 44 bow rollers, and a set of 14 belt supporting rollers,
- the subsystem S_3 composed of 1 rubber belt, 2 drums, a set of 185 bow rollers, and a set of 60 belt supporting rollers,
- the subsystem S_4 composed of three identical belt conveyors, each composed of 1 rubber belt, 2 drums, a set of 12 bow rollers, and a set of 3 belt supporting rollers,
- the subsystem S_5 composed of 1 rubber belt, 2 drums, a set of 125 bow rollers, and a set of 45 belt supporting rollers,
- the subsystem S_6 composed of 1 rubber belt, 2 drums, a set of 65 bow rollers, and a set of 20 belt supporting rollers,
- the subsystem S_7 composed of 1 rubber belt, 2 drums, a set of 12 bow rollers, and a set of 3 belt supporting rollers,
- the subsystem S_8 composed of 1 rubber belt, 2 drums, a set of 162 bow rollers, and a set of 53 belt supporting rollers,
- the subsystem S_9 composed of 3 rubber belts, 6 drums, a set of 64 bow rollers, and a set of 20 belt supporting rollers.
The scheme of the bulk cargo transportation system is presented in *Figure 2*.

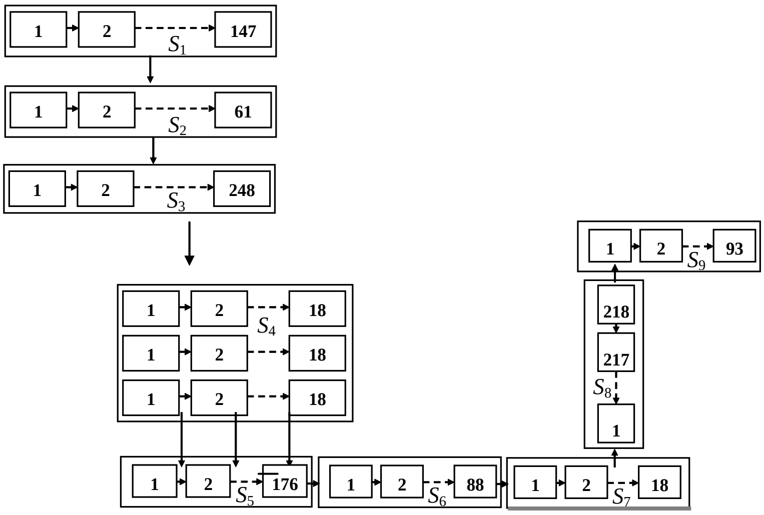

Figure 2. The scheme of port bulk cargo transportation system.

Further, assuming that the system is in the reliability state subset $\{u,u+1,\ldots,z\}$, if all of its subsystems are in this subset of reliability states, we conclude that the bulk cargo transportation system is a series system [4] of series subsystems $S_1, S_2, S_3, S_5, S_6, S_7, S_8, S_9$ and series-parallel subsystem S_4, with a scheme presented in *Figure 3*.

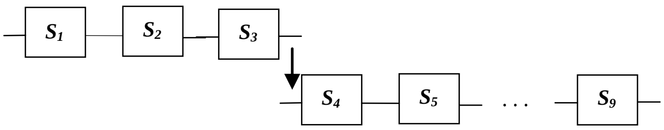

Figure 3. The scheme of port bulk cargo transportation system reliability structure

5 Reliability parameters of bulk cargo transportation system

After discussion with experts, in the reliability analysis of the bulk cargo transportation system we distinguish the following four reliability states (z = 3) of the considered system and its components:

- reliability state 3 – ensuring the highest efficiency of the conveyor,
- reliability state 2 – ensuring lower efficiency of the working conveyor, which is spilling cargo out of the belt caused by partial damage to some of the rollers or misalignment of the belt,
- reliability state 1 – ensuring lower efficiency of the working conveyor controlled directly by an operator,
- reliability state 0 – the conveyor is unable to work, which my be caused by e.g.: breakage of the belt or failure of the rollers.

We assume that the transitions between the components reliability states are possible only from a better to a worse state and we fix the system and its components critical reliability state to be $r = 2$.

Moreover, we assume that the system elements and their reserve elements $E_i^{(\upsilon)}$, $E_{ij}^{(\upsilon)}$ having the lifetimes $T_i^{(\upsilon)}(u) = T_{i1}^{(\upsilon)}(u) = T_{i2}^{(\upsilon)}(u)$, $T_{ij}^{(\upsilon)}(u) = T_{ij1}^{(\upsilon)}(u) = T_{ij2}^{(\upsilon)}(u)$, $i = 1,2,\ldots,i^{(\upsilon)}$, $j = 1,2,\ldots, j_i^{(\upsilon)}$, $u = 1,2,3$, $\upsilon = 1,2,\ldots,9$, in the reliability states subsets {1,2,3}, {2,3}, {3} respectively, have the reliability functions respectively given by the vector:

$R_i^{(\upsilon)}(t,\cdot) = [1, R_i^{(\upsilon)}(t,1), R_i^{(\upsilon)}(t,2), R_i^{(\upsilon)}(t,3)]$, $R_{ij}^{(\upsilon)}(t,\cdot) = [1, R_{ij}^{(\upsilon)}(t,1), R_{ij}^{(\upsilon)}(t,2)\ R_{ij}^{(\upsilon)}(t,3)]$

with the Weibull probability functions:

$R_i^{(\upsilon)}(t,u) = P(T_i^{(\upsilon)}(u) > t) = \exp[-\lambda_i^{(\upsilon)}(u)t^2]$, $t \in \langle 0,\infty)$, or

$R_{ij}^{(\upsilon)}(t,u) = P(T_{ij}^{(\upsilon)}(u) > t) = \exp[-\lambda_{ij}^{(\upsilon)}(u)t^2]$, $t \in \langle 0,\infty)$, with the parameters $\lambda_i^{(\upsilon)}(u)$, $\lambda_{ij}^{(\upsilon)}(u)$, $i = 1,2,\ldots,i^{(\upsilon)}$, $j = 1,2,\ldots, j_i^{(\upsilon)}$, $u = 1,2,3$, $\upsilon = 1,2\ldots,9$, presented in Tables 1-3.

S_1	$\lambda_i^{(1)}(u)$	S_2	$\lambda_i^{(2)}(u)$	S_3	$\lambda_i^{(3)}(u)$
$i=1$		$i=1$		$i=1$	
$u=1$	0,01208	$u=1$	0,01208	$u=1$	0,01208
$u=2$	0,02190	$u=2$	0,02190	$u=2$	0,02190
$u=3$	0,04909	$u=3$	0,04909	$u=3$	0,04909
$i=2,3$		$i=2,3$		$i=2,3$	
$u=1$	0,00189	$u=1$	0,00189	$u=1$	0,00189
$u=2$	0,00238	$u=2$	0,00238	$u=2$	0,00238
$u=3$	0,00292	$u=3$	0,00292	$u=3$	0,00292
$i=4,\ldots,124$		$i=4,\ldots,47$		$i=4,\ldots,188$	
$u=1$	0,00739	$u=1$	0,00739	$u=1$	0,00739
$u=2$	0,01208	$u=2$	0,01208	$u=2$	0,01208
$u=3$	0,02112	$u=3$	0,02112	$u=3$	0,02112
$i=125,\ldots,147$		$i=48,\ldots,61$		$i=189,\ldots,248$	
$u=1$	0,00204	$u=1$	0,00204	$u=1$	0,00204
$u=2$	0,00246	$u=2$	0,00246	$u=2$	0,00246
$u=3$	0,00302	$u=3$	0,00302	$u=3$	0,00302

S_4	$\lambda_{ij}^{(4)}(u)$ $j=1,2,3$	S_5	$\lambda_i^{(5)}(u)$	S_6	$\lambda_i^{(6)}(u)$
$i=1$		$i=1$		$i=1$	
$u=1$	0,01208	$u=1$	0,01208	$u=1$	0,01208
$u=2$	0,02190	$u=2$	0,02190	$u=2$	0,02190
$u=3$	0,04909	$u=3$	0,04909	$u=3$	0,04909
$i=2,3$		$i=2,3$		$i=2,3$	
$u=1$	0,00189	$u=1$	0,00189	$u=1$	0,00189
$u=2$	0,00238	$u=2$	0,00238	$u=2$	0,00238
$u=3$	0,00292	$u=3$	0,00292	$u=3$	0,00292
$i=4,\ldots,15$		$i=4,\ldots,128$		$i=4,\ldots,67$	
$u=1$	0,02806	$u=1$	0,00739	$u=1$	0,00739
$u=2$	0,02986	$u=2$	0,01208	$u=2$	0,01208
$u=3$	0,03205	$u=3$	0,02112	$u=3$	0,02112
$i=16,\ldots,18$		$i=129,\ldots,173$		$i=68,\ldots,88$	
$u=1$	0,00594	$u=1$	0,00204	$u=1$	0,00204
$u=2$	0,01003	$u=2$	0,00246	$u=2$	0,00246
$u=3$	0,02011	$u=3$	0,00302	$u=3$	0,00302

Table 1, 2 . Bulk cargo transportation subsystem S_1, S_2, S_3, S_4, S_5, S_6 component parameters $\lambda_i^{(k)}(u)$, $\lambda_{ij}^{(k)}(u)$, $u = 1,2,3$

S_7	$\lambda_i^{(7)}(u)$	S_8	$\lambda_i^{(8)}(u)$	S_9	$\lambda_i^{(9)}(u)$
$i=1$		$i=1$		$i=1,2,3$	
$u=1$	0,01208	$u=1$	0,01208	$u=1$	0,01208
$u=2$	0,02190	$u=2$	0,02190	$u=2$	0,02190
$u=3$	0,04909	$u=3$	0,04909	$u=3$	0,04909
$i=2,3$		$i=1,2,3$		$i=4,\ldots,9$	
$u=1$	0,00189	$u=1$	0,00189	$u=1$	0,00189
$u=2$	0,00238	$u=2$	0,00238	$u=2$	0,00238
$u=3$	0,00292	$u=3$	0,00292	$u=3$	0,00292
$i=4,\ldots,15$		$i=4,\ldots,165$		$i=10,\ldots,73$	
$u=1$	0,02806	$u=1$	0,00739	$u=1$	0,00466
$u=2$	0,02986	$u=2$	0,01208	$u=2$	0,00754
$u=3$	0,03205	$u=3$	0,02112	$u=3$	0,01208
$i=16,\ldots,18$		$i=167,\ldots 218$		$i=74,\ldots,93$	
$u=1$	0,00594	$u=1$	0,00204	$u=1$	0,00119
$u=2$	0,01003	$u=2$	0,00246	$u=2$	0,00181
$u=3$	0,02011	$u=3$	0,00302	$u=3$	0,00238

Table 3. Bulk cargo transportation subsystem S_7, S_8, and S_9, component parameters $\lambda_i^{(k)}(u)$, $u = 1,2,3$

6 Bulk cargo transportation system reliability prediction

Considering that the described system is a series system composed of subsystems S_υ, $\upsilon = 1,2,\ldots,9$, after applying the formulae (9)-(12), (14)-(15), its reliability function is given by

$$\boldsymbol{R}(t,\cdot) = [1, \boldsymbol{R}(t,1), \boldsymbol{R}(t,2), \boldsymbol{R}(t,3)], \ t \in \langle 0,\infty), \tag{17}$$

where the coordinates have the following forms

$$\boldsymbol{R}(t,u) = \prod_{\upsilon=1}^{9} \boldsymbol{R}^{(\upsilon)}(t,u), \ \upsilon = 1,2,\ldots,9, \text{ for } t \in \langle 0,\infty), \ u = 1,2,3,$$

$$\boldsymbol{R}^{(1)}(t,u) = \prod_{i=1}^{147} R_i^{(1)}(t,u), \ \boldsymbol{R}^{(2)}(t,u) = \prod_{i=1}^{61} R_i^{(1)}(t,u), \tag{18)-(19}$$

$$\boldsymbol{R}^{(3)}(t,u) = \prod_{i=1}^{248} R_i^{(1)}(t,u), \ \boldsymbol{R}^{(4)}(t,u) = 1 - [1 - \prod_{i=1}^{18} R_{ij}^{(4)}(t,u)]^3, \tag{20)-(21}$$

$$\boldsymbol{R}^{(5)}(t,u) = \prod_{i=1}^{173} R_i^{(5)}(t,u), \ \boldsymbol{R}^{(6)}(t,u) = \prod_{i=1}^{88} R_i^{(6)}(t,u), \tag{22)-(23}$$

$$\boldsymbol{R}^{(7)}(t,u) = \prod_{i=1}^{18} R_i^{(7)}(t,u), \ \boldsymbol{R}^{(8)}(t,u) = \prod_{i=1}^{218} R_i^{(8)}(t,u), \tag{24)-(25}$$

$$\boldsymbol{R}^{(9)}(t,u) = \prod_{i=1}^{93} R_i^{(9)}(t,u). \tag{26}$$

Applying the formulas (18)-(26) and considering the parameters given in Tables 1-3, the coordinates of the system reliability function given by (17) are as follows:

$$\begin{aligned}\boldsymbol{R}(t,1) = \ & \exp[-0.95697t^2] \cdot \exp[-0.36958t^2] \exp[-1.50541t^2] \cdot \\ & [3\exp[-0.37040t^2] - 3\exp[-0.740801t^2] + \exp[-1.11120t^2]] \\ & \exp[-1.03141t^2] \cdot \exp[-0.53701t^2] \exp[-0.37040t^2] \cdot \\ & \exp[-1.32116t^2] \ \exp[-0.36962t^2] \\ = \ & 3\exp[-6.83196t^2] - 3\exp[-7.20236t^2] + \exp[-7.57276t^2],\end{aligned} \tag{27}$$

$$\begin{aligned}\boldsymbol{R}(t,2) = \ & \exp[-1.54492t^2] \cdot \exp[-0.59262t^2] \exp[-2.40906t^2] \cdot \\ & [3\exp[-0.41507t^2] - 3\exp[-0.830141t^2] + \exp[-1.24521t^2]] \\ & \exp[-1.64736t^2] \cdot \exp[-0.86108t^2] \exp[-0.41507t^2] \cdot \\ & \exp[-2.11400t^2] \ \exp[-0.59874t^2], \\ = \ & 3\exp[-10.59790t^2] - 3\exp[-11.01297t^2] + \exp[-11.42804t^2],\end{aligned} \tag{28}$$

$$\begin{aligned}\boldsymbol{R}(t,3) = \ & \exp[-2.67991t^2] \cdot \exp[-1.02649t^2] \exp[-4.143331t^2] \cdot \\ & [3\exp[-0.49986t^2] - 3\exp[-0.999721t^2] + \exp[-1.49958t^2]] \\ & \exp[-2.83083t^2] \cdot \exp[-1.48813t^2] \exp[-0.49986t^2] \cdot \\ & \exp[-3.63643t^2] \exp[-0.98551t^2]\end{aligned}$$

$$= 3\exp[-17.79035t^2] - 3\exp[-18.29021t^2] + \exp[-18.79007t^2] \quad (29)$$

Their graphs are presented in Figure 4.

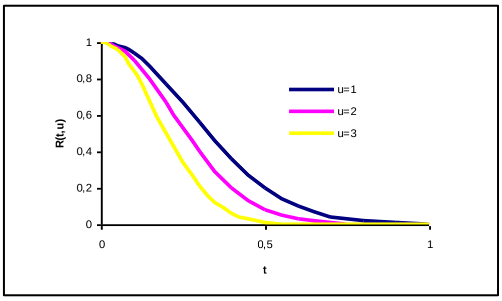

Figure 4. The graph of bulk cargo transportation system reliability function.

Considering (27)-(29), the expected values of the bulk cargo transportation system lifetimes in the reliability states subsets {1,2,3}, {2,3}, {3}, according to (5), are respectively

$$\mu(1) \cong 0.3486, \quad \mu(2) \cong 0.2777, \quad \mu(3) \cong 0.2131. \quad (30)$$

And further, the standard deviations of this system lifetimes in the reliability state subsets {1,2,3}, {2,3}, {3}, according to (6) are

$$\sigma(1) \cong 0.0176, \quad \sigma(2) \cong 0.0112, \quad \sigma(3) \cong 0.0066. \quad (31)$$

Consequently, according to (6), the mean values of the maritime ferry technical system lifetimes in the particular reliability states 1, 2, 3, are respectively:

$$\bar{\mu}(1) \cong 0.0709, \quad \bar{\mu}(2) \cong 0.0646, \quad \bar{\mu}(3) \cong 0.2131. \quad (32)$$

Since the critical reliability state is r = 2, the system risk function of the bulk cargo transportation system, according to (7), is given by

$\boldsymbol{r}(t) = 1 - \boldsymbol{R}(t,2)$,

where $\boldsymbol{R}(t,2)$ is given by (28) and $\boldsymbol{r}(t)$ is illustrated in Figure 6.

Hence, by (8), the moment when the system risk function exceeds a permitted level, for instance δ = 0.05, is given as follows

$$\tau = \boldsymbol{r}^{-1}(\delta) \cong 0.0710. \quad (33)$$

7 Bulk cargo transportation system reliability improvement prediction

To obtain better expected values of the bulk cargo transportation system lifetimes in the reliability states subsets {1,2,3}, {2,3}, {3}, we assume that the described bulk cargo transportation system is a series system with hot single redundancy of bow rollers and supporting rollers in all subsystems $S_\upsilon, \upsilon = 1,2,\ldots,9$. After applying the formulae (9)-(10), (13)-(14) and (15)-(16), its reliability function is given by

$$\boldsymbol{IR}(t,\cdot) = [1, \boldsymbol{IR}(t,1), \boldsymbol{IR}(t,2), \boldsymbol{IR}(t,3)], \; t \in \langle 0,\infty), \quad (34)$$

where

$$\boldsymbol{IR}(t,u)=\prod_{\upsilon=1}^{9}\boldsymbol{IR}^{(\upsilon)}(t,u),\ \upsilon=1,2,\ldots,9,$$

$$\boldsymbol{IR}^{(1)}(t,u)=R_1^{(1)}(t,u)[R_2^{(1)}(t,u)]^2\prod_{i=4}^{147}[1-[F_{i1}^{(1)}(t,u)]^2], \tag{35}$$

$$\boldsymbol{IR}^{(2)}(t,u)=R_1^{(2)}(t,u)[R_2^{(2)}(t,u)]^2\prod_{i=4}^{61}[1-[F_{i1}^{(2)}(t,u)]^2], \tag{36}$$

$$\boldsymbol{IR}^{(3)}(t,u)=R_1^{(3)}(t,u)[R_2^{(3)}(t,u)]^2\prod_{i=4}^{248}[1-[F_{i1}^{(3)}(t,u)]^2], \tag{37}$$

$$\boldsymbol{IR}^{(4)}(t,u)=1-[1-R_1^{(4)}(t,u)[R_2^{(4)}(t,u)]^2\prod_{i=4}^{18}[1-[F_{i1}^{(4)}(t,u)]^2]]^3, \tag{38}$$

$$\boldsymbol{IR}^{(5)}(t,u)=R_1^{(5)}(t,u)[R_2^{(5)}(t,u)]^2\prod_{i=4}^{173}[1-[F_{i1}^{(5)}(t,u)]^2], \tag{39}$$

$$\boldsymbol{IR}^{(6)}(t,u)=R_1^{(6)}(t,u)[R_2^{(6)}(t,u)]^2\prod_{i=4}^{88}[1-[F_{i1}^{(6)}(t,u)]^2], \tag{40}$$

$$\boldsymbol{IR}^{(7)}(t,u)=R_1^{(7)}(t,u)[R_2^{(7)}(t,u)]^2\prod_{i=4}^{18}[1-[F_{i1}^{(7)}(t,u)]^2], \tag{41}$$

$$\boldsymbol{IR}^{(8)}(t,u)=R_1^{(8)}(t,u)[R_2^{(8)}(t,u)]^2\prod_{i=4}^{218}[1-[F_{i1}^{(8)}(t,u)]^2], \tag{42}$$

$$\boldsymbol{IR}^{(9)}(t,u)=[R_1^{(9)}(t,u)]^3[R_2^{(9)}(t,u)]^6\prod_{i=10}^{93}[1-[F_{i1}^{(9)}(t,u)]^2], \tag{43}$$

for $t\in\langle 0,\infty)$, $u = 1,2,3$.

Applying the formulas (35)-(43) and considering the parameters given in Tables 1-3, the coordinates reliability function of the system with hot single reserve of its components given by (34) are as follows:

$$\begin{aligned}\boldsymbol{IR}(t,1)=&\exp[-6.46156t^2]\,(2-\exp[-0.00739t^2])^{702}\,(2-\exp[-0.00204t^2])^{215}\\&(2-\exp[-0.02806t^2])^{12}\,(2-\exp[-0.00466t^2])^{64}\,(2-\exp[-0.00594t^2])^{3}\\&(2-\exp[-0.00119t^2])^{20}\,[3\exp[-0.3704t^2]\,(2-\exp[-0.02806t^2])^{12}\\&(2-\exp[-0.00594t^2])^{3}-3\exp[-0.7408t^2]\,(2-\exp[-0.02806t^2])^{24}\\&(2-\exp[-0.00594t^2])^{6}+\exp[-1.1112t^2]\,(2-\exp[-0.02806t^2])^{36}\\&(2-\exp[-0.00594t^2])^{9}]\end{aligned} \tag{44}$$

$$\begin{aligned}\boldsymbol{IR}(t,2)=&\exp[-10.18283t^2]\,(2-\exp[-0.01208t^2])^{702}\,(2-\exp[-0.00246t^2])^{215}\\&(2-\exp[-0.01003t^2])^{3}\,(2-\exp[-0.00754t^2])^{64}\,(2-\exp[-0.02986t^2])^{12}\\&(2-\exp[-0.00181t^2])^{20}\,[3\exp[-0.41507t^2]\,(2-\exp[-0.02986t^2])^{12}\\&(2-\exp[-0.01003t^2])^{3}-3\exp[-0.83014t^2]\,(2-\exp[-0.02986t^2])^{24}\\&(2-\exp[-0.01003t^2])^{6}+\exp[-1.24521t^2]\,(2-\exp[-0.02986t^2])^{36}\\&(2-\exp[-0.01003t^2])^{9}]\end{aligned} \tag{45}$$

$$\boldsymbol{IR}(t,3)=\exp[-17.29049t^2]\,(2-\exp[-0.02112t^2])^{702}\,(2-\exp[-0.00302t^2])^{215}$$

$$(2-\exp[-0.02011t^2])^3\ (2-\exp[-0.01208t^2])^{64}\ (2-\exp[-0.03205t^2])^{12}$$
$$(2-\exp[-0.00238t^2])^{20}\ \ [3\exp[-0.49986t^2]\ (2-\exp[-0.03205t^2])^{12}$$
$$(2-\exp[-0.02011t^2])^3\ -3\exp[-0.9972t^2]\ (2-\exp[-0.03205t^2])^{24}$$
$$(2-\exp[-0.02011t^2])^6\ +\exp[-1.49958t^2]\ (2-\exp[-0.03205t^2])^{36}$$
$$(2-\exp[-0.02011t^2])^9\,] \tag{46}$$

Their graphs are presented in Figure 5

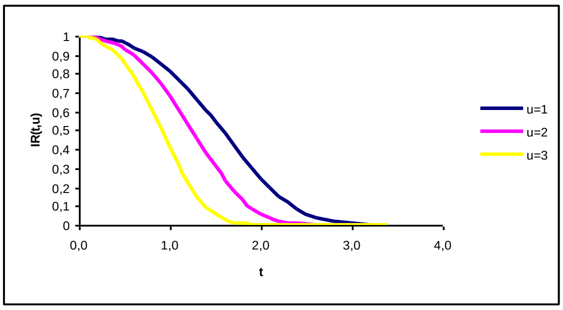

Figure 5. The graph of reliability function of the bulk cargo transportation system with hot single reserve of its components.

Considering (44)-(46), the expected values of the bulk cargo transportation system lifetimes in the reliability states subsets {1,2,3}, {2,3}, {3}, according to (5), respectively are

$$\mu(1) \cong 1.5604, \quad \mu(2) \cong 1.2375, \ \mu(3) \cong 0.9101. \tag{47}$$

And further, the standard deviations of this system lifetimes in the reliability state subsets {1,2,3}, {2,3}, {3}, are

$$\sigma(1) \cong\ 0.5973\,,\ \sigma(2) \cong\ 0.4839\,,\ \sigma(3) \cong 0.3698\,. \tag{48}$$

Consequently, according to (7), the mean values of the maritime ferry technical system lifetimes in the particular reliability states 1, 2, 3, are respectively:

$$\bar{\mu}(1) \cong 0.3229, \ \bar{\mu}(2) \cong 0.3274, \ \bar{\mu}(3) \cong 0.9101. \tag{49}$$

Since the critical reliability state is r = 2, then the system risk function of the bulk cargo transportation system with hot single redundancy, according to (7), is given by

$\boldsymbol{r_h}(t) = 1 - \boldsymbol{IR}(t,2)$,

where $\boldsymbol{IR}(t,2)$ is given by (44) and $\boldsymbol{r_h}(t)$ is illustrated in Figure 6.

Hence, by (9), the moment when the system risk function exceeds a permitted level, for instance $\delta = 0.05$, is given as follows

$$\boldsymbol{\tau} = \boldsymbol{r_h}^{-1}(\delta)\ \cong\ 0.4224. \tag{50}$$

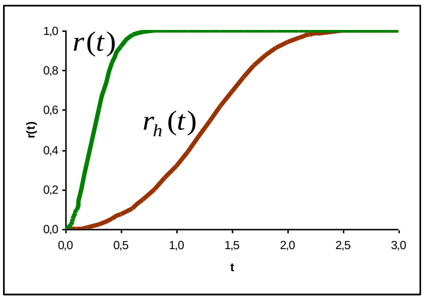

Figure 6. The graph of risk functions of a bulk cargo transportation system.

Conclusions

The multistate approach to system reliability analysis and improvement, and the reliability models of typical multistate system structures, like that considered in the paper, can be applied in the reliability analysis of a wide class of complex technical systems. This possibility is illustrated through an example of a bulk cargo transportation system, for which reliability analysis and reliability improvement and reliability characteristics predictions were achieved. From the graph of the system risk functions of a system without reserve and a system with hot reserve, we can see how the quantitative redundancy prolongs the time to the moment when the system exceeds the critical level and the mean values of system lifetimes in particular states. Finally, we can search for a factor in the Weibull reliability functions, which will allow us to improve system's basic components and obtain the same risk function and mean values like for a system with hot reserve.

References

1. Kołowrocki, K. & Soszyńska-Budny, J. 2011. Reliability and Safety of Complex Technical Systems and Processes: Modeling – Identification – Prediction – Optimization. Springer.
2. Kołowrocki, K. 2014. Reliability of large and complex systems, Elsevier.
3. Kołowrocki K. & Kwiatuszewska-Sarnecka B. (2008). Reliability and risk analysis of large systems with ageing components. Reliability Engineering & System Safety, Volume 93, 1821-182.
4. Kołowrocki K., Kwiatuszewska-Sarnecka B. & Soszyńska J. (2008). Modelling of operational processes of port bulk cargo system. Proc. 2nd Summer Safety and Reliability Seminars – SSARS 2008, Gdańsk-Sopot, Vol. 2, 217-222
5. Kwiatuszewska-Sarnecka B. Analysis of Reservation Efficiency in Series Systems, PhD. Thesis, (in Polish), 2003, Gdynia Maritime University.

The expected semi Markov rewards as a tool for the evaluation of the quality of life

Zacharias Kyritsis[1] and Aleka Papadopoulou[1]

[1] Department of Mathematics, Aristotle University of Thessaloniki, Thessaloniki 54124, Greece
(E-mail: zkyritsi@math.auth.gr, apapado@math.auth.gr)

Abstract. In the present paper, a patient's quality of life is defined through a non homogeneous semi Markov reward model. The patient's expected interval reward is calculated by means of the basic parameters of the system. The above mean reward could operate as a tool for indicating the quality of life status for all health states. The expected interval rewards are illustrated numerically with synthesized data.
Keywords: Semi Markov, Quality of Life, Rewards.

1. Introduction

In literature, basic definitions and theoretical results for the homogeneous semi-Markov reward processes can be found in Howard [5]. De Dominicis and Manca [4] provided the first results on the transient behaviour of the semi-Markov reward processes and applied them to insurance disability problems. In Balcer and Sahin [2] two extensions of a semi Markov reward model of pension accumulation are examined and expressions for the mean expected benefits are derived. A multivariate reward process defined on a semi Markov process is studied in Masuda and Sumita [12] and transform results for the distributions of the multivariate reward processes are derived. In Masuda [11] partially observable semi-Markov reward processes are examined and the conditional distribution of the vector with total rewards is studied. A general definition of rewards can be found in Limnios and Oprisan [10] and the study of the asymptotic behaviour of semi Markov reward process in Reza Soltani and Khorshidian [19]. Later, in Papadopoulou [16] closed analytic forms for the main formulas of the expected reward that the semi Markov system generates are provided. In Jianyong and Xiaobo [8] average reward semi-Markov decision processes with multichain structure are examined. Also, McClean et al. [13] provides formulas for semi Markov rewards by means of probability generating functions. In Papadopoulou and Tsaklidis [18] reward paths for semi Markov models with stochastic selection of the transition probabilities are studied. Furthermore, transition rewards are studied in Janssen and Manca [7] and higher

16th ASMDA Conference Proceedings, 30 June – 4 July 2015, Piraeus, Greece

order moments and variance for semi Markov rewards are treated numerically in Stenberg et al. [20] for the homogeneous case and Stenberg et al. [21] for the non-homogeneous case. In Papadopoulou et al [15] theoretical results concerning the moments and consequently the distribution of interval costs are obtained and provided in analytic form for a semi Markov reward model with discounting and the results are applied to an open healthcare system. Last, in Papadopoulou [17] rewards/costs are attached in a semi Markov model and analytic forms for the means, variances and moments of the total interval rewards/costs produced by Web navigation are provided.

The quality of life is recognized as an important element which is generally treated at least as primary or secondary criterion in most clinical trials. So, its measurement and statistical analysis remain an issue. Many researchers have studied the quality of life through Markov processes considering that a patient′s observed quality of life at any time is a discrete variable (state) which could be accessed through a self-rated questionnaire (Limnios et al [9], D'Amico [3], Heute and Heuber [6]). In many cases the deterioration of the patient's health status is often observed during the trial either because the toxicity of treatment or the progression of disease. This deterioration is very likely to be reflected in the patient's quality of life (Awad et al [1], Mesbah [14]).

In section 2 the expected semi Markov reward is calculated to evaluate the quality of life status in relation to each health status by means of the basic parameters of the system. In section 3 the above results are illustrated with synthesized data.

2. The expected semi Markov interval reward for the patient's quality of life

The basic idea in the present section is to provide a non homogeneous semi Markov model for which the health status is defined as an independent variable, while the quality of life is dependent on the health status (Mesbah [14]). Thus, we have two processes for each patient, one for its health status and the other for its quality of life status, related to each other.

Let us now consider a semi Markov chain with finite state space, $E=\{1,2,\ldots,l\}$, where the states define the patient's health status, $\mathbf{P_h}(t)=\{p_{ij}(t)\}_{i,j\in E}$ is the transition probability matrix of the embedded Markov chain and $\mathbf{H}(m)=\{h_{ij}(m)_{i,j\in E}$ is the holding time mass function matrix for the semi Markov chain. Also, let us consider a Markov chain with finite state space, $S=\{(1,1), (1,2),...,(l,s)\}$, where its states define a patient's status by considering the health and the quality of life status together, s denotes the number of the quality of life states and $\mathbf{P_q}(k,t)=\{p_{(i,x),(j,y)}(k,t)\}_{(i,x),(j,y)\in S}$ be the corresponding transition probability matrix for the process where $p_{(i,x),(j,y)}(k,t)$ equals to the probability of a patient which is in health state i and quality state x

to move to health state j and quality state y in the period (t, t+1] while the patient's time occupancy in state i at time t is k.

In what follows, we extend the above model by including rewards of making a transition from one (either health or quality) state to another. This model could be used for strategic approaches to planning and evaluating a patient's quality of life status.

Let now ${r_{ij}}^{health}$ be the reward produced of making a transition from the i health state to j and ${r_{xy}}^{quality}$ be the reward produced of making a transition from the x quality of life state to y.

Also, let us define as $T_{t,n,k}^{i,x}$ the interval reward produced by a patient's movement to various health and quality states through the interval (t, t+n], given that the patient was in the i health state and in the x quality of life state at time t and entered to the i health state at time t-k. Then, we can define as $V_{ix}(t,n,k)$ the interval expected reward produced by a patient as follows:

$$V_{ix}(t,n,k) = \mathrm{E}\left(T_{t,n,k}^{i,x}\right) = \mathrm{E}\ [\text{of the interval reward produced by a patient's movement through the interval } (t, t+n]\ /\ \text{the patient was in the } i \text{ health state and in the } x \text{ quality of life state at time } t \text{ and entered to the } i \text{ health state at time } t-k]$$

In the following theorem we provide with the equations for the mean of the interval reward produced by a patient's movement to various states by means of the basic parameters of the system.

Theorem 1

The interval expected reward produced by a patient's movement through the interval (t, t+n] given that the patient was in the i health state and the x quality of life state at time t and entered to the i health state at time t-k, is described by the following equation :

$$\begin{aligned} V_{ix}(t,n,k) &= \mathrm{E}\left(T_{t,n,k}^{i,x}\right) \\ &= \sum_{\mathrm{y}=1}^{\mathrm{s}} \frac{\sum_{r=k+1}^{\infty} p_{(i,x),(i,y)}(\mathrm{r},\mathrm{t})}{{}^{>}w_i(t-k,k+1)} \left({r_{xy}}^{quality} + V_{iy}(t+1,n-1,k+1)\right) \\ &\quad + \sum_{\mathrm{j}=1}^{l} \sum_{\mathrm{y}=1}^{\mathrm{s}} \frac{p_{(i,x),(j,y)}(\mathrm{k},\mathrm{t})}{p_{ij}(t-k)h_{ij}(k+1)} \left({r_{xy}}^{quality} + {r_{ij}}^{health} \right. \\ &\quad \left. + V_{jy}(t+1,n-1,0)\right) \end{aligned} \tag{1}$$

<u>Proof</u>

Using probabilistic argument we can result to the following recursive equation:

$$V_{ix}(t,n,k) = \mathrm{E}\left(T_{t,n,k}^{i,x}\right)$$

$$= \sum_{y=1}^{s} \text{Prob (of a patient to move from quality state } x \text{ to } y \text{ at}$$
$$t+1 \text{ / the patient will remain in health state } i \text{ for more than } k+1 \text{ time units)} \left(r_{xy}{}^{quality} + V_{iy}(t+1, n-1, k+1)\right)$$
$$+ \sum_{j=1}^{l} \sum_{y=1}^{s} \text{Prob (of a patient to move from quality state } x \text{ to } y \text{ at}$$
$$t+1 \text{/the patient will move from health state } i \text{ to j at time } t+1) \left(r_{xy}{}^{quality} + r_{ij}{}^{health} + V_{jy}(t+1, n-1, 0)\right)$$
$$= \sum_{y=1}^{s} \frac{\sum_{r=k+1}^{\infty} p_{(i,x),(i,y)}(\mathrm{r},\mathrm{t})}{{}^{>}w_i(t-k, k+1)} \left(r_{xy}{}^{quality} + V_{iy}(t+1, n-1, k+1)\right)$$
$$+ \sum_{j=1}^{l} \sum_{y=1}^{s} \frac{p_{(i,x),(j,y)}(\mathrm{k},\mathrm{t})}{p_{ij}(t-k) h_{ij}(k+1)} \left(r_{xy}{}^{quality} + r_{ij}{}^{health} + V_{jy}(t+1, n-1, 0)\right)$$

The initial condition for the above equation is $V_{ix}(t, 0, k) = 0$ for every k and t.

3. Illustration

In the present section we illustrate the previous theoretical results with synthesized data for HIV patients. The process of infection by HIV is characterized by two fundamental markers. The first is the viral load (VL) and the second CD4 lymphocyte. Hence, the history of the disease can be considered as a series of stages through which a patient progresses. The first stage is called primary infection. And the corresponding symptoms vary to duration that is twenty eight days in average and at least one week. At this stage there are no specific symptoms and often they are not recognized as signs of HIV infection. Even if a patient goes to a doctor or a hospital, he might be misdiagnosed. The second stage is called clinically asymptomatic stage lasts for an average of ten years and, as its name suggests, that is free from major symptoms. The HIV antibodies are detectable in the blood, so antibody tests will show a positive result. On the third stage called symptomatic HIV the lymph nodes and tissues are damaged because of the years of activity, HIV mutates and becomes more pathogenic, leading to more T helper cell destruction and the body fails to keep up with replacing the lost T helper cells. Antiretroviral treatment is usually started once an individual's CD4 index falls to a low level which is an indication that the immune system is deteriorating. Finally, on the fourth stage called progression for AIDS as the immune system becomes more and more damaged the individual may develop increasingly severe opportunistic infections and cancers, leading eventually to an AIDS diagnosis.

Using these markers and the above mentioned four stages we can describe the progress of HIV by a semi Markov model considering four health state as follows:

Primary infection → First stage: VL≤400 and CD4≤200
Asymptomatic stage → Second stage: VL≤400 and CD4>200
Symptomatic HIV → Third stage: VL>400 and CD4>200
Progression for AIDS → Fourth stage: VL>400 and CD4≤200

From the above, we can consider a non homogeneous semi Markov process with discrete and finite state space symbolized by S={1, 2, 3, 4}. Using as markers of infection the virus load and the CD4 lymphocyte we define four stage that mentioned above so, we consider that the health state space is E={1,2,3,4}.

The quality of life of a patient with HIV can be measured by different tools (questionnaires) such as FL36, MOS-HIV, MQoL-HIV and WHOQOL-HIV .
We suppose that the score of quality of life instrument ranging from 0 to 100 and we define the quality of life space S={1,2,3}.

State 1 → scores between 0-33 (low level)
State 2 → scores between 34-66 (medium level)
State 3 → scores between 67-100 (high level).

So, the state space is defined as $Z=\{(1_h, 1_q), (1_h, 2_q), (1_h, 3_q), (2_h, 1_q), (2_h, 2_q), (2_h, 3_q), (3_h,1_q), (3_h, 2_q), (3_h,3_q), (4_h, 1_q), (4_h, 2_q), (4_h, 3_q)\}$.
And we suppose that the rewards for transition in quality of life states are:

$$r_{xy}{}^{\text{quality}} = \begin{cases} -2 \text{ for transition } 3 \to 1 \\ -1 \text{ for transition } 2 \to 1 \text{ or } 3 \to 2 \\ 0 \text{ for transition } 1 \to 1 \\ 1 \text{ for transition } 1 \to 2 \text{ or } 2 \to 3 \\ 2 \text{ for transition } 1 \to 3 \end{cases}$$

Also, we suppose that the rewards for transition in health states are:

$$r_{ij}{}^{\text{health}} = \begin{cases} -2 \text{ for transition } 1 \to 3 \text{ or } 2 \to 4 \\ -1 \text{ for transition } 1 \to 2 \text{ or } 2 \to 3 \text{ or } 3 \to 4 \\ 0 \text{ for holding in any state} \\ 1 \text{ for transition } 2 \to 1 \text{ or } 3 \to 2 \text{ or } 4 \to 3 \\ 2 \text{ for transition } 3 \to 1 \text{ or } 4 \to 2 \end{cases}$$

Now by applying equation (1) we can estimate the interval reward produced by a patient movement indicating his quality of life for all health states. In Figures 1, 2 and 3 the results for the expected interval rewards given that the process started from quality of life states 1, 2 and 3 for the intervals [0,n], n=1, 2, 3, 4 and 5 are presented.

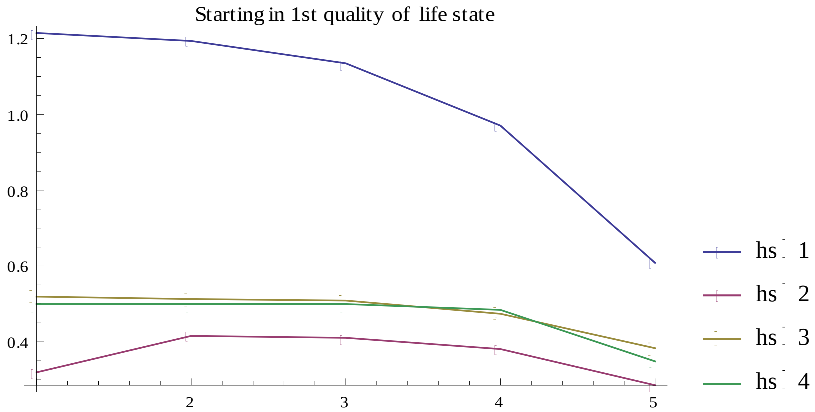

Figure 1 Expected reward given that the initial quality of life state is 1

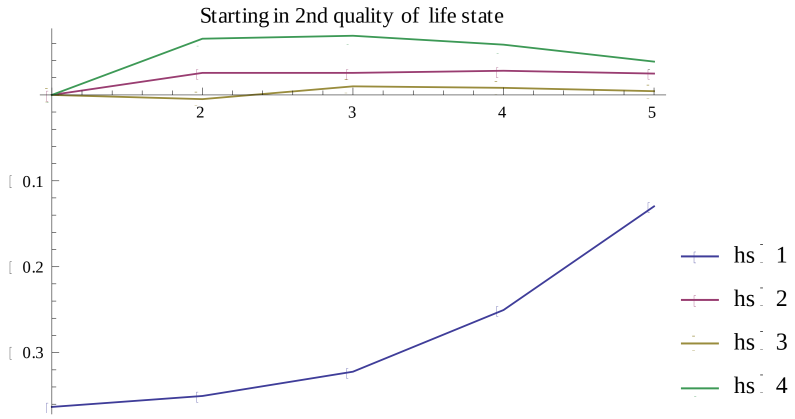

Figure 2 Expected reward given that the initial quality of life state is 2

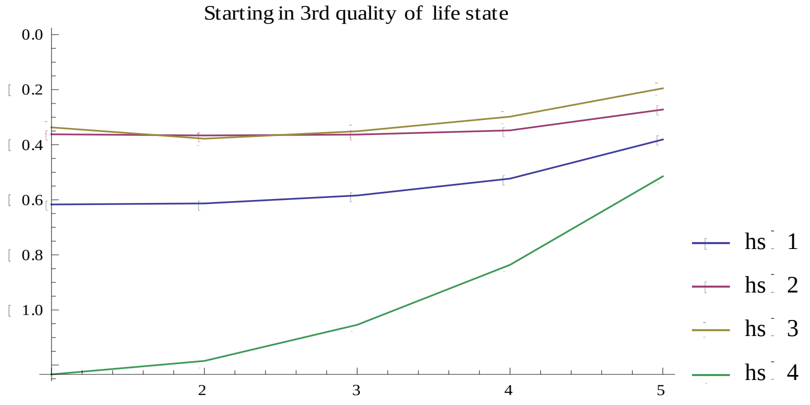

Figure 3 Expected reward given that the initial quality of life state is 3

References

1. Awad, L. Zuber,E. and Mesbah M. 2002. "Applying survival data methodology to analyze longitudinal quality of life data." In *Statistical Methods for Quality of Life Studies*, by Bernard Cole and Mei-Ling Ting Lee Munir Mesbah, 231-243. Springer.

2.Balcer, Y. Sahin I. 1986. "Pension accumulation as a semi-Markov reward process with applications to pension reform. ." In *Semi-Markov models.* , by Janssen J (ed). New York: Plenum.

3.D'Amico, Guglielmo. 2009. "Measuring quality of life through Markov Reward processes: Analysis and inference ." *Envirometrics,* June: 208-220.

4.De Dominics, R., Manca, R. 1985. "Some new results on the transient behavior of semi Markov reward processes." *Methods Oper. Res. Comput.* 13:823-838.

5.Howard, R. 1972. *Dynamic Probabilistic Sytems, vol. II.* D Wiley. .

6.Huber-Carol, C. and Heutte N. 2002. "Semi-Markov models for quality of life data with censoring." In *Statistical Methods for Quality of Life Studies: Design, Measurements and Analysis*, by Bernard Cole and Mei-Ling Ting Lee Munir Mesbah. Boston: Kluwer.

7.Janssen J, Manca R (2007) Semi-Markov risk models for finance insurance and reliability. Springer

8.Jianyong L, Xiaobo Z (2004) On average reward semi-Markov decision processes with a general multichain structure. Math Oper Res 29(2):339–352

9.Limnios N., Mesbah M. and Sadek A. 2004. "A new index for longitudinal quality of life modelling and estimation." *Envirometrics* 15: 483-490

10.Limnios N, Oprisan G (2001) Semi-Markov processes and reliability. Birkhauser, Boston.

11.Masuda Y (1993) Partially observable semi-Markov reward processes. J Appl Prob 30(3):548–560

12.Masuda, Y. Sumita U. 1991. "A multivariate reward process defined on a semi-Markov process and its first-passage-time distributions." *J Appl Prob* 28(2):360–373.

13.McClean SI, Papadopoulou A, Tsaklides G (2004) Discrete time reward models for homogeneous semi-Markov systems. Commun Stat, Theory Methods 33(3):623–638

14.Mesbah, M.Dupuy, J. F., Heutte, N. and Awad L. 2004. "Joint analysis of longitudinal quality of life and survival process." In *Handbook of Statistics.Vol22, Advances in Survival Analysis*, by N. Balakrishnan et C.R. Rao. Amsterdam: North Holland.

15. A.A. Papadopoulou, G. Tsaklidis, S. McClean, L. Garg, On the moments and the Distribution of the Cost of a semi-Markov Model for Healthcare Systems. Methodology and Computing in Applied Probability 14(3) (2012) 717-737

16.Papadopoulou, A. 2004. "Economic rewards in non homogeneous semi-Markov systems." *Commun Stat, Theory Methods* 33(3):681–696.

17.Papadopoulou A (2010) Modeling biological sequences and web navigation with a semi Markov chain. Proceedings of the Stochastic Modeling Techniques and Data Analysis International Conference, Chania, Greece, June 8–11, 2010

18. Papadopoulou AA, Tsaklidis G (2007) Some reward paths in semi Markov models with stochastic selection of the transition probabilities. Methodol Comput Appl Probab 9:399–411
19. Reza Soltani A, Khorshidian K (1998) Reward processes for semi-Markov processes asymptotic behaviour. J Appl Prob 35:833–842
20. Stenberg, F, Manca R, Silvestrov D. 2006. “Semi Markov reward models for disability insurance.” *Theory Stoch Proces* 12(28), no. 3–4:239–254.
21. Stenberg F, Silvestrov D, Manca R 2007. An algorithmic approach to discrete time nonhomogeneous backward semi-Markov reward processes with an application to disability insurance. Methodology and Computing in Appl Probab 9:497–519